Metabolites from the plant pathogen *Alternaria brassicicola*: *in vitro* and *in planta* production and biosynthesis of brassicicolin A

A Thesis Submitted to the College of
Graduate Studies and Research
In Partial Fulfillment of the Requirements
For the degree of Doctor of Philosophy
In the Department of Chemistry
University of Saskatchewan
Saskatoon

By

Myung Ryeol Park

PERMISSION TO USE

In presenting this thesis in partial fulfillment of the requirements for a postgraduate degree from the University of Saskatchewan, the author has agreed that the libraries of this University may make it freely available for inspection. The author further agrees that permission for copying of this thesis in any manner, in whole or in part, for scholarly purposes may be granted by the professor who supervised the thesis work or, in her absence, by the Head of the Department of Chemistry, or the Dean of the College of Graduate Studies and Research. It is understood that copying or publication or use of this thesis or parts thereof for financial gain shall not be allowed without the author's written permission. It is also understood that due recognition shall be given to the author and to the University of Saskatchewan in any scholarly use which may be made of any material in my thesis.

Requests for permission to copy or to make other use of material in this thesis in whole or part should be addressed to:

The Head
Department of Chemistry
University of Saskatchewan
Saskatoon, Saskatchewan, Canada
S7N 5C9

ABSTRACT

The phytopathogenic fungus *Alternaria brassicicola* (Schwein.) Wiltshire together with *A. brassicae* cause *Alternaria* black spot (also called dark leaf spot) in *Brassica* species. During infection, *A. brassicicola* produces various secondary metabolites to facilitate its colonization and invasion. A systematic investigation of the secondary metabolites produced by *A. brassicicola* was carried out.

In addition to previously reported metabolites, four metabolites, α-acetylorcinol (**210**), tyrosol (**219**), depudecin (**151**) and dihydrobrassicicolin A (**220**) were isolated and characterized from culture extracts of *A. brassicicola* for the first time. Chemical synthesis of α-acetylorcinol (**210**) was accomplished for the first time with an overall yield of 36%. Neither α-acetylorcinol (**210**) nor tyrosol (**219**) caused necrotic lesions on the leaves of or displayed elicitor activity in *Brassica juncea*, *B. napus*, or *Sinapis alba*.

A. brassicicola was incubated under different sets of culture conditions, and the culture filtrates were extracted and analyzed by HPLC-DAD. The production of brassicicolin A (**1**), depudecin (**151**) and α-acetylorcinol (**210**) was increased in low concentrations of KNO_3 or $NaNO_3$, or in the absence of nitrates. These results suggest that nitrate inhibits the biosynthesis of brassicicolin A (**1**), depudecin (**151**), and α-acetylorcinol (**210**). In the iron deficient conditions, *A. brassicicola* produced larger amounts of siderophores than in control cultures (ferric citrate 2 μM) or in high concentration of ferric citrate (200 μM). Moreover, spore germination fluids (SGFs) collected from detached leaves of *B. juncea*, *B. napus*, and *S. alba* contained fungal metabolites (i.e., siderophores and phomapyrone A (**25**)). These results suggest that siderophores may play a role in fungal colonization by obtaining iron from host plants. In addition, HPLC analyses of extracts of the detached leaves of *B. juncea*, *B. napus*, and *S. alba* infected with *A. brassicicola* revealed that phomapyrone A (**25**), a fungal metabolite and non-phytotoxin, was detected and quantified for the first time.

Brassicicolin A (**1**) is a host-selective phytotoxin produced by *A. brassicicola*. The biosynthetic precursors of brassicicolin A (**1**) were investigated using the following isotopically labeled compounds: D-[U-$^{13}C_6$]glucose, L-[^{15}N]valine, and L-[$^{2}H_8$]valine. The labeled brassicicolin A (**1e, 1j** or **1m**) was obtained from the extracts of culture filtrates of *A. brassicicola* obtained from incubation of cultures with labeled precursors. The ^{13}C NMR and

INADEQUATE spectra of ^{13}C-enriched brassicicolin A (**1e**) obtained showed ^{13}C-^{13}C coupling resulting from adjacent ^{13}C carbons. Enhancement of the isocyanide carbon resonances of the ^{13}C-enriched brassicicolin A (**1e**) suggested that the isocyanide carbons are labeled. Furthermore, spectroscopic data including ^{1}H NMR, ^{15}N NMR and HR-ESI-MS of ^{2}H-enriched (**1j**) or ^{15}N-enriched brassicicolin A (**1m**) indicated that both 2-hydroxy-3-methylbutanoyl and isocyanoisovaleryl units are derived from valine.

ACKNOWLEDGEMENTS

I would like to express my heartfelt appreciation to my supervisor Prof. M. Soledade C. Pedras, Department of Chemistry, University of Saskatchewan, for her persistent guidance, encouragement, and consistent support. Her vast knowledge in multidiscipline, professionalism, integral view on research and passion in science will remain as an inspiration for the rest of my life. Without her help, I would not have been able to complete the Ph. D. program and to make this Ph. D. thesis possible.

I would like to thank the members of my Advisory Committee: Prof. M. Majewski and Prof. D. Sanders, Department of Chemistry, University of Saskatchewan, and Prof. Y. Wei, Department of Biology, University of Saskatchewan. Their valuable advice and help during my Ph. D. program are greatly acknowledged. I also thank Prof. P. Harrison, my external examiner, Department of Chemistry, McMaster University for reviewing my thesis and making valuable comments.

I would like to thank all past and present group members in Prof. Pedras group: Dr. Z. Minic, Dr. P. Chumala, Dr. V. Sarma-Mamillapalle, Dr. S. Hossain, Dr. E. Yaya, Dr. I. Khallaf, Dr. P. Saha, Dr. M. Khan, Dr. M. Hossain, A. Abdoli, C. Thapa, H. To and M. Alavi.

I also wish to express my thanks to Dr. K. Brown and K. Thompson, Saskatchewan Structural Sciences Centre for their technical assistance. Finally, I sincerely express my deepest gratitude to S. H. Kim for her encouragement and inspiration.

DEDICATION

To my grandparents,

박 병 래 그리고 윤 단 오

(Byung Rae Park & Dan Oh Youn)

To my parents,

박 대 철 그리고 백 정 순

(Dae Chul Park & Jeong Soon Baek)

TABLE OF CONTENTS

LIST OF FIGURES

LIST OF SCHEMES

LIST OF TABLES

LIST OF ABBREVIATIONS

^{1}H NMR	proton nuclear magnetic resonance
^{13}C NMR	carbon-13 nuclear magnetic resonance
5-Aza	5-Azacytidine
A. alternata	*Alternaria alternata*
A. brassicae	*Alternaria brassicae*
A. brassicicola	*Alternaria brassicicola*
A. cassia	*Alternaria cassia*
A. fumigatus	*Aspergillus fumigatus*
A. longipes	*Alternaria longipes*
A. nidulans	*Aspergillus nidulans*
A. niger	*Aspergillus niger*
A. ochraceus	*Aspergillus ochraceus*
A. panax	*Alternaria panax*
A. phragmospora	*Alternaria phragmospora*
A. sativa	*Avena sativa*
A. sydowii	*Aspergillus sydowii*
A. tagetica	*Alternaria tagetica*
A. tenuis	*Alternaria tenuis*
A. tenuissima	*Alternaria tenuissima*
A. terpenensis	*Amphimedon terpenensis*
A. thaliana	*Arabidopsis thaliana*
Ac_2O	acetic anhydride
Aeo	2-amino-9,10- epoxi-8-oxodecanoic acid
Ala	alanine
albD	albicidin hydrolase
aq.	aqueous
B. campestris	*Brassica campestris*
B. cinerea	*Botrytis cinerea*

B. felina	*Beauveria felina*
B. juncea	*Brassica juncea*
B. napus	*Brassica napus*
B. oleracea	*Brassica oleracea*
B. rapa	*Brassica rapa*
B. subtilis	*Bacillus subtilis*
BA	brassicicolin A
BPC	base peak chromatogram
C. albicans	*Candida albicans*
C. annullata	*Cordyceps annullata*
C. arvense	*Cirsium arvense*
C. bursa-pastoris	*Capsella bursa-pastoris*
C. carbonum	*Cochliobolus carbonum*
C. heterostrophus	*Cochliobolus heterostrophus*
C. indicum	*Chaetomium indicum*
C. indigotica	*Cordyceps indigotica*
C. sativa	*Camelina sativa*
C. victoriae	*Cochliobolus victoriae*
calcd.	calculated
Col-0	*Arabidopsis thaliana* Columbia ecotype 0
CON	control
CON-S	control-autoclaved spores
CON-W	control-water
COSY	correlation spectroscopy
cv.	cultivar
D. chlamydosporia	*Diheterospora chlamydosporia*
DAD	diode array detector
DEP	depudecin
DMF	dimethylformamide
DMSO	dimethylsulfoxide
DNMT	DNA methyltransferases

E. gallicum	*Erucastrum gallicum*
E. coli	*Escherichia coli*
E. herbicola	*Erwinia herbicola*
EC	effective concentration
EDA	9,10-epoxy-8-hydroxy-9-methyldecatrienoic acid
EI	electron impact
EIC	extracted ion chromatogram
ESI	electrospray ionization
Et_2O	diethyl ether
EtOAc	ethyl acetate
EtOH	ethanol
FAB	fast atom bombardment
F. amygdali	*Fusicoccum amygdali*
F. graminearum	*Fusarium graminearum*
F. oxysporum	*Fusarium oxysporum*
F. verticillioides	*Fusarium verticillioides*
FCC	flash column chromatography
FD	field desorption
FT-IR	fourier transformed infrared
G. formosana	*Gibellula formosana*
GC-MS	gas chromatography-mass spectrometry
glc	glucose
GSH	glutathione
h	hours
H. victoriae	*Helminthosporium victoriae*
HDAC	histone deacetylase
HMBC	heteronuclear multiple bond correlation
HMQC	heteronuclear multiple quantum correlation
HSQC	heteronuclear single quantum coherence spectroscopy
HPLC	high performance liquid chromatography
HRMS	high resolution mass spectrometry

HSTs	host selective toxins
Hz	Hertz
Hx	hexane
I. tenuipes	*Isaria tenuipes*
IC	inhibitory concentration
INADEQUATE	incredible natural abundance double quantum transfer experiment
Isn	isocyanide or isonitrile
J	coupling constant
L. maculans/P. lingam	*Leptosphaeria maculans/Phoma lingam*
LAH	lithium aluminum hydride
m.p.	melting point
m/z	mass/charge ratio
Me	methyl
MeCN	acetonitrile
MeO	methoxy
MeOH	methanol
MHz	megahertz
min	minutes
MM	minimal medium
mmol	millimole
MRSA	methicillin-resistant *Staphylococcus aureus*
MS	mass spectrometry
N. scuroucicola	*Nimbya scuroucicola*
N. sphaerica	*Nigrospora sphaerica*
ND	not detected
NHST	non-host-selective toxin
nps6	non-ribosomal peptide synthetase 6 mutant
NRPS	non-ribosomal peptide synthetase
OSMAC	one strain many compounds
P. dispersa	*Pantoea dispersa*
P. quinquefolius	*Panax quinquefolius*

P. syringae	*Pseudomonas syringae*
Pad	phytoalexin deficient
PCC	pyridinium chlorochromate
PDA	potato dextrose agar
PDB	potato dextrose broth
Pen	penetration
Phe	phenylalanine
PK	polyketide
PKS	polyketide synthase
ppm	parts per million
prep. TLC	preparative thin layer chromatography
Pro	proline
quant.	quantative yield
R. solani	*Rhizoctonia solani*
ROS	reactive oxygen species
RP-FCC	reverse phase flash column chromatography
rpm	revolutions per minute
rt	room temperature
s	seconds
S. alba	*Sinapis alba*
S. aureus	*Staphylococcus aureus*
S. sclerotiorum	*Sclerotinia sclerotiorum*
SAHA	suberoylanilide hydroxamic acid
SBHA	suberoylanilide bis-hydroxamic acid
SD	standard deviation
SGF	spore germination fluids
T. aestivum	*Triticum aestivum*
T. erecta	*Tagetes erecta*
T. luteorostrata	*Torrubiella luteorostrata*
T. salsuginea	*Thellungiella salsuginea*
TEA	triethylamine

THF	tetrahydrofuran
TIC	total ion current
TLC	thin layer chromatography
t_R	retention time
UV/Vis	ultraviolet/visible
v	volume
val	valine
X. albilineans	*Xanthomonas albilineans*
zwf	glucose-6-phosphate-1-dehydrogenase

1 Introduction

1.1 General objectives

The plant pathogenic fungus *Alternaria brassicicola* (Schwein.) Wiltshire together with *A. brassicae* (Berk.) Sacc. cause *Alternaria* black spot disease in crucifers. *A. brassicicola* produces various secondary metabolites including phytotoxin(s). This thesis describes a systematic investigation of the metabolites of *A. brassicicola* produced in aseptic cultures and *in planta*. In addition, the biosynthetic study of brassicicolin A, a host-selective phytotoxin is presented. The overall goal of this project is to understand the chemical interactions between *A. brassicicola* and its host plants. This knowledge could lead to the development of novel strategies to control *A. brassicicola*. The specific objectives of my Ph. D. research work are summarized below.

A. Investigation of the components of culture media and conditions that influence the production of secondary metabolites by *A. brassicicola,* including:
    a. Carbon and nitrogen sources, organic and inorganic components, and temperature;
    b. Inhibitors of histone deacetylases and DNA methyltransferases;
    c. Co-cultivation with *A. brassicae*.
B. Investigation of metabolites produced on leaf tissues of plants (susceptible and resistant) infected with *A. brassicicola*, including:
    a. Comparative chemical analyses of metabolites produced in infected and control leaves of *Brassica juncea* cv. Cutlass (susceptible), *B. napus* cv. Westar (susceptible) and *Sinapis alba* cv. Ochre (resistant);
    b. Comparative chemical analyses of metabolites produced in infected and control leaves of *Arabidopsis thaliana* Columbia (Col-0) and mutants (*pad3-1* and *pen2-1*).
C. Investigation of the biosynthetic pathway of brassicicolin A (**1**) using isotopically labeled precursors.

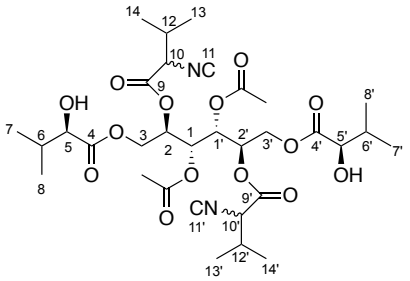

1

1.2 Secondary metabolites produced by phytopathogenic fungi

Secondary metabolites (SMs) are defined as metabolites that "*are found in only specific organisms, or groups of organism, and are an expression of the individuality of species"* (Dewick, 2002). To be specific, secondary metabolites are "*low-molecular-weight natural products with restricted taxonomic distribution, often synthesized after active growth has ceased, which do not have an obvious function in producer species*" (Keller, Turner *et al.*, 2005). Moreover, natural products are "*organic compounds of natural origin that are unique to one organism, or common to a small number of closely related organisms*" (Mann, 1987). Although SMs are one of the subclasses of natural products (Hanson, 2003), the terms "natural product" and "secondary metabolite" are interchangeable (Mann, 1987).

SMs have chemical-ecological roles in adaptation, fitness, and survival of living organisms (O'Brien and Wright, 2011) rather than having basic cellular functions like primary metabolites. Among various SMs, it has been demonstrated that toxic metabolites produced by phytopathogenic fungi facilitate the development of plant diseases that may lead to serious yield losses of economically important crops (Muria-Gonzalez, Chooi *et al.*, 2015; Pusztahelyi, Holb *et al.*, 2015). Toxic metabolites that cause damage to plants are known as phytotoxins. Although many efforts to establish the role(s) of phytotoxins in plant disease have been made during the last decades, a better understanding of the chemical-ecological roles of phytotoxins is essential to control plant pathogens in effective ways.

1.2.1 Phytotoxins produced in culture and *in planta*

The definition of phytotoxins has evolved substantially (Graniti, 1991), since it was first used (Wheeler and Luke, 1963). In a more recent review on phytotoxins, Strange suggested that

phytotoxins are "*compounds synthesized by plant pathogens, which adversely affect their hosts*" (Strange, 2007). Phytopathogenic fungi and bacteria biosynthesize and secrete phytotoxins during infection. Phytotoxins can be classified into host-selective (or host-specific) toxins (HSTs) and non-host-selective (or non-host-specific) toxins (NHSTs). HSTs have a specific range of host plants that are susceptible to the pathogens, whereas NHSTs have a wide spectrum of host plants irrespective of host specificity (Scheffer and Livingston, 1984).

Phytotoxins have mostly been isolated from culture extracts of phytopathogens. In certain cases, chemical syntheses and derivatization of phytotoxins, and/or genetic manipulation of phytopathogens are required to establish the importance of phytotoxins (Strange, 2007). A review article published in 2007 covered about 126 phytotoxins produced by microbial phytopathogens (up to end of 2005) (Strange, 2007). In this section, a few examples of phytotoxins produced by microbial phytopathogens that cause disease symptoms are described below.

HC-Toxin **(2)**, a cyclic tetrapetide, is produced by *Cochliobolus carbonum,* one of the most virulent pathogens on maize. HC-toxin **(2)** is a cyclic compound containing D-Pro-L-Ala-D-Ala-L-Aeo, where Aeo represents 2-amino-9,10- epoxi-8-oxodecanoic acid (Kawai, Rich *et al.*, 1983). The absolute configurations of HC-toxin **(2)** were confirmed by total synthesis (Kawai and Rich, 1983).

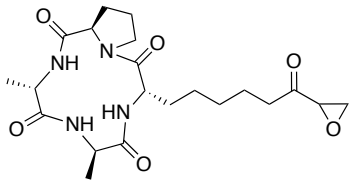

2

Interestingly, resistant maize having HC-toxin reductase can transform HC-toxin **(2)** by reducing the carbonyl group in the Aeo residue (Johal and Briggs, 1992; Meeley and Walton, 1991). The host specificity of HC-toxin **(2)** was confirmed by observing HC-toxin reductase activity in cereal crops (e.g. barley, sorghum, oats) that are resistant to *C. carbonum* (Walton, 2006). Meeley and Walton reported that resistant maize reduced HC-toxin **(2)** to less toxic 8-hydroxy HC-toxin (**3**), where a NAD(P)H-dependent HC-reductase catalyzed this detoxification

(Meeley and Walton, 1991). Further investigation on detoxification of HC-toxin **(2)** and host susceptibility revealed that plants expressing HC-toxin reductase activity (**Scheme 1.1**) were resistant to *C. carbonum* (Meeley, Johal *et al.*, 1992). This is an example of detoxification of phytotoxins in which host plants acquire resistance to virulent isolates by transforming phytotoxins to less toxic metabolites.

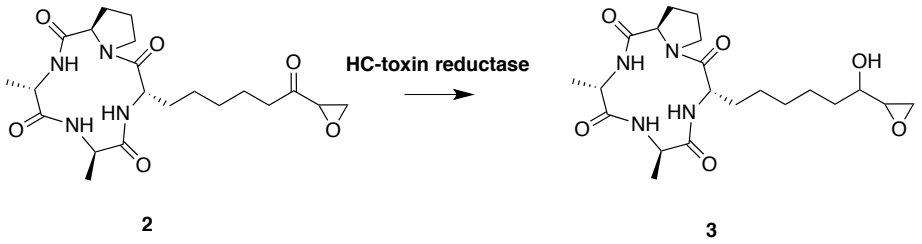

Scheme 1.1 Detoxification of HC-toxin (**2**) by resistant maize.

Albicidin **(4)** was first reported as a phytotoxin produced by *Xanthomonas albilineans* causing leaf scald disease of sugarcane (Birch and Patil, 1985). Strains that do not produce albicidin **(4)** fail to cause disease, whereas albicidin-producing strains cause disease in susceptible sugarcane. Albicidin **(4)** also showed antibacterial activity by inhibiting DNA replication in *Escherichia coli* at nanomolar concentrations (Birch and Patil, 1985). The complete structure of albicidin **(4)**, however, remained unknown for more than 30 years because the strain produced albicidin (**4**) in low amount. Cociancich *et al*., finally, elucidated the structure of albicidin **(4)** on the basis of HR-MS and NMR spectroscopic data; 1 mg of albicidin **(4)** was purified from 100 L cultures (Cociancich, Pesic *et al.*, 2015). Kretz *et al*. carried out the total synthesis of albicidin **(4)** and confirmed the structure (Kretz, Kerwat *et al.*, 2015).

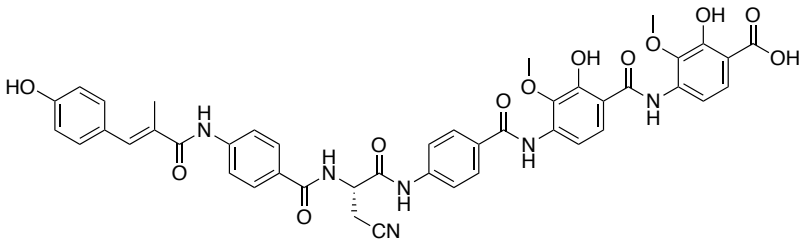

Zhang and Birch first reported that *Pantoea dispersa* (syn. *Erwinia herbicola*) detoxified albicidin (**4**) almost completely (Zhang and Birch, 1997a), and later on cloned and sequenced a gene (*albD*) responsible for enzymatic detoxification of albicidin (Zhang and Birch, 1997b). Zhang and Birch suggested that the gene (*albD*, albicidin hydrolase) could be transferred into sugarcane to confer disease resistance to susceptible sugarcanes (Zhang and Birch, 1997b). Zhang et al. reported that transgenic sugarcane harboring the *albD* gene showed no damage on infected leaves, whereas non-transgenic sugarcane showed severe disease symptoms (Zhang, Xu *et al.*, 1999).

It is worth noting that HC-toxin (**2**) and albicidin (**4**) are detoxified differently. That is, HC-toxin is detoxified by naturally resistant plants, whereas albicidin is detoxified by transgenic plants having a detoxification gene cloned from a bacterium. In both cases, one single gene is involved in detoxification of phytotoxins. Those two detoxification strategies are important to further develop crops resistant to devastating microbial pathogens.

Fusicoccin (**5**) is another example of a phytotoxin. Fusicoccin (**5**) is produced by *Fusicoccum amygdali* Del., the causal agent of drupe canker of almond trees (*Prunus amygdalus* St.) and peaches (Ballio, Chain *et al.*, 1964). The structure of fusicoccin **(5)**, elucidated by Ballio *et al*., is a diterpenoid containing a 5-8-5 ring structure (called fusicoccane) (Ballio, Brufani *et al.*, 1968). Unlike HSTs, fusicoccin **(5)** has been known as a non-host-selective toxin (NHST) and has been shown to display various biological activities such as opening leaf stomata, awaking seed dormancy, stimulating seed germination, inducing root formation and promoting cell enlargement (Ballio, 1991; Marre, 1979; Muromtsev, Voblikova *et al.*, 1994). Interestingly, fusicoccin **(5)** was isolated from peach pulp (ca. 5 mg/kg) and almond shoots (ca. 10 mg/kg) after infection with *F. amygdali* Del. (Ballio, D'Alessio *et al.*, 1976).

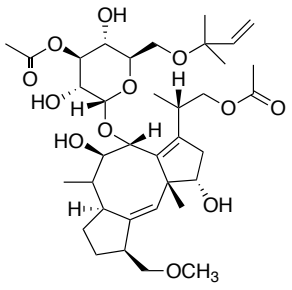

5

Phomalide (**6**) was first isolated from *Leptosphaeria maculans* [asexual stage of *Phoma lingam* (Tode ex Fr.) Desm.] and its chemical structure was elucidated by Pedras *et al*. (Pedras, Taylor *et al.*, 1993). Phomalide (**6**) is a depsipeptide, which contains both ester and amide bonds. Phomalide (**6**) exhibited phytotoxicity on *B. napus* cv. Westar (susceptible to *L. maculans*) but not on *B. juncea* cv. Cutlass (resistant to *L. maculans*) (Pedras and Biesenthal, 1998). Phomalide (**6**) was detected in leaf-extracts of *B. napus* after infection with *L. maculans/P. lingam* (Pedras and Biesenthal, 1998). Pedras *et al*. reported that phomalide (**6**) was detected in liquid cultures during the early stages of fungal growth (24–60h), and once sirodesmins (NHST) were produced in culture, the production of phomalide (**6**) was inhibited (Pedras, Taylor *et al.*, 1993). Pedras and Biesenthal also reported that prodution of phomalide (**6**) was not detected in cultures incubated with sirodesmin PL (**7**) (Pedras and Biesenthal, 1998). Elliott et al. reported that sirodesmin PL (**7**) was detected in extacts of stem and cotyledonary tissues of *B. napus* infected with *L. maculans/P. lingam* (Elliott, Gardiner *et al.*, 2007).

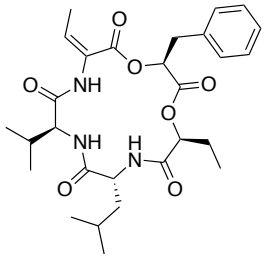

6

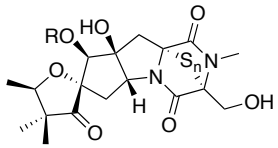

7

In general, phytotoxins are isolated from culture filtrates of phytopathogenic fungi. However, such phytotoxins are not always detected *in planta* after fungal infection. Detection of phytotoxins in infected plants can be strong evidence to establish the involvement of phytotoxins during infection. However, phytotoxins have not been detected in many cases, even though severe disease symptoms are observed in infected plant tissues. Since artificial conditions for fungal growth are different from natural environments, where fungi interact dynamically with plants, phytopathogenic fungi might not produce such phytotoxins *in vitro*. In addition, synergistic effects by multiple phytotoxins might cause plant disease symptoms. Detection of phytotoxins could be hindered by complex mixtures of plant metabolites produced in infected tissues. Furthermore, in some cases, metabolism of phytotoxins by plants or production in small quantities could prevent detection of phytotoxins *in planta* (Hohn, 1997).

1.2.2 Orphan pathways

During the past decades, whole-genome sequence projects of many microorganisms have been completed. As a result, it has become evident that there are genes encoding numerous metabolites that are not produced (Gross, 2007). Such metabolites belong to orphan biosynthetic pathways that are "*gene clusters for which the encoded natural product is unknown*"; thus, numerous metabolites present in orphan biosynthetic pathways await to be discovered (Gross, 2007). Many efforts to activate these cryptic or silent gene clusters particularly in microorganisms have been made; as a result, numerous metabolites have been reported (Brakhage, 2013; Brakhage and Schroeckh, 2011; Cichewicz, 2010; Gross, 2007; Höfs, Walker *et al.*, 2000; Scherlach and Hertweck, 2009; Strauss and Reyes-Dominguez, 2011; Wiemann and Keller, 2014). The following sections cover various strategies to activate silent and/or cryptic gene clusters encoding secondary metabolites.

1.2.2.1 Modification of culture conditions

Bode *et al*. proposed OSMAC (One Strain MAny Compounds) approach to activate cryptic or silent biosynthetic gene clusters by changing cultivation parameters such as media components, temperature, pH, aeration, light etc. (Bode, Bethe *et al.*, 2002). Simple modifications of cultivation parameters might induce a given organism to produce hidden metabolites. For example, *Aspergillus ochraceus* DSM7428 produced only one metabolite, named aspinonene (**8**); however, DSM7428 produced more metabolites (**8**–**21**) under different culture conditions (e.g., different culture vessels, fermenters, shaken or static cultures) (**Figure 1.1**). Newly characterized orphan metabolites are polyketides (**9**–**15**), and nonribosomal peptides (**16**–**18**) (Bode, Bethe *et al.*, 2002).

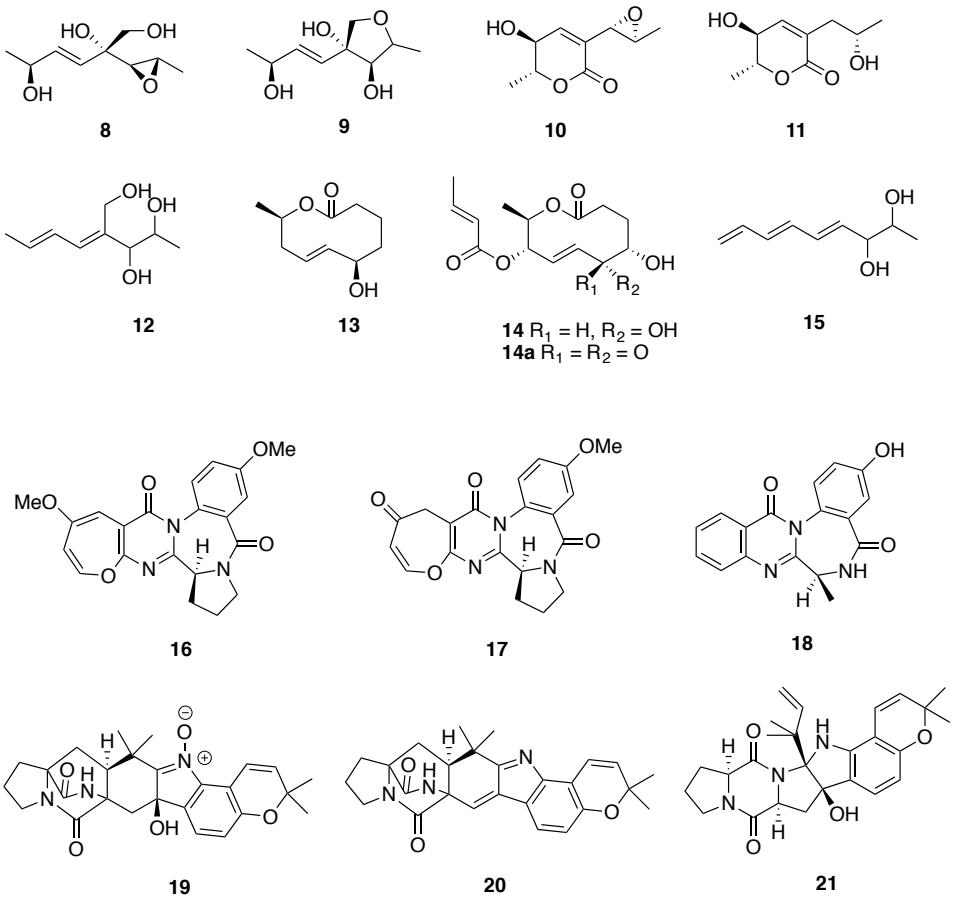

Figure 1.1 Secondary metabolites isolated from cultures of *Aspergillus ochraceus* grown under various culture conditions (Bode, Bethe *et al.*, 2002).

The phytopathogenic fungus *L. maculans* causes blackleg disease on crucifers. A systematic investigation of metabolites of *L. maculans* produced under various culture conditions was carried out (Pedras and Chumala, 2011; Pedras and Yu, 2008a, b, 2009b). Briefly, *L. maculans/P. lingam* produced phomalide (**6**), sirodesmin PL (**7**), deacetylsirodesmin PL (**7a**), sirodesmin H (**7b**), sirodesmin J (**7c**), sirodesmin, K (**7d**) and phomamide (**22**) in minimal medium (MM), components of which are chemically defined. *L. maculans* L2/M2 produced depsilairdin (**23**) a HST, polanrazine B (**24**), phomapyrone A (**25**), and phomalairdenone A (**26**)

in MM (**Figure 1.2**) (Pedras and Yu, 2009a). In potato dextrose broth (PDB) media, *L. maculans/P. lingam* produced maculansins A (**27**), B (**28**), and 2,4-dihydroxy-3,6-dimethylbenzaldehyde (**29**) (Pedras and Yu, 2008b). None of the previously reported metabolites (**6–7, 7a–7d, 22**) produced in MM were detected in PDB. Interestingly, maculansin A (**27**) was more toxic to *B. juncea* cv. Cutlass (resistant to *L. maculans*, susceptible to *A. brassicicola*) than to *B. napus* cv. Westar (susceptible to *L. maculans*). 2,4-Dihydroxy-3,6-dimethylbenzaldehyde (**29**) showed a strong inhibitory activity of root growth in *B. juncea* and *B. napus* (Pedras and Yu, 2008b). Furthermore, high NaCl concentration in MM induced production of 8-hydroxynaphthalene-1-sulfate (**30**) and bulgarein (**31, 31a**) in *L. maculans/P. lingam* cultures (Pedras and Yu, 2009b). Considering these metabolites associated with melanin biosynthesis, it was suggested that *L. maculans/P. lingam* produces those metabolites for self-protection in high salt. None of those metabolites (**30–31b**) exhibited phytotoxic activity or elicitor activity in crucifers (Pedras and Yu, 2009b).

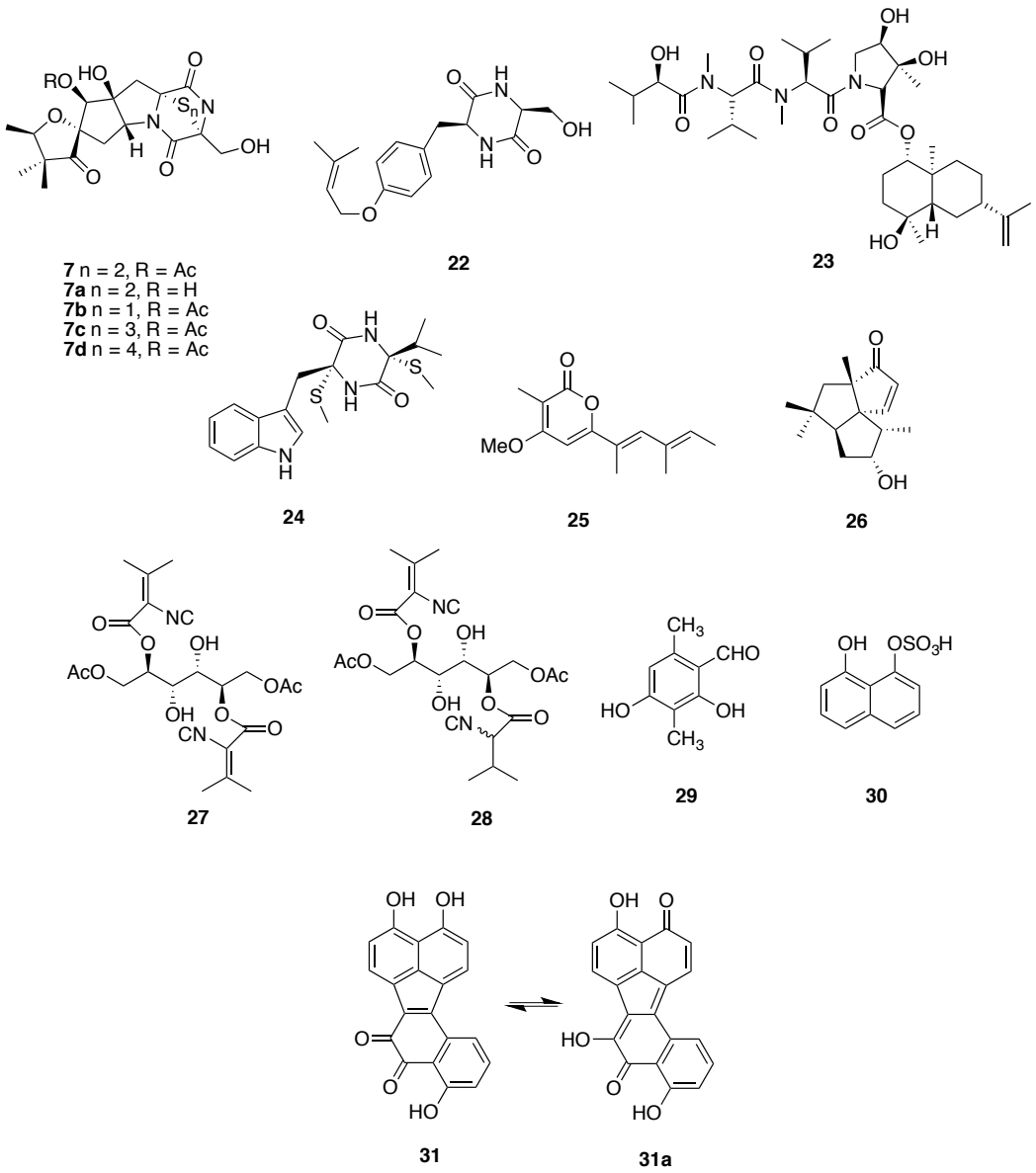

Figure 1.2 Secondary metabolites produced by *Leptosphaeria maculans/Phoma lingam* (Pedras and Chumala, 2011; Pedras and Yu, 2008a, b, 2009b).

1.2.2.2 Epigenetic modifiers

Epigenetics is "*the study of changes in gene functions that are mitotically and/or meiotically heritable and that do not entail a change in DNA sequence*" (Wu and Morris, 2001). From the viewpoint of natural product chemistry, epigenetic modifications including histone modification (i.e., acetylation, methylation, or phosphorylation of residues in histones) and DNA

methylation have led to discovery of various secondary metabolites in several species. Small molecules responsible for epigenetic modifications (**Figure 1.3**) have shown that inhibition of histone deacetylases (HDAC) or DNA methyltransferases (DNMT) activates silent or cryptic secondary metabolite gene clusters (Cichewicz, 2010). As an example, a study showed that in *Aspergillus niger*, more than 70% of polyketide synthase (PKS), non-ribosomal peptide synthetase (NRPS), and hybrid PKS-NRPS gene clusters were not expressed under general growth conditions (e.g., shake and static culture conditions). However, treatment with SAHA (**32**) and 5-Aza (**35**) led to substantial induction of many biosynthetic gene clusters (Fisch, Gillaspy *et al.*, 2009). As summarized in **Table 1**, epigenetic modifiers (**32–35**) have enabled the discovery of secondary metabolites in various species (**Figure 1.4**–**Figure 1.12**).

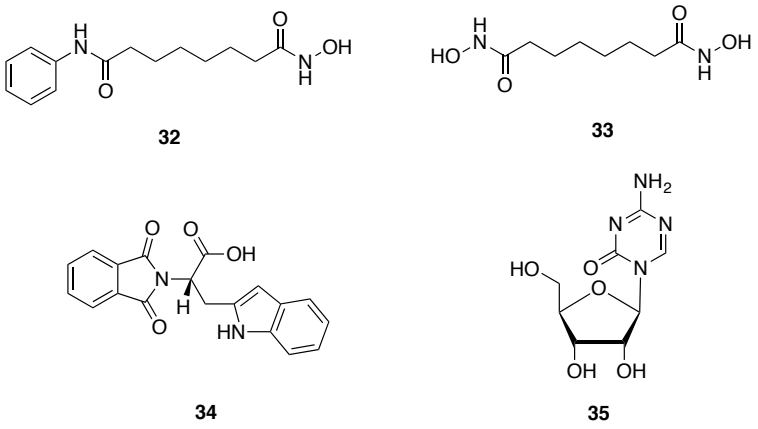

Figure 1.3 Chemical structures of representative epigenetic modifiers. HDAC inhibitors, SAHA (**32**), SBHA (**33**), RG-108 (**34**); DNMT inhibitor, 5-Aza (**35**).

Table 1 Selected secondary metabolites of terrestrial filamentous fungi and marine-derived fungi grown in the presence of epigenetic modifiers.

Classification	Name	Species	Modifier	References
PK	Indigotide A (**36**, 4.8 mg) Indigotide B (**37**, 1.3 mg)	*Cordyceps indigotica*	5-Aza (**35**, 0.1 mM)	(Asai, Yamamoto *et al.*, 2012a)
PK	Indigotide C (**38**, 5.6 mg) Indigotide D (**38a**, 2.3 mg) Indigotide E (**39**, 18.4 mg) Indigotide F (**40**, 9.2 mg) 13-Hydroxyindigotide A (**41**, 11.4 mg) 8-*O*-Methylindigotide B (**42**, 9.6 mg).	*Cordyceps indigotica*	SBHA (**33**, 1.0 mM)	(Asai, Yamamoto *et al.*, 2012b)
PK	Annullatin A (**43**, 12.3 mg) Annullatin B (**44**, 55.0 mg) Annullatin C (**44a**, 5.2 mg) Annullatin D (**45**, 5.8 mg) Annullatin E (**46**, 10.9 mg)	*Cordyceps annullata*	SBHA (**33**, 0.5 mM)	(Asai, Luo *et al.*, 2012)
PK	Chaetophenol A (**47**, 8.3 mg) Chaetophenol B (**48**, 35.3 mg) Chaetophenol C (**49**, 22.1 mg) Chaetophenol D (**50**, 2.8 mg), Chaetophenol E (**51**, 2.2 mg) Chaetophenol F (**52**, 22.7 mg)	*Chaetomium indicum*	SBHA (**33**, 0.5 mM)	(Asai, Yamamoto *et al.*, 2013)
PK	Daldinone E (**53**, 7.2 mg)	*Daldinia* sp.	SAHA (**32**,0.8 mM)	(Du, King *et al.*, 2014)
PK	Tenuipyrone (**54**, 1.2 mg)	*Isaria tenuipes*	SBHA (**33**, 0.5 mM), RG-108 (**34**, 0.5 mM)	(Asai, Chung *et al.*, 2012b)
Mixed	EGM-556 (**55**, 3.5 mg)	*Microascus* sp.	SAHA (**32**, 10 μM)	(Vervoort, Drašković *et al.*, 2011)
Mixed	Nygerone A (**56**, 1.9 mg)	*Aspergillus niger*	SAHA (**32**, 10 μM)	(Henrikson, Hoover *et al.*, 2009)

Classification	Name	Species	Modifier	References
Mixed	Luteoride A (**57**, 3.8 mg) Luteoride B (**58**, 1.2 mg) Luteoride C (**59**, 2.0 mg)	*Torrubiella luteorostrata*	SBHA (**33**, 1.0 mM)	(Asai, Yamamoto *et al.*, 2011)
Mixed	Desmethylisaridin E (**60**, 3.5 mg) Desmethylisaridin C2 (**61**, 2.5 mg) Isaridin F (**62**, 1.0 mg)	*Beauveria felina*	SAHA (**32**, 0.5 mM)	(Chung, El-Shazly *et al.*, 2013)
Mixed	12'-*O*-Acetylisariotin A (**63**, 50.4mg) 1-*epi*-Isariotin A (**64**, 6.3 mg) Isariotin K (**65**, 14.4 mg) Isariotin L (**66**, 29.4 mg) Isariotin M (**67**, 6.3 mg) Formosterol A (**68**, 22.4 mg) Formosterol B (**69**, 5.6 mg)	*Gibellula formosana*	SBHA (**33**, 1.0 mM), RG-108 (**34**, 1.0 mM)	(Asai, Chung *et al.*, 2012a)
Mixed	(7*S*)-(+)-7-*O*-Methylsydonol (**70**, 18.9 mg) (7*S*,11*S*)-(+)-12-Hydroxysydonic acid (**70a**, 3.1 mg) 7-Deoxy-7,14-didehydrosydonol (**71**, 2.1 mg)	*Aspergillus sydowii*	5-Aza (**35**, 0.1 mM)	(Chung, Wei *et al.*, 2013)
Mixed	Sclerotiorin (**72**, 2 mg) Sclerotioramine (**72a**, 27 mg) Ochrephilone (**73**, 1 mg) Dechloroisochromophilone III (**74**, 1mg) Dechloroisochromophilone IV (**74a**, 1 mg) 6-((3*E*,5*E*)-5,7-Dimethyl-2-methylenenona-3,5-dienyl)-2,4-dihydroxy-3- methylbenzaldehyde (**75**, 1mg) Pencolide (**76**, 40 mg), Atlantinone A (**77**, 7 mg) Atlantinone B (**78**, 3 mg)	*Penicillium citreonigrum*	5-Aza (**35**, 0.05 mM)	(Wang, Sena Filho *et al.*, 2010)

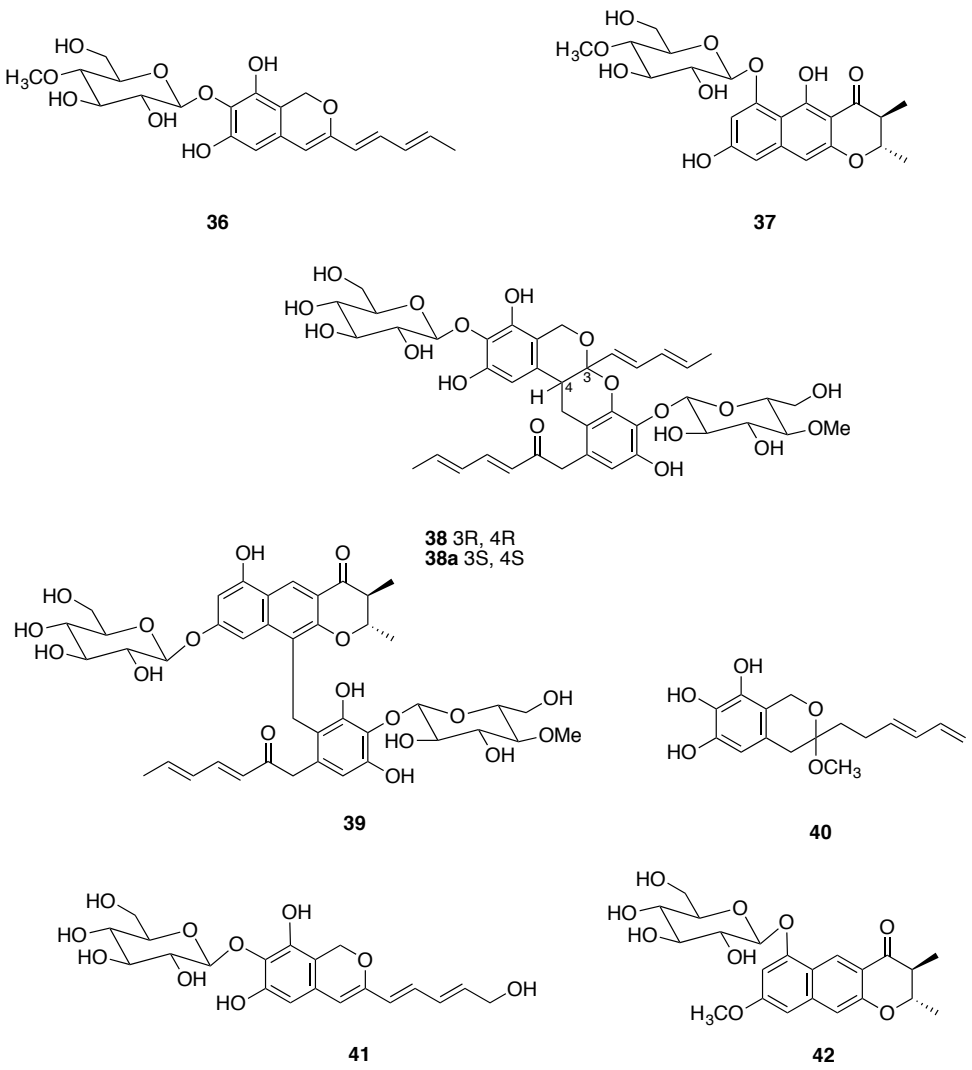

Figure 1.4 Metabolites of *Cordyceps indigotica* induced by SBHA (**33**) and 5-Aza (**35**) (Asai, Yamamoto *et al.*, 2012a; Asai, Yamamoto *et al.*, 2012b).

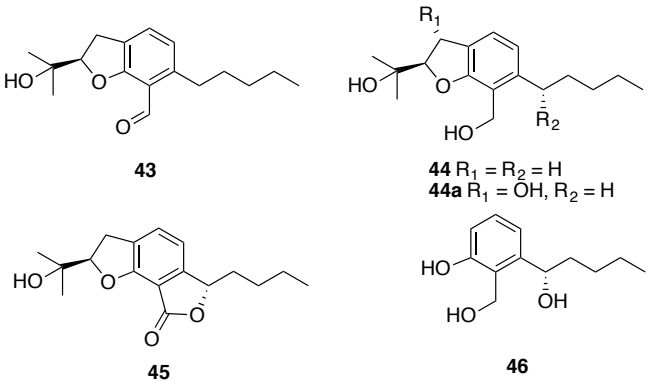

Figure 1.5 Metabolites of *Cordyceps annullata* induced by SBHA (**33**) (Asai, Luo *et al.*, 2012).

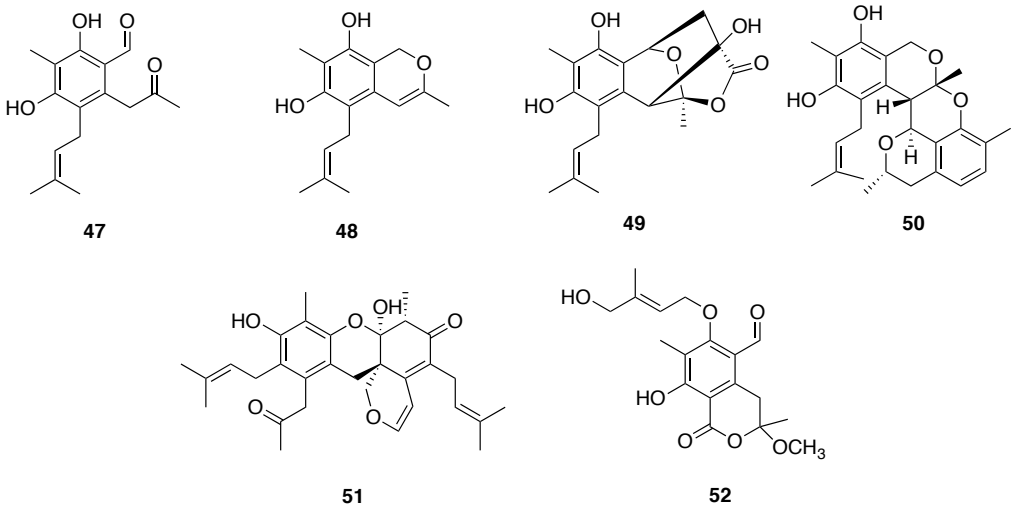

Figure 1.6 Metabolites of *Chaetomium indicum* induced by SBHA (**33**) (Asai, Yamamoto *et al.*, 2013).

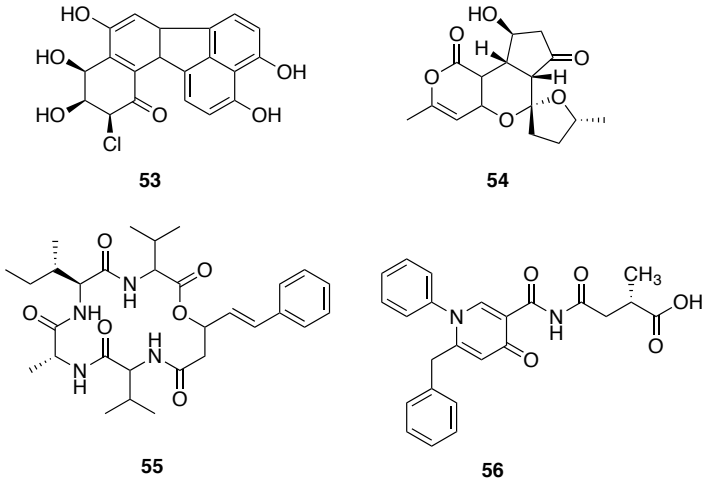

Figure 1.7 Metabolites induced by epigenetic modifiers; Daldinone E (**53**) (Du, King *et al.*, 2014), tenuipyrone (**54**) (Asai, Chung *et al.*, 2012b), EGM-556 (**55**) (Vervoort, Drašković *et al.*, 2011), nygerone A (**56**) (Henrikson, Hoover *et al.*, 2009).

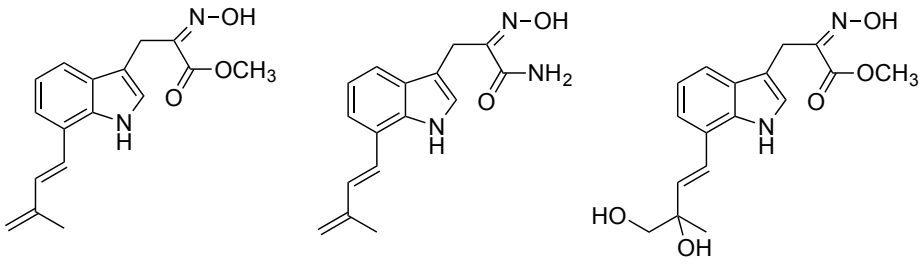

Figure 1.8 Metabolites of *Torrubiella luteorostrata* induced by SBHA (**33**) (Asai, Yamamoto *et al.*, 2011).

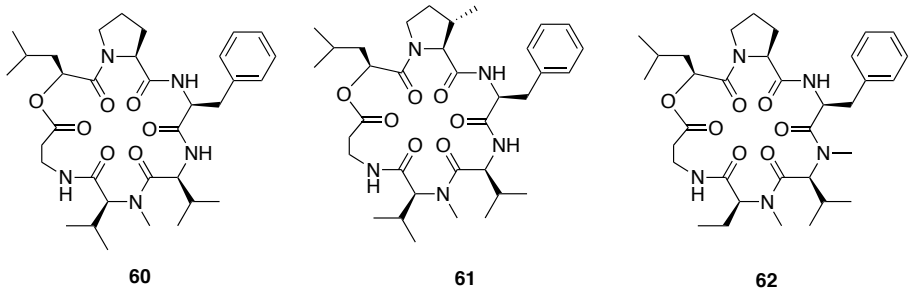

Figure 1.9 Metabolites of *Beauveria felina* induced by SAHA (**32**) (Chung, El-Shazly *et al.*, 2013).

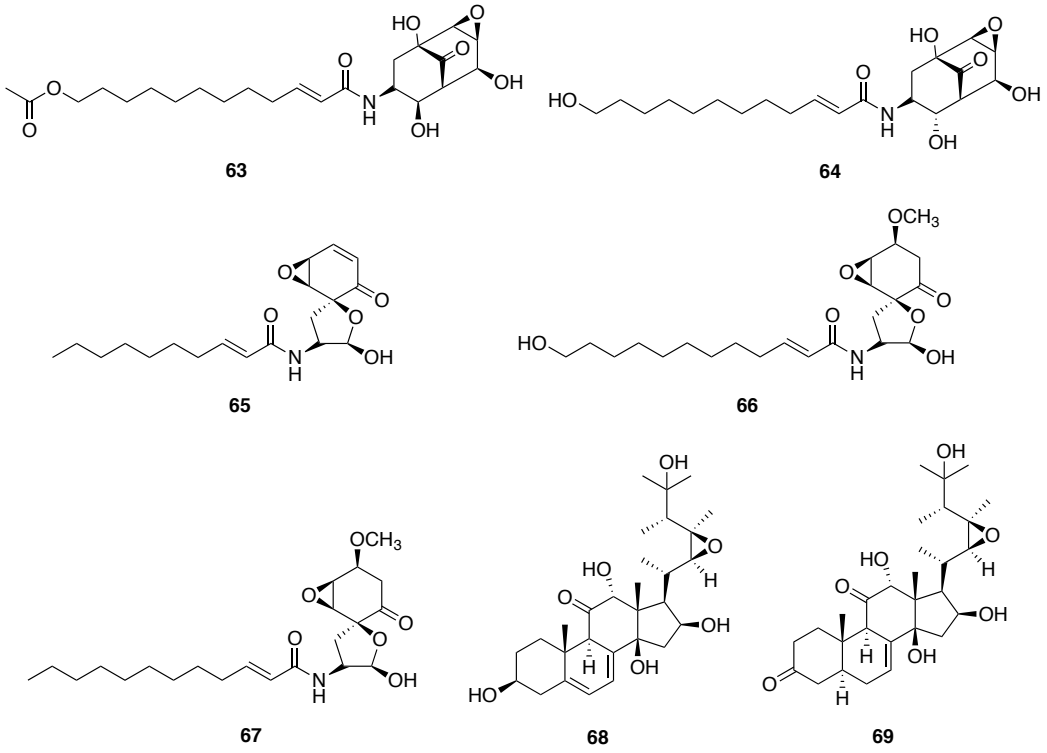

Figure 1.10 Metabolites of *Gibellula formosana* induced by SBHA (**33**) and RG-108 (**34**) (Asai, Chung *et al.*, 2012a).

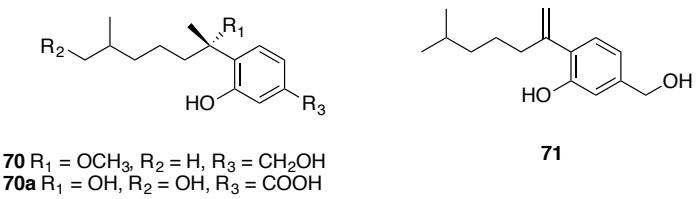

70 R_1 = OCH_3, R_2 = H, R_3 = CH_2OH
70a R_1 = OH, R_2 = OH, R_3 = COOH

71

Figure 1.11 Metabolites of *Aspergillus sydowii* induced by SAHA (**32**) (Chung, Wei *et al.*, 2013).

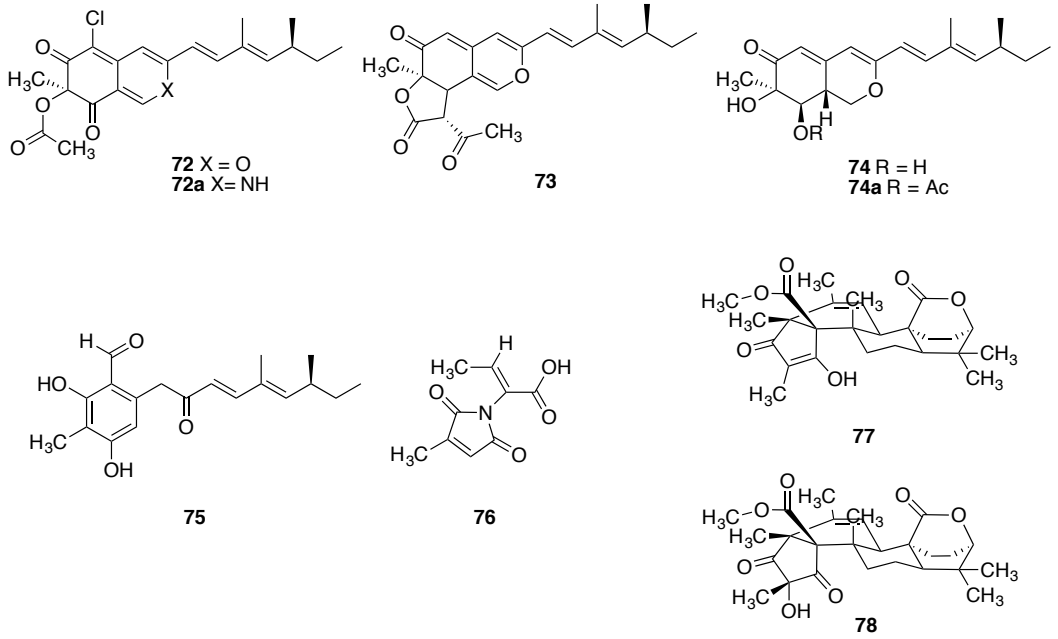

72 X = O
72a X= NH

73

74 R = H
74a R = Ac

75

76

77

78

Figure 1.12 Metabolites of *Aspergillus sydowii* induced by 5-Aza (**35**) (Wang, Sena Filho *et al.*, 2010).

1.2.2.3 Co-cultivation

Numerous secondary metabolites have been isolated from shake or static cultures that are prepared with sufficient nutrient components; however, such conditions are not comparable to natural environments. Media to grow single cells of microorganisms are prepared in sterile conditions to prevent unwanted contamination by other microorganisms. The sterile growth conditions might not reflect the complex natural environments in which chemical interactions between a given organism and its neighboring organisms occur. In addition, microorganisms

cultivated in artificial media might not biosynthesize secondary metabolites that are exclusively produced due to interactions with other organisms. Thus, co-cultivation of a given microorganism with one or multiple antagonists could be a way to mimic complex natural environments. For example, co-cultivation of *A. nidulans* with soil bacteria (actinomycetes) led to activation of cryptic gene clusters encoding orsellinic acid (**79**), lecanoric acid (**80**), and two phenolic compounds (**81** and **82**) (Schroeckh, Scherlach *et al.*, 2009). In addition, novel prenylated polyketides (**83** and **84**) were isolated from *A. fumigatus* culture filtrates after co-culturing with *Streptomyces rapamycinicus* (König, Scherlach *et al.*, 2013).

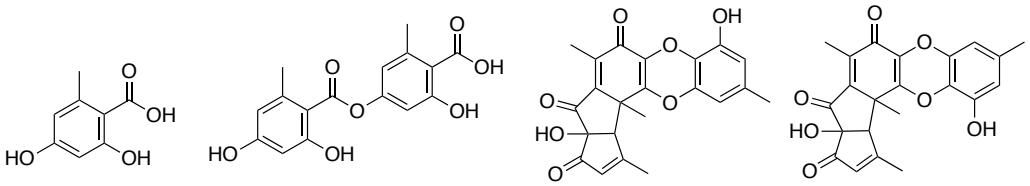

79 **80** **81** **82**

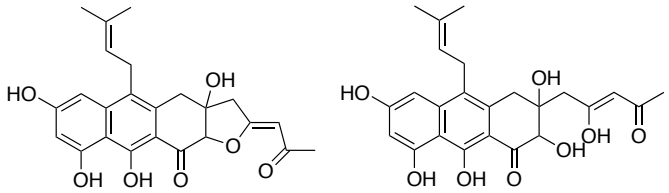

83 **84**

Co-cultivation of *Alternaria* species with other species led to the discovery of metabolites. The endophytic fungus, *A. tenuissima*, was cultivated with *Nigrospora sphaerica*, another endophytic fungus, leading to induction of two polyketides (**85** and **86**) in co-culture extracts (Chagas, Dias *et al.*, 2013). Neither *A. tenuissima* nor *N. sphaerica* produced stemphyperylenol (**85). T**he production of alterperylenol (**86)** was increased when they are co-cultured. Interestingly, stemphyperylenol (**85**) showed antifungal activity against *N. sphaerica* at 0.2 mM, while a 10-fold higher concentration did not cause phytotoxicity in the host plant (*Smallanthus sonchifolius*). Stemphyperylenol (**85)** might play an important role in maintaining ecological relationships between endophyte-endophyte and endophyte-plant (Chagas, Dias *et al.*, 2013). A review addressing microbial interactions that increased the chemodiversity of metabolites produced in co-cultures has been published recently (Bertrand, Bohni *et al.*, 2014).

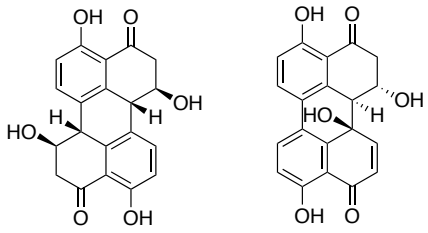

85 86

1.2.3 Chemistry of phytopathogenic *Alternaria* species

In general, *Alternaria* species infect aerial parts of host plants, and produce metabolites including phytotoxins to facilitate infection processes. *Alternaria* species cause economically important diseases in various oilseed and horticultured crops, fruits, and cereals (Thomma, 2003).

1.2.3.1 Secondary metabolites produced by *Alternaria* species

A comprehensive review was published in 2013 regarding metabolites (more than 268 metabolites covered from 1965 to 2013) of *Alternaria* species and their biological activities. In this article, more than 268 metabolites (covered from 1965 to 2013) produced by *Alternaria* species were reviewed (Lou, Fu *et al.*, 2013) (**Table 2**). More recently reported (2014–2015) secondary metabolites produced by *Alternaria* species are summarized in **Table 3**.

Table 2 Structural types of secondary metabolites produced by *Alternaria* species (Lou, Fu *et al.*, 2013).

Class	Number
Alkaloids	61
Cyclopeptides	22
Steroids	7
Terpenoids	49
Pyranones	56
Quinones	45
Phenolics	38
Miscellaneous	12

Table 3 Secondary metabolites of *Alternaria* species.

Metabolites[a]	***Alternaria* species**	**Biological activity**	**References**
5-Butyl-4-methoxy-6-methyl-2*H*-pyran-2-one (**87**, 17 mg) 5-Butyl-6-(hydroxymethyl)-4-methoxy- 2*H*-pyran-2-one (**87a**, 12.4 mg) 5-(1-hydroxybutyl)-4-methoxy-6-methyl-2*H*-pyran-2-one (**87b**, 4.2 mg) 4-methoxy-6- methyl-5-(3-oxobutyl)-2*H*-pyran-2-one (**87c**, 2.6mg)	*Alternaria phragmospora*	Antileukemic activity; HL60 cells (IC_{50}) **87a**, 0.45 μg/mL **87c**, 0.18 μg/mL	(Metwaly, Fronczek *et al.*, 2014)
(+)-1-[(+)- (2*S*, 3*S*, 4a*S*)-Altenuene-2-acetoxy ester] ((+)-**88**, 3.7 mg) (−)-1-[(−)-(2*R*, 3*R*, 4a*R*)-Altenuene-2-acetoxy ester] ((−)-**88**, 0.9mg) (+)-2-[(+)-(2*S*, 3*S*, 4a*S*)- Altenuene-3-acetoxy ester] ((+)-**89**, 1.5 mg) (−)-2-[(−)-(2*R*, 3*R*, 4a*R*)- Altenuene-3-acetoxy ester] ((−)-**89**, 1.2 mg) (+)-(10*R*)-7-Hydroxy-3-(2-hydroxy-propyl)-5,6-dimethyl-isochromen-1-one (**90**, 0.7 mg)	*Alternaria alternata*	Antibacterial activity (IC_{80}) *Staphylococcus aureus* (+)-**88**, 17.1 ± 1.2 μg/mL (−)-**88**, 15.4 ± 1.1 μg/mL (−)-**89**, 45.0 ± 1.7 μg/mL *Candida albicans* (+)-**89**, 24.0 ± 1.0 μg/mL *Bacillus subtilis* **90**, 19.7 ± 1.0 μg/mL	(Wang, Yang *et al.*, 2014)
2-*O*-Methylalternariol 4-*O*-β-[4-methoxyl-glucopyranoside] (**91**, 4.5 mg)	*Alternaria alternate*cib-137	N/A [b]	(Xu, Pu *et al.*, 2015)
Deoxyphomalone (**92**) Dimethyl 4-methyl-2,6-pyridinedicarboxylate (**93**) Stemphyperylenol (**85**) *N*-Methyl-2-pyrrolidone (**94**)	*Alternaria tenuissima*	N/A [b]	(Anyanwu and Sorensen, 2015)
Solanapyrone P (**95**, 1.6 mg) Solanapyrone Q (**96**, 0.6mg) Solanapyrone R (**97**, 0.8 mg)	*Alternaria tenuissima* SP-07	N/A [b]	(Wang, Luo *et al.*, 2014)
Altertoxin V (**98**, 3.1 mg) Altertoxin VI (**99**, 3.7 mg)	*Alternaria tenuissima* QUE1Se	Anti-HIV activity (IC_{50}) **98**, 0.09 μM,	(Bashyal, Wellensiek *et al.*, 2014)

Metabolites[a]	*Alternaria* species	Biological activity	References
6-Methoxy-3,6a,7,10-tetrahydroxy-4,9-dioxo-4,5,6,6a,6b,7,8,9-octa- hydroperylene (**100**, 6 mg) 3,6a,9,10-Tetrahydroxy-7,8-epoxy-4-oxo-4,5,6,6a,6b,7,8,9-octahydroperylene (**101**, 10 mg) 6-Methoxy-3,6a,9,10-tetrahydroxy-7,8-epoxy-4-oxo-4,5,6,6a,6b,7,8,9-octahydroperylene (**102**, 7 mg)	*Alternaria* sp. DC401	Antimalarial activity (IC_{50}) **102**, 3.2 μg/mL Cytotoxicity **102**, 4.4 μg/mL Antileishmanial activity (IC_{50}) **100**, 3.1 μg/mL **102**, 1.4 μg/mL	(Idris, Tantry *et al.*, 2015)
Tricycloalternarene I (**103**, 5 mg) Tricycloalternarene J (**104**, 3 mg)	*Alternaria* sp.	N/A[b]	(Shi, Wei *et al.*, 2015)
Altersolanol O (**105**, 2.4 mg) Altersolanol S (**106**, 2.0 mg) Altersolanol T (**107**, 22 mg) Altersolanol V (**108**, 16 mg)	Alternaria sp. XZSBG-1	Inhibition of α-glucosidase (Du, Liu *et al.*, 2006) (IC_{50}) **107**, 7.2 μM,	(Chen, Shen *et al.*, 2014)
Polluxochrin (**109**, 8.0 mg) Dioschrin (**110**, 7.5 mg), Castochrin (**111**) Pyrenochaetic acid D (**112**, 15 mg) Pyrenochaetic acid E (**112a**, 2.5 mg) Pyrenochaetic acid F (**112b**, 2.8 mg) Pyrenochaetic acid G (**113**, 3.0 mg) Pyrenochaetic acid H (**114**, 2.3 mg) Dimethylamide asterrate (**115**, 6.5 mg) Blennolide G (**116**, 4.0 mg) Blennolide H (**117**, 5.1 mg) Blennolide J (**118**, 5.0 mg)	*Alternaria* sp.	Methicillin-resistant *S. aureus* (MRSA) activity, MIC **116**, 2.9 μg/mL **117**, 3.2 μg/mL **118**, 2.0 μg/mL	(Cai, King *et al.*, 2014)

[a] Secondary metabolites of *Alternaria* species reported from 2014 to 2015.

[b] N/A = Data on bioassays are not available.

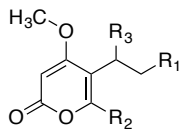

87 $R_1 = CH_2CH_3$, $R_2 = CH_3$, $R_3 = H$
87a $R_1 = CH_2CH_3$, $R_2 = CH_2OH$, $R_3 = H$
87b $R_1 = CH_2CH_3$, $R_2 = CH_3$, $R_3 = OH$
87c $R_1 = C(O)CH_3$, $R_2 = CH_3$, $R_3 = H$

Figure 1.13 Metabolites isolated from *Alternaria phragmospora* (Metwaly, Fronczek *et al.*, 2014).

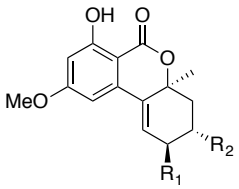

(+)-**88** R_1 = OAc R_2 = OH
(+)-**89** R_1 = OH R_2 = OAc

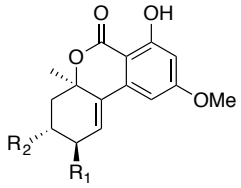

(-)-**88** R_1 = OAc R_2 = OH
(-)-**89** R_1 = OH R_2 = OAc

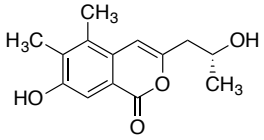

90

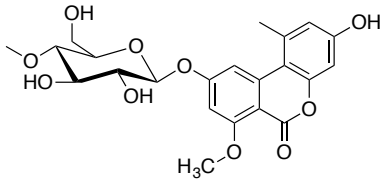

91

Figure 1.14 Metabolites isolated from *Alternaria alternata* (Wang, Yang *et al.*, 2014; Xu, Pu *et al.*, 2015).

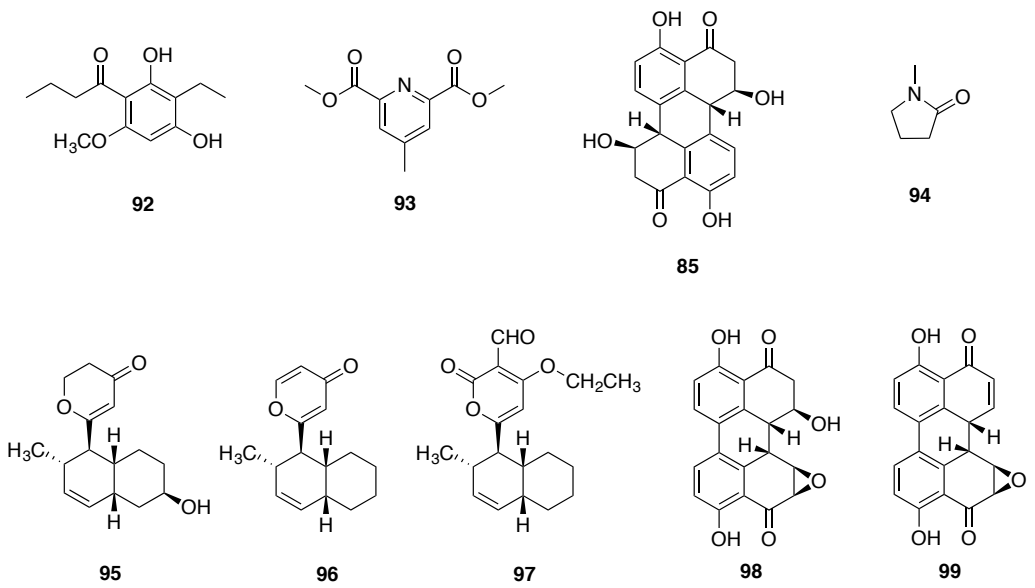

Figure 1.15 Metabolites isolated from *Alternaria tenuissima* (Anyanwu and Sorensen, 2015; Bashyal, Wellensiek *et al.*, 2014; Wang, Luo *et al.*, 2014).

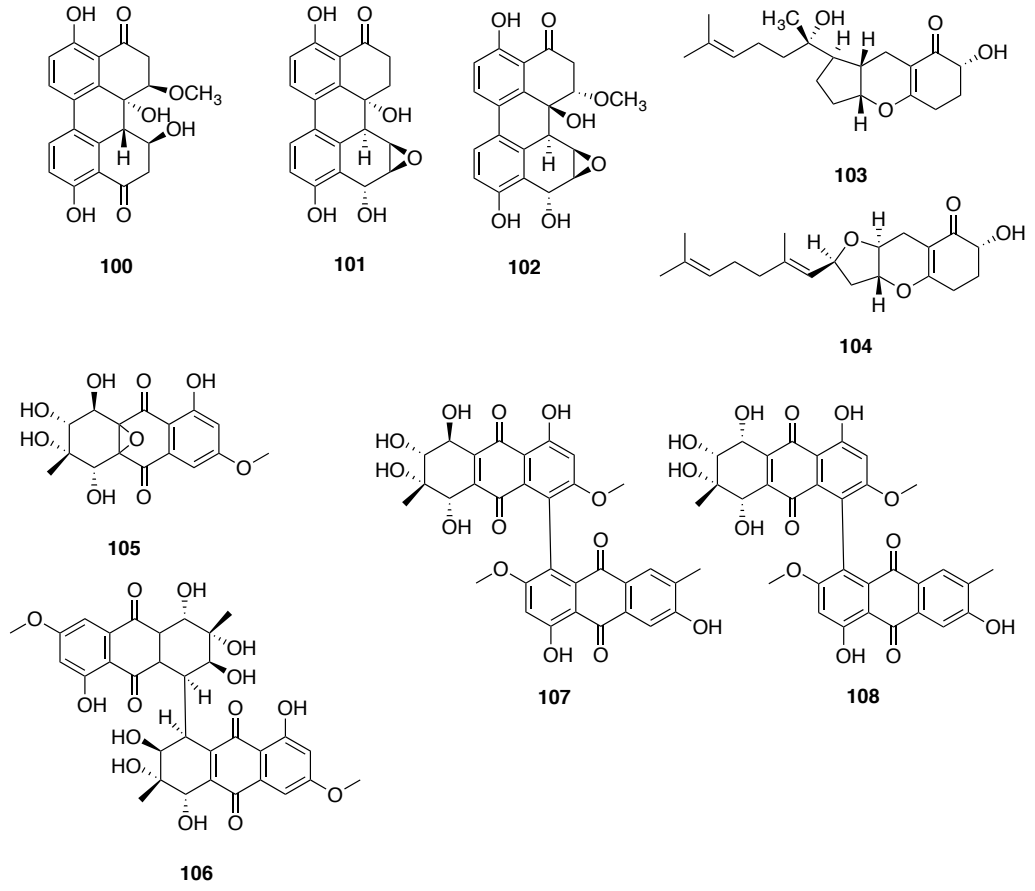

Figure 1.16 Metabolites isolated from *Alternaria* species (Chen, Shen *et al.*, 2014; Idris, Tantry *et al.*, 2015; Shi, Wei *et al.*, 2015).

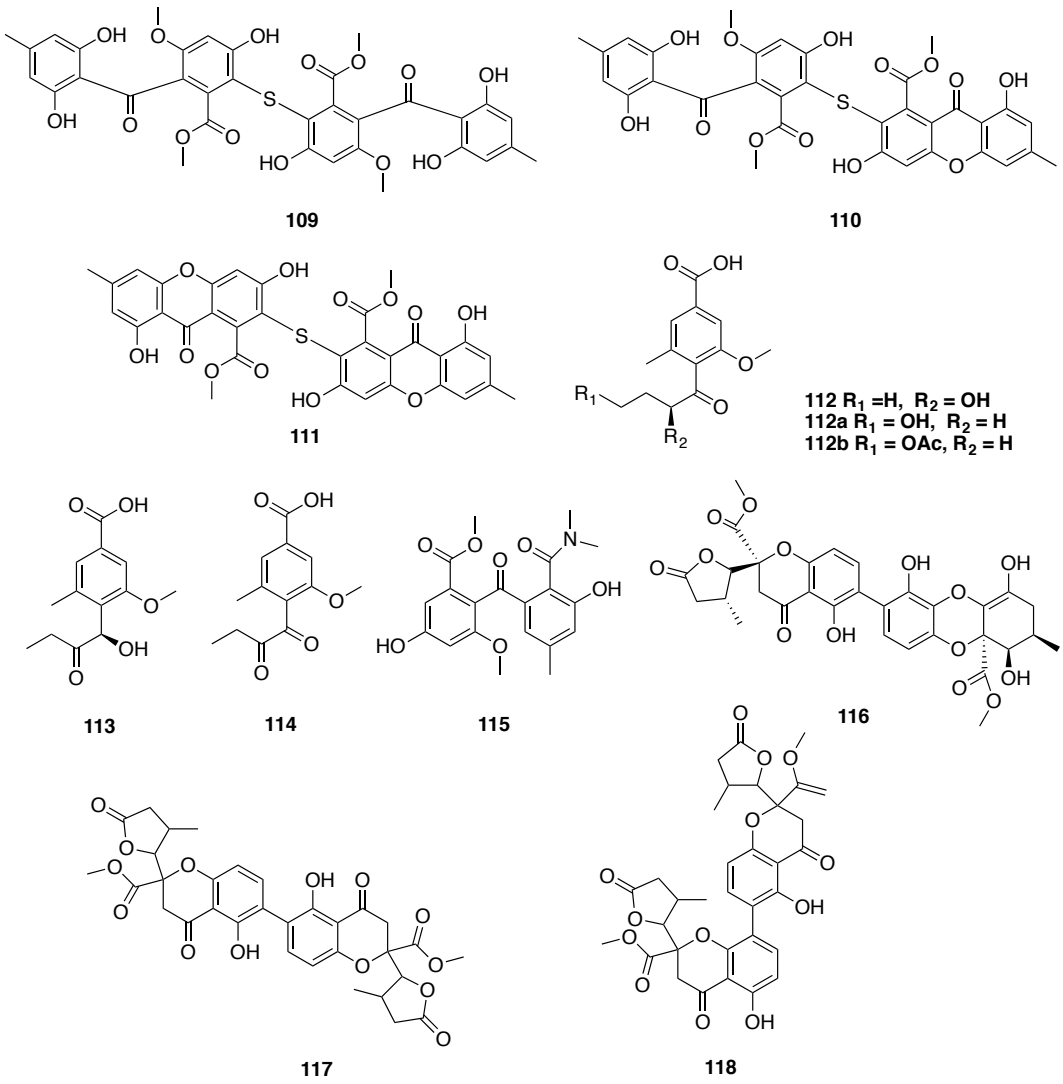

Figure 1.17 Metabolites isolated from *Alternaria* species (Cai, King *et al.*, 2014).

1.2.3.2 Phytotoxins produced in culture and *in planta*

1.2.3.2.1 Host-selective toxins

Host-selective toxins (HST) are usually defined as low-molecular-weight metabolites produced by plant pathogens that damage (e.g. necrosis, chlorosis, wilting, water-soaking symptoms) susceptible plants. More recently, several studies have shown that protein toxins produced in spore germination fluids (SGFs) also cause disease symptoms in susceptible plants (Akimitsu, Tsuge *et al.*, 2014). In general, the HST-producing isolates cause disease, whereas the non-producing isolates fail to cause disease. HSTs produced by *Alternaria* species have been reviewed (Akimitsu, Tsuge *et al.*, 2014; Tsuge, Harimoto *et al.*, 2013). To date, more than 20 HSTs have been isolated and characterized. Several examples of *Alternaria* HSTs of fruits (e.g., strawberry, tangerine, or apple) and crops (e.g., crucifers) are described below.

Structurally, AK toxins (**119** and **119a**) have a 9,10-epoxy-8-hydroxy-9-methyldecatrienoic acid (EDA) moiety connected with an *N*-acetyl-β-methyl-phenylalanyl moiety through an ester linkage. AF- and ACT-toxins also contain EDA. AF toxins are produced by *A. alternata* strawberry pathotype. The AF toxin producer biosynthesizes three AF toxins (**120, 120a,** and **120b**), where the AF toxin I (**120**) is a major component (Hayashi, 1990; Maekawa, Yamamoto *et al.*, 1984). The structure of AF toxin II (**120a**) was first elucidated by Nakatsuka *et al*. (Nakatsuka, Ueda *et al.*, 1986), while the structures of the other toxins were determined by 2'-*O*-acyl derivatization of AF toxin II (**120a**). Furthermore, 2'-*O*-acyl derivatives of AF toxin II (e.g., acetyl, propionyl, or isovaleryl) exhibited phytotoxicity in both strawberries and pears, whereas AF toxin II (**120a**) was toxic to strawberries (Tsuge, Harimoto *et al.*, 2013).

ACT toxins (named ACT I **121**, and II **121a**) were isolated from culture filtrates of *A. alternata* tangerine pathotype (Kohmoto, Itoh *et al.*, 1993). ACT toxin I (**121**) is a major component of SGFs of *A. alternata* tangerine pathotype. ACT-toxin I (**121**) exhibited phytotoxicity on *Citrus reticulata* Blanco (Emperor mandarin) at 20 nM, whereas a 10^4-fold increase in ACT-toxin I (**121**) did not affect resistant citrus or Japanese pear (Kohmoto, Itoh *et al.*, 1993).

AM toxins (**122, 122a,** and **122b**) are produced by the apple pathotype of *A. alternata*, the chemical structures of which were elucidated as a cyclic tetrapeptide consisting of L-α-hydroxy-isovaleric acid, L-alanine, α-amino acrylic acid, and l-α-amino(methoxyphenyl)valeric acid (Ueno, Nakashima *et al.*, 1975b). AM toxins I (**122**, 0.002 μg/mL) and III (**122b,** 0.010

μg/mL) caused necrosis on leaves of susceptible cultivars, whereas resistant cultivars did not show necrosis at 200 μg/mL of **122** and 10 μg/mL of **122b**, respectively. The biological activity of AM toxin II (**122a**) is unknown (Ueno, Hayashi *et al.*, 1975; Ueno, Nakashima *et al.*, 1975a).

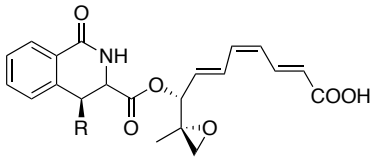

119 R = CH_3
119a R = H

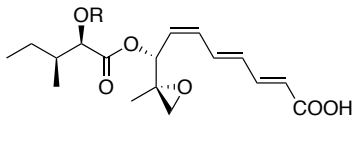

120 R =C(O)CH(OH)$C(CH_3)_2$OH
120a R = H
120b R = C(O)CH(OH)$CH(CH_3)_2$

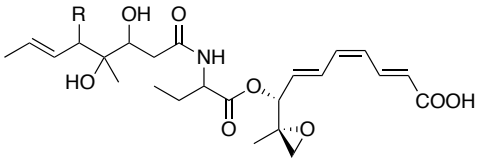

121 R = OH
121a R = H

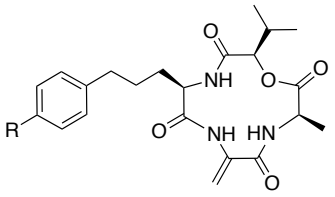

122 R = OCH_3
122a R = H
122b R = OH

Destruxin B (**123**) was first isolated from *Oospora destructor* (Metch.) Delac., (Kodaira, 1962) and the chemical structure of destruxin B (**123**) was elucidated (Païs, Das *et al.*, 1981). Destruxin B (**123**) was reported as a host-selective toxin produced by *Alternaria brassicae* (Berkeley) Saccardo (Ayer and Peña-Rodriguez, 1987).

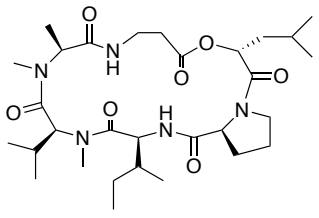

123

Destruxin B (**123**) was found to cause severe toxicity in *B. campestris* cv. Yellow Sarson, and Toria, whereas *B. campestris* cv. Candle showed mild symptom. Considering sensitivity to destruxin B (**123**) and susceptibility to *A. brassicae*, Bains and Tewari first proposed that destruxin B (**123**) is a host-selective toxin (Bains and Tewari, 1987). Furthermore, Buchwaldt and Green insisted that destruxin B (**123**) should be regarded as a host-selective toxin based upon

observations that *Brassica* species are most sensitive to the toxin **123**, whereas the taxonomically far-distant plants from *Brassica* species are much less sensitive (Buchwaldt and Green, 1992).

Evidence of detoxification of destruxin B (**123**) by susceptible or resistant plants supports that destruxin B (**123**) is a host-selective toxin. Biotransformation of destruxin B (**123**) occurred with hydroxylation followed by glycosylation; *S. alba* (resistant) metabolized destruxin B (**123**) to hydroxydestruxin B (**124**) substantially faster than susceptible *Brassica* species. On the other hand, *B. napus* (susceptible) transformed hydroxydestruxin B (**124**) to β-D-glucosyl hydroxydestruxin B (**125**) substantially faster than *S. alba* (resistant) (**Scheme 1.2**). Furthermore, hydroxydestruxin B (**124**) induced production of phytoalexins (e.g., sinalexin and sinalbin A) in *S. alba*, whereas no phytoalexins were detected in susceptible *Brassica* species. On the basis of these observations, Pedras *et al.* suggested that *S. alba* (resistant) can overcome fungal pathogen attack through detoxification of destruxin B (**123**) as well as production of phytoalexins (Pedras, Zaharia *et al.*, 2001). Furthermore, *Camelina sativa* and *Capsella bursa-pastoris* also detoxified hydroxydestruxin B (**124)** to non-toxic hydroxydestruxin B glucoside (**125**) and 6-*O*-malonylhydroxydestruxin-β-D-glucopyranoside (**126**) (Pedras, Montaut *et al.*, 2003).

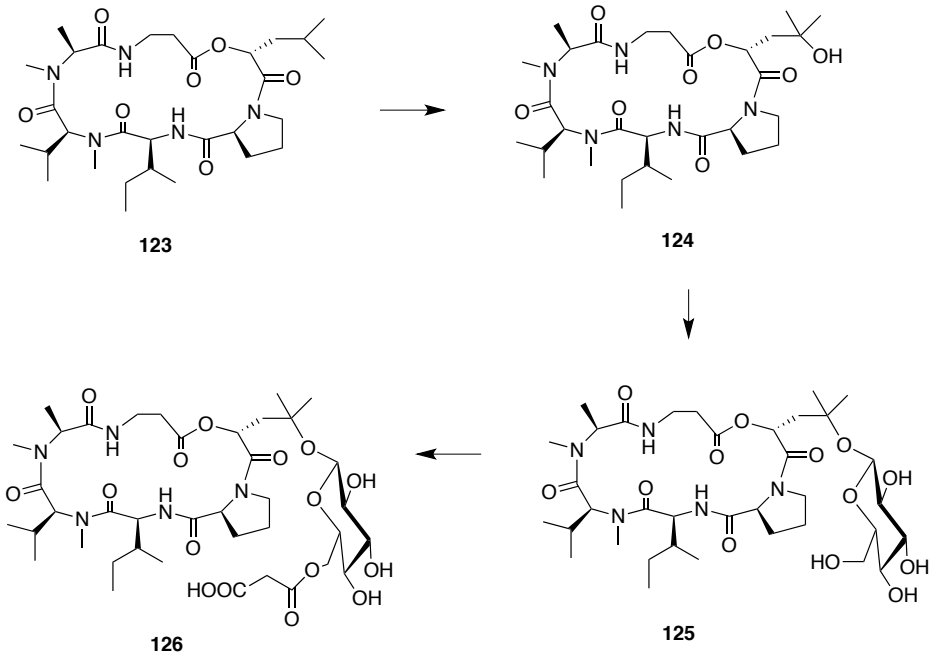

Scheme 1.2 Biotransformation of destruxin B (**123**) in crucifers (Pedras, Montaut *et al.*, 2003; Pedras, Zaharia *et al.*, 2001).

Pedras and Khallaf carried out studies on detoxification of destruxin B (**123**) using crucifers and cereal crops (Pedras and Khallaf, 2012). It was reported that *A. thaliana*, *Thellungiella salsuginea*, *Erucastrum gallicum*, *B. rapa* and *B. napus* transformed destruxin B (**123**) to hydroxydestruxin B (**124**), whereas cereals *Avena sativa* and *Triticum aestivum* transformed it to hydroxydestruxin B (**124**), dehydrodestruxin B (**127**/**127a**), and desmethyldestruxin B (**128**). Furthermore, phytoalexins were elicited by destruxin B (**123**) in *A. thaliana*, *T. salsuginea*, and *E. gallicum*, whereas no phytoalexins were detected in *B. rapa*, *B. napus, A. sativa* and *T. aestivum.* They suggested that in detoxifying destruxin B (**123**), the tested crucifers appear to have destruxin B hydrolase, while in cases of cereals, multiple enzymatic reactions are likely to be involved (Pedras and Khallaf, 2012).

Four analogs of destruxin B—desmethyldestruxin B (**128**), homodestruxin B (**129**), hydroxyhomodestruxin B (**129a**), hydroxydestruxin B (**124**)—were investigated for a structure-phytotoxic activity relationship. In leaves of *S. alba* cv. Ochre, destruxin B (**123**), and homodestruxin B (**129**) are converted to hydroxydestruxin B (**124**), and hydroxyhomodestruxin B (**129a**), respectively (Pedras, Zaharia *et al.*, 1999). Cell suspension culture assays of *S. alba* cv. Ochre (resistant) revealed that homodestruxin B (**129**, $EC_{50} = 3\times10^{-4}$ M) showed the most toxicity followed by destruxin B (**122**) and desmethyldestruxin B (**128**), whereas the phytotoxicity of hydroxylated destruxins was significantly decreased compared to the parent compounds (Pedras, Biesenthal *et al.*, 2000). A comprehensive review on destruxins was published (Pedras, Irina Zaharia *et al.*, 2002).

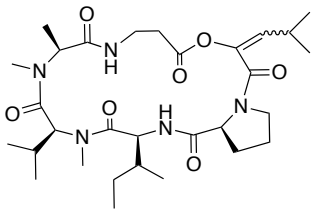

127

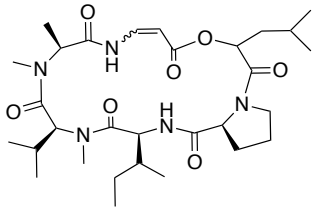

127a

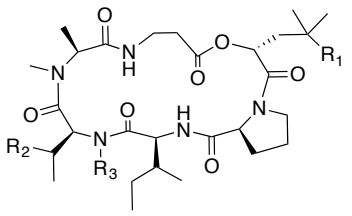

128 R_1 = H, R_2 = CH_3, R_3 = H
129 R_1 = H, R_2 = CH_2CH_3, R_3 = CH_3
129a R_1 = OH, R_2 = CH_2CH_3, R_3 = CH_3

1.2.3.2.2 Non-host-selective toxins

Non-host-selective toxins exhibit phytotoxicity against a broad spectrum of plants. While many studies on host-selective toxins have been reported, relatively fewer studies on non-host-selective toxins have been published (Ballio, 1991; Mitchell, 1984). Non-host-selective toxins produced by *Alternaria* species were briefly covered in the most recent review (Lou, Fu *et al.*, 2013).

Tentoxin (**130**), a cyclic tetrapeptide, is produced by *Alternaria tenuis*. Initially, culture extracts of *A. tenuis* induced albinism—chlorophyll deficiency—in citrus seedlings (Ryan, Greenblatt *et al.*, 1961). Fulton *et al*. reported the causal agent of albinism from *A. tenuis* culture filtrates to be tentoxin (Fulton, Bollenbacher *et al.*, 1965). The chemical structure of tentoxin (**130**) was confirmed by total synthesis (Rich and Mathiaparanam, 1974).

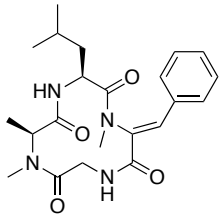

130

Zinniol (**131**) produced by *A. tagetica* was established as a non-host-selective toxin. Zinniol induced necrosis in unrelated plant species such as carrot, cucumber, barley, zinnia, and marigold (Cotty, 1983; Robeson and Strobel, 1984; White and Starratt, 1967). In addition to necrosis, zinniol (**131**) inhibited germination of seeds of zinnia, tomato, lettuce, watermelon, and carrot (White and Starratt, 1967). A structure activity relationship study was carried out using natural and synthetic zinniol derivatives against marigold (*Tagetes erecta*) (Gamboa-Angulo, Escalante-Erosa *et al.*, 2002). They reported that zinniol (**131**) caused severe necrosis on *T. eracta*. Monosubstituted derivatives (**131b**, **131f**) showed weak phytotoxicity, whereas **131a** and **131c** did not cause damage. Furthermore, carboxylated methyl ether derivatives **131d** and **131e** showed strong phytotoxicity (Gamboa-Angulo, Escalante-Erosa *et al.*, 2002).

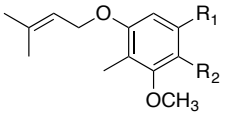

131 $R_1 = CH_2OH$, $R_2 = CH_2OH$

131a $R_1 = CH_2OH$, $R_2 = CH_2OCH_2CH_2Ph$

131b $R_1 = CH_2OH$, $R_2 = CH_2OCH_3$

131c $R_1 = CH_2OAc$, $R_2 = CH_2OH$

131d $R_1 = COOH$, $R_2 = CH_2OCH_3$

131e $R_1 = CH_2OCH_3$, $R_2 = COOH$

131f $R_1 = CH_2OCH_3$, $R_2 = CH_2OH$

1.2.3.2.3 Spore germination fluids

Nishimura and Kohmoto initially used the term "*released toxin*" when a metabolite was detected and isolated from *spore germination fluids* (SGFs) of virulent isolates of *Alternaria* species (Nishimura and Kohmoto, 1983b). This concept was proposed by Nishimura and Scheffer (1965), when HV-toxin was released from SGFs of *Helminthosporium victoriae* on oat leaves. Many HSTs produced by *Alternaria* species were detected in SGFs (Hayashi, 1990; Nishimura and Kohmoto, 1983a). In general, spore germination fluids (SGFs) of a fungus are harvested from spore suspensions on leaves of susceptible plants after appropriate incubation time (ca. 24–48 h). Filtrates of SGFs are assayed to determine phytotoxicity in susceptible and resistant plants. SGFs could be collected from non-plant materials such as glass surface, or plastic plates. But, such SGFs generally do not show phytotoxicity (Oka, Akamatsu *et al.*, 2005; Quayyum, Gijzen *et al.*, 2003).

Host recognition and HST production by phytopathogenic fungi take place on the sites of initial contact at the early stage of infection. Thus, investigation of SGFs containing HSTs would establish the roles of fungal metabolites in disease development. This section covers host-selective protein toxins produced by the phytopathgenic fungi *Alternaria* species during the early germination of spores.

Otani *et al*. reported the first protein toxin produced by *A. brassicicola* (Otani, Kohnobe *et al.*, 1998). SGFs were obtained from spore suspension of *A. brassicicola* germinated on leaves of susceptible *B. oleracea* (cabbage). SGFs caused necrosis and/or chlorosis in susceptible *Brassica* species, but they did not show phytotoxicity to non-host plants. Furthermore, proteinase

K and heat led to loss of phytotoxicity, suggesting SGFs contained protein toxin(s). Purification of the SGF toxin resulted in isolation of a 35 kDa protein toxin, named AB-toxin.

The fungus *A. panax* Whetzel causes *Alternaria* blight in American ginseng (*Panax quinquefolius* L.). SGFs of *A. panax* collected from ginseng leaves caused disease symptoms in *P. quinquefolius,* but not in non-host plants. SGFs did not display phytotoxic activity after heating or treating with proteinase A. After chromatography of SGFs produced by *A. panax*, a 35 kDa host-selective protein toxin, named AP-toxin, was isolated (Quayyum, Gijzen *et al.*, 2003). Despite having the same molecular weight as that of AB-toxin, AP-toxin did not cause damage on hosts of *A. brassicicola*; it was concluded that AP-toxin is different from AB-toxin (Quayyum, Gijzen *et al.*, 2003).

A host-selective protein toxin in SGFs from *A. brassicae* called ABR-toxin (27.5 kDa) was produced in host plants, but not in non-host plants, suggesting production of ABR-toxin might be affected by factors of host plants (Parada, Sakuno *et al.*, 2008). SGFs of *A. brassicae* collected from *B. oleracea* (cabbage) caused chlorosis only in *Brassica* leaves (Parada, Sakuno *et al.*, 2008).

1.2.3.3 Metabolites produced by *Alternaria brassicicola*

Pedras *et al*. reported a fungal metabolite (named brassicicolin A) produced by *A. brassicicola*, which exhibits phytotoxicity on leaves of *B. juncea* cv. Cutlass susceptible to *A. brassicicola* (Pedras, Chumala *et al.*, 2009). Initially, brassicicolin A (**1**) was isolated from *A. brassicicola* and reported as an antibiotic complex against *B. subtilis* and *S. aureus* (Ciegler and Lindenfelser, 1969). The structure of brassicicolin A (**1**) was elucidated by Gloer *et al*. and confirmed by chemical degradation studies (Gloer, Poch *et al.*, 1988). In addition to antibiotic activity, brassicicolin A (**1**) showed phytotoxicity only on *B. juncea* (susceptible) at 0.05 mM, whereas phytotoxicity was not observed on *S. alba* cv. Ochre (resistant) at 0.5 mM (Pedras, Chumala *et al.*, 2009).

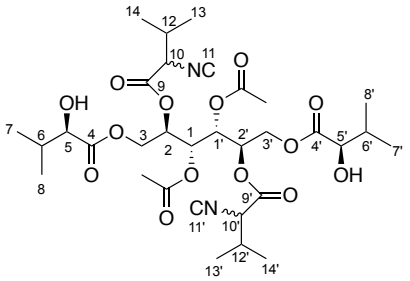

1

MacKinnon *et al*. reported six fusicoccane-like diterpenoids (named brassicicenes A to F) (**Figure 1.18**) isolated from the extracts of culture filtrates of *A. brassicicola*. MacKinnon *et al*. proposed that brassicicenes A to F (**132**–**137**) might have phytotoxicity, but phytotoxic bioassays were not carried out due to small quantities of those metabolites (MacKinnon, Keifer *et al.*, 1999). Pedras *et al*. reported brassicicenes G to I (**138**–**140**) isolated from the extracts of culture filtrates of *A. brassicicola*, but phytotoxicity assays were not carried out due to small amounts. Considering brassicicenes G to I (**138**–**140**) were isolated from fractions exhibiting low phytotoxicity, it is likely that they have no phytotoxicity (Pedras, Chumala *et al.*, 2009). Most recently, Kenmoku et al. reported brassicicenes J (**141)** and K (**142)** (Kenmoku, Takeue *et al.*, 2014).

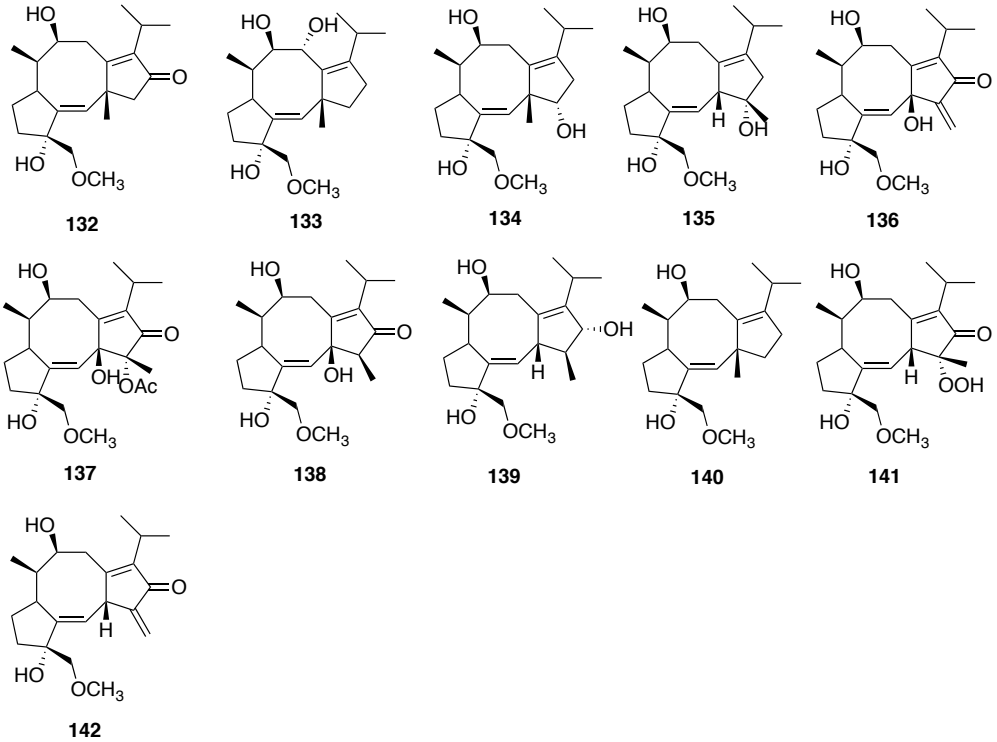

132 **133** **134** **135** **136**

137 **138** **139** **140** **141**

142

Figure 1.18 Structures of brassicicenes produced by *Alternaria brassicicola.*

Pedras *et al*. reported that phomapyrones A (**25**), F (**147**) and G (**148**), and infectopyrone (**149**) were isolated from non-phytotoxic fractions of extracts of *A. brassicicola* culture filtrates (Pedras, Chumala *et al.*, 2009). Initially, phomapyrones A (**25**) to G (**148**) and infectopyrone were isolated and characterized from the culture filtrates of *L. maculans*/*P. lingam* (Pedras and Chumala, 2005; Pedras, Morales *et al.*, 1994) (**Figure 1.19**). Although crude extracts of the fungal cultures showed phytotoxic effects (Pedras, Morales *et al.*, 1994), purified phomapyrones A (**25)** and D (**145**) did not exhibit phytotoxicity (Pedras and Chumala, 2005).

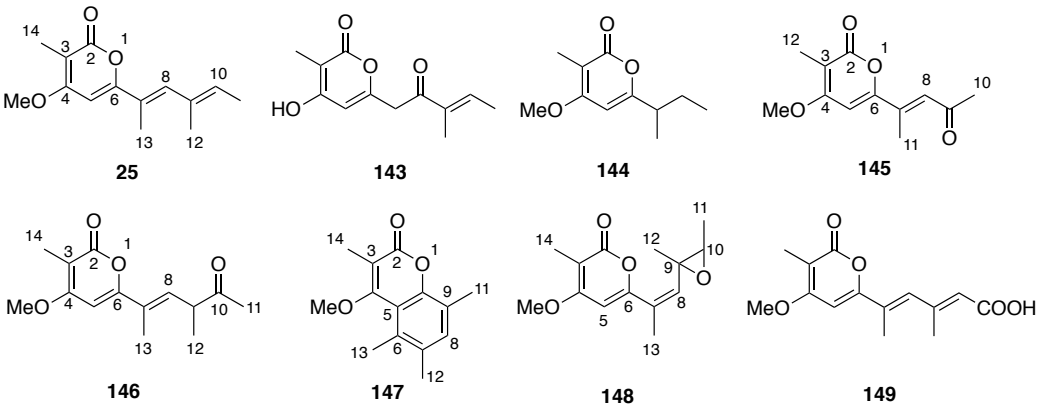

Figure 1.19 Structures of phomapyrones.

1.2.3.4 Biosynthesis of secondary metabolites of *Alternaria* species

After structure elucidation of a metabolite of interest, biosynthetic building blocks can be proposed from a retrobiosynthetic analysis. To carry out biosynthetic studies of a metabolite of interest, isotopically labeled precursors (e.g., ^{13}C, ^{2}H, ^{15}N, ^{18}O) of primary building blocks are administered to cultures of the producing organism and the labeled intermediates or final products are isolated. The precursor/metabolite relationship can be confirmed by analyses of the labeled metabolites using nuclear magnetic resonance (NMR) spectroscopy and mass spectrometry (Schneider, 2007).

Depudecin and phomapyrone A

Administration of [1-^{13}C], [2-^{13}C], [1,2-$^{13}C_2$], [2-$^{2}H_3$], or [2-^{2}H,2-^{13}C]acetate into *Nimbya scuroucicola* culture, a producer of depudecin (**151**), revealed that depudecin (**151**) is derived from an acetate-derived hexaketide (**Scheme 1.3**) (Tanaka, Fujimori *et al.*, 2000). Wight *et al*. reported that the depudecin (**151**) gene cluster contains six genes, *DEP1–DEP6,* and *A. brassicicola dep5* mutant showed reduced virulence on *B. oleracea* (Wight, Kim *et al.*, 2009).

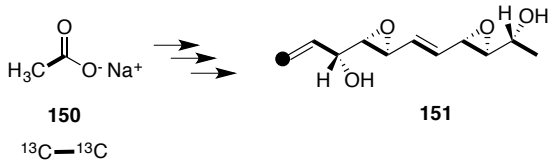

Scheme 1.3 Labeling pattern of depudecin (**151**) (Tanaka, Fujimori *et al.*, 2000).

A biosynthetic study of phomapyrone A (**25**) produced by the fungus *L. maculans/P. lingam* demonstrated the polyketide origin; **25** is derived from a pentaketide containing four methyl groups derived from methionine (**Scheme 1.4**) (Pedras and Chumala, 2005).

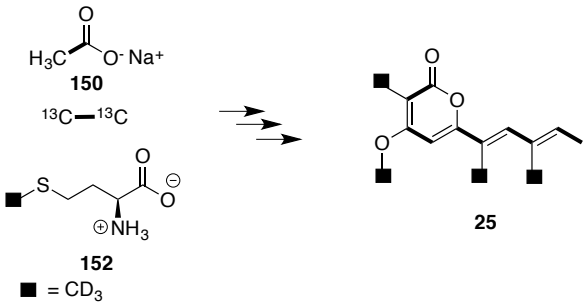

Scheme 1.4 Labeling pattern of phomapyrone A (**25**) (Pedras and Chumala, 2005).

Brassicicolin A and the origin of isocyanide carbon

Brassicicolin A ($C_{32}H_{48}N_2O_{14}$) consists of one D-mannitol, two isocyanoisovaleryl, two 2-hydroxy-3-methylbutanoyl, and two acetyl units. Since the structure of brassicicolin A (**1**) was elucidated in 1988 (Gloer, Poch *et al.*, 1988), no biosynthetic studies have been published to date. Brassicicolin A (**1**) has an isocyanide group. While the biosynthetic origins of the nitrogen in isocyanide group are likely derived from (*S*)-valine, the origin of carbon remains elusive. Reviews on naturally occurring isocyanides and related metabolites were published in 1988 and 2004 (Edenborough and Herbert, 1988; Garson and Simpson, 2004).

An organic isocyanide (also called isonitrile) contains a functional group having nitrogen and carbon with an R group (alkyl or aryl) directly attached to nitrogen (**Figure 1.20**). The isocyanide group has both nucleophilic and electrophilic atoms. The presence of an isocyanide group in a given compound might be confirmed by spectroscopic data such as IR (ca. 2165–2110 cm^{-1}) and ^{13}C NMR (ca. δ_C 154–170 ppm). Mild acidic conditions might promote hydrolysis of isocyanides to formamides (Edenborough and Herbert, 1988).

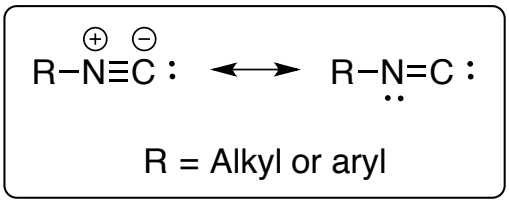

Figure 1.20 Resonance structures of isocyanides.

Xanthocillin (**153**) produced by *Penicillium notatum* Westling was isolated (Rothe, 1950). A complex mixture of xanthocillins exhibited antibiotic activity against a wide spectrum of microorganisms. A biosynthetic study of xanthocillin (**153**) revealed that [2-^{14}C]tyrosine was incorporated into xanthocillin (**153**), whereas neither ^{14}C-formate nor [methyl-^{14}C]methionine was incorporated into the isocyanide carbon (Edenborough and Herbert, 1988). Similarly, [2-^{13}C,^{14}C]glycine was incorporated into *O*-methyl groups of xanthocillin X monomethyl ether (**153a**), whereas neither ^{14}C-formate nor [3-^{14}C]serine was incorporated into the isocyanide carbon (Herbert and Mann, 1984; Kitahara and Endo, 1981). It is likely that in terrestrial isocyanides, the nitrogen is derived from amino acids; however, the biosynthetic origin of the isocyanide carbon has not been established in many cases.

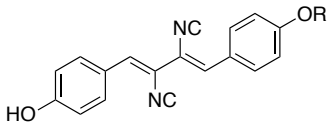

153 R = H
153a R = CH_3

Brady and Clardy proposed the biosynthetic origins of nitrogen and carbon of isocyanide containing antibiotic metabolite (**158**) (Brady and Clardy, 2005a, b). A biosynthetic study was carried out using recombinant *E. coli* strains and labeled precursors (**155**, **157a**, **159**, **160**) (**Scheme 1.5**). As a result of feeding experiments, ^{15}N-enriched **158** was detected in cultures expressing the *is*ocya*n*ide/*is*o*n*itrile genes (IsnA/IsnB) after administration of ^{15}N-labled tryptophan (**155)**; *N*-formyl tryptophan (**159**), and *N*-formyl tryptamine (**160**) were not incorporated into **158**. If each gene is expressed separately, incorporation of ^{15}N-labeled precursors does not occur. IsnA and IsnB are involved in the biosynthesis of the isocyanide **158**. To establish the role of IsnB, the ^{15}N-labeled methyl ester (**157a**) was administered due to instability of the synthetic **157**. The ^{15}N-enriched **158** was detected in the cultures, where IsnB was expressed in the presence of ^{15}N-labeled methyl ester **157a**, suggesting that IsnB is responsible for decarboxylation of isocyanide-containing intermediate **157.** The role of IsnA is unclear (Brady and Clardy, 2005a) **(Scheme 1.5)**.

Next, to establish the biosynthetic origin of carbon of isocyanide **158**, mutants deficient in key primary metabolic enzymes were used (Brady and Clardy, 2005b). In brief, the mutant deficient in glucose-6-phosphate-1-dehydrogenase (*zwf*) (Fraenkel and Banerjee, 1972) grown in either [U-$^{13}C_6$]glucose or [2-^{13}C]glucose produced the ^{13}C-enriched isocyanide **158**, but when grown in [1-^{13}C]glucose did not produce the ^{13}C-enriched isocyanide **158**. Furthermore, [2-^{13}C]ribose led to production of ^{13}C-enriched isocyanide **158**; whereas [1-^{13}C]ribose did not. It was concluded that ribulose-5-phosphate (**156**) could be the final carbon donor of isocyanide **158** because it is a tautomer of both arabinose-5-phosphate and ribose-5-phosphate (**156a**) (Brady and Clardy, 2005b).

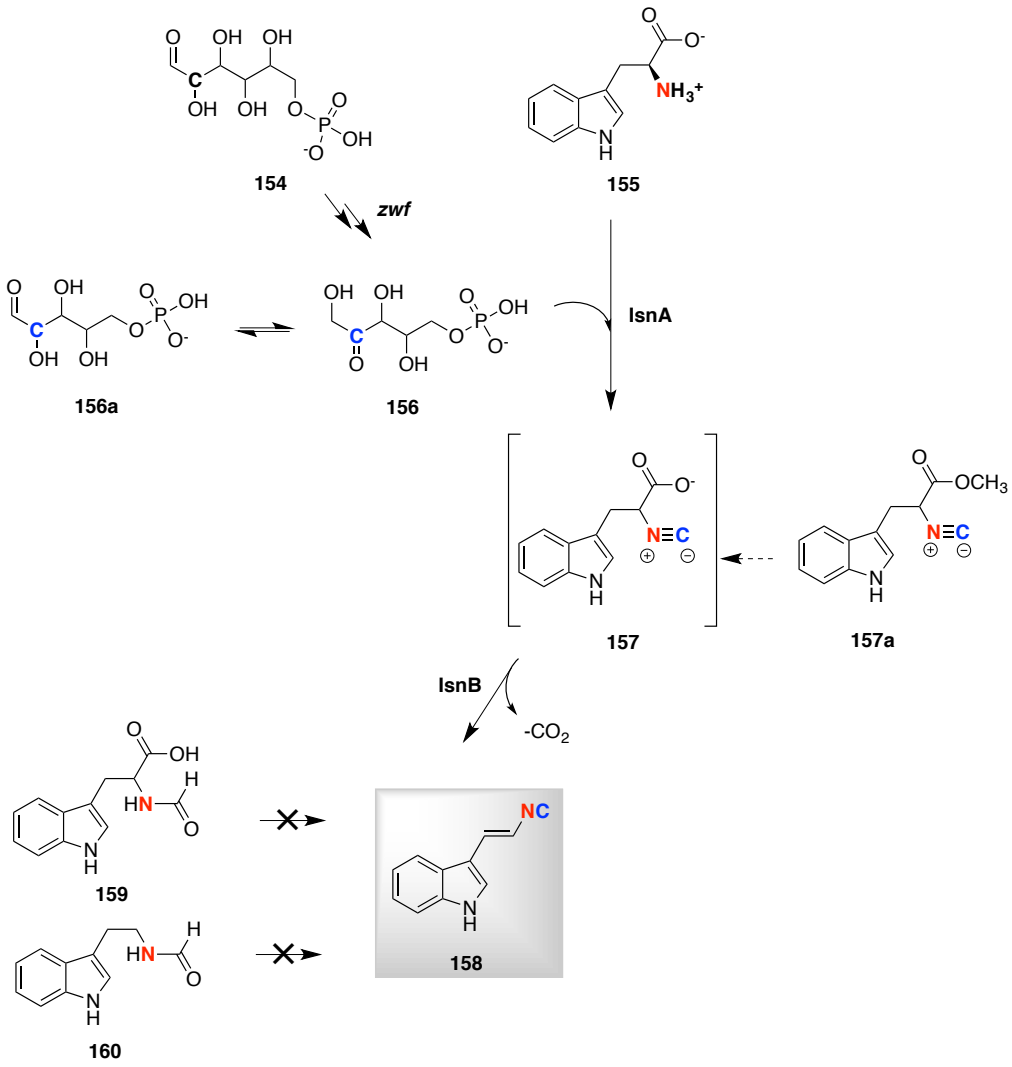

Scheme 1.5 Biosynthesis of indole vinylisocyanide (**158**). *zwf* = glucose-6-phosphate-1-dehydrogenase, Isn = isocyanide or isonitrile (Brady and Clardy, 2005a, b).

Pedras and Yaya reported a plant-derived isocyanide (named isocyalexin A (**166**)) (Pedras and Yaya, 2012) as a phytoalexin isolated from UV-irradiated rutabaga. The structure of isocyalexin (**166**) was confirmed by chemical synthesis (Pedras and Yaya, 2012). Isocyalexin A (**166**) showed a strong antifungal activity against *Rhizoctonia solani* (complete inhibition at 0.50 mM), whereas moderate or weak antifungal activity against *A. brassicicola*, *L. maculans*, and *Sclerotinia sclerotiorum*. Biosynthetic studies of isocyalexin A (**166**) were carried out using perdeuterated compounds and (*S*)-[$^{13}C_{11}$,$^{15}N_2$]-enriched **155** (Pedras and Yaya, 2013). Based on

the incorporation of labeled compounds into isocyalexin (**166**), a biosynthetic pathway to isocyalexin (**166**) was proposed (**Scheme 1.6**). Pedras and Yaya pointed out that transformation of 4'-methoxyindolyl-3'-glycine (**163**) from aziridine intermediate **162** is one of the key steps to biosynthesis of isocyalexin A (**166**). Interestingly, the carbon source of the isocyanide group in isocyalexin A (**166**) is derived from (*S*)-tryptophan (**155)** (Pedras and Yaya, 2013).

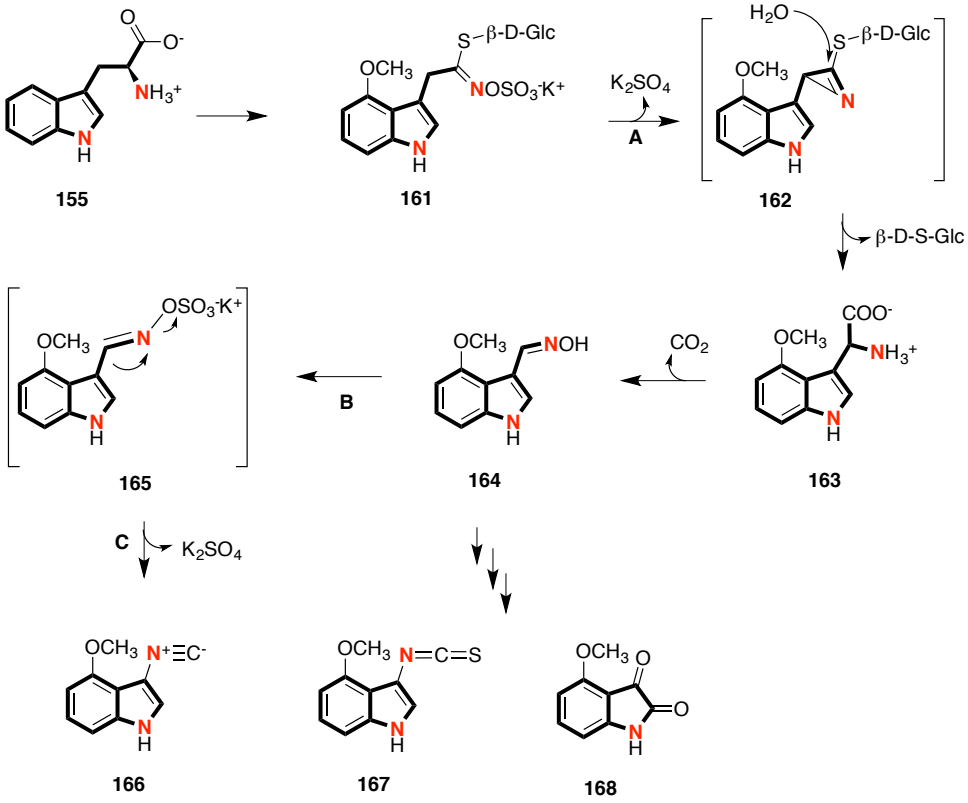

Scheme 1.6 A proposed biosynthetic pathway of isocyalexin A (**166**): A, Neber-type rearrangement; B, sulfation; C, Beckmann-type rearrangement (Pedras and Yaya, 2013).

Although terrestrial isocyanides are rarely found, marine organisms produce isocyanide compounds along with the corresponding formamide and/or isothiocyanate derivatives (Faulkner, 1984). Despite efforts to identify the origin of isocyanide carbons in marine organisms using *N*-formyl precursors, data have shown that the isocyanide carbon is not derived from the corresponding formamides or the C-1 of tetrahydrofolate pool (Garson and Simpson,

2004). However, it is possible that marine organisms can utilize the cyanide produced by microbial symbionts that are using amino acids such as glycine, methionine, or serine to generate inorganic cyanides (Bornemann, Patterson *et al.*, 1988). Karuso and Scheuer reported that [^{14}C]cyanide was incorporated into 2-isocyanopupukeanane (**169**) and 9-isocyanopupukeanane (**170**) in *Ciocalypta* sp. and *Acanthella* sp., respectively (Karuso and Scheuer, 1989). Intact incorporation of [^{13}C, ^{15}N]cyanide into 9-isocyanopupukeanane (**170b**) was also observed in *Acanthella* sp. (Karuso and Scheuer, 1989) (**Scheme 1.7**).

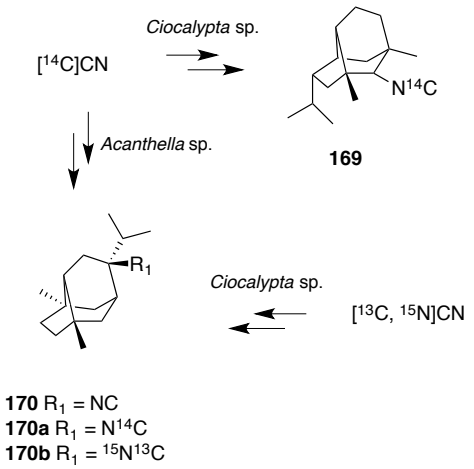

Scheme 1.7 Proposed biosynthetic pathways of 2-isocyanopupukeanane (**169**) and 9-isocyanoneopupukeanane (**170**) (Karuso and Scheuer, 1989)

Garson first established that sodium [^{14}C]cyanide was incorporated (up to 1.8%) into the isocyanide carbon in diisocyanoadociane (**171**) using the Great Barrier Reef sponge *Amphimedon terpenensis* (Garson, 1986). Feeding experiments were carried out using more advanced precursors to establish biosynthetic relationships between cyanide and isocyanide and thiocyanate and isothiocyanate (Simpson and Garson, 2004). Administration of [^{14}C]thiocyante to *A. terpenensis* led to detection of ^{14}C-labeled diisocyanoadociane (**171**), ^{14}C-labeled 9-isothiocyanatopupukeanane (**174**), and ^{14}C-labeled 2-thiocyanatoneopupukeanane (**173**), suggesting that thiocyanate could be a biosynthetic precursor of isocyanide, thiocyanate, and isothiocyanate compounds. Administration of [^{14}C]cyanide to *A. terpenensis* led to detection of

^{14}C-labeled 2-thiocyanatoneopupukeanane (**173**) and ^{14}C-labeled -9-isocyanopupukeanane (**175**). Considering the incorporation of [^{14}C]cyanide and [^{14}C]thiocyante into 2-thiocyanatoneopupukeanane (**173**), interconversion between cyanide and thiocyante might occur. Furthermore, administration of [^{14}C]9-isothiocyanatopupukeanane (**174**) to *Axinyssa* n. sp. resulted in detection of ^{14}C-labeled-9-isocyanopupukeanane (**175**), while feeding of **175** led to isolation of **174** in *Axinyssa* n. sp.. However, administration of [$^{14}C_2$]–bisisothiocyanatodociane (**172**) to *A. terpenensis* did not lead to detection of labeled diisocyanoadociane (**171**) (**Scheme 1.8**). That is, isothiocyanate is not a precursor of isocyanide; instead, interconversion between isocyanide and isothiocyanate might take place as a strategy for homeostasis of two compounds (Garson and Simpson, 2004).

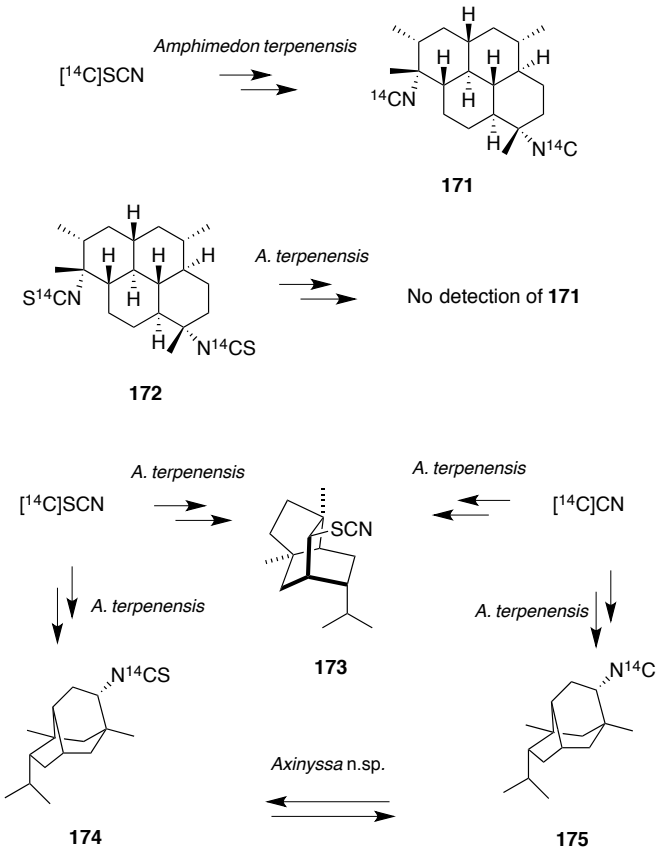

Scheme 1.8 Administration of ^{14}C-labeled precursors to two marine sponges *Amphimedon terpenensis* and *Axinyssa* n.sp. (Simpson and Garson, 2004)

1.2.3.5 Siderophores

To overcome low bioavailability of iron and to detoxify reactive oxygen species (ROS) produced by plants, certain plant pathogens produce siderophores, a family of low-molecular-weight Fe^{3+} chelators. Siderophores as high-affinity iron (Fe^{3+}) chelators not only enable fungal pathogens to utilize iron, but also act as antioxidants to detoxify (ROS) (Haas, Eisendle *et al.*, 2008). The roles of siderophores produced by phytopathogenic fungi have been studied and several comprehensive reviews have been published (Chen, Yang *et al.*, 2014; Dixon and Stockwell, 2014; Expert, Enard *et al.*, 1996; Expert, Franza *et al.*, 2012; Haas, Eisendle *et al.*, 2008; Hider and Kong, 2010; Renshaw, Robson *et al.*, 2002).

Several siderophores produced by phytopathogenic *Alternaria* species were reported during the last decades. Jalal *et al*. reported that *A. longipes* ATCC 26293 produced coprogen (**176**), neocoprogen I (**177)**, isoneocoprogen I (**178)**, and N^{α}-dimethylcoprogen (**179)** based upon ^{1}H and ^{13}C NMR spectroscopic data, and fast-atom-bombardment (FAB) mass spectrometric data (Jalal, Love *et al.*, 1988). Hydroxycoprogen (**180)**, hydroxyneocoprogen I (**181)**, and hydroxyisoneocoprogen I (**182)** produced by *A. longipes* were reported (Jalal and van der Helm, 1989). Ohra *et al*. tested the phytotoxicity of siderophores using ferricrocin **(183)** and coprogen (**176**) isolated from *A. cassia*, a phytopathogen in diseased seedlings of sicklepod (*Cassia obtusifolia* L.). Ferricrocin **(183)** caused necrosis in cowpea, whereas coprogen (**176**) caused weak necrosis in cowpea (Ohra, Morita *et al.*, 1995).

More recently, Oide *et al*. proposed that the siderophores produced by fungal pathogens might obtain iron from host plants (Oide, Moeder *et al.*, 2006). The *A. brassicicola* non-ribosomal peptide synthetase deficient mutant (*nps6*) caused smaller lesions in *Arabidopsis thaliana,* compared to lesions caused by the wild type isolate. Furthermore, increased sensitivity to oxidative stress was observed in *A. brassicicola nps6* mutant. HPLC analysis of the culture filtrates of wild type and *nps6* mutant revealed that only wild type produced siderophores; coprogen (**176**), N^{α}-dimethylcoprogen (**179)**, and dimerumic acid (**184**). Furthermore, addition of iron either to spore suspensions or to *A. thaliana* enhanced the virulence of the *nps6* mutant. These findings suggest that non-ribosomal peptide synthetase (NPS6) is involved in biosynthesis of siderophores and such siderophores play an important role in taking iron from host plants (Oide, Moeder *et al.*, 2006).

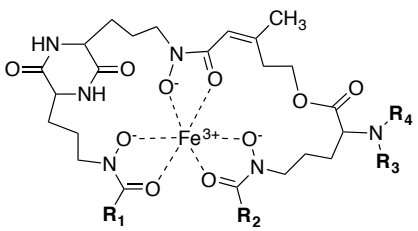

	R_1	R_2	R_3	R_4
176	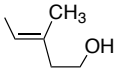	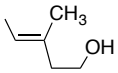	CH_3CO	H
177	CH_3	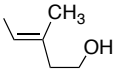	CH_3CO	H
178	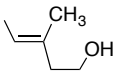	CH_3	CH_3CO	H
179	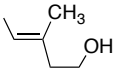	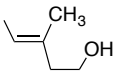	CH_3	CH_3
180	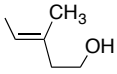	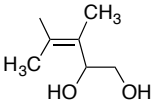	CH_3CO	H
181	CH_3	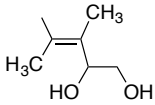	CH_3CO	H
182	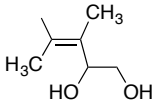	CH_3	CH_3CO	H

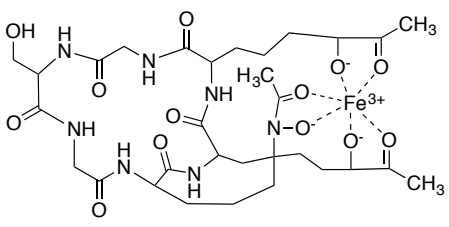

183

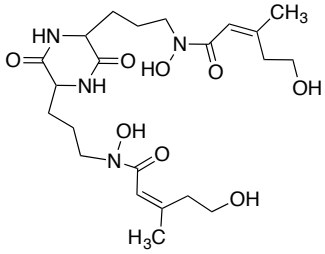

184

1.3 Secondary metabolites produced by plants

1.3.1 Phytoalexins and phytoanticipins

Plants produce numerous secondary metabolites active against plant pathogens and having diverse chemical structures. The secondary metabolites that plants produce to defend themselves are largely classified into two groups: phytoanticipins and phytoalexins (Dixon, 2001; VanEtten, Mansfield *et al.*, 1994). Over the past decades, a great variety of chemical structures of phytoanticipins and phytoalexins have been elucidated. Phytoalexins are secondary metabolites having antimicrobial activity and are produced *de novo* under different abiotic and/or biotic stress (e.g. microbial infection, UV irradiation, and heavy metal salts). It is essential that these plant metabolites exhibit antifungal or antibacterial activities and that they are absent in healthy plants to belong to the phytoalexin group (Pedras, Yaya *et al.*, 2011). More than 50 phytoalexins have been characterized in crucifers (the Brassicaceae family) since Takasugi et al. first reported cruciferous phytoalexins (Takasugi, Katsui *et al.*, 1986). The phytoalexins produced in *B. juncea* (brown mustard), *B napus* (rapeseed) and *S. alba* (white mustard) are summarized in **Table 4**. Comprehensive reviews on phytoalexins produced by crucifers are available (Pedras and Yaya, 2010; Pedras, Yaya *et al.*, 2011).

Table 4 Selected phytoalexins produced in *Brassica juncea* cv. Cutlass (brown mustard), *Brassica napus* cv. Westar (canola) and *Sinapis alba* cv. Ochre (Pedras, Yaya *et al.*, 2011).

Species	Elicitation	Phytoalexins
***Brassica juncea* (brown mustard)**	$CuCl_2$, $AgNO_3$ *A. brassicae*, *L. maculans*	Brassilexin (**185**) Cyclobrassinin (**186**) Cyclobrassinin sulfoxide (**187**) Indolyl-3-acetonitrile (**188**) Spirobrassinin (**189**)
***Brassica napus* (rapeseed)**	$CuCl_2$ *L. maculans*	1-Methoxybrassinin (**190**) 4-Methoxycyclobrassinin (**191**) Brassilexin (**185**) Cyclobrassinin (**186**) Cyclobrassinin sulfoxide (**187**) Dehydrocyclobrassinin (**192**) Spirobrassinin (**189**)
***Sinapis alba* (white mustard)**	Destruxin B (**123**) *A. brassicae*, *L. maculans*	Sinalbin A (**193**) Sinalbin B (**194**), Sinalexin (**195**)

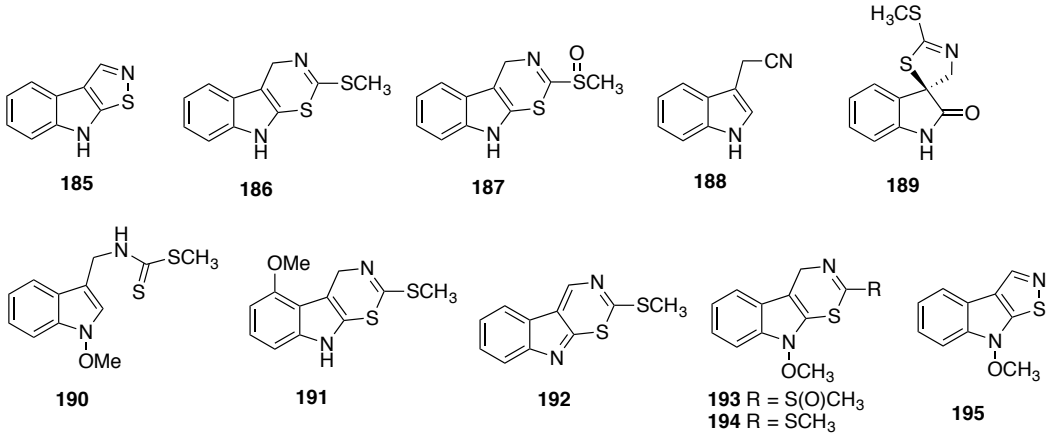

Phytoanticipins are defined as "*low molecular weight, antimicrobial compounds that are present in plants before challenge by microbial infection*" (VanEtten, Mansfield *et al.*, 1994). Although these plant metabolites are clearly defined, there has been confusion in certain cases. For example, three nitriles, indolyl-3-acetonitrile (**188**), arvelexin (**188a**) caulilexin C (**188b**) were considered phytoanticipins in *Thellungiella halophile* (Pedras, Zheng *et al.*, 2009; Pedras and Zheng, 2010), although previously indole-3-acetonitrile (**188**) was reported as a phytoalexin in brown mustard (*B. juncea*) (Pedras, Nycholat *et al.*, 2002). A recent review article covers issues of definition and ecological roles of phytoanticipins (Pedras and Yaya, 2015).

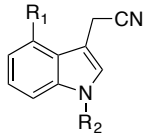

188 R1 = R2 = H
188a R_1 = OMe R_2, = H
188b R_1 = H, R_2 = OCH_3

More than 130 glucosinolates have been reported from the order Brassicales (Agerbirk and Olsen, 2012). Glucosinolates are constitutively present in crucifers, thus they are considered phytoanticipins (Morant, Jørgensen *et al.*, 2008). The biologically active isothiocyanates and

nitriles are hydrolysis products of glucosinolates. Stable isothiocyanates formed by enzymatic reactions (i.e., myrosinase) have shown strong antimicrobial activity than the corresponding glucosinolates (**Scheme 1.9**) (Pedras and Yaya, 2015).

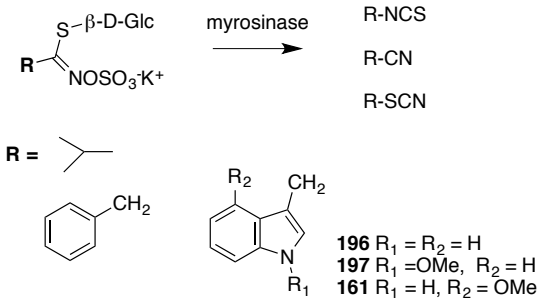

Scheme 1.9 General scheme for hydrolysis of glucosinolates

Indole glucosinolates (**196, 197,** and **161**) are of interest in this work because they are biosynthetic precursors of almost all (*S*)-tryptophan-derived phytoalexins (Pedras, Yaya *et al.*, 2011). For example, once indolyl-3-methylisothiocyanates (**199**) are formed from indole glucosinolates via myrosinase-mediated reaction, brassinin and related phytoalexins (**199–201**) having scaffold A are biosynthesized (Takasugi, Katsui *et al.*, 1986). Other phytoalexins (such as rapalexins **204**) containing scaffold B are derived from indole glucosinolates but their biosynthetic pathway is independent from those of brassinin-type phytoalexins (**Scheme 1.10**) (Pedras, Montaut *et al.*, 2004; Pedras and Yaya, 2013).

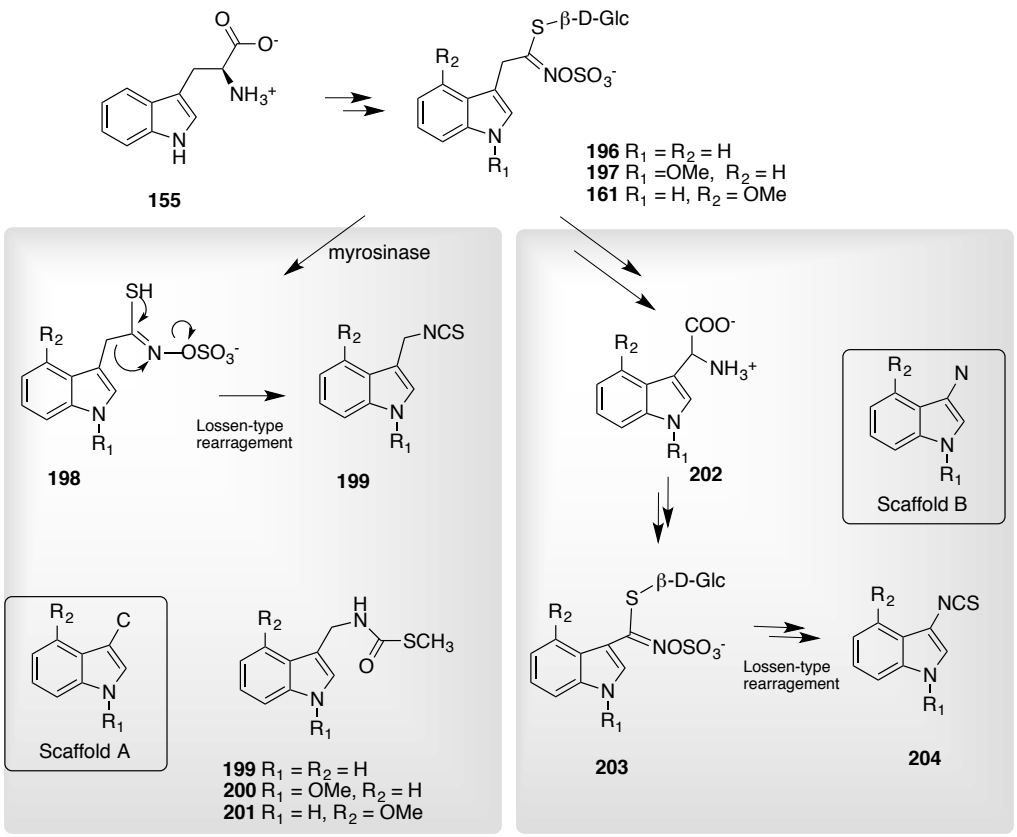

Scheme 1.10 Biosynthetic relationship of indole glucosinolates and phytoalexins containing two different scaffolds (Pedras and Yaya, 2013).

Since the whole genome sequence of *A. thaliana* was completed (TheArabidopsisInitiative, 2000), numerous studies have been carried out using ecotypes and mutants. Camalexin was first reported as a phytoalexin from *C. sativa* (Browne, Conn *et al.*, 1991), and Tsuji *et al*. reported camalexin from *A. thaliana* induced upon infection with *Pseudomonas syringae* (Tsuji, Jackson *et al.*, 1992). The biosynthesis of camalexin, including the relevant enzymes and genes has been reviewed (Pedras, Yaya *et al.*, 2011). In brief, camalexin is derived from (*S*)-tryptophan (**155**) and cysteine. The biosynthesis of indole-3-acetaldoxime (**205**) is mediated by CYP79B2 and CYP79B3, and indolyl-3-acetonitrile (**188**) is presumably activated by conjugation with glutathione (GSH) (**206**) to yield (*R*)-*S*-(cyano-1*H*-indolyl-3-methyl)cysteine (**207**). In the last step, CYP71B15 catalyzes the biosynthesis of camalexin (**209**) from (*S*)-dihydrocamalexic acid (**208**) (**Scheme 1.11**). Schuhegger *et al*. reported that a camalexin-deficient (*pad3*) mutant of *A. thaliana* accumulated dihydrocamalexic

acid (**208**) in leaves. Furthermore, the recombinant yeast expressing PAD3 converted dihydrocamalexic acid (**208**) to camalexin (**209**) (Schuhegger, Nafisi *et al.*, 2006).

The peroxisome-associated myrosinase (PEN2) is responsible for hydrolyzing the β-thioglycosidic bond of indole glucosinolates (Bednarek, Pislewska-Bednarek *et al.*, 2009). Unlike PAD3, this enzyme is not involved in the biosynthesis of camalexin.

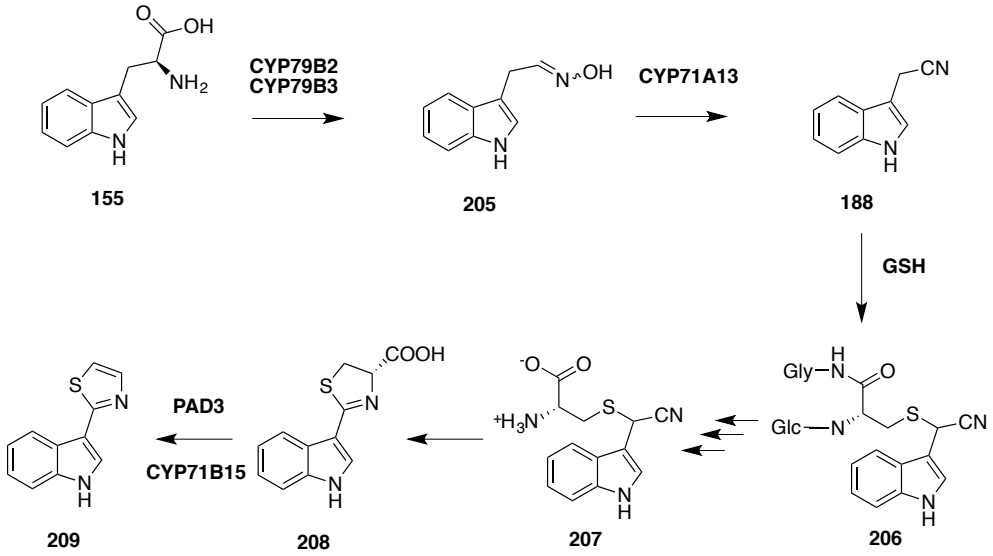

Scheme 1.11 Camalexin (**209**) biosynthesis (Pedras, Yaya *et al.*, 2011).

1.4 Summary

Phytopathogenic fungi biosynthesize and secrete SMs known as phytotoxins that cause damage to plants during fungal invasion. The phytopathogenic fungus *Alternaria brassicicola* (Schwein.) Wiltshire causes *Alternaria* black spot (also called dark leaf spot) in *Brassica* species. Many SMs of *A. brassicicola* grown under standard fermentation conditions have been reported; however, with the exception of siderophores, no fungal SMs have been detected in plants infected with *A. brassicicola*. One of the major challenges for detection is due to plants biotransforming fungal metabolites produced during infection. Unknown phytotoxins of *A. brassicicola* that are not produced in standard growth conditions could participate in disease

development. Detection of phytotoxins could be hindered by complex plant metabolites produced in infected tissues. For those reasons, it is difficult to detect fungal metabolites in infected tissues.

So far, brassicicolin A (**1**), a host-selective toxin produced by *A. brassicicola,* has not been detected in host plants infected with *A. brassicicola*. To clarify the involvement of SMs in disease development, a systematic investigation of SMs produced by *A. brassicicola* and its host plants is necessary. In this work, components of culture media and conditions that influence production of SMs by *A. brassicicola* will be investigated for a better understanding of the chemical interactions between *A. brassicicola* and its host plants. Then, the comparative chemical analysis of SMs produced in infected plants and control plants will be carried out. Finally, a biosynthetic study of brassicicolin A (**1**), a host-selective phytotoxin, will be conducted. Completion of my Ph. D. research work could lead to the development of novel strategies to control *A. brassicicola.*

2 Results and discussion

2.1 Metabolites of *A. brassicicola*

A comprehensive investigation of secondary metabolites produced by *A. brassicicola* grown under various conditions was carried out. Two standard media, minimal medium (MM) and potato dextrose broth (PDB) as well as modified MM were employed for growth of *A. brassicicola* (Pedras and Park, 2015).

2.1.1 Isolation and structure elucidation of metabolites produced in standard media

A. brassicicola was incubated in standard minimal medium (MM) and potato dextrose broth (PDB) at 23 °C and 30 °C under shaking. After seven days of incubation, cultures were filtered and the mycelia were separated from the broths. The resulting culture filtrates were extracted with EtOAc, the extracts were concentrated and analyzed by HPLC-DAD and HPLC-ESI-MS.

The amounts of crude extracts from cultures in PDB were significantly larger than those in MM, while the mycelial weights did not show significant differences. HPLC chromatograms of crude extracts showed more complex metabolite profiles in MM than in PDB (**Figure 2.1**). The reported metabolites were screened by comparison of UV spectra in Dr. Pedras' HPLC libraries (**Figure 2.2**). Four known metabolites were confirmed by comparing spectroscopic data of the metabolites isolated in this work with previously reported data of each metabolite.

Brassicicolin A (**1**) was produced with a larger amount in MM than in PDB. High temperature (30 °C) increased production of brassicicolin A (**1**) in either MM or PDB. Spectral data of brassicicolin A (**1**) were consistent with those previously reported (Pedras, Chumala *et al.*, 2009). Although HPLC method A did not resolve phomapyrone A (**25**) from brassicicolin A (**1**) (**Figure 2.1**), phomapyrone A (**25**) displayed a unique UV absorption, which makes two metabolites distinguishable (**Figure 2.2**). Spectral data of phomapyrone A (**25**) isolated in this work were consistent with those previously reported (Pedras, Morales *et al.*, 1994). UV spectra of phomapyrones E (**146**) and G (**148**) were fairly similar (**Figure 2.2**), but multiplicity in ^{1}H NMR spectra of those metabolites allowed differentiation of two phomapyrones. Pedras and

Chumala reported that H-10 in phomapyrone G (**148**) shows quartet at δ_H 3.05 (1H, 6Hz), whereas phomapyrone E does not have H-10. H-12 in phomapyrone E (**146**) shows doublet at δ_H1.30 (3H, 6 Hz), whereas phomapyrone G (**148**) shows singlet δ_H1.50 (3H) (Pedras and Chumala, 2005). Based on comparison of spectral data of each metabolite, t_R = 20.1 min, and t_R = 24.1 min were assigned as phomapyrone E (**146**) and phomapyrone G (**148**), respectively.

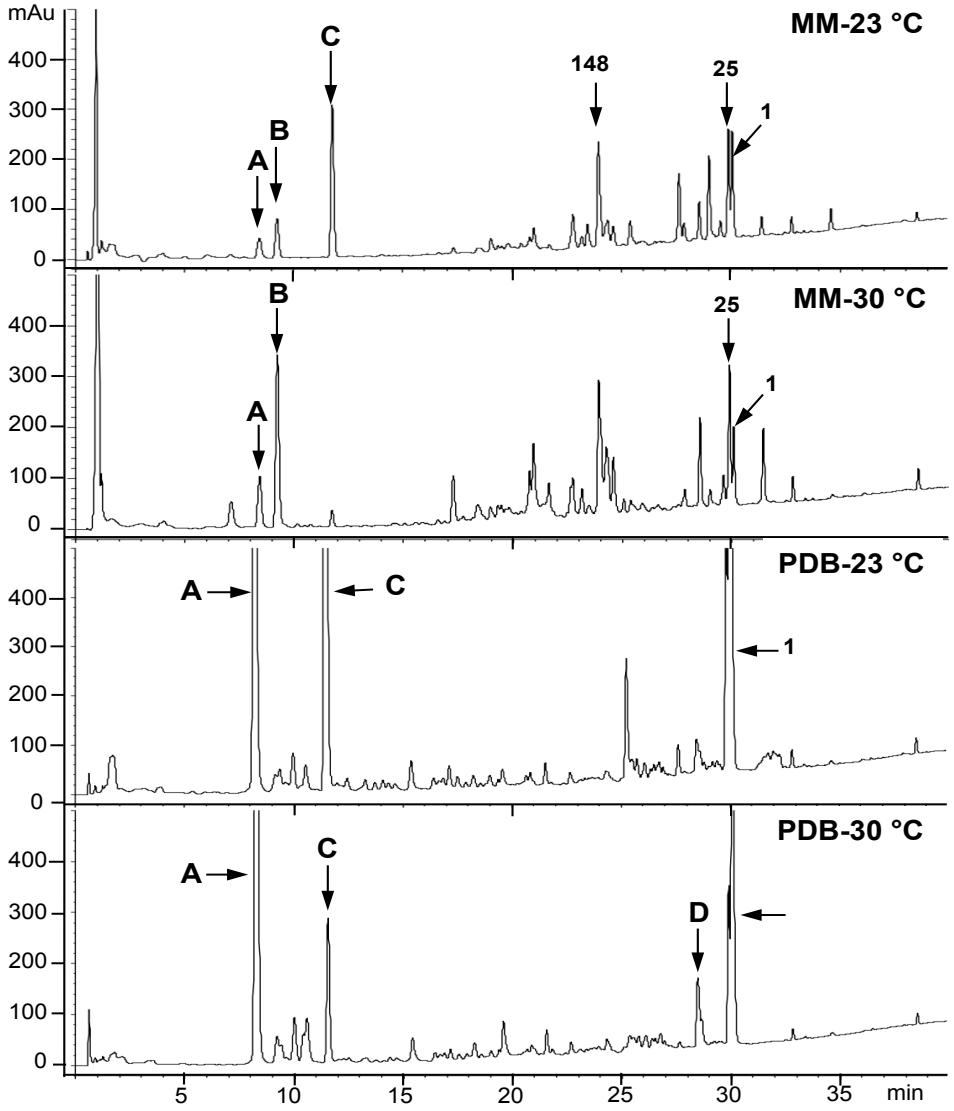

Figure 2.1 HPLC-DAD chromatograms of crude extracts of culture filtrates of *Alternaria brassicicola* grown in minimal medium (MM) and potato dextrose broth (PDB) at 23°C and 30°C (Method A, detection 220 nm): Metabolites A, t_R = 8.4 min; B, t_R = 9.2 min; C, t_R = 11.6 min.

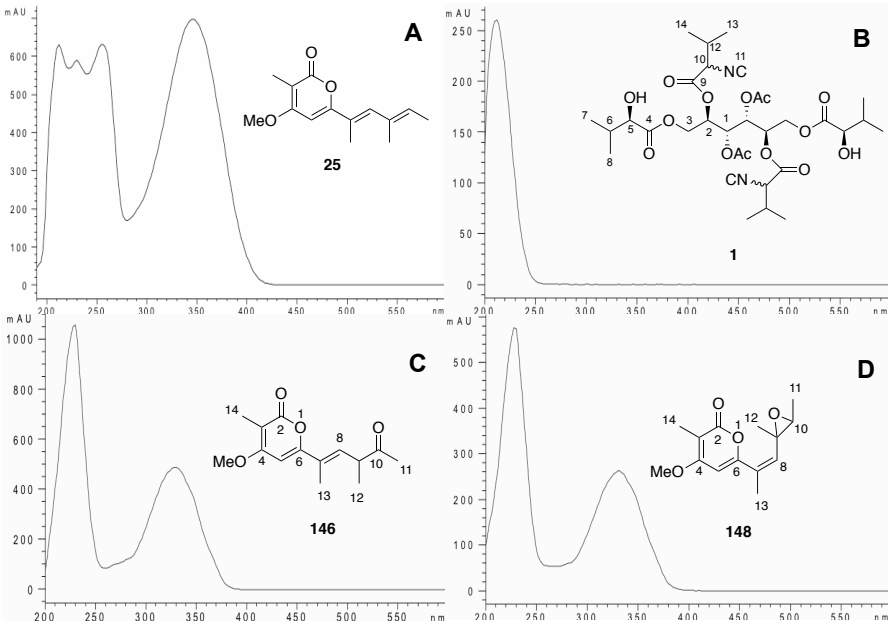

Figure 2.2 UV spectra of four reported metabolites of *Alternaria brassicicola*. A, Phomapyrone A (**25**); B, brassicicolin A (**1**); C, phomapyrone E (**146**); D, phomapyrone G (**148**).

The chromatograms of cultures in MM displayed three peaks in the polar region (peaks A, B, and C) and one peak (peak D) in the non-polar region that did not match UV spectral data stored in Dr. Pedras' HPLC libraries. Metabolites A, B and C were detected in both MM and PDB, whereas metabolite D was solely detected in PDB. To elucidate chemical structures of metabolites A–D, culture filtrates were extracted and fractionated by flash column chromatography (FCC) (**Scheme 4.1** and **Scheme 4.2**). Spectroscopic data (^{1}H and ^{13}C NMR, HR-MS, and FT-IR) were used to characterize the chemical structures of these metabolites as described below.

2.1.1.1 α-Acetylorcinol

Metabolite A (2.5 mg, t_R = 8.4 min, method A) was a yellowish-oily compound. The HREI-MS detected a strong peak at *m/z* 166.0626, establishing the molecular formula of metabolite A as $C_9H_{10}O_3$ (five degrees of unsaturation). The strong IR band at 1701 cm^{-1} and broad band at 3347 cm^{-1} indicated a carbonyl group and an alcohol with O-H, respectively. The ^{1}H NMR spectrum shows three spin systems of eight protons, the ratios of which were 1:2:2:3

(**Table 5**). The proton spectrum in the aromatic region showed mulitplets at δ_H 6.14 (2H)–6.17 (1H) that suggested *meta* coupling. Hence, metabolite A has a trisubstituted benzene ring with two hydroxyl groups at 3,5-positions. The other substituent has a carbonyl group, and two singlets in the aliphatic region in the ^{1}H NMR spectrum (**Table 5**).

The proton-decoupled ^{13}C NMR spectrum of metabolite A showed seven peaks: one ketone, two sp^3 hybridized carbons and in the aromatic region, three quaternary carbons and two sets of protonated carbons indicated a trisubstituted benzene ring. The most deshielded peak at δ_C 160.1 represented the carbon atom containing a hydroxyl group.

In HMBC, methylene protons at δ_H 3.54 showed correlations with three carbon resonances at δ_C 209.7, δ_C 138.0 and δ_C 109.1, suggesting the methylene fragment exists between the benzene ring and the acetyl group. In addition, correlations between the carbonyl carbon at δc 209.7 and the methyl proton at δ_H 2.12 indicated an acetyl group. Based on spectroscopic data, metabolite A was assigned as α-acetylorcinol (**210**) (**Figure 2.3**).

Table 5 ^{1}H (500 MHz, CD_3OD) and ^{13}C (125 MHz, CD_3OD) NMR spectroscopic data of α-acetylorcinol (**210**).

C/H #	δ_C	δ_H, multiplicity ($^3J_{HH}$, Hz)
1	102.4	6.17, 1H, m
2, 2a	160.1	—
3, 3a	109.1	6.14, 2H, m
4	138.0	—
1’	51.8	3.54, 2H, s
2’	209.7	—
3’	29.1	2.12, 3H, s

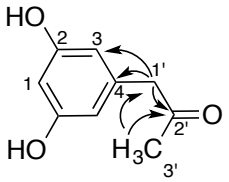

210

Figure 2.3 HMBC correlations of α-acetylorcinol (**210**)

Synthesis of α-acetylorcinol

The chemical synthesis of α-acetylorcinol (**210**) does not appear to have been published. To confirm the chemical structure and to obtain sufficient quantity for further experiments, synthesis of α-acetylorcinol (**210**) was carried out. Retrosynthetic analysis of α-acetylorcinol (**210**) suggested 3,5-dimethoxyphenylacetic acid (**211**) could be a starting material. Reduction of ester **212** to alcohol **213** followed by oxidation to aldehyde **214** and Grignard reaction yielded 1-(3,5-dimethoxy)propan-2-one (**216**). Since this synthetic route required more than 5 steps and led to a low yield (29%) (**Scheme 2.1**), another synthetic route was devised.

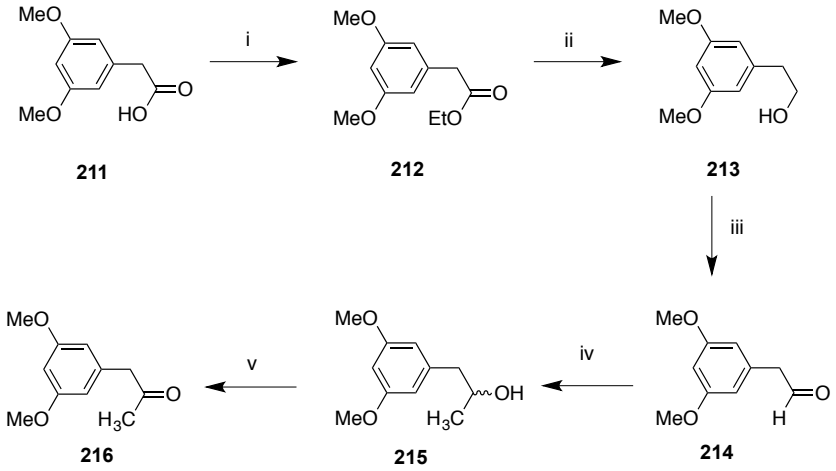

Scheme 2.1 Synthesis of 1-(3,5-dimethoxy)propan-2-one (**216**). Reagents and conditions: (i) EtOH, H_2SO_4, reflux, 2 h, quant.; (ii) LAH, THF, ice-water bath → rt, 1.5 h 83%; (iii) PCC, CH_2Cl_2, rt, 1.5 h 42%; (iv) Mg, CH_3I, Et_2O, NH_4Cl, rt 15 min, quant.; (v) PCC, CH_2Cl_2, rt, 1.5 h, 82%.

To improve overall yield and to shorten the synthetic route, Weinreb amide (*N*-methoxy-*N*-methylamide) was employed (Wang, Denton *et al.*, 2011). The first two steps yielded 2-(3,5-dimethoxyphenyl)-*N*-methoxy-*N*-methylacetamide (**218**) under mild conditions (92%) (**Scheme 2.2**). In the subsequent step, the Weinreb amide **218** yielded the ketone **216** in 76% yield (De Luca, Giacomelli *et al.*, 2001). In the final step, both methoxy groups in 1-(3,5-dimethoxy) propan-2-one (**216**) were deprotected using iodocyclohexane in DMF under reflux (Zuo, Yao *et*

al., 2008). Using this synthetic method, α-acetylorcinol (**210**) was synthesized in four steps with 36% overall yield. The spectroscopic data were identical with those of naturally occurring α-acetylorcinol (**210**) (Pedras and Park, 2015).

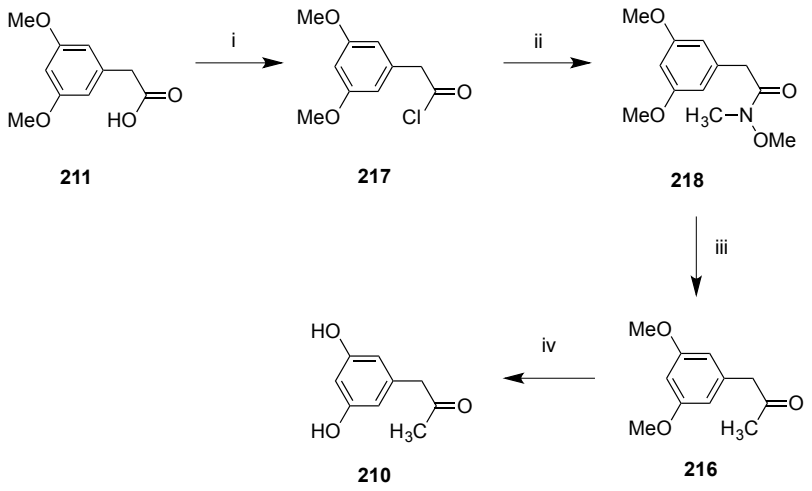

Scheme 2.2 Synthesis of α-acetylorcinol (**210**). Reagents and conditions: (i) Oxalyl chloride, DMF, CH_2Cl_2, rt, 30 min; (ii) *N,O*-dimethylhydroxylamine hydrochloride, pyridine, CH_2Cl_2, rt, 30 min, 92% overt two steps; (iii) CH_3MgI, THF, rt, 30 min, 76%; (iv) Iodocyclohexane, DMF, reflux, 52%.

2.1.1.2 Tyrosol

Metabolite B was a white solid (2.5 mg, t_R = 9.2 min, method A). HREI-MS detected a peak at *m/z* 138.0682, establishing its molecular formula as $C_8H_{10}O_2$ (four degrees of unsaturation). The IR spectrum showed intense OH peaks at 3392 cm^{-1} and 3170 cm^{-1}.

The ^1H NMR spectrum of metabolite B showed two different spin systems: two sets of doublets in the aromatic region and two sets of triplets in the aliphatic region. In aromatic region, the doublets at δ_H 7.04 (2H) and δ_H 6.72 (2H) with J = 8.5 Hz represented protons with *ortho* coupling in a 1,4-disusbstituted benzene ring. In the aliphatic region, one methylene proton at δ_H 3.70 and the other methylene proton at δ_H 2.73 represented a hydroxyethyl moiety (**Table 6**).

The ^{13}C NMR of metabolite B provided six distinct carbon signals: four signals of sp^2 hybridized carbon and, two signals in the aliphatic region. Two quaternary carbons at δ_C 156.9 and δ_C 131.2 and two sp^2-hybridized carbons δ_C 131.0 and δ_C 116.3 indicated a 1,4-disubstituted benzene ring. Furthermore, one sp^3-hybrdized carbon at δ_C 64.8 was deshielded by oxygen and the other sp^3-hybrized carbon at δ_C 39.6 was affected by the aromatic ring. The other substituent of the benzene ring was assigned as OH based on IR spectrum and an index of hydrogen deficiency. Therefore, metabolite B was assigned as tyrosol (**219**). Spectroscopic data of commercially available tyrosol (2-(4-hydroxyphenyl)ethanol) was identical to those of naturally occurring tyrosol (**219**).

Table 6 ^1H (500 MHz, CD_3OD) and ^{13}C (125MHz, CD_3OD) NMR spectroscopic data of tyrosol (**219**).

C/H #	δ_C	δ_H, multiplicity ($^3J_{HH}$, Hz)
1	156.9	-
2, 2a	116.3	6.72, 2H, d (8.5)
3, 3a	131.0	7.04, 2H, d (8.5)
4	131.2	-
1’	39.6	2.73, 2H, t (7)
2’	64.8	3.70, 2H, t (7)

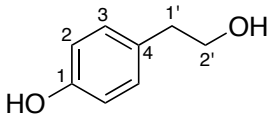

219

2.1.1.3 Depudecin

Metabolite C (57 mg, t_R = 11.6 min, method A) was a colorless oily compound. HREI-MS and HPLC-ESI-MS spectra gave neither a molecular nor quasi-molecular ion. The ^{1}H NMR spectrum of metabolite C exhibited signals for one methyl group, six methine protons, and five olefinic protons, including two terminal olefinic protons. The ^{13}C NMR spectrum detected 11 signals: one methyl group, six sp^3 hybridized carbons containing oxygen, and four sp^2 hybridized carbons (**Table 7**).

In HSQC, one methyl group at δ_H 1.30 was attached to one methyl carbon at δ_C 20.1, suggesting metabolite C has terminal methyl group (C-1) in the structure. One sp^2-hybridized carbon at δ_C 117.2 showed correlations with two olefinic protons at δ_H 5.39 and at δ_H 5.26, which suggested metabolite C has allyl group (C-11) at the terminal position. In HMBC, intensive correlations of δ_H 1.30 with δ_C 67.2 and δ_C 64.4 allowed the assignment of C-2 and C-3, respectively. The proton at δ_H 5.39 (H-11) displayed correlations with δ_C 71.8 and δ_C 136.2, allowing assignment C-9 and C-10, respectively. Further correlations of the carbon δ_C 71.8 (C-9) with one methine proton δ_H 3.01 allowed the assignment of H-8. Likewise, the correlation of δ_C 64.4 with one methine proton δ_H 2.90 allowed the assignment of H-3. While δ_C 55.6 and δ_C 55.2 did not display correlations with δ_H 3.43 and δ_H 3.38, δ_C 132.2 and δ_C 131.7 showed correlations with δ_H 3.43, δ_H 3.38, and δ_H 5.66–5.73. Furthermore, δ_H 5.66–5.73 displayed correlations with δ_C 55.6 and δ_C 55.2, allowing the complete assignment of C-4, C-5, C-6, and C-7 (**Table 7**).

Based on these spectroscopic data and a previous report (Matsumoto, Matsutani *et al.*, 1992), metabolite C was assigned as depudecin (**151**). The stereochemistry of depudecin (**151**) isolated in this work was identical to that of depudecin (**151**) in the literature by comparison of optical rotation ($[\alpha]_D$ = −35 (*c* 0.50, MeOH)), lit. ($[\alpha]_D$ = −36 (*c* 0.52, $CHCl_3$)).

Table 7 ^{1}H (500 MHz, $CDCl_3$) and ^{13}C (125 MHz, $CDCl_3$) NMR spectroscopic data of depudecin (**151**).

C/H #	δ_C	δ_H, multiplicity ($^{3}J_{HH}$, Hz)	HMBC
1	20.1	1.30, 3H, d (6.5)	2-OH
2	67.2	3.72, 1H, dq (4.5, 6.5)	H-1, H-3, 2-OH
3	64.4	2.90, 1H, dd (4.5, 2)	H-1
4	55.6	3.43–3.38, 1H m	H-5, H-6
5	132.2	5.69–5.66, 1H, m	H-4, H-6
6	131.7	5.73–5.69, 1H, m	H-5,H-7
7	55.2	3.43–3.42, 1H, m	H-5, H-6
8	62.7	3.01, 1H, dd (4.5, 2)	9-OH
9	71.8	4.13–4.11, 1H, m	H-8, 9-OH, H-10, H-11
10	136.2	5.92, 1H, ddd (5.5, 11, 17)	H-9, H-11, 9-OH
11	117.2	5.26, 1H, d (11); 5.39, 1H, d (17)	H-9
OH (C-2)	–	2.17–2.16, 1H, m	–
OH (C-9)	–	2.33–2.32, 1H, m	–

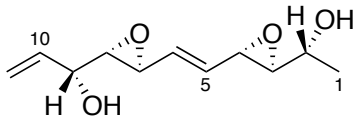

151

2.1.1.4 Dihydrobrassicicolin A

The purified metabolite D was analyzed by ^{1}H NMR and HPLC-ESI-MS. The HPLC-ESI-MS detected an ion peak at *m/z* 703 attributed to a mass shift of 18 from the molecular ion peak of brassicicolin A (at *m/z* 685 $[M+H]^+$). The HRESI-MS established $C_{32}H_{50}N_2O_{15}Na$ as molecular formula of a sodium adduct ion of metabolite D. The ^{1}H NMR spectrum of metabolite D showed high similarity to that of brassicicolin A (**1)** except for two proton signals at δ_H 8.30 and δ_H 8.26 (**Figure 2.4**). Those diagnostic proton signals suggested two isocyanide groups in brassicicolin A (**1**) might be hydrolyzed to two formamide groups (-NHCHO). Therefore, hydrolyzed brassicicolin A (**1**) was potentially assigned as a structure of metabolite D**.**

Hydrolysis of brassicicolin A

To confirm structure of metabolite D, chemical hydrolysis of brassicicolin A (**1**) was carried out in acidic conditions at room temperature. HPLC analysis showed that the reaction mixture contained the hydrolysis product (metabolite D, t_R = 23.3 min) as well as unidentified products. Thus, acidic hydrolysis of brassicicolin A (**1**) was carried out at 4 °C to prevent formation of byproducts (**Scheme 2.3**); the reaction was quenched and analyzed by HPLC-ESI-MS. A quasi-molecular ion peak at *m/z* 703 $[M\text{-}H_2O+H]^+$ was detected by HPLC-ESI-MS analysis.

Comparison of the ^{1}H NMR spectrum of brassicicolin A (**1**) and that of the reaction mixture suggested the presence of formamide groups (-NHCHO) in the reaction mixture (δ_H 8.30 and δ_H 8.26) due to a mixture of three epimers of metabolite D as shown in brassicicolin A (**1**). The ^{1}H NMR spectrum of acid-hydrolyzed brassicicolin A was identical to that of the isolated metabolite D obtained from fungal cultures. Thus, metabolite D was assigned as dihydrobrassiciolin A (**220**).

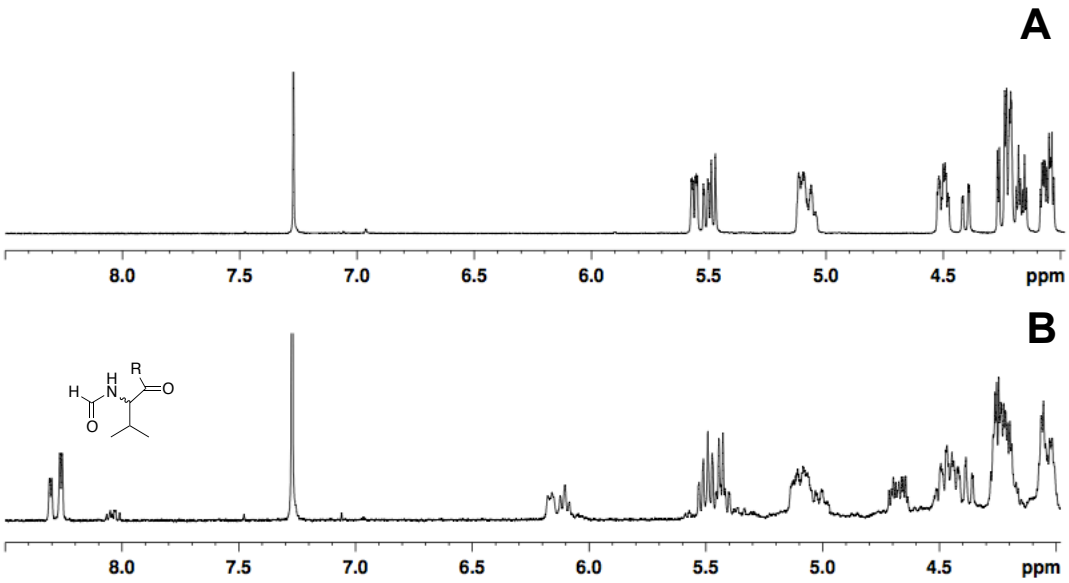

Figure 2.4 Partial ^{1}H NMR spectra of brassicicolin A (**1**, A) and metabolite D (**220**, B).

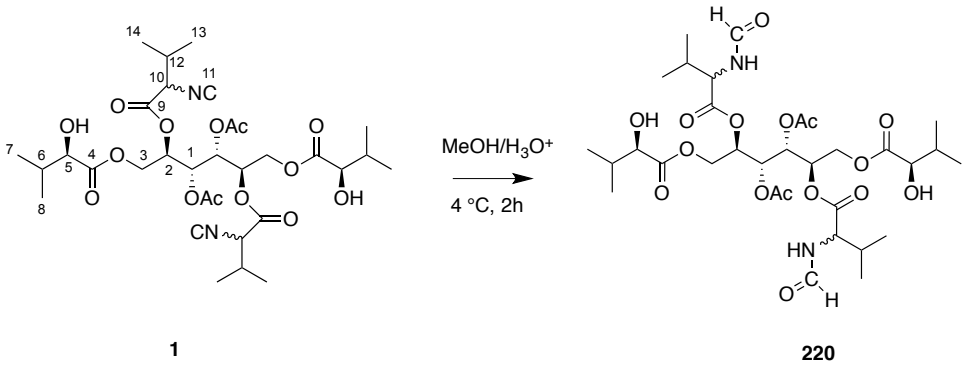

1 220

Scheme 2.3 Acidic hydrolysis of brassicicolin A (**1**).

To determine whether dihydrobrassicicolin A (**220**) is a fungal metabolite or results from spontaneous hydrolysis of brassicicolin A (**1**), brassicicolin A (**1**) was incubated in PDB at 30 °C. After 7 days (maximum production of brassicicolin A), PDB was extracted and brassicicolin A (**1**) and dihydrobrassicicolin A (**220**) were quantified. Brassicicolin A (**1**, 2.3 mg) was hydrolyzed (ca. 50%) spontaneously in PDB media in seven days (1.3 mg), indicating dihydrobrassicicolin A (**220**, 1.7 mg) is a hydrolysis product of brassicicolin A (**1**) formed spontaneously during incubation of *A. brassicicola* (Pedras and Park, 2015).

2.1.2 Modification of culture conditions and quantification of metabolites

Considering that cultures of *A. brassicicola* grown in MM produced more complex mixtures of metabolites than those grown in PDB (**Figure 2.1**), it was necessary to deconstruct the MM to determine the effects of some components on the biosynthesis of metabolites. Specifically, carbon and nitrogen sources are known to affect strongly the production and regulation of secondary metabolites of fungi (Tudzynski, 2014) (**Table 8**).

Table 8 Different culture conditions to grow *Alternaria brassicicola.*

Entry	Modification of standard MM and PDB [a]
1	Standard MM
2	High glucose (45 g/L, 250 mM)
3	Low glucose (3 g/L, 17 mM)
4	Sucrose (15 g/L, 44 mM) substitute for glucose
5	Fructose (15 g/L, 83 mM) substitute for glucose
6	Mannitol or sorbitol (15 g/L, 82 mM) substitute for glucose
7	No asparagine
8	No thiamine
9	Low KNO_3 (0.31 g/L, 3.1 mM)
10	$NaNO_3$ (2.5 g/L, 29 mM) substitute for KNO_3
11	Low $NaNO_3$ (0.25 g/L, 2.9 mM)
12	No nitrate
13	NH_4Cl (0.16 g/L, 3.0 mM) substitute for KNO_3
14	High ferric citrate (54 mg/L, 200 μM)
15	No ferric citrate
16	NaCl[b] (10 g/L)
17	PDB[c]

[a] All cultures were incubated at 23 °C and 30 °C unless stated otherwise.
[b] NaCl was added to 60-hour-old cultures of *A. brassicicola* in standard MM.
[c] PDB (potato dextrose broth) was considered a standard medium

2.1.2.1 Standard conditions and carbon sources

A. brassicicola was grown in modified MM (entries 1–16) and PDB (entry 17) at 23 °C and 30 °C. After seven days, cultures were filtered and mycelia were weighed. Culture filtrates were extracted with EtOAc and each extract was analyzed by HPLC-DAD. Five fungal metabolites (**1, 151, 25, 210**, and **219**) were also quantified using calibration curves (**Table 18**).

The cultures grown in MM (entry 1) and PDB (entry 17) were considered standard culture conditions at low and high temperatures (23 °C and 30 °C). The mycelial weights were

similar among standard conditions (entries 1 and 17), while cultures in PDB (entry 17) produced significantly larger amounts of extractable metabolites than standard MM (entry 1). In addition, high temperature led to increase in extract weights in either PDB or MM (**Table 9**) (Pedras and Park, 2015).

Table 9 Weights of mycelia and extract of culture filtrates of *Alternaria brassicicola* grown in modified MM and PDB.

Entry	Modification of standard MM and PDB[a]	Wet mycelia weight (g/100 mL)		Dry extracts of culture filtrates (mg/100mL)	
		23 °C	30 °C	23 °C	30 °C
1	Standard MM	$1.5 \pm 0.3^{g–j}$	$1.6 \pm 0.5^{g–l}$	3.7 ± 0.7^{abc}	$9 \pm 3^{a–f}$
2	High glucose	2.0 ± 0.1^{jkl}	2.0 ± 0.1^{jkl}	4.5 ± 0.7^{abc}	$11 \pm 1^{a–f}$
3	Low glucose	0.4 ± 0.1^{a}	0.4 ± 0.1^{a}	1.0 ± 0.4^{a}	2.8 ± 0.5^{ab}
4	Sucrose	2.2 ± 0.0^{l}	$1.1 \pm 0.2^{b–g}$	4 ± 3^{abc}	$10 \pm 2^{a–f}$
5	Fructose	$1.6 \pm 0.1^{g–k}$	$1.7 \pm 0.1^{h–l}$	$9.7 \pm 0.6^{a–f}$	$10 \pm 4^{a–f}$
6	Mannitol or sorbitol	No growth	No growth	No growth	No growth
7	No asparagine	$1.8 \pm 0.1^{i–l}$	2.0 ± 0.1^{jkl}	$8.7 \pm 0.8^{a–e}$	$9.1 \pm 0.7^{a–f}$
8	No thiamine	2.0 ± 0.1^{jkl}	2.1 ± 0.1^{jkl}	$6 \pm 1^{a–d}$	$7.9 \pm 0.7^{a–e}$
9	Low KNO_3	$1.4 \pm 0.1^{f–i}$	$0.8 \pm 0.0^{a–f}$	$12 \pm 4^{b-f}$	$19 \pm 10^{e–i}$
10	$NaNO_3$	2.1 ± 0.1^{kl}	$1.5 \pm 0.2^{g–j}$	$5.1 \pm 0.9^{a–d}$	$12 \pm 2^{a–f}$
11	Low $NaNO_3$	$1.2 \pm 0.1^{e–h}$	$0.6 \pm 0.1^{a–d}$	$10.4 \pm 0.6^{a–f}$	27 ± 2^{hi}
12	No nitrate	$0.7 \pm 0.1^{a–e}$	0.5 ± 0.0^{a}	$8.3 \pm 0.2^{a–e}$	27.0 ± 0.9^{hi}
13	NH_4Cl	$1.2 \pm 0.1^{d–h}$	0.5 ± 0.1^{abc}	$15 \pm 2^{c–g}$	$25 \pm 2^{g–i}$
14	High ferric citrate	$1.8 \pm 0.3^{i–l}$	$1.2 \pm 0.3^{e–h}$	$11 \pm 1^{a–f}$	$16 \pm 2^{d–h}$
15	No ferric citrate	0.5 ± 0.2^{ab}	0.3 ± 0.2^{a}	4.0 ± 0.2^{abc}	$20 \pm 10^{f–i}$
16	NaCl	$1.9 \pm 0.1^{i–l}$	1.4 ± 0.3^{ghi}	$6 \pm 1^{a–d}$	$14 \pm 3^{b–g}$
17	PDB	$1.6 \pm 0.1^{g–k}$	$1.1 \pm 0.1^{c–g}$	30 ± 10^{i}	51 ± 1^{j}

[a] PDB (potato dextrose broth) was considered a standard medium.

Values are means ± standard deviation of three replicates ($n \geq 3$) randomly selected in cases where $n > 3$. The means in each treatment were analyzed by one-way ANOVA with Tukey's test. Weights of wet mycelia and extracts of culture filtrates within the same column with the same letters are not significantly different at $P < 0.05$.

HPLC analysis of the extracts of culture filtrates obtained from standard conditions reveled that the amount of brassicicolin A (**1**) was approximately 10-fold larger in PDB than that in MM, while phomapyrone A (**25**), α-acetylorcinol (**210**) and tyrosol (**219**) were detected in relatively much smaller amounts than brassicicolin A (**1**) in all standard conditions. Furthermore, at 30 °C production of brassicicolin A (**1**) was increased, whereas production of depudecin (**151**) decreased (**Table 10**).

The metabolite profiles of cultures containing glucose (entry 1) as the carbon source were similar to those of cultures containing sucrose (entry 4), with no statistically significant differences. Reducing 5-fold the amount of glucose in the MM (entry 3) clearly affected both the mycelial growth and the extract weight, relative to standard cultures (entry 1). By contrast, increasing 3-fold the amount of glucose (entry 2) did not affect the mycelial mass or extract weight. Cultures grown in sucrose (entry 4) or fructose (entry 5) had similar mycelial weights and extract weights relative to control MM. However, *A. brassicicola* did not grow when sorbitol or mannitol were used as carbon sources (entry 6) (**Table 9** and **Table 10**) (Pedras and Park, 2015).

Table 10 Quantification by HPLC-DAD of the major metabolites produced by *Alternaria brassicicola* in minimal medium (MM), modified MM and potato dextrose broth (PDB).

	MM modification	Brassicicolin A (**1**) (µmol/100 mL)		Depudecin (**151**) (µmol/100 mL)		Phomapyrone A (**25**) (µmol/100 mL)		α-Acetylorcinol (**210**) (µmol/100 mL)		Tyrosol (**219**) (µmol/100 mL)	
		23 °C	30 °C	23 °C	30 °C	23 °C	30 C	23 C	30 C	23 C	30 C
1	Standard MM	2 ± 1^{a}	4 ± 2^{ab}	0.4 ± 0.4^{a}	0.04 ± 0.04^{a}	0.6 ± 0.2^{fg}	$0.4\pm0.2^{d–g}$	0.03 ± 0.01^{abc}	$0.07\pm0.05^{a–d}$	0.07 ± 0.02^{ab}	0.4 ± 0.1^{def}
2	High glucose	0.6 ± 0.3^{a}	1.4 ± 0.1^{a}	0^{a}	0^{a}	0.24 ± 0.02^{bcd}	0.60 ± 0.02^{g}	0.01 ± 0.00^{ab}	$0.04\pm0.01^{a–d}$	0.11 ± 0.02^{abc}	0.6 ± 0.2^{f}
3	Low glucose	0^{a}	0^{a}	0.03 ± 0.05^{a}	0^{a}	0.18 ± 0.02^{abc}	$0.35\pm0.09^{c–f}$	0^{a}	$0.06\pm0.02^{a–d}$	0^{a}	0^{a}
4	Sucrose	0.5 ± 0.2^{a}	3.7 ± 0.9^{ab}	0.2 ± 0.2^{a}	0.07 ± 0.07^{a}	$0.30\pm0.05^{b–e}$	0.23 ± 0.04^{bcd}	$0.16\pm0.06^{a–e}$	$0.38\pm0.05^{a–f}$	0^{a}	$0.29\pm0.05^{b–e}$
5	Fructose	3.2 ± 0.4^{ab}	2 ± 1^{a}	0.10 ± 0.04^{a}	0.07 ± 0.07^{a}	0.23 ± 0.04^{bcd}	0.31 ± 0.07^{cde}	$0.07\pm0.02^{a–d}$	$0.2\pm0.1^{a–e}$	0.03 ± 0.01^{a}	$0.24\pm0.09^{a–d}$
6	Sorbitol or mannitol	No growth	No growth	No growth	No growth	No growth	No growth	No growth	No growth	No growth	No growth
7	No asparagine	4 ± 2^{abc}	2.4 ± 0.0^{a}	0.9 ± 0.4^{ab}	0^{a}	0.29 ± 0.05^{bcd}	0.29 ± 0.05^{bcd}	$0.12\pm0.02^{a–e}$	$0.05\pm0.03^{a–d}$	0.05 ± 0.01^{a}	$0.2\pm0.2^{a–d}$
8	No thiamine	2.6 ± 0.7^{a}	3.2 ± 0.7^{ab}	0.8 ± 0.7^{ab}	0^{a}	0.50 ± 0.04^{efg}	0.6 ± 0.1^{g}	$0.05\pm0.02^{a–d}$	$0.1\pm0.1^{a–e}$	0.04 ± 0.00^{a}	$0.18\pm0.02^{a–d}$
9	Low KNO_3	2 ± 2^{a}	14 ± 4^{cde}	31 ± 10^{e}	12 ± 7^{d}	0^{a}	0^{a}	$0.6\pm0.2^{c–g}$	1.1 ± 0.4^{ghi}	0^{a}	0.4 ± 0.2^{def}
10	$NaNO_3$	0.8 ± 0.2^{a}	3 ± 1^{ab}	0^{a}	0^{a}	0.32 ± 0.03^{cde}	0.26 ± 0.04^{bcd}	0.01 ± 0.01^{ab}	$0.13\pm0.07^{a–e}$	0.06 ± 0.02^{ab}	$0.35\pm0.04^{c–f}$
11	Low $NaNO_3$	2.8 ± 0.6^{a}	15.2 ± 0.8^{de}	26 ± 4^{e}	10 ± 6^{cd}	0^{a}	0^{a}	$0.53\pm0.09^{b–f}$	1.4 ± 0.4^{i}	0^{a}	0^{a}
12	No nitrate	1.77 ± 0.06^{a}	16 ± 3^{e}	17 ± 6^{d}	9.5 ± 0.4^{bcd}	0^{a}	0^{a}	$0.42\pm0.06^{a–f}$	$0.6\pm0.1^{e–h}$	0^{a}	0^{a}
13	NH_4Cl	2.4 ± 0.5^{a}	$9\pm1^{a–e}$	12 ± 2^{d}	0.2 ± 0.1^{a}	0^{a}	0^{a}	$0.6\pm0.2^{e–h}$	1.1 ± 0.3^{hi}	0^{a}	0^{a}
14	High ferric citrate	3 ± 1^{a}	$6\pm2^{a–d}$	0.03 ± 0.03^{a}	0.04 ± 0.05^{a}	0.19 ± 0.05^{abc}	0.17 ± 0.06^{abc}	0.02 ± 0.02^{ab}	$0.08\pm0.06^{a–d}$	0.01 ± 0.01^{a}	0.42 ± 0.06^{def}
15	No ferric citrate	4 ± 2^{abc}	$13\pm9^{b–e}$	0^{a}	0.4 ± 0.3^{a}	$0.35\pm0.04^{c–f}$	0.28 ± 0.05^{bcd}	0^{a}	$0.09\pm0.02^{a–d}$	0^{a}	0^{a}
16	NaCl	2.3 ± 0.3^{a}	$9\pm4^{a–e}$	0.05 ± 0.04^{a}	0.1 ± 0.1^{a}	0.18 ± 0.01^{abc}	0.10 ± 0.02^{ab}	$0.12\pm0.05^{a–e}$	$0.6\pm0.4^{d–g}$	0.06 ± 0.01^{ab}	0.5 ± 0.1^{ef}
17	PDB	33 ± 12^{f}	33 ± 1^{f}	2.0 ± 0.9^{ab}	0.9 ± 0.2^{abc}	0^{a}	0^{a}	0.7 ± 0.1^{fgh}	1.1 ± 0.4^{ghi}	0^{a}	0^{a}

Note: Values are means ± standard deviation of three replicates ($n \geq 3$) randomly selected in cases where $n > 3$. The means in each treatment were analyzed by one-way ANOVA with Tukey's test. Values with the same letters within each metabolite column are not significantly different at $P < 0.05$; 0 µmol/100 mL indicates that metabolites are not detected under reported conditions; minimum detectable amounts at 220 nm: brassicicolin A (**1**) = 1.25 nmoles, depudecin (**151**) = 0.063 nmoles, phomapyrone A (**25**) = 0.025 nmoles, α-acetylorcinol (**210**) = 0.005 nmoles, tyrosol (**219**) = 0.005 nmoles.

2.1.2.2 Effect of nitrogen sources

MM has two nitrogen sources: KNO_3 (3.1 g/L, 31 mM, inorganic component) and asparagine (0.28 g/L, 2.1 mM, organic component). The preliminary results of cultures incubated in low concentration of KNO_3 (3 mM) showed a substantial increase in depudecin (**151**) at 23 °C and brassicicolin A (**1**) at 30 °C. These results led to an analysis of effects of nitrogen on metabolite profiles of *A. brassicicola*. A 10-fold decrease in the amount of nitrate (entry 11) or its complete removal (entry 12) caused an increase in extract weights, whereas replacing KNO_3 with $NaNO_3$ (entry 10) did not affect extract weights. Similarly, substituting NH_4Cl for KNO_3 (entry 13) increased extract weights at 30 °C. High temperature (30 °C) negatively affected mycelial growth in nitrogen limitation conditions, while extract weights were significantly increased (**Table 9**) (Pedras and Park, 2015).

The HPLC chromatograms of culture extracts obtained from low nitrogen (3 mM) showed that α-acetylorcinol (**210**), depudecin (**151**), and brassicicolin A (**1**) were detected, whereas other metabolites were detected in extremely low amounts (**Figure 2.5**). Interestingly, a low concentration of nitrate (sodium or potassium) or complete removal of nitrate from MM increased significantly the production of brassicicolin A (**1**) at 30 °C, depudecin (**151**) 23 °C and α-acetylorcinol (**210**) at 30 °C (entries 8, 10 and 11). Similarly, low NH_4Cl increased the amounts of depudecin (**151**) at 23 °C and α-acetylorcinol (**210**) at 23 °C and 30 °C (entry 12).

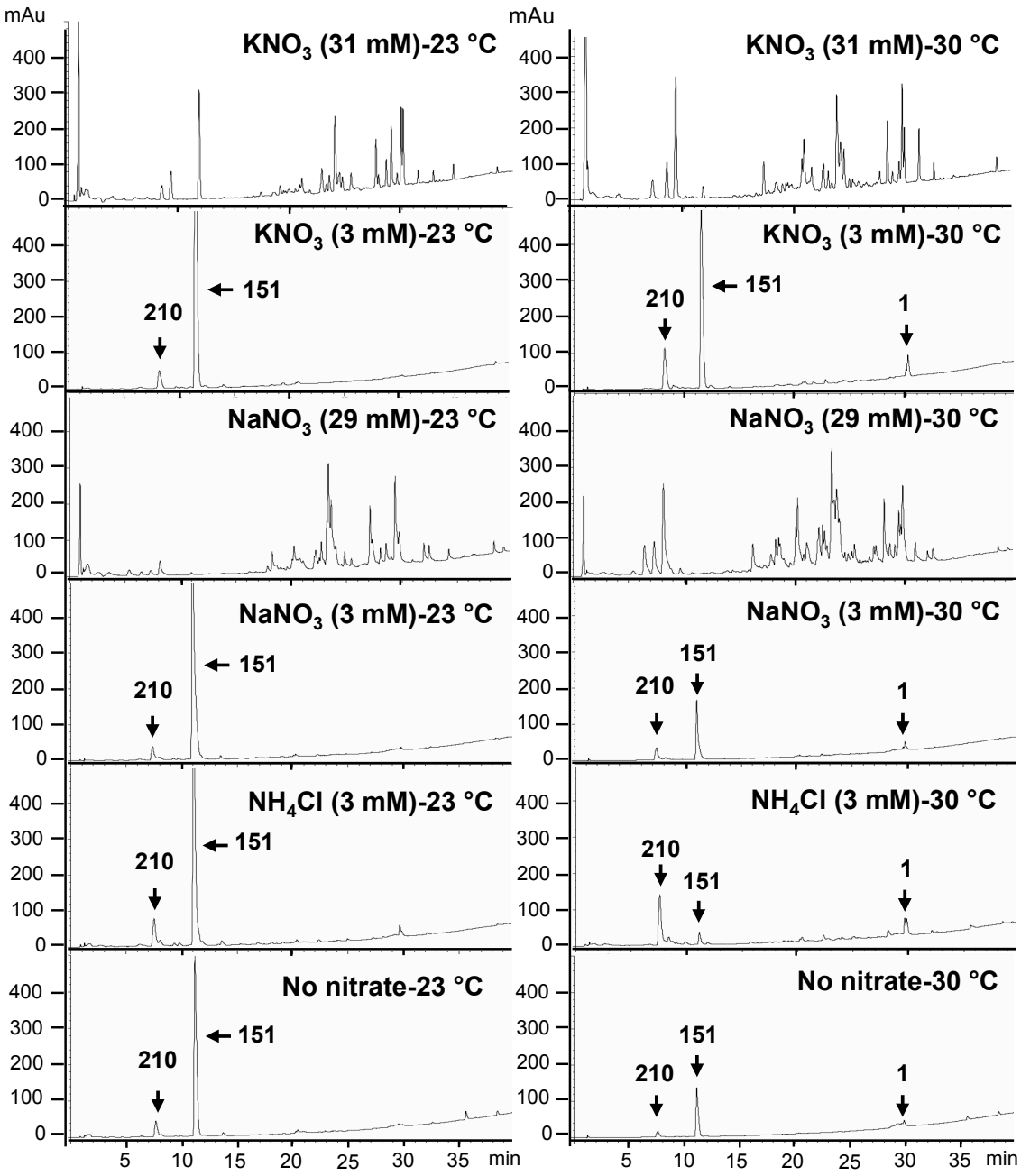

Figure 2.5 HPLC-DAD chromatograms (method A, detection 220 nm) of extracts of the culture filtrates of *Alternaria brassicicola* grown under different nitrogen sources: Arrows indicate α-acetylorcinol (**210**, t_R = 8.4 min), depudecin (**151**, t_R = 11.6 min), and brassicicolin A (**1**, t_R = 29.5 min).

A. brassicicola grown under low concentration of nitrogen showed darker mycelia at either temperature (**Figure 2.6**). To examine the cause of this darker color, mycelia obtained from nitrogen-depleted conditions were extracted in either neutral or acidic condition. However, the extraction of dark pigments from mycelia was unsuccessful.

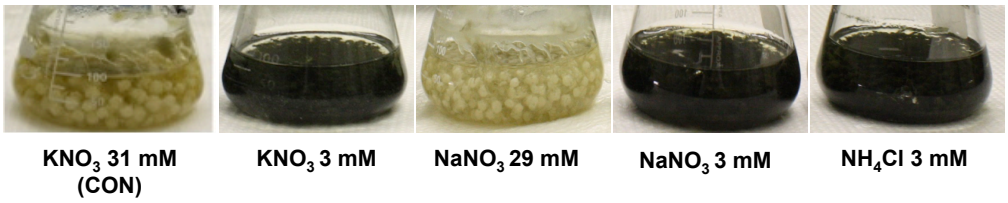

Figure 2.6 *Alternaria brassicicola* (7-d-old) grown under different nitrogen sources.

2.1.2.3 Iron and siderophores

MM has ferric citrate (0.54 mg/L, 2 μM) as a sole iron source. To determine whether ferric citrate affects the metabolite profiles of *A. brassicicola*, three different concentrations of ferric citrate were tested: 0, 2, and 200 μM. A 100-fold increase in ferric citrate (entry 14) showed similar mycelial weight, while extract weights were not significantly different compared to control (2 μM) cultures. Complete removal of ferric citrate from MM (entry 15) significantly inhibited mycelial growth (**Table 9**) whereas high ferric citrate (entry 14) exhibited similar metabolites profiles compared to standard MM (**Table 10**).

Siderophores

The production of siderophores in cultures of *A. brassicicola* in the absence of Fe^{3+} was investigated in more detail. Five-day-old cultures were examined for production of siderophores by HPLC-ESI-MS and colorimetric detection at 435 nm (absorption is due to chelation of hydroxamic acids with $FeCl_3$) (Jalal, Love *et al.*, 1988; Konetschny-Rapp, Huschka *et al.*, 1988). Culture broths grown in MM without ferric citrate showed a stronger reddish color than cultures grown in either standard MM (2 μM) or high ferric citrate (200 μM), suggesting a higher concentration of siderophores in MM without ferric citrate as previously reported (Oide, Moeder *et al.*, 2006) (**Figure 2.7**).

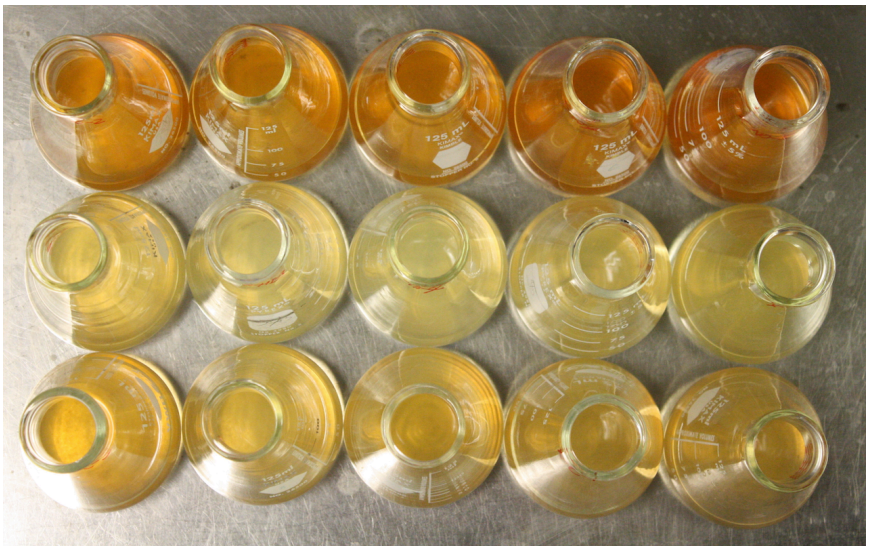

Figure 2.7 Culture filtrates of *Alternaria brassicicola* after addition of $FeCl_3 \cdot 6H_2O$: Top row, cultures grown in ferric citrate 0 µM; middle row, ferric citrate 200 µM; bottom row, ferric citrate 2 µM.

The extracellular siderophores were partially purified using an amberlite XAD-4 column by elution with MeOH. Eluents having red coloration were collected and analyzed by HPLC-ESI-MS and HR-LC-ESI-MS. The MeOH-fractions contained several peaks that are not detected in EtOAc extracts. Removal of ferric citrate significantly increased production of siderophores, whereas high ferric citrate and control showed similar metabolite profiles (**Figure 2.8**). UV and high resolution mass spectra (HR-ESIMS) suggest that the structures of the components are dimerumic acid (**184**, t_R = 9.0 min, *m/z* = 538), unknown (t_R = 11.1 min, *m/z* = 824), *N,N*-dimethyltriornicin (**221**, t_R = 11.3 min, *m/z* = 738), coprogen B (**222**, t_R = 11.7 min, *m/z* = 780), N^{α}-methylcoprogen B (**223**, t_R = 12.0 min, *m/z* = 794), hydroxycoprogen (**180**, t_R = 12.2 min, *m/z* = 838), *N,N*-dimethylcoprogen (**179**, t_R = 12.6 min, *m/z* = 808) and neocoprogen I (**177**, t_R = 12.9 min, *m/z* = 752) (**Table 11**). Furthermore, the presence of peaks of low intensity at *m/z* 752 (808-56), 768 (824-56) and 682 (738-56) indicated loss of Fe^{3+} from the respective quasi-molecular ions $[M-56]^+$, which is consistent with the structures of these siderophores (Hider and Kong, 2010). In addition, their UV spectra were similar to published data (Konetschny-Rapp, Huschka *et al.*, 1988).

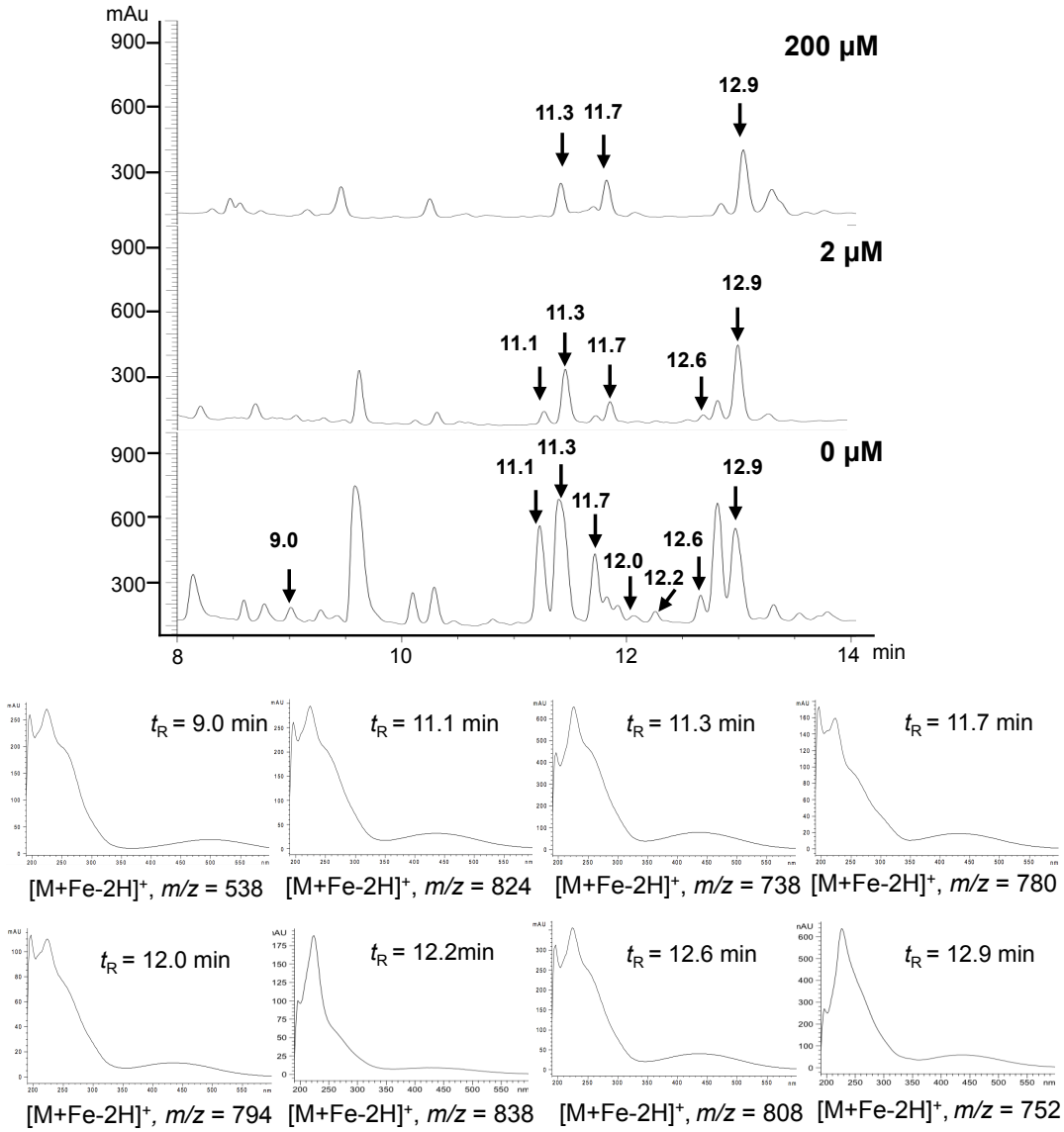

Figure 2.8 HPLC chromatograms (method D, detection 220 nm), and UV spectra of MeOH fractions obtained from culture filtrates-$FeCl_3$ of *A. brassicicola* grown under different concentrations of ferric citrate. t_R = 9.0 min, dimerumic acid (**184**); t_R = 11.1 min, unknown; t_R = 11.3 min, *N,N*-dimethyltriornicin (**221**); t_R = 11.7 min, coprogen B (**222**); t_R = 12.0 min, N^{α}-methylcoprogen B (**223**); t_R = 12.2 min, hydroxycoprogen (**180**); t_R = 12.6 min, *N,N*-dimethylcoprogen (**179**); t_R = 12.9 min, neocoprogen I (**177**).

Table 11 High resolution mass spectral data of siderophores produced by *Alternaria brassicicola*.

t_R	Siderophores	Molecular formula	Observed value as $[M+Fe-2H]^+$, *m/z*	mDa error
9.0	Dimerumic acid (**184**)	$C_{22}H_{34}FeN_4O_8$	538.1777	5.64
11.3	*N,N*-Dimethyltriornicin (**221**)	$C_{31}H_{50}FeN_6O_{11}$	738.2955 369.6521[a]	7.35 8.77
11.7	Coprogen B (**222**)	$C_{33}H_{52}FeN_6O_{12}$	780.3086 390.6573[a]	9.88 8.61
12.0	N^{α}-methylcoprogen B (**223**)	$C_{34}H_{54}FeN_6O_{12}$	794.3315 397.6651[a]	17.14 8.56
12.2	Hydroxycoprogen (**180**)	$C_{35}H_{54}FeN_6O_{14}$	838.3163	12.11
12.6	*N,N*-Dimethylcoprogen (**179**)	$C_{35}H_{56}FeN_6O_{12}$	808.3263 404.6704[a]	-3.7 3.5
12.9	Neocoprogen I (**177**)	$C_{31}H_{48}FeN_6O_{12}$	752.2757	8.29

[a] Doubly charged ions

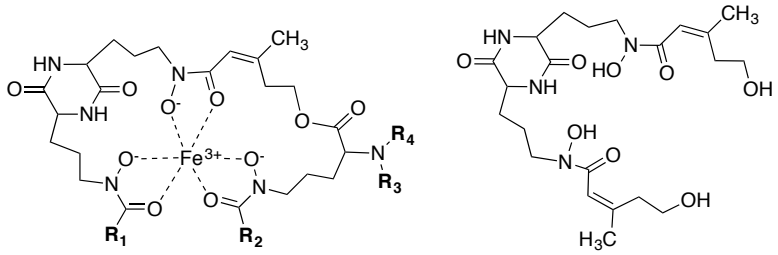

184

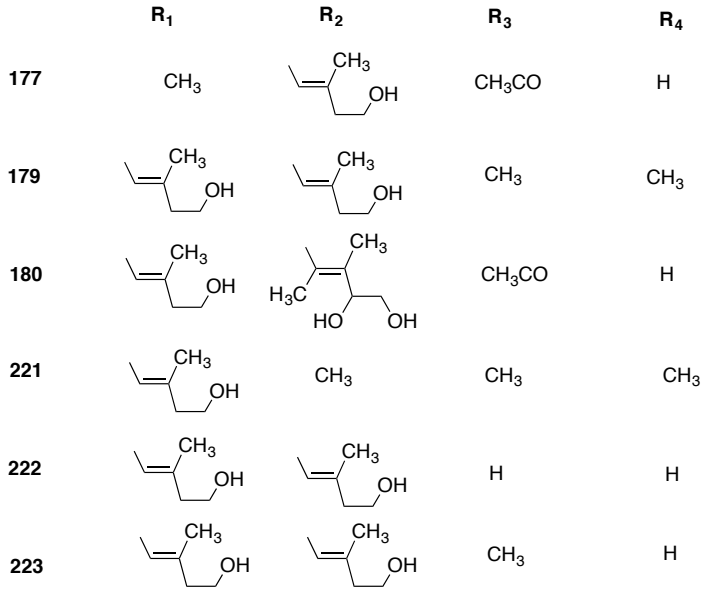

To examine whether the EtOAc extracts of the second half culture filtrate contain siderophores, the extracts were analyzed by HPLC-ESI-MS. Siderophores were detected in EtOAc extract of culture filtrates grown in Fe^{3+} depleted MM and standard MM, albeit in relatively lower amount than when using fractionation by XAD-4 column (Pedras and Park, 2015).

2.1.2.4 Other conditions

Removal of asparagine or thiamine from MM did not appear to affect the metabolite profiles of *A. brassicicola,* but decreased the amount of phomapyrone A (**25**) at 23 °C compared to standard MM (entry 1). Since a ten-fold increase in NaCl (entry 16) completely inhibited conidia germination, NaCl was added to 60-hour-old cultures. No significant effects of NaCl on the mycelial growth or the fungal metabolites were observed. (**Table 9** and **Table 10**)

2.1.3 Epigenetic modifiers

DNA methyltransferase and HDAC inhibitors are epigenetic modifiers known to induce metabolites present in orphan pathways in fungi and bacteria (Scherlach and Hertweck, 2009; VanderMolen, Darveaux *et al.*, 2014; Williams, Henrikson *et al.*, 2008). For example, SAHA (**32**) SBHA (**33**), and 5-Aza (**35)** triggered modifications of the secondary metabolite profiles of various fungal species (**Table 1**). In this context, two HDAC inhibitors (SAHA **32**, and SBHA **33**) and a DNA methyltransferase inhibitor (5-Aza, **35**) were tested to determine whether these epigenetic modifiers affect *A. brassicicola* metabolite profiles.

2.1.3.1 Synthesis of SAHA and SBHA

Two histone deacetylase inhibitors, SAHA (**32)** and SBHA (**33)** were synthesized according to published procedures (Mai et al., 2001). Synthesis of SAHA (**32**) was carried out from suberic acid (**224**) by refluxing with Ac_2O. Aniline was added to the cyclic anhydride **225** to yield acid **226**. In the final step, SAHA (**32**) was obtained upon treatment with hydroxylamine solution in overall 22% yield. The synthesis of SBHA (**33**) was accomplished by adding freshly prepared hydroxylamine solution to suberic acid (**224**) in quantitative yield (**Scheme 2.4**).

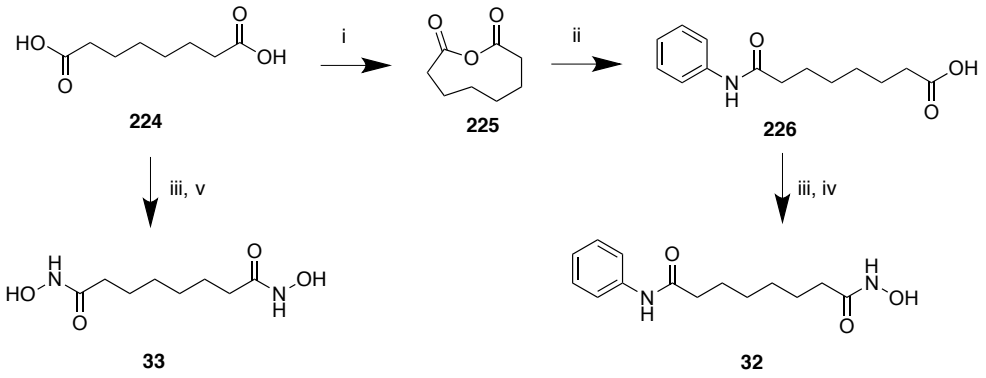

Scheme 2.4 Synthesis of suberoylanilide hydroxamic acid (SAHA, **32**) and suberoyl bis-hydroxamic acid (SBHA, **33**). Reagents and conditions: (i) Ac_2O, reflux 1h; (ii) Aniline, rt, 30 min, 40% yield over two steps; (iii) $ClCO_2Me$, Et_3N in ice-water bath, (iv) $NH_2OH{\cdot}HCl$, KOH in ice-water bath, 55% yield over two step; (v) $NH_2OH{\cdot}HCl$, Na_2CO_3 0 °C, quantitative for SBHA (**33**).

2.1.3.2 Administration of epigenetic modifiers

To investigate effects of histone deacetylase inhibitors on induction of secondary metabolism of *A. brassicicola,* the fungal spores were incubated in presence of SAHA (**32**) and SBHA (**33**) in standard MM. After seven days, the culture filtrates of *A. brassicicola* were extracted and analyzed by HPLC-DAD. Those culture extracts were compared with control culture extracts to examine whether SAHA (**32**) or SBHA (**33**) affects metabolite profiles of *A. brassicicola*.

The HPLC chromatograms of culture extracts of *A. brassicicola* grown in MM containing SAHA (**32**) were similar to those of control cultures in MM, except for an increase in metabolite E (t_R = 12.9 min, method A) and a decrease in SAHA (**32**) (**Figure 2.9**). On the other hand, the HPLC chromatograms of extracts of the culture filtrates containing SBHA (**33**) were similar to those of extracts of the culture filtrates in standard MM. While the extracts of culture filtrates containing 5-Aza (**35**) exhibited similar metabolite profiles compared to standard culture, 5-Aza (**35**) appeared to reduce amounts of metabolites of the *A. brassicicola* (**Figure 2.9**)

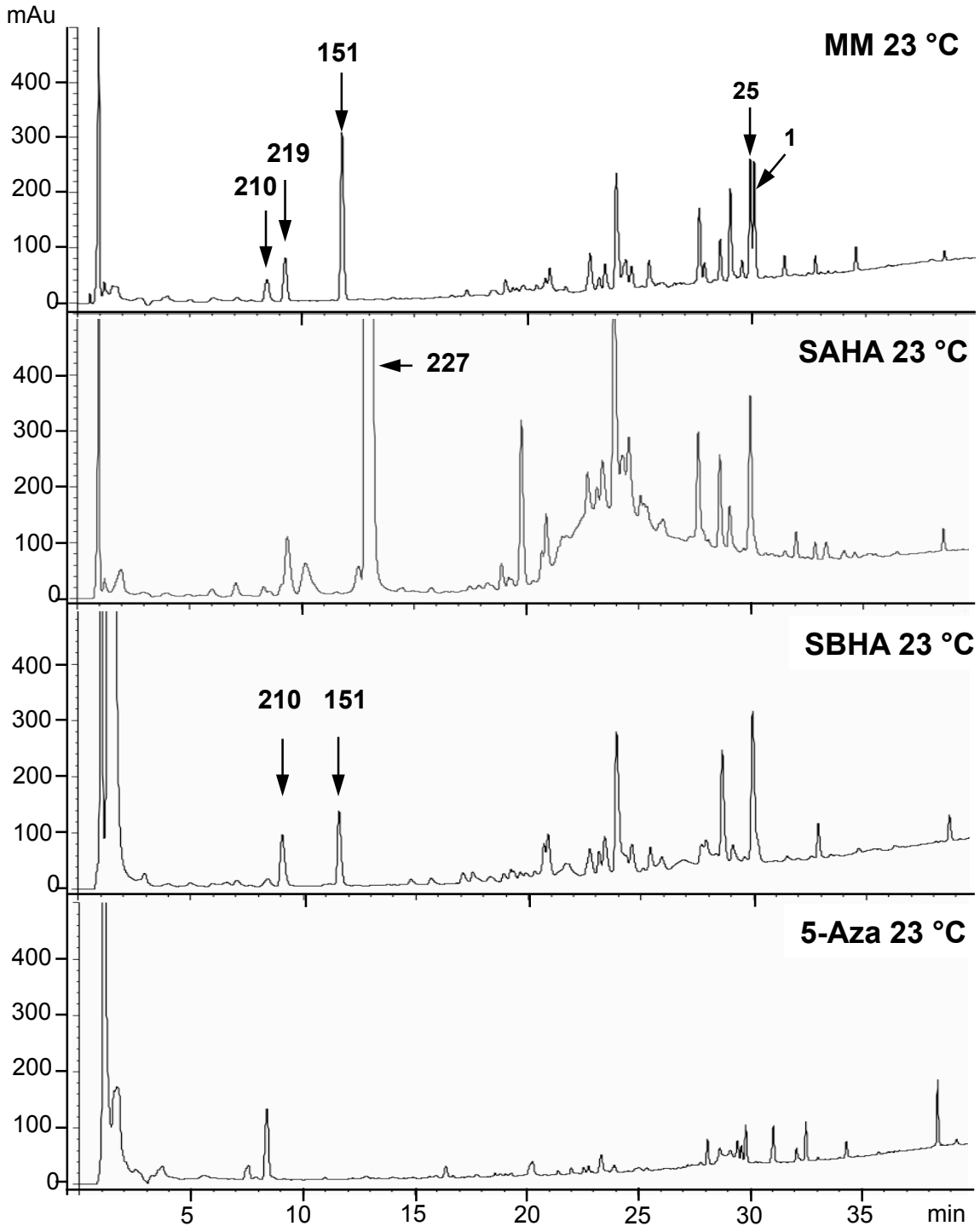

Figure 2.9 HPLC-DAD chromatograms of extracts of the *Alternaria brassicicola* culture filtrates incubated with SAHA (**32**, 0.50 mM), SBHA (**33**, 0.50 mM) or 5-Aza (**35**, 0.30 mM) (method A, detection 220 nm): Metabolite E (**227**), t_R = 12.9 min.

N-*Phenylacetamide (**227**)*

The chemical structure of the metabolite E (t_R = 12.9 min) was elucidated after purification of the culture filtrate extract followed by analyses by ^{1}H NMR and MS spectroscopy. The molecular formula obtained by HREI-MS analysis (*m/z* 135.0688, C_8H_9NO) indicated five degrees of unsaturation. The ^{1}H NMR spectrum displayed spin systems; one spin system containing five aromatic protons and another a singlet of three protons at 2.19 ppm. Based on these spectroscopic data, the structure of this metabolite was assigned as *N*-phenylacetamide (**227**), and was confirmed by comparison with an authentic sample, prepared by standard acetylation of aniline using acetic anhydride.

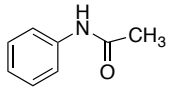

227

2.1.3.3 Biotransformation of SAHA

The time course analysis of SAHA (**32**) in cultures of *A. brassicicola* was carried out to examine the biotransformation of SAHA (**32**). Cultures incubated with SAHA (**32**) and *N*-phenylacetamide (**227**) were monitored for 5 days using HPLC-DAD. The stability of SAHA (**32**) in standard MM was also examined. The concentration of SAHA (**32**) remained constant for the first 24 h and decreased faster at 30 °C than at 23 °C. HPLC analysis of cultures incubated with SAHA (**32**) indicated that *A. brassicicola* completely transformed SAHA (**32**) to *N*-phenylacetamide (**227**) at 30 °C in five days, while at 23 °C SAHA (**32**) was converted much slower (**Figure 2.10**).

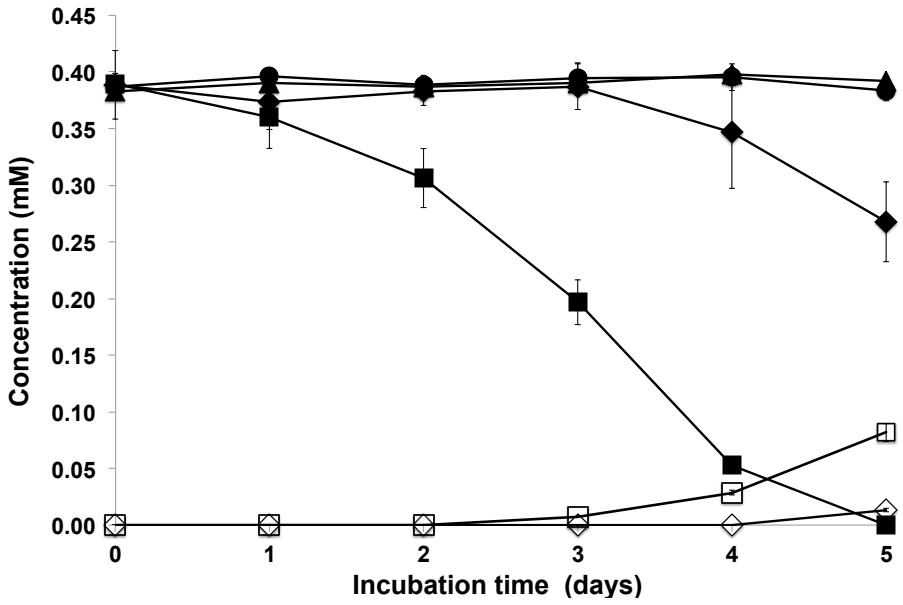

Figure 2.10 Progress curve of biotransformation of SAHA (**32**, 0.40 mM) by *Alternaria brassicicola*: ◆ SAHA (**32**) + *A. brassicicola* at 23 °C; ■ SAHA (**32**) + *A. brassicicola* at 30 °C; ● SAHA (**32**) at 23 °C;▲ SAHA (**32**) at 30 °C; ◇ *N*- phenylacetamide (**227**), 23 °C; □ *N*-phenylacetamide (**227**) 30 °C.

2.1.3.4 Biotransformation of aniline

Biotransformation of SAHA (**32**) suggested that *A. brassicicola* might enzymatically hydrolyze SAHA (**32**) followed by enzymatic acetylation of aniline (**228**). To confirm this hypothesis, aniline (**228**) was added to standard MM and the cultures were monitored by HPLC-DAD. Aniline (**228**) was added to two-day-old cultures of *A. brassicicola*. Cultures were collected at different time intervals and then lyophilized immediately. The lyophilized cultures were dissolved in water and analyzed by HPLC-DAD. *A. brassicicola* started to biotransform aniline (**228**) to *N*-phenylacetamide (**227**) four hours after addition of aniline (**228**) (**Figure 2.11** and **Figure 2.12**) and formation of *N*-phenylacetamide (**227**) increased up to 48 h with no further changes. Quantification of aniline (**228**) was not feasible because it formed an adduct with glucose (**230**, t_R = 8.7 min, method C). The amount of this adduct did not change in control cultures, but decreased as *N*-phenylacetamide (**227**) was formed (**Figure 2.12**). Elucidation of the structure of this product follows.

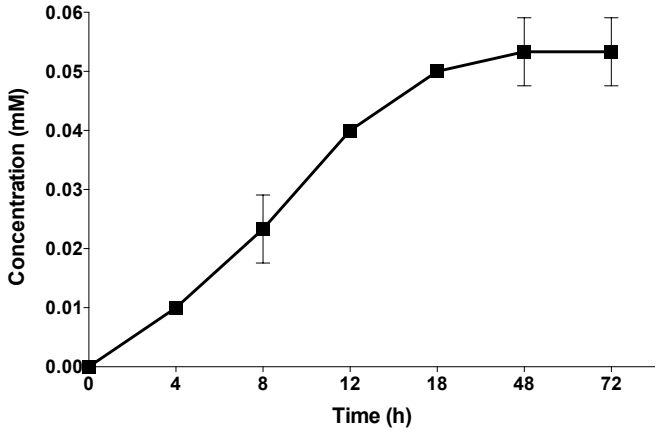

Figure 2.11 Progress curve of formation of *N*-phenylacetamide (**227**) from aniline (**228**) in cultures of *Alternaria brassicicola* in MM at 23 °C: ■ *N*-phenylacetamide (**227**).

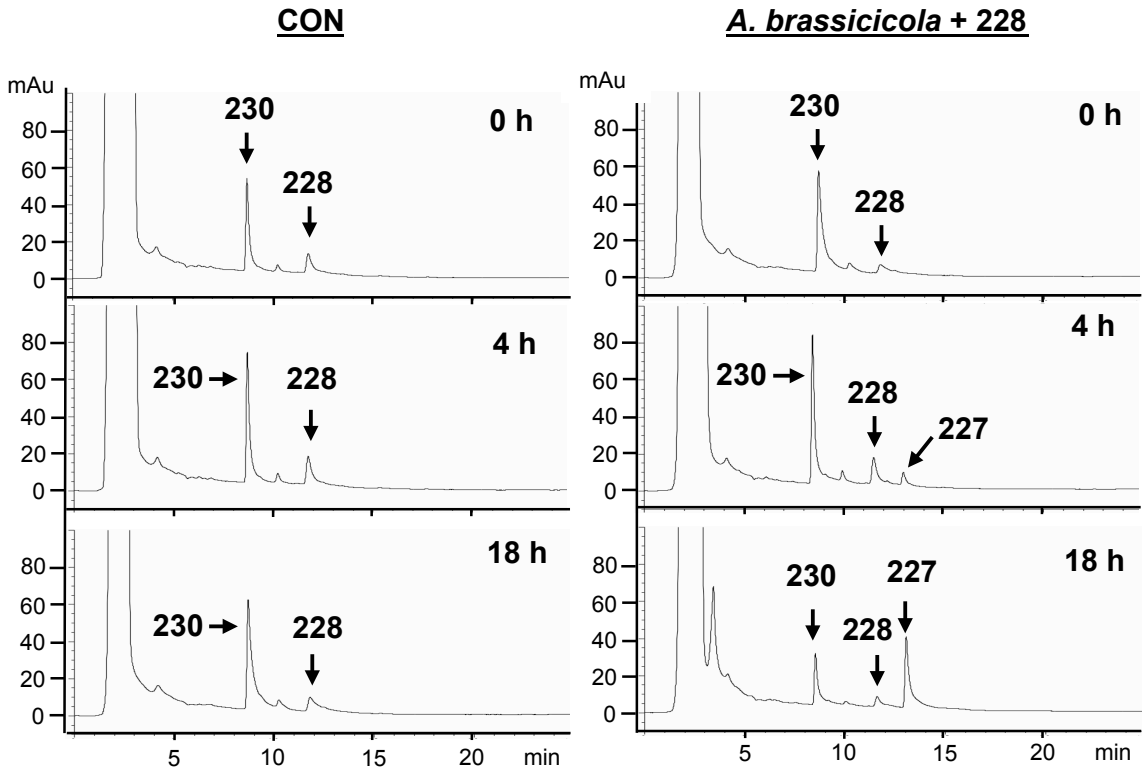

Figure 2.12 HPLC-DAD chromatograms (method C, detection 220 nm) of cultures of *Alternaria brassicicola*: CON, standard MM containing 0.20 mM aniline (**228**); *A. brassicicola* was incubated in MM containing 0.20 mM aniline (**228**).

First, the stability of aniline (**228**) in H_2O was examined. Aniline (**228**) was dissolved in H_2O (0.20 mM), and the solution was analyzed by HPLC-DAD. The concentration of aniline (**228**) remained constant, suggesting it was stable in H_2O (**Figure 2.13**). Next, aniline (**228**) was added to MM without glucose and with glucose, and the solutions were analyzed by HPLC-DAD. A product was detected only in MM containing glucose and aniline (**228**), whereas it was not detected in MM without glucose (**Figure 2.13**).

To characterize the unknown product, aniline (**228**) and glucose (**229**) were stirred in H_2O at room temperature and the reaction was monitored by HPLC-DAD. The HPLC chromatograms showed an increase in the peak area of the unknown component (t_R = 8.7 min) and a decrease in aniline (**228**) as the reaction progressed (**Figure 2.13**). The solution was lyophilized and then analyzed by NMR spectroscopy. The ^{1}H NMR and ^{13}C NMR spectra of this reaction mixture showed the characteristic anomeric carbon and proton signals of α- and β-D-glucopyranoses (δ_C 92.8 and 96.6 ppm; δ_H 4.59 and 5.17 ppm), in addition to δ 85.5 ppm and δ 4.72 ppm (1H, d, 8.8 Hz), respectively. The chemical shifts of the anomeric carbon and proton signals of α- and β-D-glucopyranoses were similar to those of published data (Roslund, Tähtinen *et al.*, 2008). The additional ^{1}H NMR and ^{13}C NMR spectral data suggested that the unknown component was *N*-β-D-glucopyranosyl aniline (**230**) (Bridiau, Benmansour *et al.*, 2007) (**Scheme 2.5**).

Quantification of *N*-phenylacetamide (**227**) in the extract of culture filtrates of *A. brassicicola* showed that only ca. 25% of aniline (**228**) was converted to *N*-phenylacetamide (**227**) by *A. brassicicola* in 48 h.

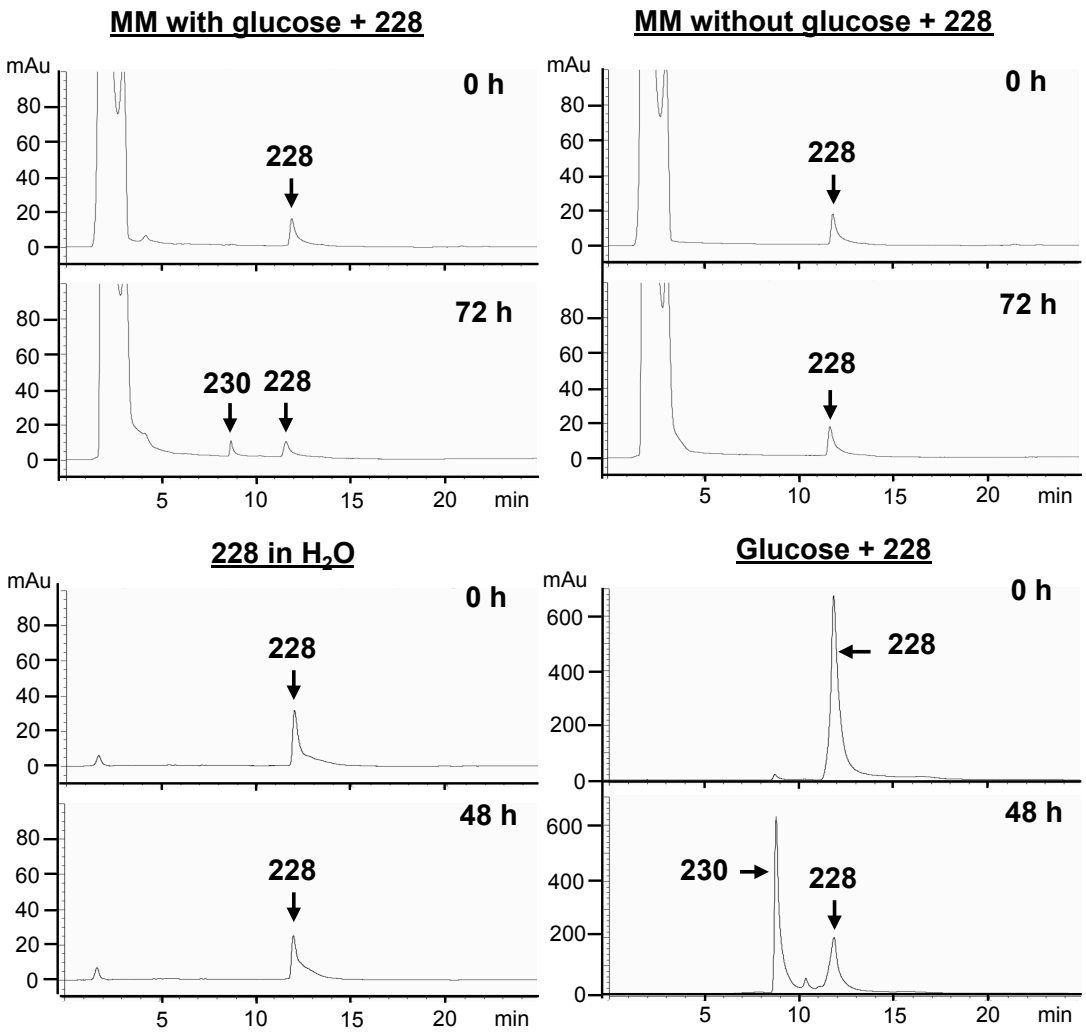

Figure 2.13 HPLC-DAD chromatograms (method C, detection 220 nm) of MM (aniline (**228**) with glucose and without glucose) and aniline (**228**) in H_2O.

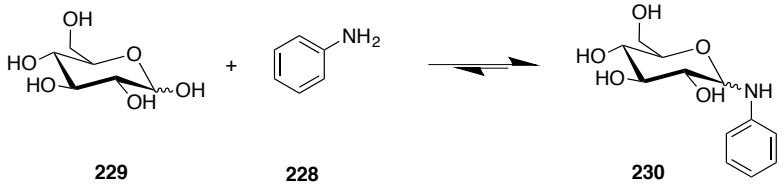

Scheme 2.5 Reaction of aniline (**228**) with glucose.

2.1.4 Co-cultivation of *A. brassicicola* and *A. brassicae*

Alternaria black spot disease in most Brassica species is caused by *A. brassicae*, *A. brassicicola*, and *A. raphani*. It was hypothesized *A. brassicicola* might produce potential phytotoxin(s) that are not present in standard growth conditions if *A. brassicicola* was co-incubated with either *A. brassicae* or *A. raphani*. Hence, *A. brassicicola* and *A. brassicae* were co-cultivated in PDB and MM to examine changes in metabolite production of *A. brassicicola*.

Two weeks later, culture broths obtained from each 6-well plate were extracted and then analyzed by HPLC-DAD. HPLC analyses of culture extracts of *A. brassicae* indicated that *A. brassicae* produced destruxin B (**123**, t_R = 29.6 min, Method A) and homodestruxin B (**129**, t_R = 30.5 min, Method A) in both PDB and MM. Metabolite profiles of co-inoculation were similar to those of *A. brassicicola* in either PDB or MM. However, destruxin B (**123**) and homodestruxin B (**129**) did not appear to be produced by *A. brassicae* in co-culture regardless of media. It indicates that *A. brassicicola* might dominate in these growth conditions leading to less growth of *A. brassicae* in co-culture with *A. brassicicola*.

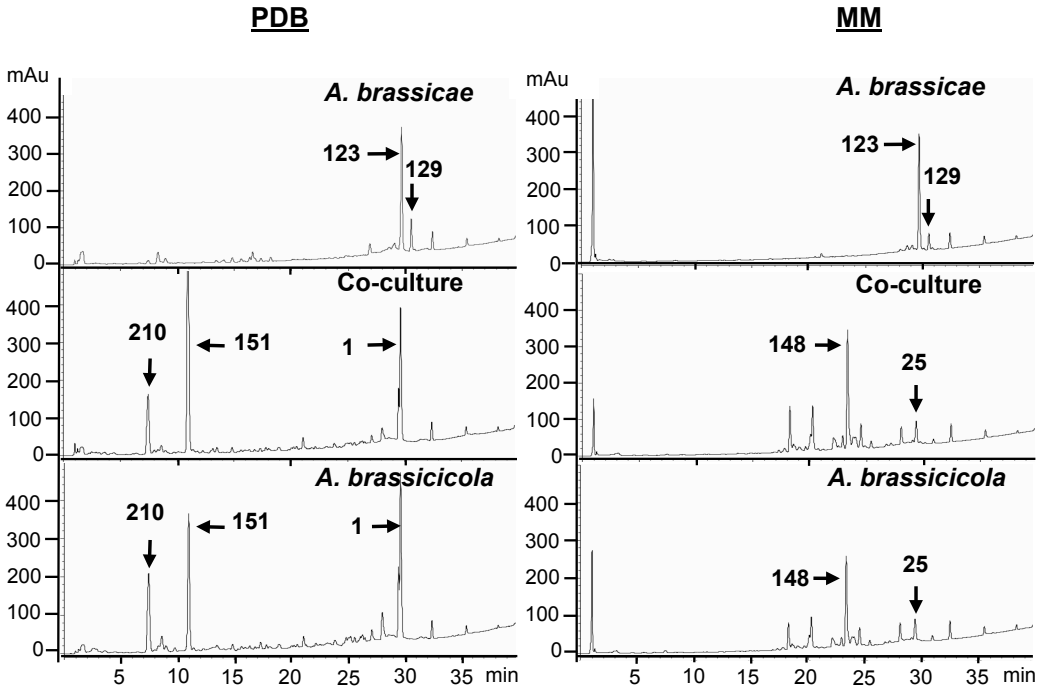

Figure 2.14 HPLC-DAD chromatograms (method A, detection 220 nm) of culture extracts of *Alternaria brassicae*, co-culture, and *A. brassicicola.*

2.1.5 Biological activity - conidia germination

To determine if any of the metabolites produced by *A. brassicicola* affects its conidia germination and germ tube growth, a microplate reader was used to evaluate conidial germination over a period of 36 h. Cultures of *A. brassicicola* in MM amended with brassicicolin A (**1**), depudecin (**151**), α-acetylorcinol (**210**), and tyrosol (**219**) were incubated in 48-well microplates. Comparison of the absorbance of wells containing conidia incubated with the various compounds (**Figure 2.15**) indicated that brassicicolin A (**1**) caused a slight inhibition of spore germination and mycelial growth at early growth stages, but no other effects were registered relative to control wells. In addition, similar experiments were carried out with SAHA (**32**), which displayed no effect on conidial germination relative to control cultures.

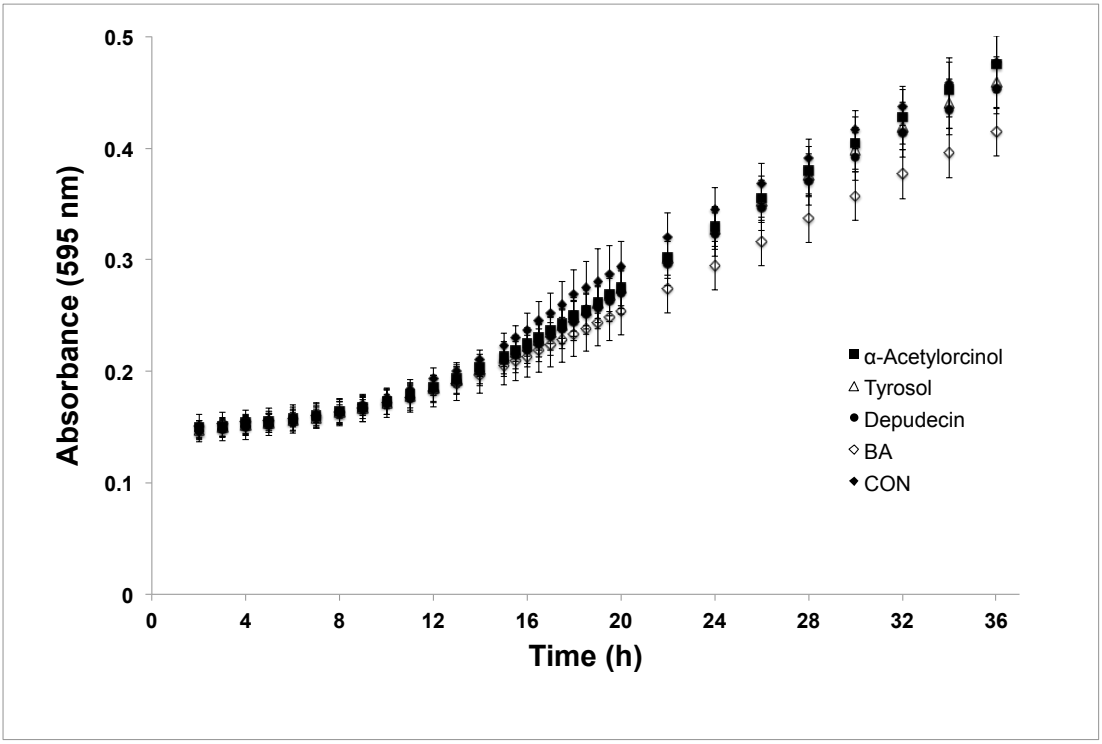

Figure 2.15 Growth curve of *Alternaria brassicicola* in MM containing four fungal metabolites (all metabolites at 0.50 mM).

2.1.6 Discussion

A comprehensive investigation of the metabolites produced by *A. brassicicola* under various culture conditions was carried out. Four metabolites—α-acetylorcinol (**210**), tyrosol (**219**) depudecin (**151**), dihydrobrassicicolin A (**220**)—were isolated from the extract of *A. brassicicola* culture filtrates and their structures were elucidated (Pedras and Park, 2015). The synthesis of α-acetylorcinol (**210**) was accomplished for the first time (Pedras and Park, 2015). It was reported that both tyrosol (**219**) and α-acetylorcinol (**210**) were isolated from cultures of fungal plant pathogens including *A. tagetica* (Gamboa-Angulo, García-Sosa *et al.*, 2001), *Stagonospora apocyni* (Venkatasubbaiah, Baudoin *et al.*, 1992) and *Ceratocystis species* (Ayer, Browne *et al.*, 1986).

Production of secondary metabolites of *A. brassicicola* is strongly affected by culture conditions, specifically temperature, nitrogen sources, and ferric ion (Pedras and Park, 2015). Production of brassicicolin A (**1**) was increased in low nitrate conditions at 30 °C, whereas depudecin (**151**) production was increased in media containing low amounts of nitrate at 23 °C, compared to control cultures (**Table 10** and **Figure 2.6**) (Pedras and Park, 2015).

Low concentration of nitrate is likely to activate the pathway(s) that are suppressed (or silent) in high concentration of nitrate. For example, *A. nidulans* grown under nitrogen-starvation produced two novel polyketides, sanghaspirodins A and B that are not present in nutrient-rich growth conditions (Scherlach, Sarkar *et al.*, 2011). Production of alternariol in cultures of *A. alternata* also was significantly dependent on nitrogen sources. A decrease in the ratio of ammonium and nitrate (from 1:2.6 to 1:1) produced ca. 40-fold higher amounts of alternariol (Brzonkalik, Herrling *et al.*, 2011). Another study reported that a 2-fold increase in nitrate led to a decrease in alternariol and alternariol monomethyl ether in *A. alternata* cultures (Orvehed, Haggblom *et al.*, 1988). Many previously published reports support this concept that nitrogen represses certain polyketide-derived secondary metabolites produced by fungal pathogens; deoxynivalenol, fusarielin H, and zearalenone produced by *Fusarium graminearum*, (Giese, Sondergaard *et al.*, 2013) and fumonisin produced by *Fusarium verticillioides* (Kim and Woloshuk, 2008).

Dark mycelia of *A. brassicicola* grown under low concentration of nitrogen sources could be explained by melanin biosynthesis (**Figure 2.6**). Many *Alternaria species* have been known to produce melanin (Kimura and Tsuge, 1993). Pedras and Yu also reported that under high salt

condition, *L. maculans/P. Lingam* produced 8-hydroxynaphthalene-1-sulfate (**30**) and bulgarein (**31a/b**), which are related to melanin biosynthesis (Pedras and Yu, 2009b). Cramer *et al*. reported that under nitrogen-starvation condition, *A. brassicicola* expressed "*altr015xf07.b1.ab1*" gene, which has significant similarity with 1,3,8-trihydroxynaphthalene (1,3,8-THN, a precursor of melanin) reductase in *A. alternata* (Cramer, La Rota *et al.*, 2006). In addition, UV irradiation activated the 1,3,8-THN reductase gene in *A. alternata* (Kihara, Moriwaki *et al.*, 2004). Therefore, melanin accumulation is most likely to provide fungal spores with resistance to stress conditions such as UV irradiation, high temperature, nutrient scarcity, enzymatic lysis, and oxidative stresses. However, further experiments are necessary to establish whether nitrogen deprivation induces melanin biosynthesis and sporulation in *A. brassicicola*.

Iron is an essential element in almost all microorganisms, plants and animals. They utilize iron in many metabolic processes such as respiration and photosynthesis. Many microorganisms produce iron-chelating agents (termed siderophores) to transport iron into the intercellular space. In addition, siderophores play an important role in detoxifying ROS produced by plants. A mutant of *A. brassicicola* deficient in siderophore production was less virulent on *A. thaliana* than the wild-type isolate. It was proposed that siderophores supply iron to pathogens for survival in their hosts, but are not phytotoxic (Oide, Moeder *et al.*, 2006). The results of this work are consistent with the data of Oide et al. (2006).

Genome sequences revealed that biosynthetic gene clusters are not expressed in standard fermentation conditions (Gross, 2007). One of the strategies to activate cryptic and/or silent gene clusters is to use histone deacetylase inhibitors, leading to discovery of secondary metabolites from microorganisms (**Table 1**). In this work, three epigenetic modifiers (**32, 33,** and **35**) were tested to examine whether these compounds affect the metabolite profiles of *A. brassicicola.* As a result, those epigenetic modifiers did not appear to induce novel metabolites; instead, *A. brassicicola* hydrolyzed SAHA (**32**) to *N*-phenylacetamide (**227**) via hydrolysis followed by acetylation. 5-Aza (**35**) down-regulated production of metabolites of *A. brassicicola* (**Figure 2.9**). According to Sigma-Aldrich product information, the half-life of 5-Aza (**35**) is short ($t_{1/2}$ = 90 min at 50 °C in KPO_4 buffer (pH = 7.4). Moreover, Beisler (1978) reported that 5-Aza is hydrolyzed into *N*-(formylamidino)-*N′*-β-D-ribofuranosylurea (**35a**), and l- β -D-ribofuranosyl-3-guanylurea (**35b**) (Beisler, 1978). Thus, the degradation products of 5-Aza (**35**) might down-regulate production of *A. brassicicola* metabolites.

SBHA (**33**) did not induce the production of novel metabolites. A possible explanation is that *A. brassicicola* is likely to have resistance mechanism(s) to exogenous HDAC inhibitors. Brosch et al. reported that *C. carbonum*, a HDAC inhibitor-producing fungus (i.e., HC-toxin **2**), is resistant to HC-toxin (**2**) and trichostatin A (a HDAC inhibitor) (Brosch, Dangl *et al.*, 2001). Baidyaroy *et al*. reported that *A. brassicicola* and *Diheterospora chlamydosporia* (a HDAC-inhibitor producing fungus) did not inhibit HDAC (Baidyaroy, Brosch *et al.*, 2002). It was established that *A. brassicicola* hydrolyzed SAHA (**32**) to aniline (**228**) followed by acetylation to yield *N*-phenylacetamide (**227**) (**Figure 2.10**). It has been reported that *A. brassicicola* hydrolyzed carbamates and dithiocarbamates followed by acetylation of the resulting amines to yield the corresponding amide (Pedras, Minic *et al.*, 2012; Pedras, Minic *et al.*, 2009). Therefore, *A. brassicicola* is most likely to have a protection mechanism against hydroxamate HDAC inhibitors, which could be biotransformed via hydrolysis-acetylation (Pedras and Park, 2015).

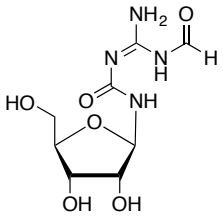

35a

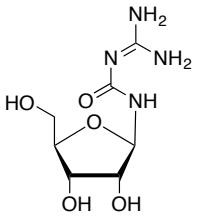

35b

2.2 Analyses of metabolites produced on infected leaves

To understand the chemical-ecological interactions between *A. brassicicola* and its host plants, it is important to know the metabolites produced by *A. brassicicola* and inducible metabolites produced in the host plants. The comparative chemical analyses of the fungal metabolites produced on infected leaves of *Brassica juncea* cv. Cutlass (susceptible), *B. napus* cv. Westar (susceptible) and *Sinapis alba* cv. Ochre (resistant) are one of the important steps to understand the involvement of fungal metabolites in infection processes. In addition, these analyses can establish the ecological roles of metabolites involved in plant responses to fungal pathogen attack. Toward this end, work described in this section involves phytotoxicity assays, and HPLC analyses of infected and control leaves and spore germination fluids (SGFs).

2.2.1 Phytotoxicity assays

Whole plant assays

It was established that *A. brassicicola* produced brassicicolin A (**1**) as a host-selective toxin. Brassicicolin A (**1**) caused severe necrosis in *B. juncea* and *B. napus* (Pedras, Chumala *et al.*, 2009). Depudecin (**151**) has been known to be produced by *A. brassicicola* (Matsumoto, Matsutani *et al.*, 1992), but its phytotoxicity has not been established. But, Wight *et al*. recently reported that the depudecin-minus mutants of *A. brassicicola* were less virulent on *B. oleracea* (Wight, Kim *et al.*, 2009). For this reason, it was hypothesized that depudecin (**151**) might play an important role in phytotoxicity in susceptible cultivars. To determine whether depudecin (**151**) shows phytotoxic activity and/or synergistic effects on phytotoxicity, brassicicolin A (**1**) and depudecin (**151**) were tested using leaves of whole plants of *B. juncea* (susceptible), and *B. napus* (susceptible). Various concentrations of brassicicolin A (**1**) and depudecin (**151**) were combined and the mixtures were inoculated onto leaves of whole plants (see Section 4.4.2).

Brassicicolin A (0.25–5.0 mM) displayed necrotic/chlorotic spots on both *B. juncea* and *B. napus*, while depudecin (**151**) did not cause visible necrotic lesions at any concentration except for 5.0 mM in *B. napus* (**Figure 2.16**). Although a mixture of brassicicolin A (0.25 mM) and depudecin (**151,** 1.0 mM or 0.50 mM) showed slightly larger lesions on *B. napus* than brassicicolin A (**1**, 0.25 mM) did, no substantial differences among mixtures of both compounds (**1** and **151**) were observed in *B. juncea* and *B. napus* (**Figure 2.16**). In addition, certain

combinations did not exhibit concentration-dependent necrotic lesions. For example, a mixture of brassicicolin (**1**) 0.50 mM and depudecin (**151**) 1.0 mM caused smaller lesions than a mixture of brassicicolin (**1**) 0.50 mM and depudecin (**151**) 0.50 mM (**Figure 2.16**). From these observations, it is unclear whether brassicicolin A (**1**) and depudecin (**151**) have a synergistic effect on the phytotoxicity to B. *juncea* and *B. napus*.

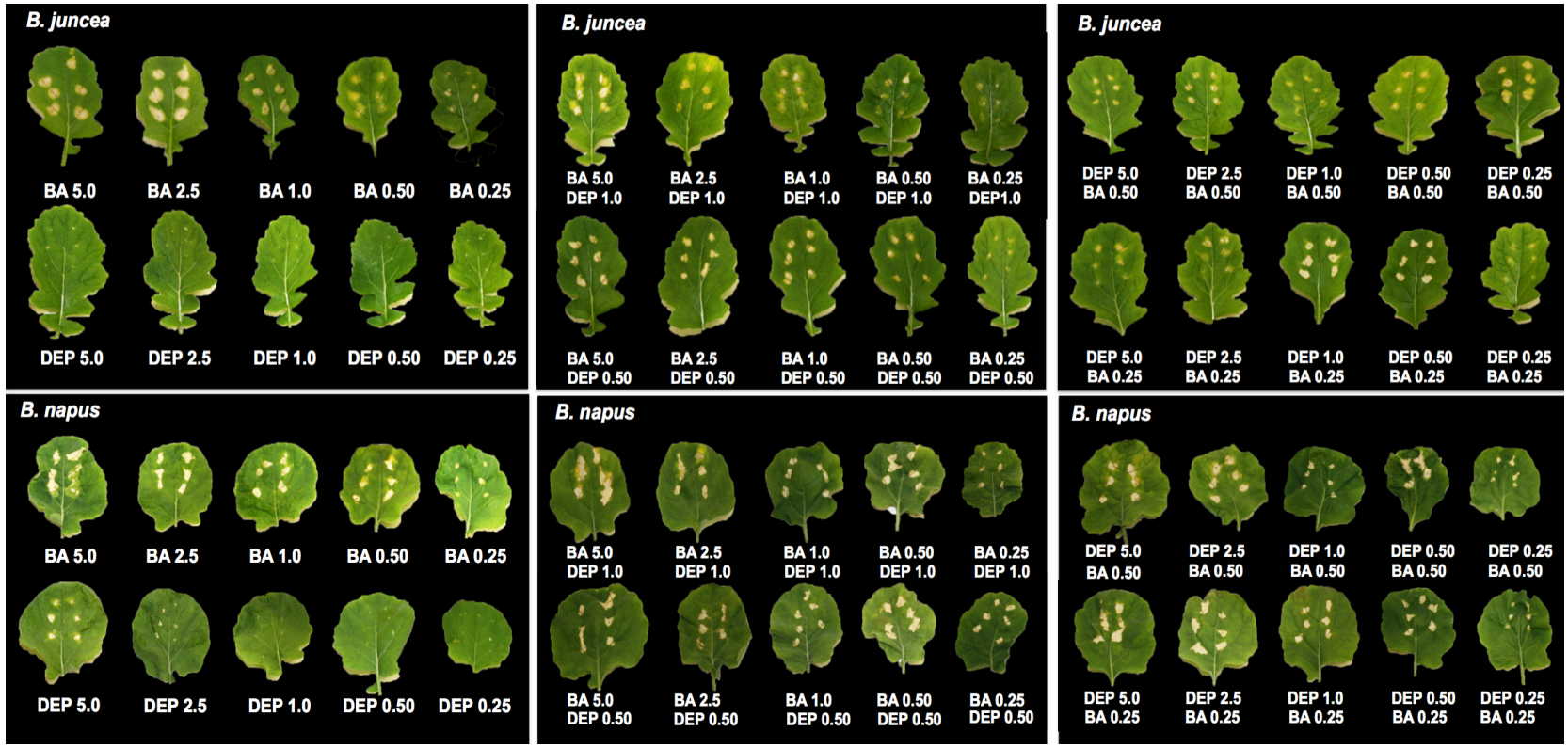

Figure 2.16 Effects of brassicicolin A (BA, **1**) and depudecin (DEP, **151**) on leaves of whole plants of *Brassica juncea* cv. Cutlass (susceptible), and *B. napus* cv. Westar (susceptible). Numbers refer to concentration of each metabolite (mM).

Detached leaf assays

Phytotoxicity of brassicicolin A (**1**), depudecin (**151**), α-acetylorcinol (**210**), tyrosol (**219**), and phomapyrone A (**25**) was investigated using detached leaves of *Brassica* species; *B. juncea* cv. Cutlass (susceptible), *B. napus* cv. Westar (susceptible) and *S. alba* cv. Ochre (resistant). Brassicicolin A (**1**) caused necrotic/chlorotic lesions around inoculation sites (**Figure 2.17**) regardless of the plant species resistance to *A. brassicicola*. Lesion sizes caused by brassicicolin A (0.10–1.0 mM) (**1**) in the three crucifers were similar in terms of concentration-dependent necrosis (**Table 12**).

Interestingly, detached leaves and leaves whole plants of *S. alba* showed opposite results; whereas no differences between both assays were observed in *B. juncea* and *B. napus* (**Figure 2.17**). Brassicicolin A (**1**) caused necrosis in detached leaves of *S. alba* and did not cause any damage at any of the concentrations on leaves of whole plants of *S. alba*. These results in leveas of whole plants are consistent with published data establishing that brassicicolin A (**1**) did not show phytotoxicity in leaves of whole plants of *S. alba* (Pedras, Chumala *et al.*, 2009). In this work, however, a significant difference was observed between leaves of whole plants and detached leaves of *S. alba* responding to brassicicolin A (**1**)..

The other fungal metabolites— α-acetylorcinol (**210**) tyrosol (**219**), phomapyrone A (**25**)—were tested for phytotoxicity using detached leaves *of B. juncea*, *B. napus*, and *S. alba*. As a result, α-acetylorcinol (**210**) tyrosol (**219**), depudecin (**151**), and phomapyrone A (**25**) did not cause any damage at three concentrations (1.0, 0.50 and 0.10 mM) (**Table 12**).

Table 12 Phytotoxicity of fungal metabolites in *Brassica juncea* cv. Cutlass (brown mustard, susceptible), *B. napus* cv. Westar (canola, susceptible) and *Sinapis alba* cv. Ochre (white mustard, resistant) [a].

	B. juncea cv. Cutlass			*B. napus* cv. Westar			*S. alba* cv. Ochre		
Metabolites (mM)	1.0	0.5	0.1	1.0	0.5	0.1	1.0	0.5	0.1
Brassicicolin A (**1**)	3	3	2	3	2	1	3	2	1
Depudecin (**151**)		ND			ND			ND	
Phomapyrone A (**25**)		ND			ND			ND	
α-Acetylorcinol (**210**)		ND			ND			ND	
Tyrosol (**219**)		ND			ND			ND	

[a] Data represent the means of lesion diameters of treated leaves (n = 36).
Lesion size scale: 0 = 0.0–1.9 mm; 1 = 2.0–2.9 mm; 2 = 3.0–3.9 mm; 3 = 4.0–4.5 mm; 4 = 4.6–5.5 mm; 5 = 5.6–6.5 mm; 6 = 6.5–7.5 mm.
[b] ND = No damage.

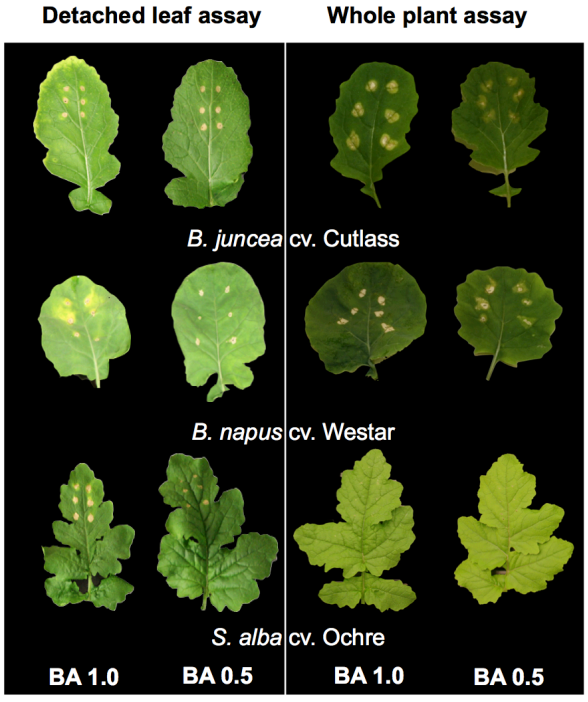

Figure 2.17 Effects of brassicicolin A (**1**) (1.0 mM and 0.50 mM) on detached leaves of *Brassica juncea* cv. Cutlass (susceptible), *B. napus* cv. Westar (susceptible) and *Sinapis alba* cv. Ochre (resistant).

2.2.2 Analyses and phytotoxicity of spore germination fluids

Certain phytotoxins are found in spore germination fluids (SGFs) at the early growth stage of phytopathogenic fungi in host plants. In addition, host recognition followed by HST production by fungal pathogens is one of the important processes during fungal invasion. Thus, analyses of SGFs are important to establish roles of fungal metabolites in the early infection process on the site of initial contact with the host plants.

Spore germination fluids (SGFs), initially, were collected from six spots in each leaf of *B. juncea*, *B. napus*, or *S. alba.* However, it turned out that amounts of SGFs are too small to analyze fungal metabolites. Furthermore, it was difficult to retain moisture in droplets of spore suspensions during a period of germination. That is, the droplets of spore suspensions were completely dried so that spores stayed on leaves without germination. After several trials to optimize conditions by changing spore concentrations (1×10^5 spores/mL, 20μL), the number of inoculation spots (40 spots per a leaf), and incubation time (72 h), reasonable amounts of SGFs were collected from detached leaves of the three crucifers (see Experimental section 4.4.3). All spore suspensions placed on leaves have dark-yellowish (or brownish) color—initially, spore suspensions were transparent—and yellowish necrotic/chlorotic lesions were observed around inoculation spots in all species tested (**Figure 2.18**). Regardless of the resistance to *A. brassicicola*, the three species exhibited macroscopic stress responses such as necrotic/chlorotic, water soak lesion, or wilting in infected leaves.

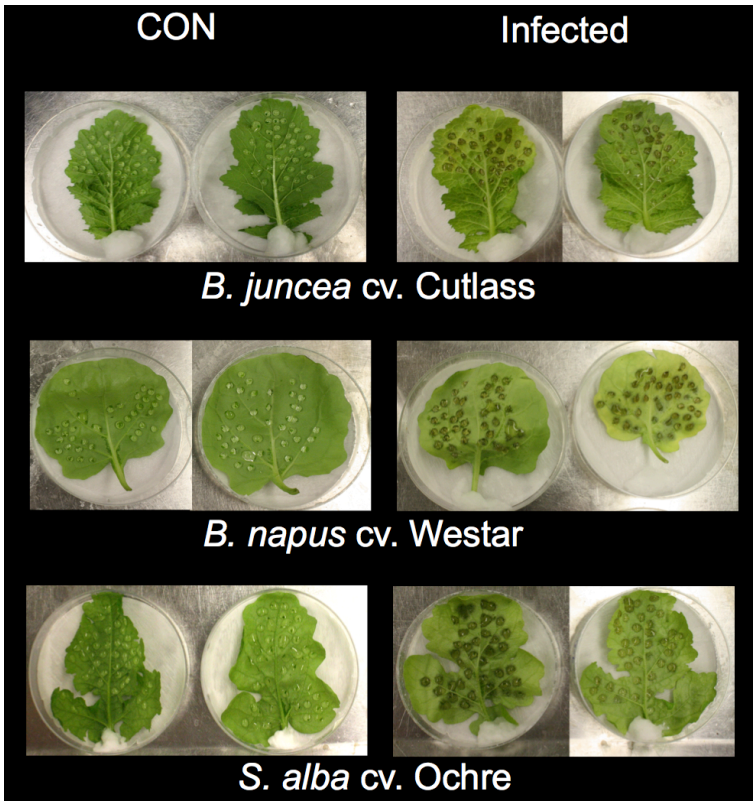

Figure 2.18 Detached leaves (3-day post inoculation) of *Brassica juncea* (susceptible), *B. napus* (susceptible), and *Sinapis alba* (resistant) after inoculation with *A. brassicicola* spores. Control leaves were similarly treated with distilled water.

SGFs collected from each species were filtered, lyophilized, concentrated and analyzed by HPLC-ESI-MS. The MS spectra of SGFs collected from each species revealed that *A. brassicicola* produced several siderophores (see Section 2.1.2.3) as well as phomapyrone A (**25**). These metabolites were not detected in control leaves (H_2O-treatment) (**Figure 2.19**, **Figure 2.20**, and **Figure 2.21**). Fungal metabolites (siderophores and phomapyrone A (**25**)) in SGFs collected from different crucifers were detected in this work for the first time.

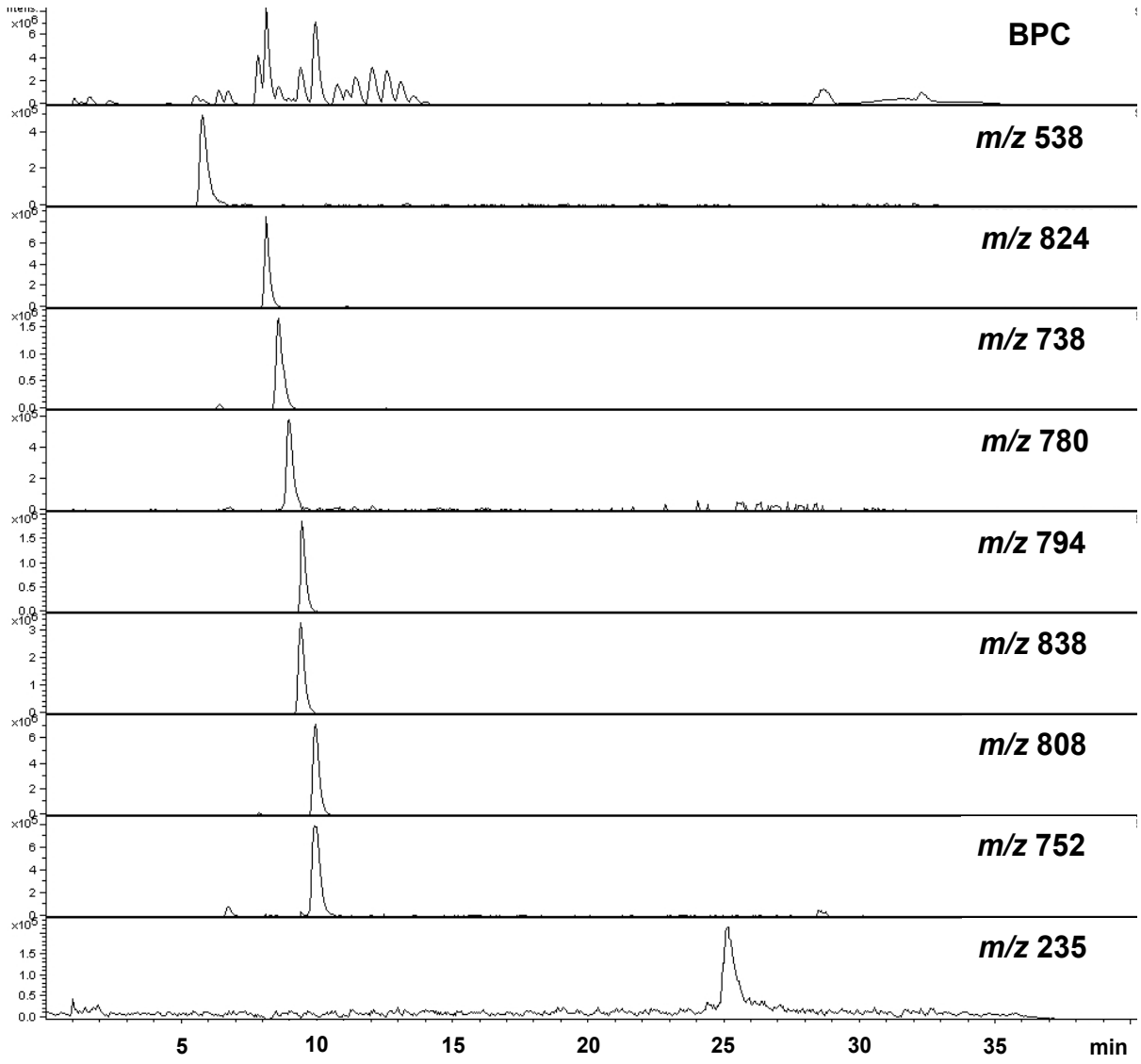

Figure 2.19 HPLC-ESI-MS chromatograms (base peak chromatogram (BPC) and extract ion chromatograms) of SGF collected from detached leaves of *Brassica juncea* cv. Cutlass (susceptible). EIC: *m/z* = 538, dimerumic acid, **184**; *m/z* = 824, unknown; *m/z* = 738, *N,N*-Dimethyltriornicin, **220**; *m/z* = 780, coprogen B, **221**; *m/z* = 794, N^{α}-methylcoprogen B, **222**; *m/z* = 838, hydroxycoprogen **180**; *m/z* = 808, *N,N*-dimethylcoprogen **179**; , *m/z* = 752, neocoprogen I, **177**; *m/z* = 235, phomapyrone A (**25**).

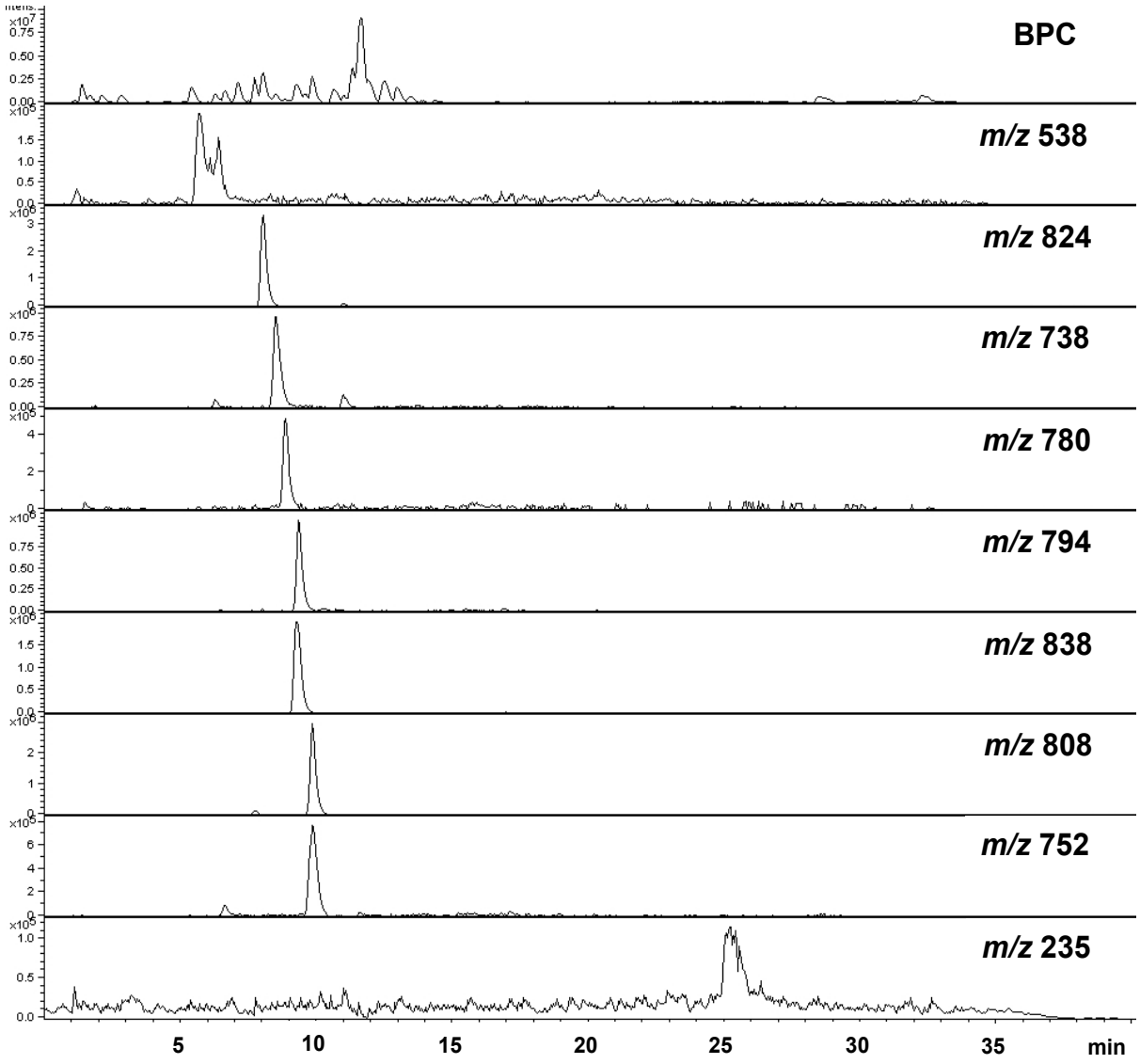

Figure 2.20 HPLC-ESI-MS chromatograms (base peak chromatogram (BPC) and extract ion chromatograms) of SGF collected from detached leaves of *Brassica napus* cv. Westar (susceptible). EIC: *m/z* = 538, dimerumic acid, **184**; *m/z* = 824, unknown; *m/z* = 738, *N,N*-Dimethyltriornicin, **220**; *m/z* = 780, coprogen B, **221**; *m/z* = 794, N^{α}-methylcoprogen B, **222**; *m/z* = 838, hydroxycoprogen **180**; *m/z* = 808, *N,N*-dimethylcoprogen **179**; , *m/z* = 752, neocoprogen I, **177**; *m/z* = 235, phomapyrone A (**25**).

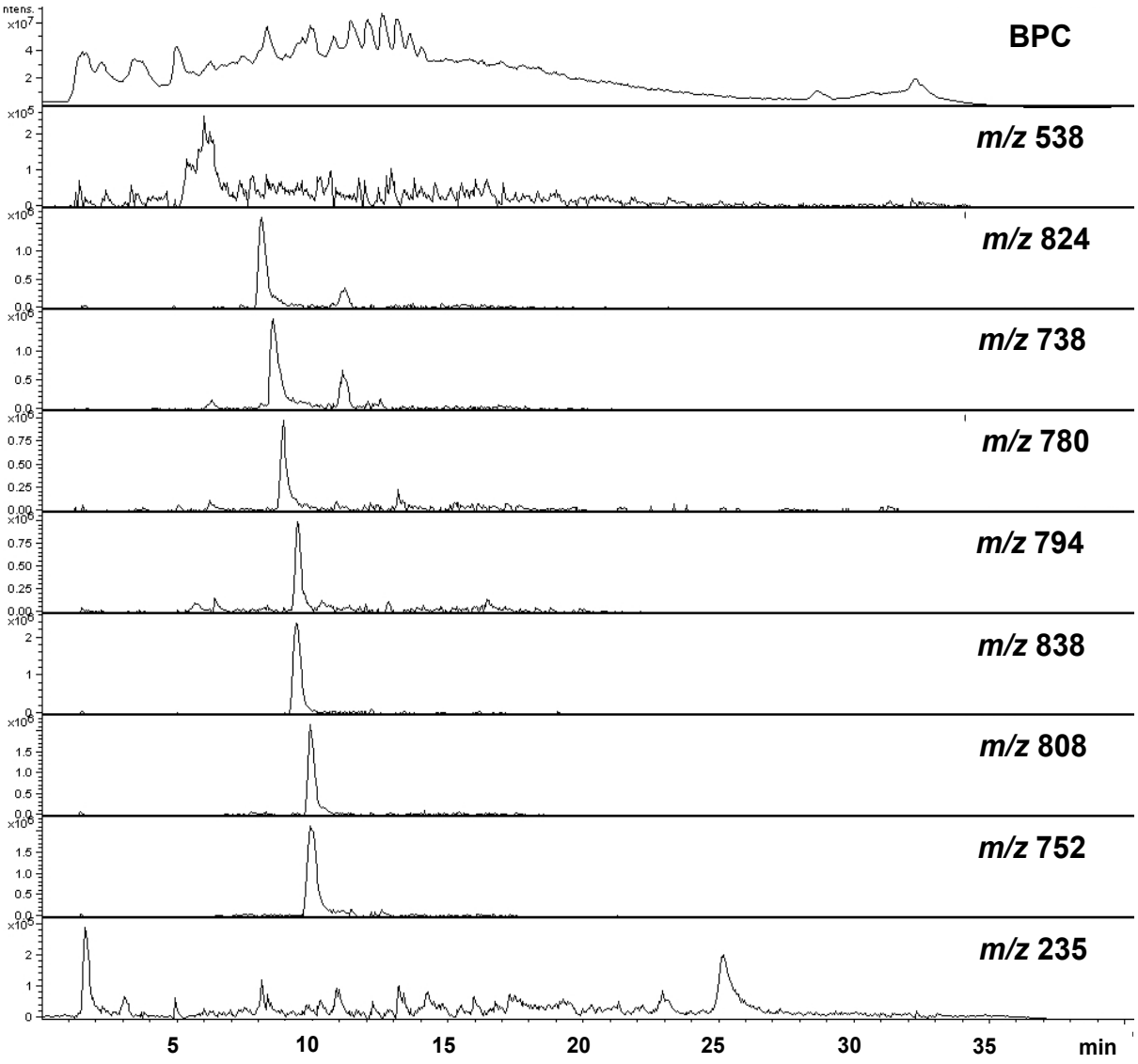

Figure 2.21 HPLC-ESI-MS chromatograms (base peak chromatogram (BPC) and extract ion chromatograms) of SGF collected from detached leaves of *Sinapis alba* cv. Ochre (resistant). EIC: *m/z* = 538, dimerumic acid, **184**; *m/z* = 824, unknown; *m/z* = 738, *N,N*-Dimethyltriornicin, **220**; *m/z* = 780, coprogen B, **221**; *m/z* = 794, N^{α}-methylcoprogen B, **222**; *m/z* = 838, hydroxycoprogen **180**; *m/z* = 808, *N,N*-dimethylcoprogen **179**; , *m/z* = 752, neocoprogen I, **177**; *m/z* = 235, phomapyrone A (**25**) .

2.2.3 Analyses of infected leaves of crucifers

Brassicicolin A (**1**) is a host-selective phytotoxin of susceptible species *B. juncea* and *B. napus* (Pedras, Chumala *et al.*, 2009). Although brassicicolin A (**1**) showed phytotoxicity to susceptible *Brassica* species, experiments to detect brassicicolin A (**1**) in infected leaves of whole plants were not successful (Pedras, Chumala *et al.*, 2009). Detached leaves of three crucifer species: *B. juncea* cv. Cutlass (susceptible), *B. napus* cv. Westar (susceptible), *S. alba* cv. Ochre (resistant) were infected with *A. brassicicola* and incubated up to five days. The extracts of infected leaves were analyzed by HPLC-DAD. Control leaves were treated with either water or autoclaved spores.

2.2.3.1 *Brassica juncea* cv. Cutlass (brown mustard)

Two days after inoculation with *A. brassicicola* spores, detached leaves of *B. juncea* started showing yellowish spots around spore inoculation sites (**Figure 2.22**). As fungal spores germinated in *B. juncea*, the inoculation sites appeared darker and brownish, but these symptoms were absent in controls. Leaves displayed a higher degree of necrotic/chlorotic lesions around inoculation sites.

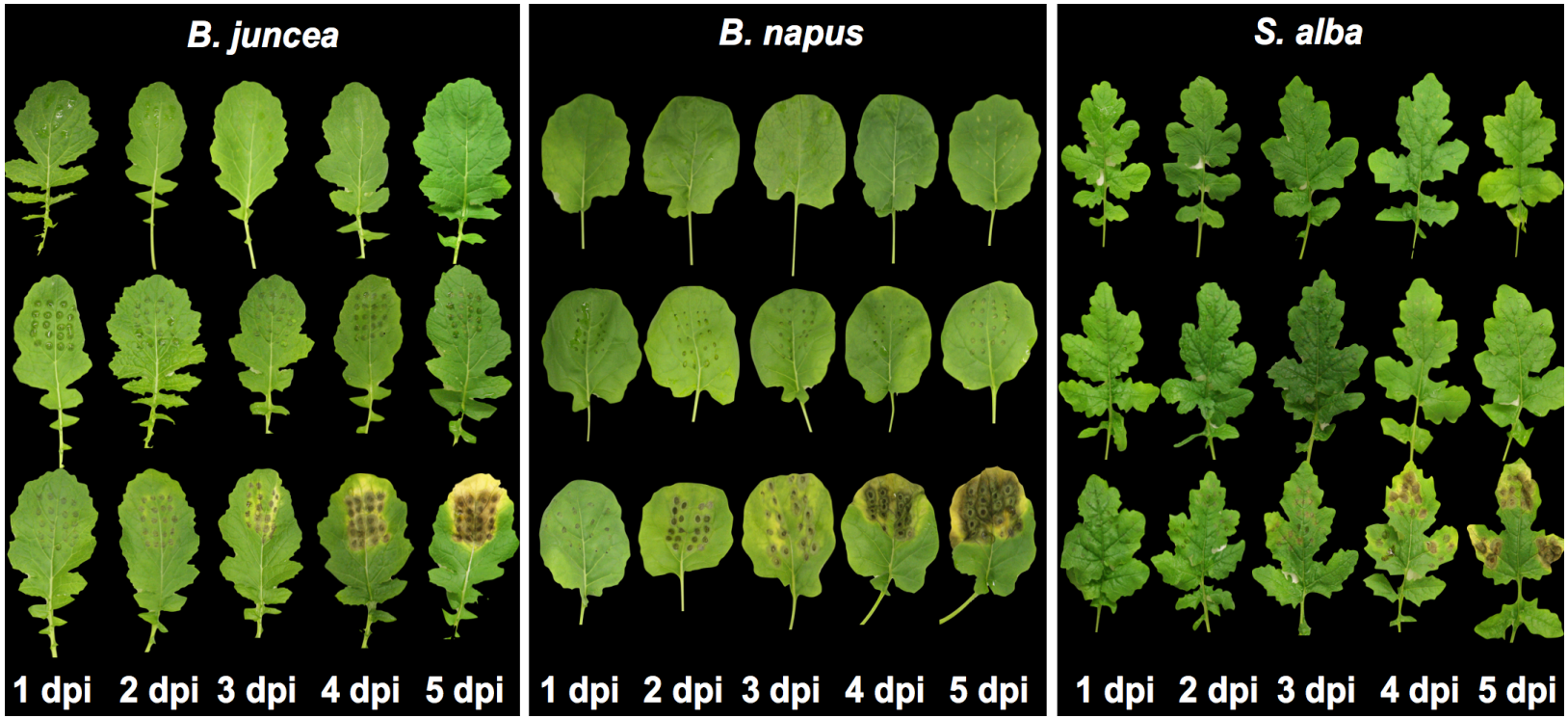

Figure 2.22 Leaves of *Brassica juncea*, *B. napus*, and *Sinapis alba,* five days after inoculation with *Alternaria brassicicola*; control (top row); autoclaved *A. brassicicola* spores (middle row); *A. brassicicola* spores (bottom row).

HPLC chromatograms of extracts of leaves showed that fungal infection induced the production of plant metabolites (**Figure 2.23**). Plant metabolites were assigned by comparing with authentic samples and UV spectral libraries available in Dr. Pedras' group.

HPLC-DAD analysis of MeOH-extracts of leaves indicated production of the phytoalexins: brassilexin (**185**), rutalexin (**231**), and cyclobrassinin (**186)**. Three phytoalexins were consistently detected over a five-day inoculation period. Extracts of control leaves did not contain phytoalexins. Interestingly, phomapyrone A (**25**) was detected in 4-d-old and 5-d-old infected leaves extracts (**Figure 2.24**). HPLC-ESI-MS of extracts of infected leaves also detected phomapyrone A (**25**) in *B. juncea* (**Figure 2.29**). However, brassicicolin A (**1**) was not detected in extracts of infected leaves of *B. juncea*.

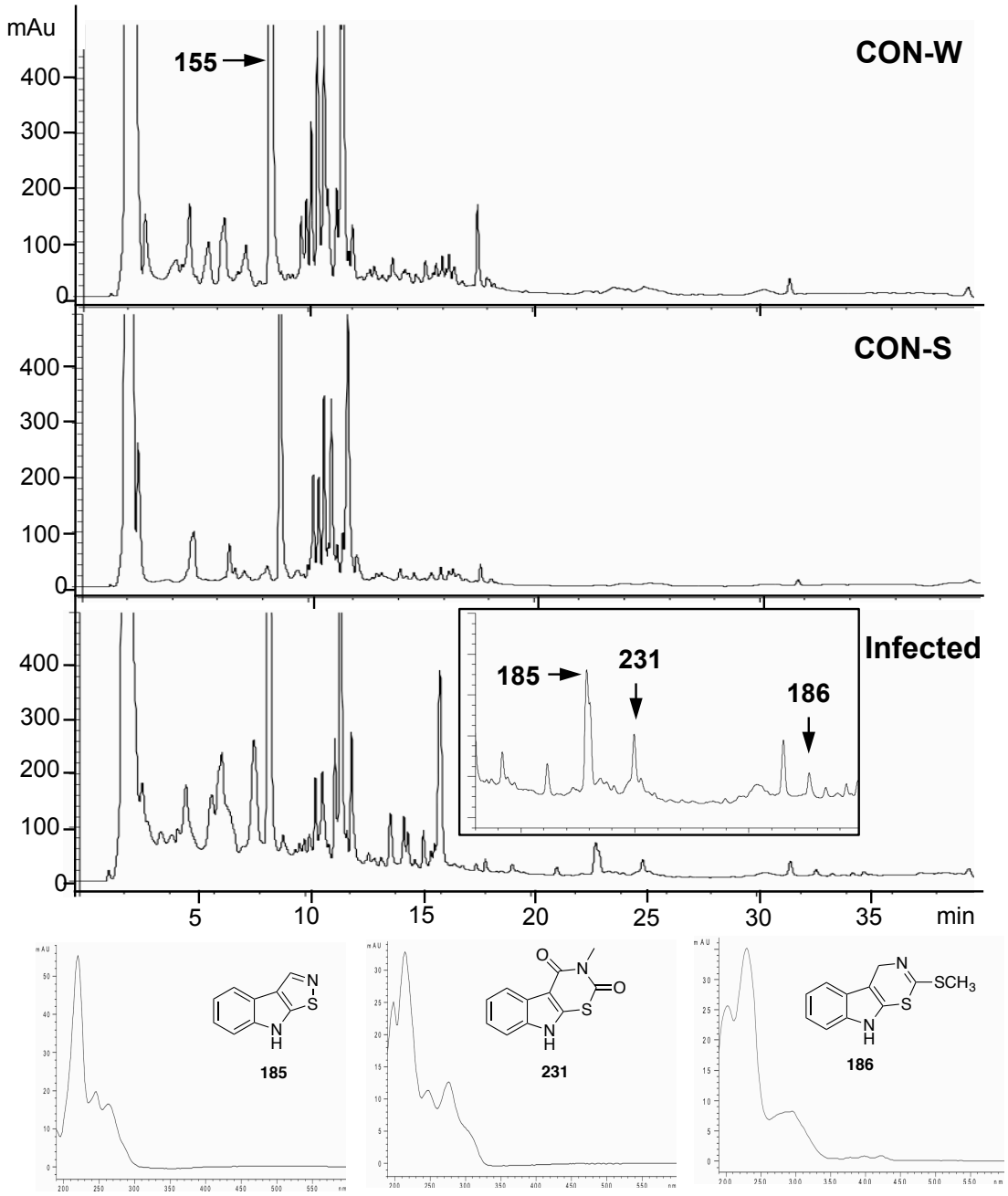

Figure 2.23 HPLC-DAD chromatograms (method C, detection 220 nm) of extracts of control leaves (CON-W, H_2O; CON-S, autoclaved spores) and infected leaves of *Brassica juncea* (3-day post inoculation) and UV spectra of the corresponding phytoalexins detected in infected leaves. The insert in the HPLC chromatogram refers to the expansion of HPLC chromatogram.

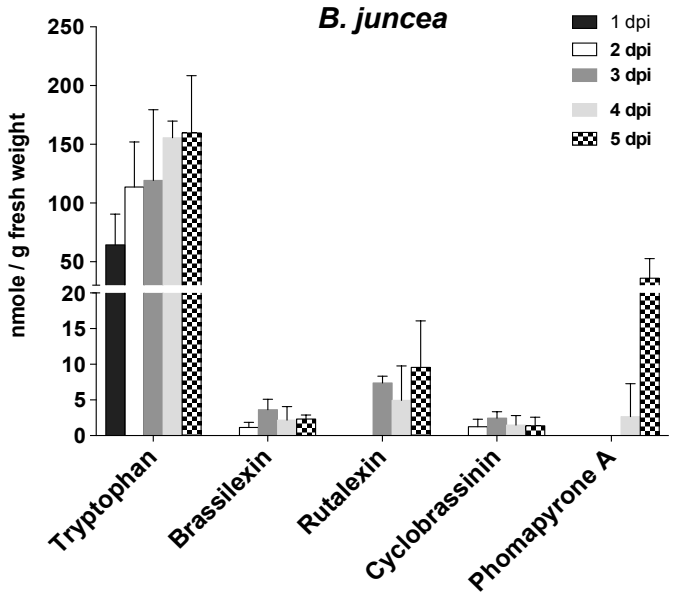

Figure 2.24 Production of plant and fungal metabolites on infected leaves (n = 3) of *Brassica juncea* cv. Cutlass (susceptible).

2.2.3.2 *Brassica napus* cv. Westar (canola)

Leaves of *Brassica napus* displayed symptoms similar to those of leaves of *B. juncea* (whole plants and detached leaf assays) (**Figure 2.17**). Three days after inoculation with *A. brassicicola* spores, *B. napus* started to show necrotic/chlorotic lesions around inoculation sites. Five-day-old infected leaves exhibited the most severe damage (dark brown color, and necrosis/chlorosis).

HPLC-DAD analyses of leaf extracts revealed that fungal infection induced the production of the phytoalexins, arvelexin (**188a**), caulilexin (**188b**) within 24 h (**Figure 2.25**) and phytoanticipins such as glucobrassicin (**196**), 4-MeO-glucobrassicin (**161**), and indole-3-acetonitrile (**188)** within 48 h. However, neither phytoalexins nor phytoanticipins were detected three days after incubation, suggesting production might be below the current detection limits. Phomapyrone A (**25**) was detected in 4-day-old infected leaves of *B. napus* (**Figure 2.26**).

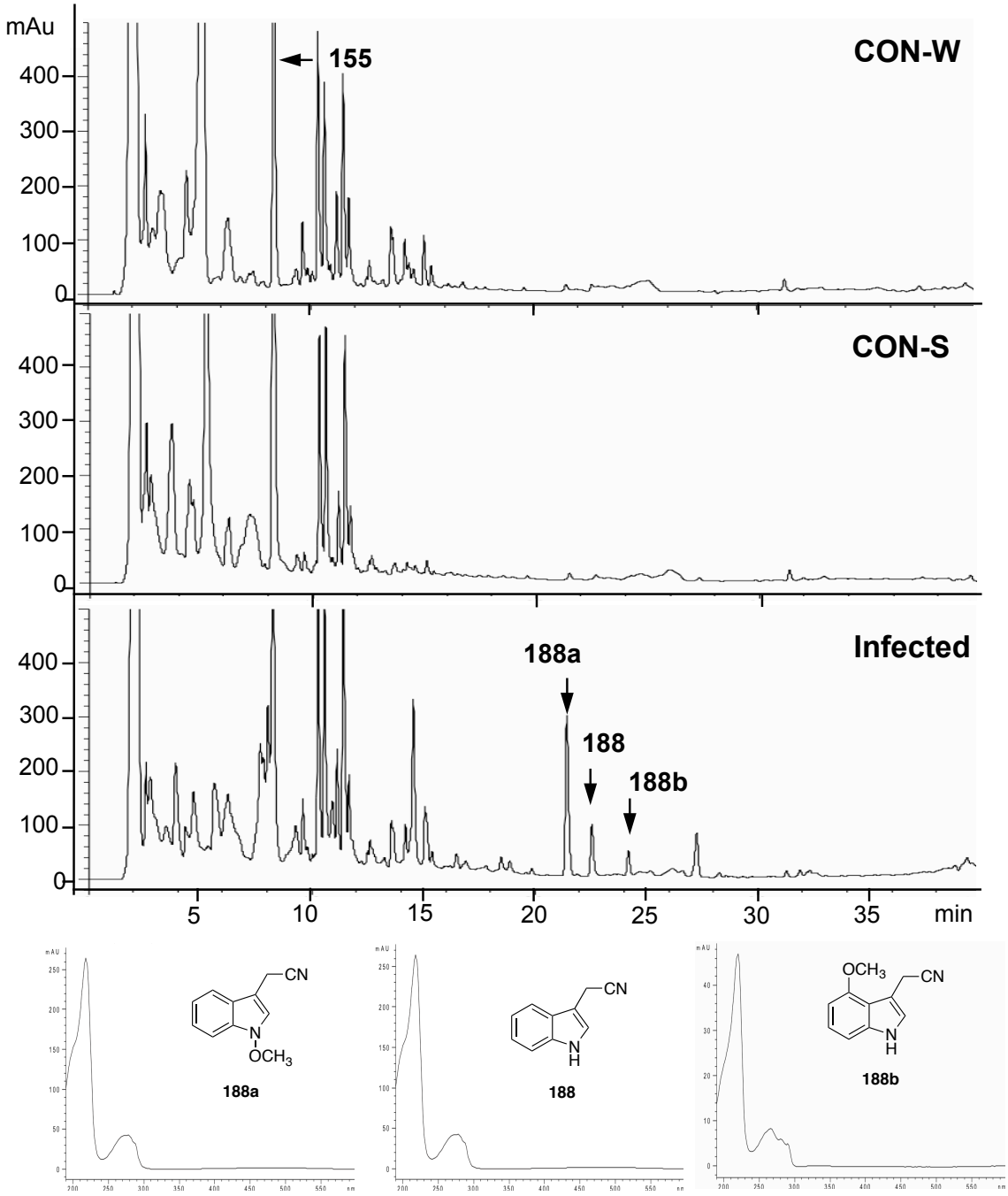

Figure 2.25 HPLC-DAD chromatograms (method C, detection 220 nm) of extracts of control leaves (CON-W, H_2O; CON-S, autoclaved spores) and infected leaves of *Brassica napus* cv. Westar (1-day after post inoculation) and UV spectra of the corresponding phytoalexins were detected in infected leaves.

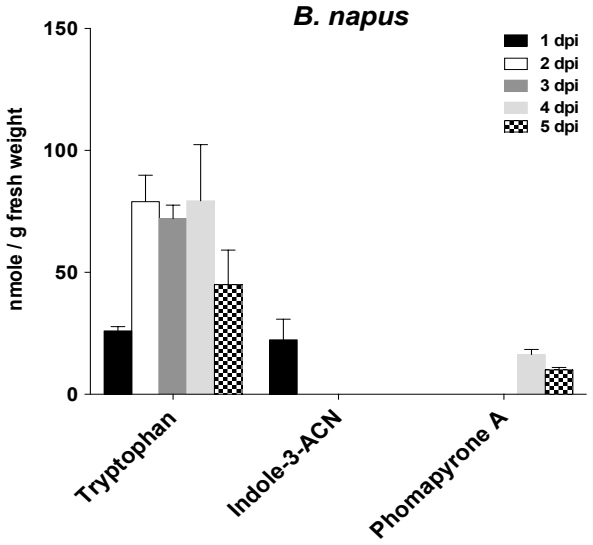

Figure 2.26 Production of plant and fungal metabolites on infected leaves (n = 3) of *Brassica napus* cv. Westar (susceptible).

2.2.3.3 *Sinapis alba* cv. Ochre (white mustard)

Sinapis alba is resistant to *Alternaria* species. While *B. juncea* (susceptible) and *B. napus* (susceptible) exhibited similar necrotic/chlorotic lesions, *S. alba* responded differently. That is, leaves of whole plants did not show necrosis and/or chlorosis, whereas detached leaves showed necrosis caused by brassicicolin A (1.0 mM, 0.5 mM, and 0.1 mM, see Section 2.2.1).

In the detached leaf assay, three days after inoculation with fungal spores, *S. alba* started to show dark brown color, necrosis and/or chlorosis. Although the most severe damage was observed in infected leaves, five days post inoculation, the severity of symptoms on *S. alba* was lower than in leaves of *B. juncea* and *B. napus* (**Figure 2.22**). These results were consistent with those observed in detached leaves of *S. alba* after inoculation with brassicicolin A (**1**) (**Figure 2.17**). Detached leaves of *S. alba* are less resistant to *A. brassicicola* than leaves of whole plants. However, the severity of symptoms appears to be lower than the symptoms observed in leaves of *B. napus* and *B. juncea*.

HPLC-DAD analyses of extracts of control leaves and infected leaves of *S. alba* showed that the production of sinalexin (**195**) and sinalbin A (**193**) was induced by fungal infection. 4-Hydroxybenzyl isothiocyante (**232**) was detected in both control and infected leaf extracts (**Figure 2.27**). Sinalexin (**195**), a phytoalexin and phomapyrone A (**25**) were detected in 5-d-old infected leaves (**Figure 2.28**).

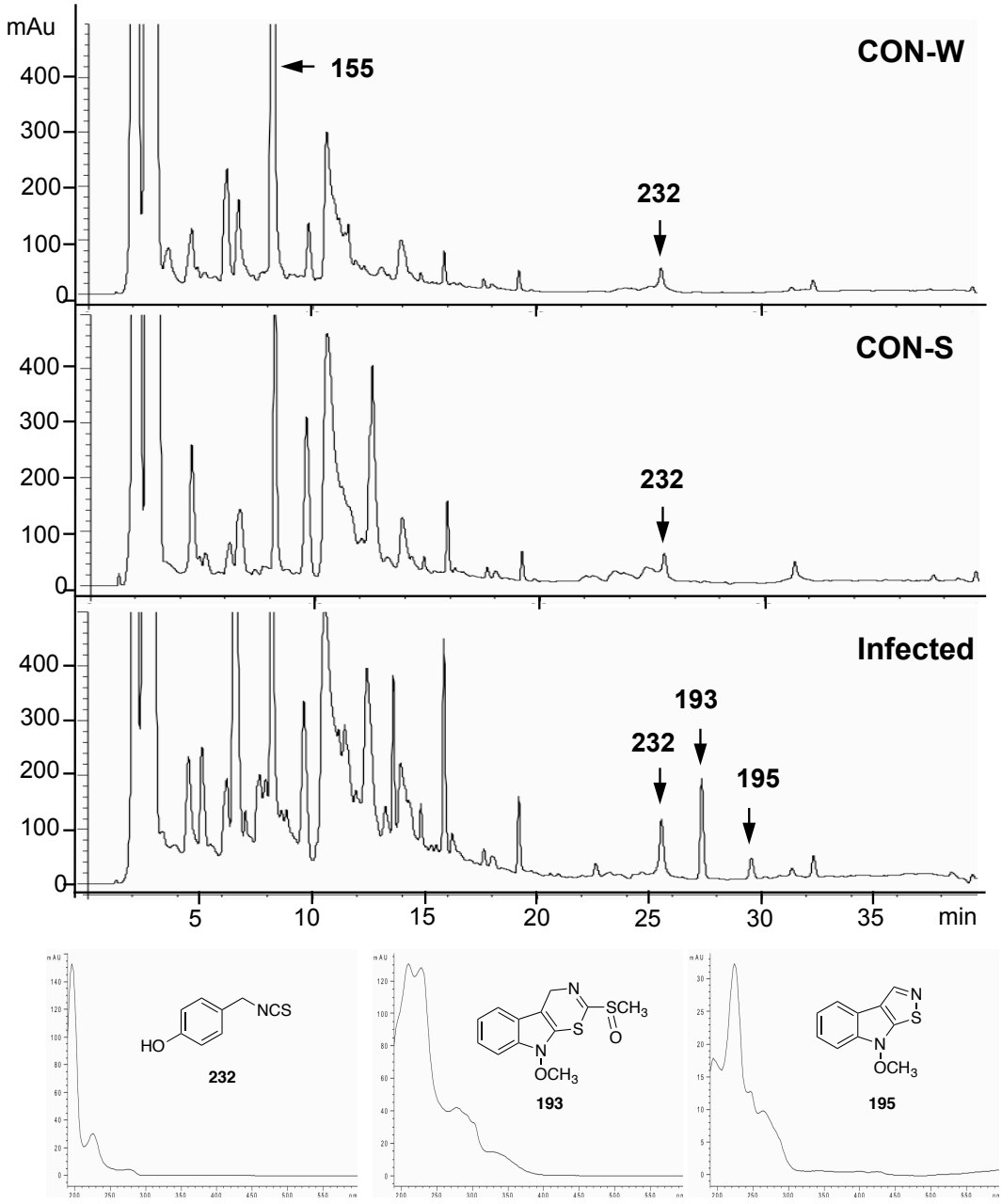

Figure 2.27 HPLC-DAD chromatograms (method C, detection 220 nm) of extracts of control (CON-W, H_2O; CON-S, autoclaved spores) and infected leaves of *Sinapis alba* cv. Ochre (3-day after post inoculation) and UV spectra of the corresponding phytoalexins detected in infected leaves.

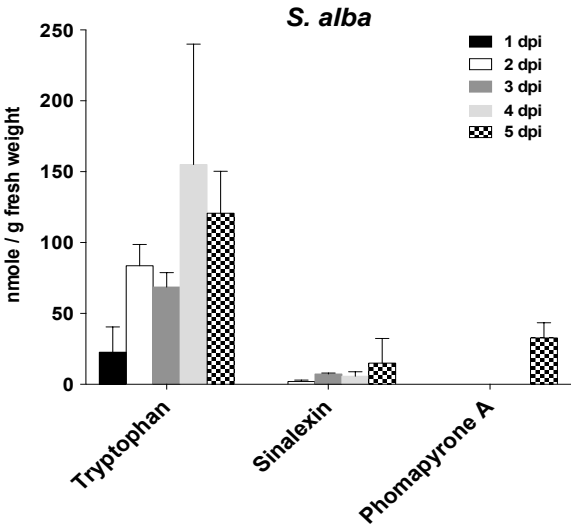

Figure 2.28 Production of plant and fungal metabolites on infected leaves (n = 3) of *Sinapis alba* cv. Ochre (resistant).

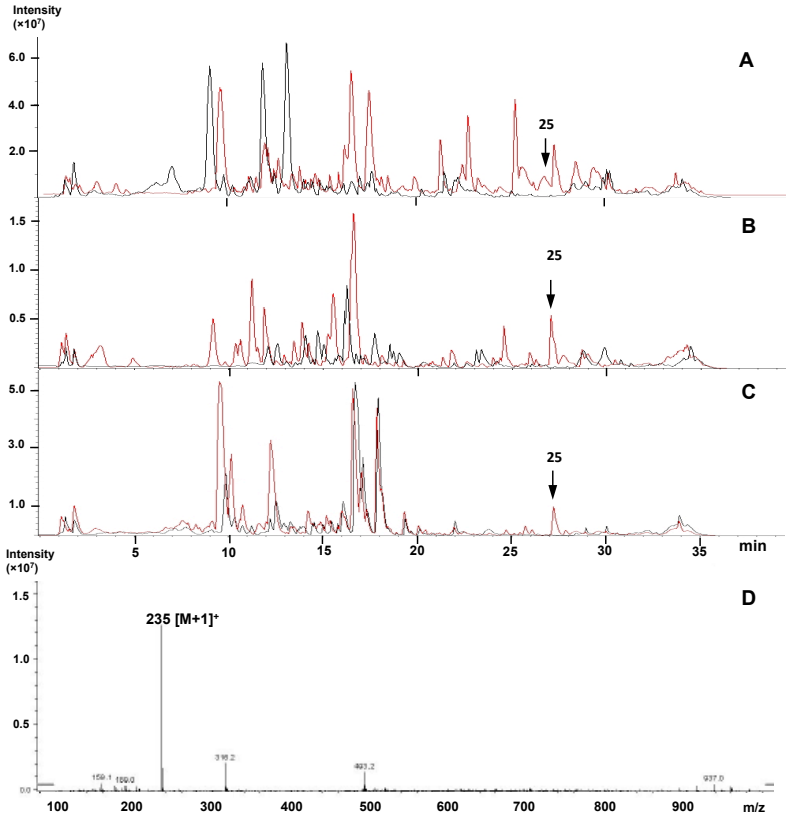

Figure 2.29 HPLC-ESI-MS chromatograms (base peak chromatogram) of the extracts of infected tissues (5-day post inoculation): A, *Brassica juncea*; B, *B. napus*; C, *Sinapis alba*; D, mass spectrum of the peak at t_R 28 min; red, infected tissue extract; black, control leaf extract. The arrow indicates the peak corresponding to phomapyrone A (**25**) in infected tissue extracts.

2.2.3.4 *Arabidopsis thaliana* Col-0, *pen*2-1 and *pad*3-1

Arabidopsis thaliana is a well-known model in the plant field. Since the genome sequencing of *A. thaliana* has been completed (TheArabidopsisInitiative, 2000), numerous studies have been carried out using *A. thaliana* wild types and mutants. Investigation of secondary metabolites of *A. brassicicola* in infected *A. thaliana* and its mutants could help to understand the importance of metabolites in plant-pathogen interactions. It was hypothesized that *A. brassicicola* might produce larger amounts of fungal metabolites in susceptible mutants *pen2-1* and *pad3-1* than in the resistant ecotype Col-0. To test this hypothesis, *A. thaliana* Col-0, *pad3-1,* and *pen2-1* seedlings were grown in hydroponic kits. Plants (4–5-week-old) were inoculated with fungal spore suspensions and incubated for two days. No substantial differences around inoculation sites in Col-0, *pad3-1,* and *pen2-1* were observed (**Figure 2.30**).

To examine the fungal metabolites produced during infection, SGFs were collected and analyzed by HPLC-ESI-MS. While the known plant metabolites, glucobrassicin (**196**), 4-MeO-glucobrassicin (**161**), and camalexin (**209)** were detected, none of the fungal metabolites including siderophores and phomapyrone A (**25**) was observed in SGFs collected from Col-0, *pad3-1,* or *pen2-1*. The infected leaves and control leaves were extracted and the extracts were analyzed by HPLC-DAD. HPLC chromatograms of leaf extracts of infected Col-0 and *pen2-1* showed induction of camalexin (**209**) and unknown metabolites (t_R 11–13 min); but no fungal metabolites were detected in Col-0, *pen2-1* and *pad3-1*. In addition, *pad3-1* did not produce camalexin (**209**) in infected leaves, whereas unknown metabolites (t_R 11–13 min) appeared to accumulate (**Figure 2.31**). In the MS spectrum of the unknown metabolites, one metabolite (t_R 12.2 min) showed a quasimolecular ion peak $[M+1]^+$ at *m/z* 247. Considering the molecular weight and UV spectrum of the peak at t_R 12.2 min in *pad3-1*, presumably, the peak might be (*S*)-dihydrocamalexic acid (**208**), a precursor of camalexin (**209**) (Schuhegger, Nafisi *et al.*, 2006). However, further experiments are needed to characterize the peak at t_R 12.2 min.

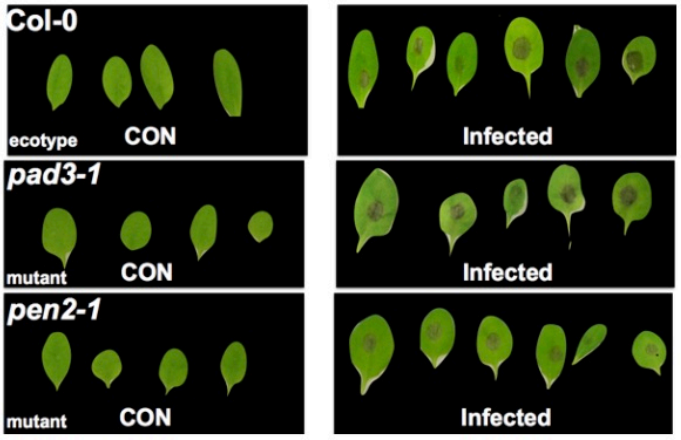

Figure 2.30 Leaves of *Arabidopsis thaliana* ecotype (Col-0) and mutants (*pad3-1* and *pen2-1*) infected with spores of *A. brassiciola* (2-day post inoculation).

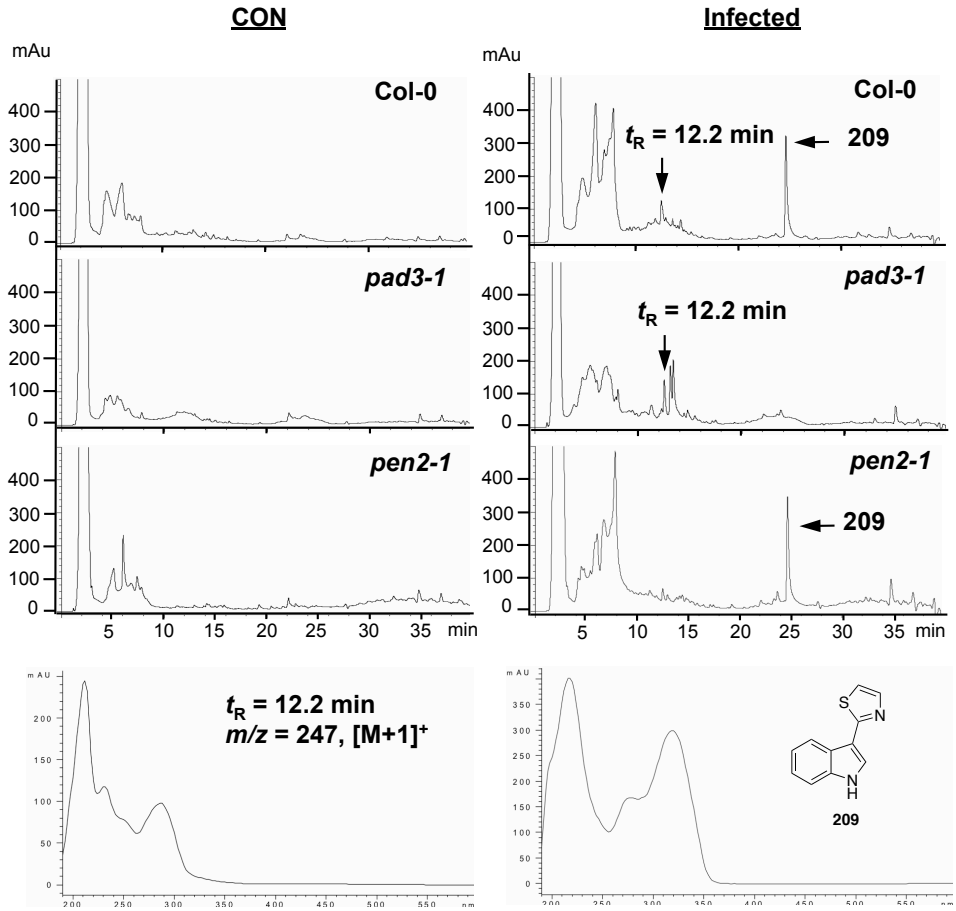

Figure 2.31 HPLC-DAD chromatograms (method C, detection 220 nm) of extracts of *Arabidopsis thaliana* Col-0 and mutants (*pad3-1* and *pen2-1*) (2-day post inoculation). Arrows indicate plant metabolites induced by *Alternaria brassicicola.* UV spectra of the unknown metabolite (t_R = 12.2 min) and camalexin (**209**).

Quantification of plant metabolites produced in Col-0, *pen2-1*, and *pad3-1* was carried out using calibration curves built with authentic compounds. Although quantification of glucobrassicin (**196**) and 4-MeO-glucobrassicin (**161**) in polar region (t_R = 5–8min in **Figure 2.31**) was not successful due to poor resolution, those metabolites appeared to increase in infected leaves in all of the *A. thaliana* lines. Camalexin **(209)** was induced by fungal infection in Col-0 and *pen2-1,* whereas it was not detected in *pad3-1* (**Figure 2.32**).

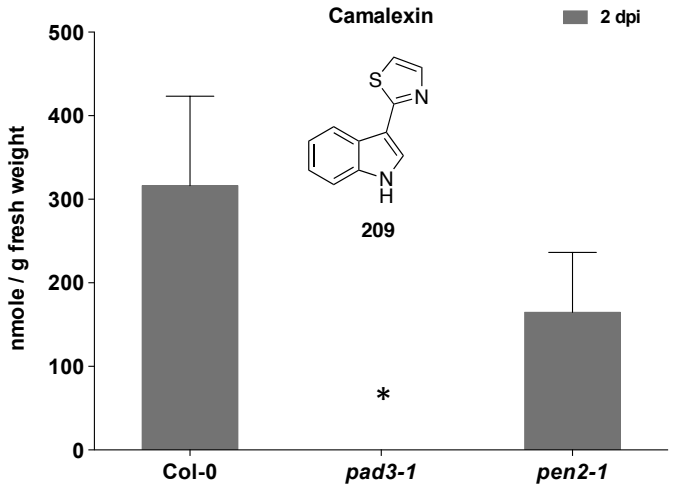

Figure 2.32 Production of camalexin (**209**) in infected leaves of *Arabidopsis thaliana* Col-0 and mutants (*pad3-1* and *pen2-1*) (2-day post inoculation). Asterisk indicates that camalexin was not detected.

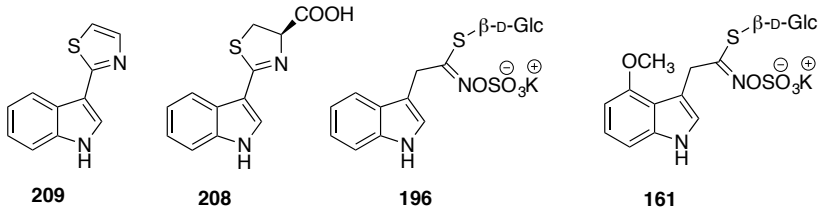

2.2.4 Discussion

The comparative chemical analyses of the fungal metabolites produced on infected and control leaves of *B. juncea* cv. Cutlass (susceptible), *B. napus* cv. Westar (susceptible) and *S. alba* cv. Ochre (resistant) were carried out to understand the involvement of fungal metabolites during fungal invasion. In this work, depudecin (**151**) exhibited phytotoxicity only at 5.0 mM in leaves of whole plants of *B. napus*. Considering phytotoxic activity of other metabolites (e.g., brassicicolin A – 0.1 mM), depudecin (**151**) does not seem to have phytotoxic activity in the tested crucifers. Further experiments are needed to establish if depudecin (**151**) might have synergistic effects on phytotoxicity in susceptible plants.

Depudecin (**151**) has been known as a HDAC inhibitor (Kwon, Owa *et al.*, 1998). However, other biological activities of depudecin (**151**) are unknown, except for low virulence of the depudecin minus mutants of *A. brassicicola* (Wight, Kim *et al.*, 2009). Considering that HC-toxin (**2**), a HDAC inhibitor produced by *C. carbonum*, exhibited severe phytotoxicity in susceptible maize cultivars (Walton, 2006), depudecin (**151**) might have an important role in *A. brassicicola*–crucifers pathosystems. To establish biological activity, further experiments are necessary.

None of the metabolites (except for brassicicolin A (**1**)) did exhibit phytotoxicity in the three crucifers in whole plant assays. Previously published results showed that tyrosol (**219**) was phytotoxic to leaves of marigold (*Tagetes erecta* L.) (Gamboa-Angulo, García-Sosa *et al.*, 2001), prickly sida (*Sida spinosa* L.) and lamb's quarters (*Chenopodium album* L.), whereas α-acetylorcinol (**210**) displayed relatively lower phytotoxicity to prickly sida and lamb's quarters (Venkatasubbaiah, Baudoin *et al.*, 1992). Furthermore, tyrosol (**219**) inhibited seed germination of lettuce (Kimura and Tamura, 1973), while **219** promoted germination of spores of the fungus, *C. albicans* (Chen, Fujita *et al.*, 2004).

Pedras *et al*. established that brassicicolin A (**1**) exhibited phytotoxic activity in leaves of whole plants of *B. juncea,* and *B. napus*, but not on *S. alba* showed necrosis caused by brassicicolin A (**1**) (Pedras, Chumala *et al.*, 2009). In this work, a significant difference was observed in between leaves of whole plants and detached leaves of *S. alba* responding to brassicicolin A (**1**) (**Figure 2.17**). *S. alba* might lose resistance to *A. brassicicola* in excised leaves. Furthermore, loss of resistance is likely to allow *A. brassicicola* to infect *S. alba* (**Figure**

2.22). On the other hand, the lower severity of disease symptoms on *S. alba* is probably due to other defense mechanisms regardless of physical stress (i.e., excision of leaves).

Spore germination fluids (SGFs) produced by *Alternaria* species during germination contain various phytotoxic metabolites, resulting in visible necrosis and/or chlorosis in susceptible plants (Oka, Akamatsu *et al.*, 2005; Otani, Kohnobe *et al.*, 1998; Parada, Sakuno *et al.*, 2008; Quayyum, Gijzen *et al.*, 2003). SGF is one of the useful tools for the investigation of plant-pathogen interactions because SGF is involved in host recognition and HST production on the sites of initial contact at the early stage of infection. SGFs collected from *B. juncea, B. napus*, and *S. alba* were analyzed by HPLC-ESI-MS to determine whether SGFs contain potentially toxic metabolites rather than known protein toxins (i.e., AB-toxin) (Oka, Akamatsu *et al.*, 2005). Eight siderophores plus phomapyrone A (**25**) were detected in SGFs collected from the three crucifers for the first time (**Figure 2.19**–**Figure 2.21**). Production of siderophores is considered one of the essential processes to utilize iron from the plants and to have resistance to localized reactive oxygen species (ROS) produced by plants (Haas, Eisendle *et al.*, 2008; Oide, Moeder *et al.*, 2006).

Considering antifungal activity of phytoalexins and hydrolyzed products of indole glucosinolates, the *pen2* mutant is more vulnerable to fungal pathogens than the eco type (Bednarek, Pislewska-Bednarek *et al.*, 2009). It was expected that *A. brassicicola* might be able to infect the *pen2* mutant. However, no germination was observed in the *pen2* mutants. None of the fungal metabolites were detected in either HPLC-DAD or HPLC-ESI-MS. Presumably, improper incubation conditions (e.g., short incubation time or spore concentration) might prevent germination and further fungal invasion.

Camalexin has shown strong antifungal activity against *A. brassicicola* (Pedras and Abdoli, 2013). PAD3 (phytoalexin deficient 3) is a key enzyme associated with camalexin (**209**) biosynthesis (Schuhegger, Nafisi *et al.*, 2006). The *Arabidopsis pad3* exhibited more susceptibility than in wild-type against *A. brassicicola* (Thomma, Nelissen *et al.*, 1999). After infection with *A. brassicicola*, the enhanced peak (t_R = 12.9 min, *m/z* 247) was detected in extracts of the *pad3* (**Figure 2.31**). It can be deduced from UV and MS spectra that the peak is most likely to be (*S*)-dihydrocamalexic acid (**208**) (Schuhegger, Nafisi *et al.*, 2006). None of the fugal metabolites were detected in SGFs and extracts of infected *pad3*. Further experiments are

needed to establish roles of fungal metabolites in the chemical-ecological interactions between *A. brassicicola* and *A. thaliana*.

2.3 Biosynthesis of brassicicolin A

The structure of brassicicolin A (**1**) was first elucidated by Gloer *et al*. and confirmed through chemical degradation studies (Gloer, Poch *et al.*, 1988). Brassicicolin A (**1**) ($C_{32}H_{48}N_2O_{14}$) has a D-mannitol unit (**233**) to which two isocyanoisovaleryl (C-9/C-9'–C-14/C-14'), two 2-hydroxy-3-methylbutanoyl (C-4/C-4'–C8/C-8'), and two acetyl (C15/C15'–C-16/C-16') units are connected through ester linkages. The chemical structure of brassicicolin A (**1**) has an axis of symmetry (C_2) and two epimerizable centers at the α-carbons of isocyanoisovaleryl units. Theoretically, four diastereomers are possible (**Figure 2.33**); however, since two (**1c** and **1d**) of the potential four isomers are identical (a meso-compound), three diastereomers would be observed. Furthermore, these stereoisomers are in equilibrium due to labile protons at α to the isocyanogroups, which makes these isomers interconvertible in solution. As shown in **Figure 2.34** and **Figure 2.35**, a total of 16 carbon resonances are detected in the ^{13}C NMR spectrum with each carbon displaying three signals in the ^{13}C due to a mixture of three stereoisomers.

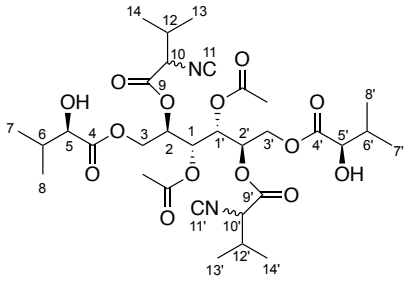

1

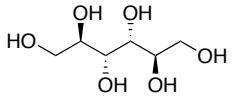

233

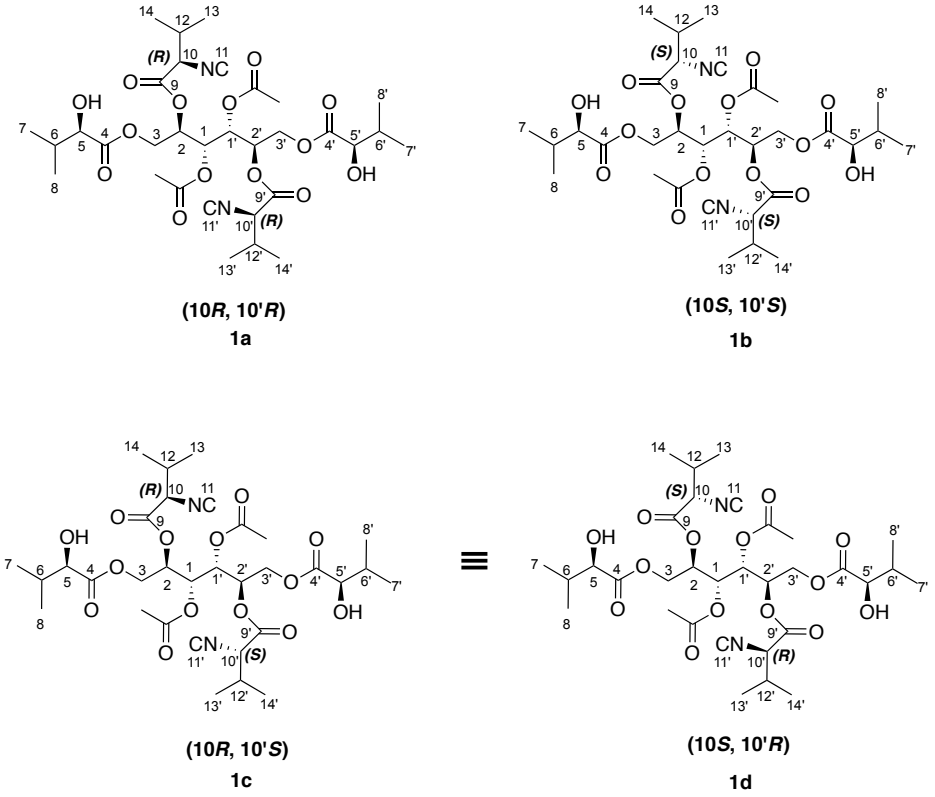

Figure 2.33 Brassicicolin A (**1**) as a mixture of three diastereomers.

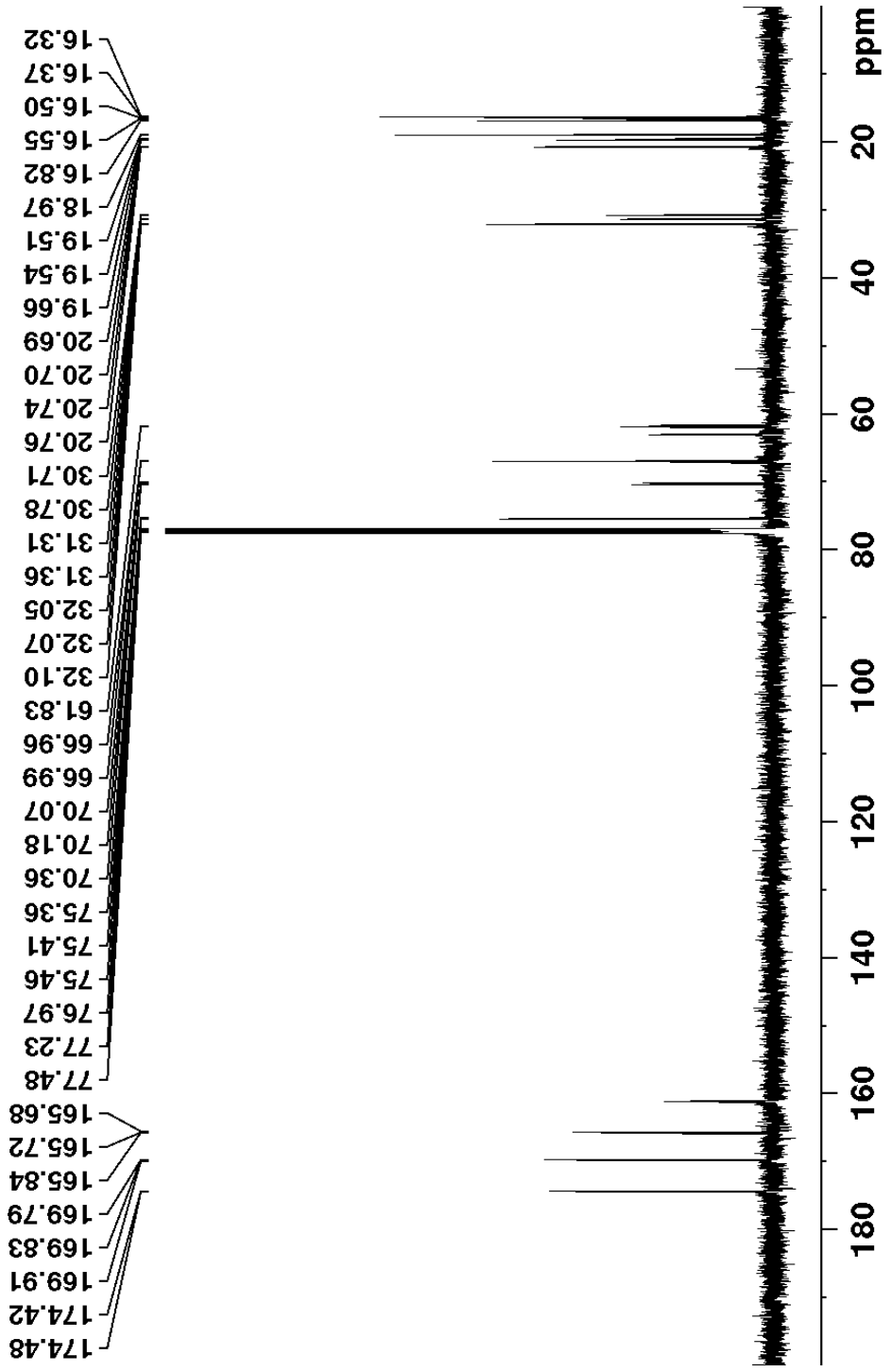

Figure 2.34 ^{13}C NMR (125 MHz, $CDCl_3$) spectrum of natural abundance brassicicolin A (**1**).

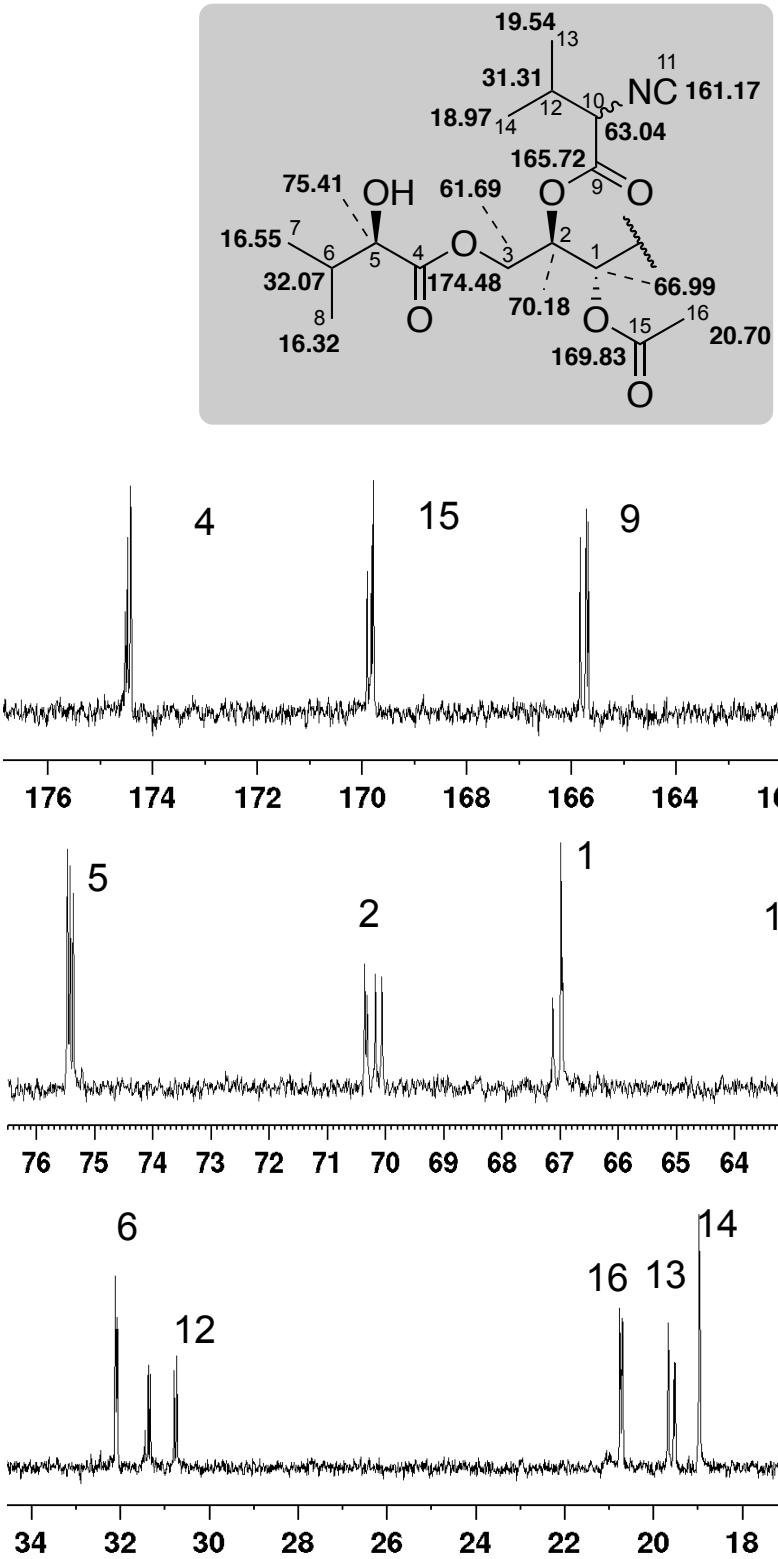

Figure 2.35 Expansions of the ^{13}C NMR (125 MHz, $CDCl_3$) spectrum of natural abundance brassicicolin A (**1**). Numbers on peaks refer to carbon numbers of brassicicolin A (**1**).

Based on previous reports on the structure of brassicicolin A (**1**) (Gloer, Poch *et al.*, 1988; Pedras, Chumala *et al.*, 2009), all carbon resonances were assigned as shown in **Table 13**.

Table 13 ^{1}H (500 MHz, $CDCl_3$) and ^{13}C (125MHz, $CDCl_3$) NMR spectroscopic data of brassicicolin A (**1**)

Carbon number	δ_C[a]	δ_H[b]
1/1’	67.13, 66.99, 66.96	5.57–5.47, m, 2H
2/3’	70.36, 70.32, 70.18, 70.07	5.13–5.04, m, 2H
3/3’	62.03, 61.83, 61.69, 61.66	4.27–4.15, m, 2H
4/4’	174.52, 174.48, 174.42	—
5/5’	75.46, 75.41, 75.36	4.09–4.03, m, 2H
6/6’	32.10, 32.07, 32.05	2.10–2.05, m, 2H
7/7’[†]	16.82, 16.55, 16.50	0.90–0.87, m, 6H
8/8’[†]	16.37, 16.32	1.04–1.02, m, 6H
9/9’	165.84, 165.72, 165.68	—
10/10’	63.04	4.53–4.39, m, 4H
11/11’	161.27, 161.17, 161.04	—
12/12’	31.36, 31.31, 30.78, 30.71	2.39–2.31, m, 2H
13/13’[§]	19.66, 19.54, 19.51	1.16–1.13, m, 6H
14/14’[§]	18.97	1.02–0.99, m, 6H
15/15’	169.91, 169.83, 169.79	—
16/16’	20.76, 20.74, 20.70, 20.69	2.16–2.13, m, 6H
OH (5/5’)	—	2.71–2.63, m, 2H

[a,b] Chemical shifts of carbons and protons were consistent with those previously reported (Gloer, Poch *et al.*, 1988; Pedras, Chumala *et al.*, 2009)

[†] C-7/C-7’ and C-8/C-8’ are interchangeable.

[§] C-13/C-13’ and C-14/C-14’ are interchangeable.

2.3.1 Incorporation of D-[U-$^{13}C_6$]glucose into brassicicolin A

Retrobiosynthetic analysis of brassicicolin A (**1**) suggested that the main skeleton (C-1/C-1'–C-3/C-3') could derive from mannitol (**233**) and the isocyanoisovaleryl (C-9/C-9'–C-14/C-14'), and 2-hydroxy-3-methylbutanoyl (C-4/C-4'–C-8/C-8') groups could derive from valine. Two acetyl groups (C-15/C-15'–C-16/C-16') could derive from acetyl-CoA. The origin of the carbons C-11 and C-11' of the isocyanide groups, however, is unclear.

In the previous section (See Section 2.1.2), carbon, nitrogen, and temperature affected production of brassicicolin A (**1**) in modified MM. Briefly, high temperature (30 °C) increased the amount of brassicicolin A (**1**), while it was not produced in media containing 5-fold lower amounts of glucose. *A. brassicicola* did not grow in MM containing mannitol (**233**) instead of glucose. The amount of brassicicolin A (**1**) in PDB was significantly larger (ca. 16-fold) than in standard MM (**Table 10**). Although production of brassicicolin A (**1**) increased in PDB, PDB was excluded in this biosynthetic study of brassicicolin A (**1)** due to its carbohydrate content (potato starch 4 g/L; glucose 20 g/L), which would dilute isotopically labeled glucose, potentially, leading to lower incorporation. Standard MM at 30 °C was employed in feeding experiments because of lager production (ca. 2.5-fold) of brassicicolin A (**1**) compared to standard MM at 23 °C. Furthermore, since brassicicolin A (**1**) appeared to be produced at later growth stage, isotopically labeled glucose were administered twice: the earlier (2–3d-old culture) and later (4–5d-old culture) growth stages.

Cultures of *A. brassicicola* in standard MM were grown at 30 °C. D-[U-$^{13}C_6$]glucose was administered to 72-h-old culture (100 mg in 100 mL of MM), and 120-h-old culture (100 mg in 100 mL of MM). After 8 days, cultures were extracted and brassicicolin A (**1**) was isolated from the crude extracts by FCC (see **Scheme 4.6**). After obtaining brassicicolin A (**1**) (2.7 mg from 300 mL of MM), the resultant brassicicolin A (**1**) was analyzed by NMR (^{1}H, ^{13}C, and 2D INADEQUATE) and HPLC-ESI-MS.

^{13}C NMR analysis

As shown in **Figure 2.36** (entire spectrum) and **Figure 2.37** (expanded spectrum), the ^{13}C NMR spectrum of ^{13}C-enriched brassicicolin A (**1**) obtained from incubation of cultures with D-[U-$^{13}C_6$]glucose was complex. This is due to the presence of an inseparable mixture of diastereomers and one-bond couplings ($^1J_{13C\text{-}13C}$) of ^{13}C-labeled carbons. For instance, the carbonyl carbon of the acetyl group (C-15/C-15') in brassicicolin A (δ_C 169.8 ppm) showed the expected three resonances with each resonance showing coupling with adjacent ^{13}C-labeled carbons. All carbon signals showed couplings except for the isocyanide carbon at C-11/C-11' (δ_C 161.1 ppm) as expected, since there is no ^{13}C-labeled carbon adjacent to C-11/C-11'.

To determine whether isocyanide carbons (C-11/C-11') in brassicicolin A (**1**) are labeled, natural abundance brassicicolin A (**1**) (2.7 mg in $CDCl_3$) was analyzed by ^{13}C NMR using the identical parameters as those used for ^{13}C-enriched brassicicolin A (**1**) (2.7 mg in $CDCl_3$). After the peaks were aligned, the ^{13}C NMR spectra were compared. For example, resonances of C-4/C-4' show doublets due to adjacent ^{13}Cs (C-5/C-5') plus singlets in the center due to the natural abundance of ^{13}C. A significant enhancement was observed at isocyanide carbons at C-11/C-11' (δ_C 161.1 ppm), suggesting isocyanide carbons derived from D-[U-$^{13}C_6$]glucose.

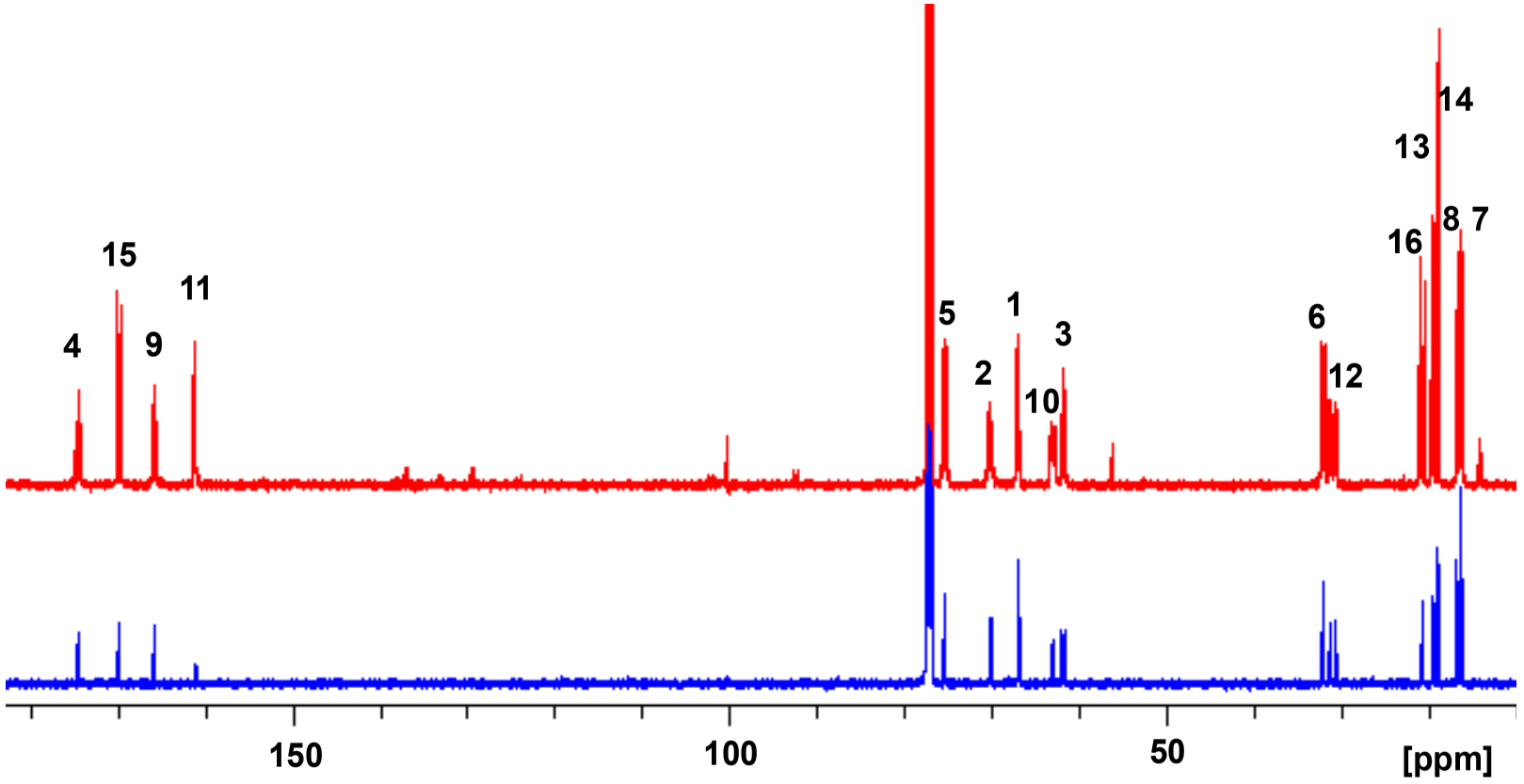

Figure 2.36 ^{13}C NMR (125 MHz, $CDCl_3$) spectra of ^{13}C-enriched brassicicolin A (**1e**) (red, 2.7 mg) and natural abundance brassicicolin A (blue, 2.7mg). Numbers indicate carbon numbers in the structure of brassicicolin A (**1**). Spectra were recorded under identical conditions (see Experimental).

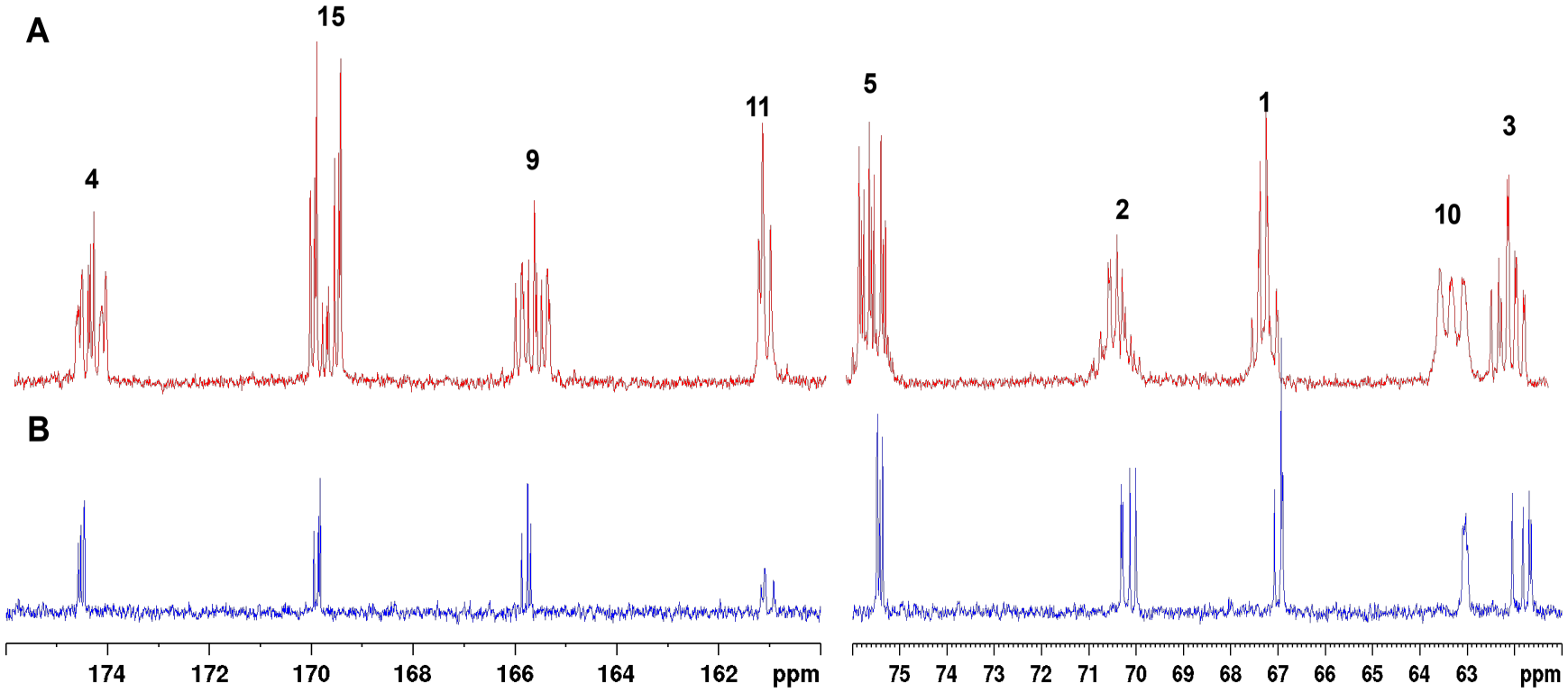

Figure 2.37 Expansion of ^{13}C NMR (125MHz, $CDCl_3$) spectra: A, ^{13}C-enriched brassicicolin A (**1e**) obtained from incubation of cultures with D-[U-$^{13}C_6$]glucose; B, natural abundance of brassicicolin A (**1**).

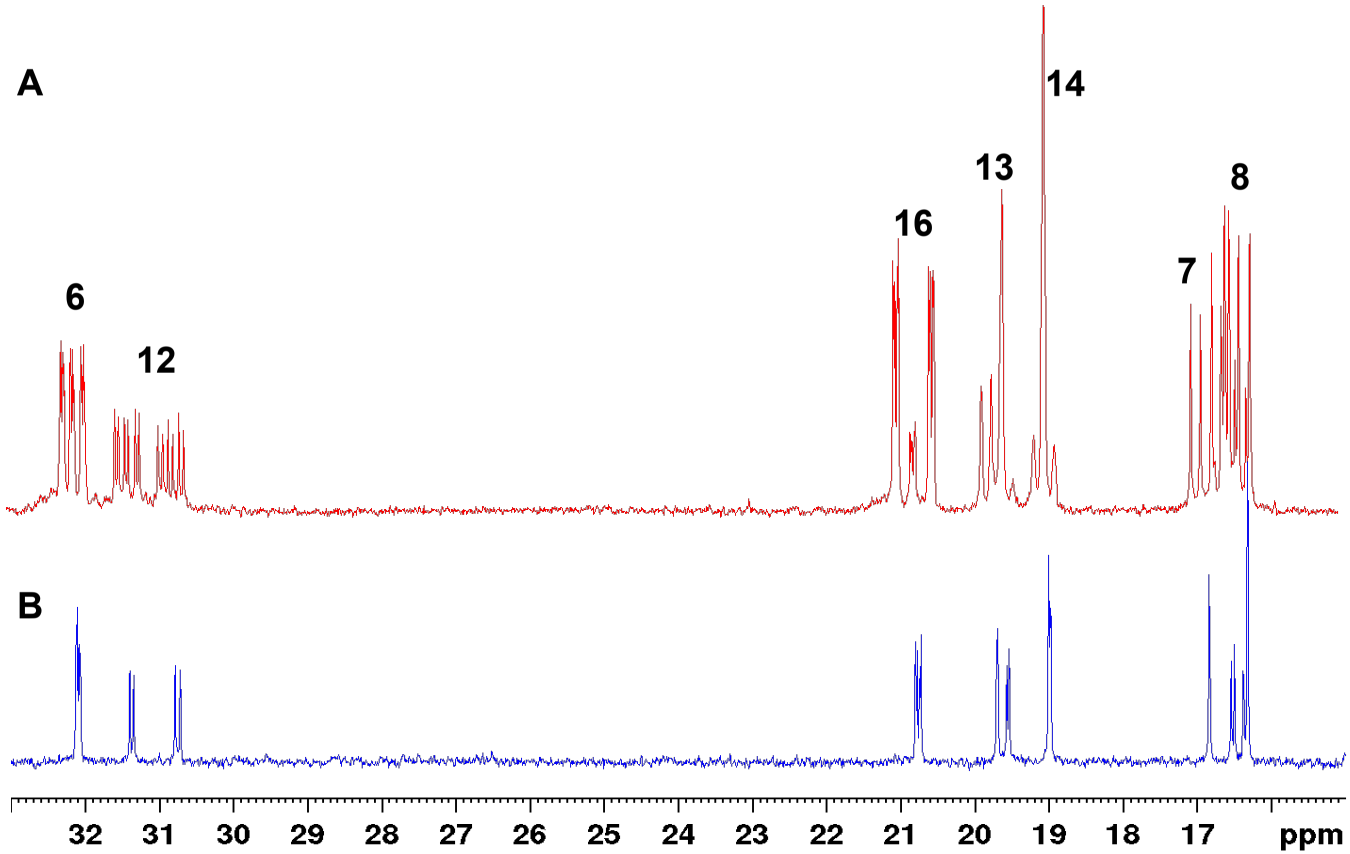

Figure 2.37 (Continued). Expansion of ^{13}C NMR (125MHz, $CDCl_3$) spectra: A, ^{13}C-enriched brassicicolin A (**1e**) obtained from incubation of cultures with D-[U-$^{13}C_6$]glucose; B, natural abundance of brassicicolin A (**1**).

Incorporation of [U-$^{13}C_6$]glucose into brassicicolin A (**1**) was established using NMR spectroscopy. INADEQUATE spectrum showed intense correlations between δ_C 174.5 (C-4/C-4') and 75.4 (C-5/C-5'), δ_C 32.1 (C-6/C-6') and 16.3 (C-7/C-7') or 16.7 (C-8/C-8'), δ_C 165.7 (C-9/C-9') and 63.1 (C-10/C-10'), and δ_C 31.2 (C-12/C-12') and 18.9 (C-14/C-14') or 19.7 (C-13/C13') (**Figure 2.38**). In the mannitol (**233**) unit, correlations between δ_C 67.0 (C-1/C-1') and 70.2 (C-2/C-2') and δ_C 70.2 (C-2/C-2') and 61.7 (C-3/C-3') were observed. Because C-1 and C-1' show the same chemical shift, a correlation cannot be established. A strong correlation between δ_C 169.8 (C-15/C-15') and 20.7 (C-16/C-16') indicated incorporation of D-[U-$^{13}C_6$]glucose into acetyl groups of brassicicolin A (**1**) (**Figure 2.38**). Based on those observations in the INADEQUATE spectrum, the labeling pattern of the ^{13}C-enriched brassicicolin A (**1e**) was established (**Figure 2.39**).

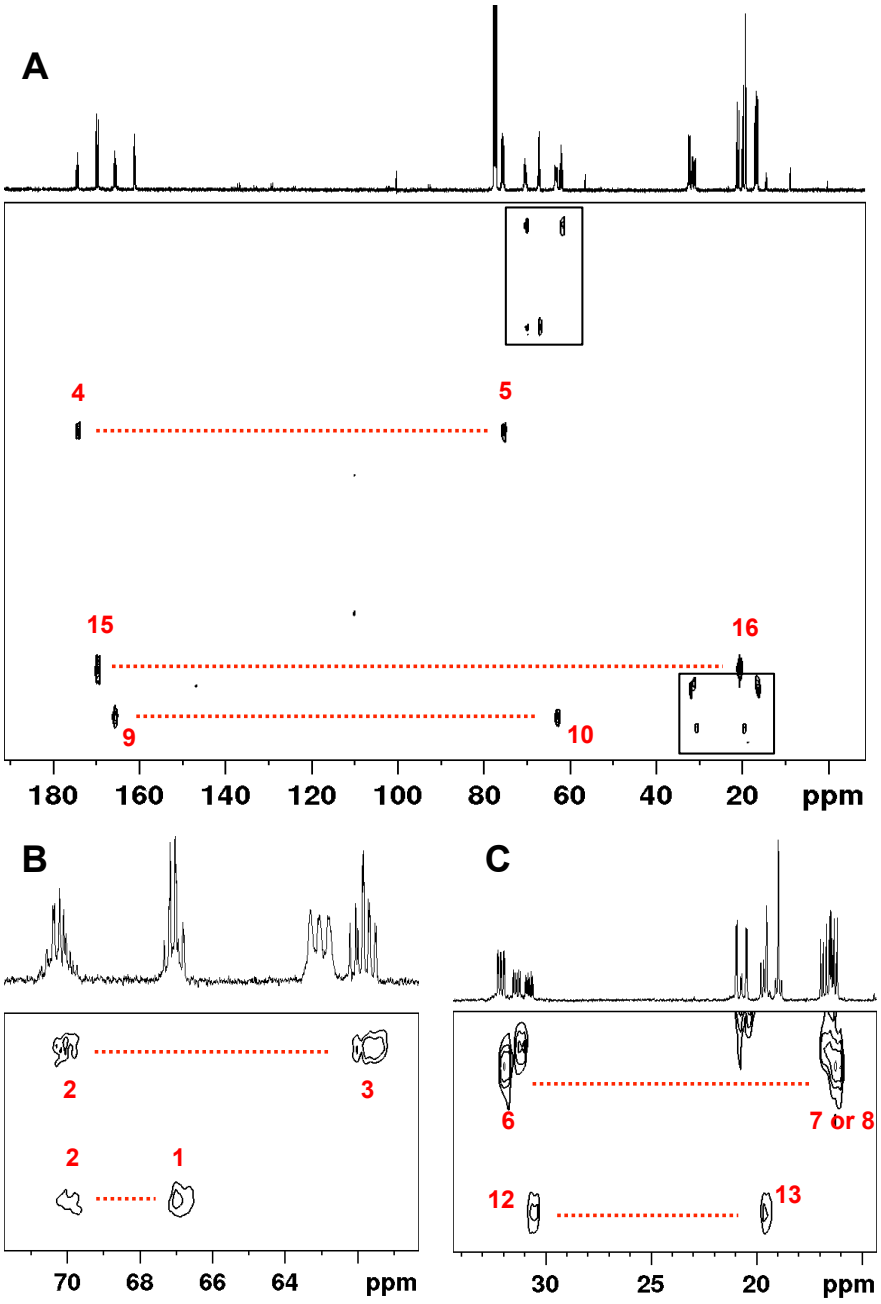

Figure 2.38 INADEQUATE spectrum of ^{13}C-enriched brassicicolin A (**1e**) obtained from incubation of cultures with D-[U-$^{13}C_6$]glucose (A). B and C represent expanded INADEQUATE spectra. Dashed red lines indicate couplings ($^{1}J_{13C\text{-}13C}$) between the adjacent carbons. Numbers indicate carbon numbers of brassicicolin A (**1**).

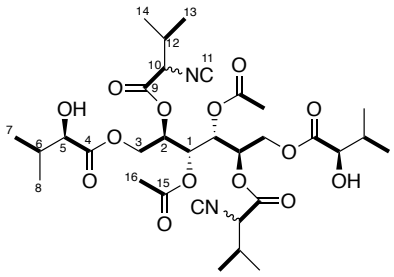

1e

Figure 2.39 Labeling patterns in ^{13}C-enriched brassicicolin A (**1e**) obtained from incubation of cultures with D-[U-$^{13}C_6$]glucose. Bold lines indicate correlations detected in the 2D INADEQUATE spectrum.

ESI-MS analysis

According to IUPAC, an isotopologue is "*a molecular entity that differs only in isotopic composition*"; whereas, isotopomers have "*the same number of each isotopic atom but differing in their position*" (IUPAC, 1997). For example, [1,2,3,4,5,6-$^{13}C_6$]glucose (**229a**), and [1,2-$^{13}C_2$]glucose (**229b**) are isotopologues; whereas, [1,2-$^{13}C_2$]glucose (**229c**) and [1,3-$^{13}C_2$]glucose (**229d**) are isotopomers (**Figure 2.40**).

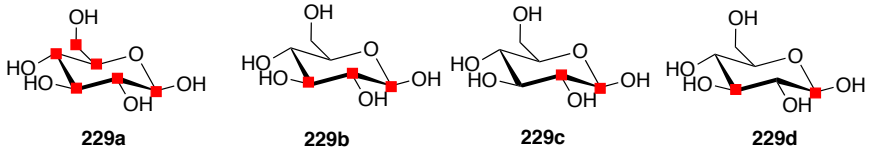

229a **229b** **229c** **229d**

Figure 2.40 Examples of isotopologues and isotopomers of glucose. Red squares refer to ^{13}C atoms.

HPLC-ESI-MS analysis confirmed incorporation of D-[U-$^{13}C_6$]glucose (**229a**) into brassicicolin A (**1**). Natural abundance brassicicolin A (**1**) (molecular weight 684) displayed three quasimolecular ion peaks at *m/z* 685 $[M+1]^+$, 703 $[M+H_2O+1]^+$, 707 $[M+Na]^+$ in HPLC-ESI-MS spectrum (**Figure 2.41**). Although ^{13}C-enriched brassicicolin A (**1e**) displayed a complicated MS spectrum, it clearly showed a peak at *m/z* 716 $[M+32]^+$ that is not present in

natural abundance brassicicolin A (**1**) (**Figure 2.41**), indicating all carbons in ^{13}C-enriched brassicicolin A (**1**) are labeled.

Detection of various quasi-molecular ions (686, 687, 688, etc.) indicates a mixture of isotopologues and isotopomers of the ^{13}C-enriched brassicicolin A (**1**). D-[U-$^{13}C_6$]Glucose is metabolized by *A. brassicicola* providing various labeled precursors of brassicicolin A (**1**). For example, D-[U-$^{13}C_6$]glucose is converted to doubly labeled [1,2-$^{13}C_2$]acetyl-CoA thorough glycolysis. The doubly labeled acetyl-CoA could be incorporated into C-15/C-15' and C-16/C-16' in brassicicolin A (**1**) leading to detection of a peak at *m/z* 688 $[M+2+H]^+$. However, detection of a peak at *m/z* 688 does not necessarily mean that one of two acetyl groups (C-15/C-15' and C-16/C-16') of brassicicolin A (**1**) is labeled with ^{13}C. In other words, another isotopomer that has two ^{13}Cs in any two positions in brassicicolin A (**1**) could give a peak at *m/z* 688 $[M+2+H]^+$. Similarly, detection of a peak at *m/z* 689 $[M+3+H]^+$ indicates three carbons are labeled in brassicicolin A (**1**), but it is not feasible to determine the exact positions of labeled carbons in brassicicolin A (**1**).

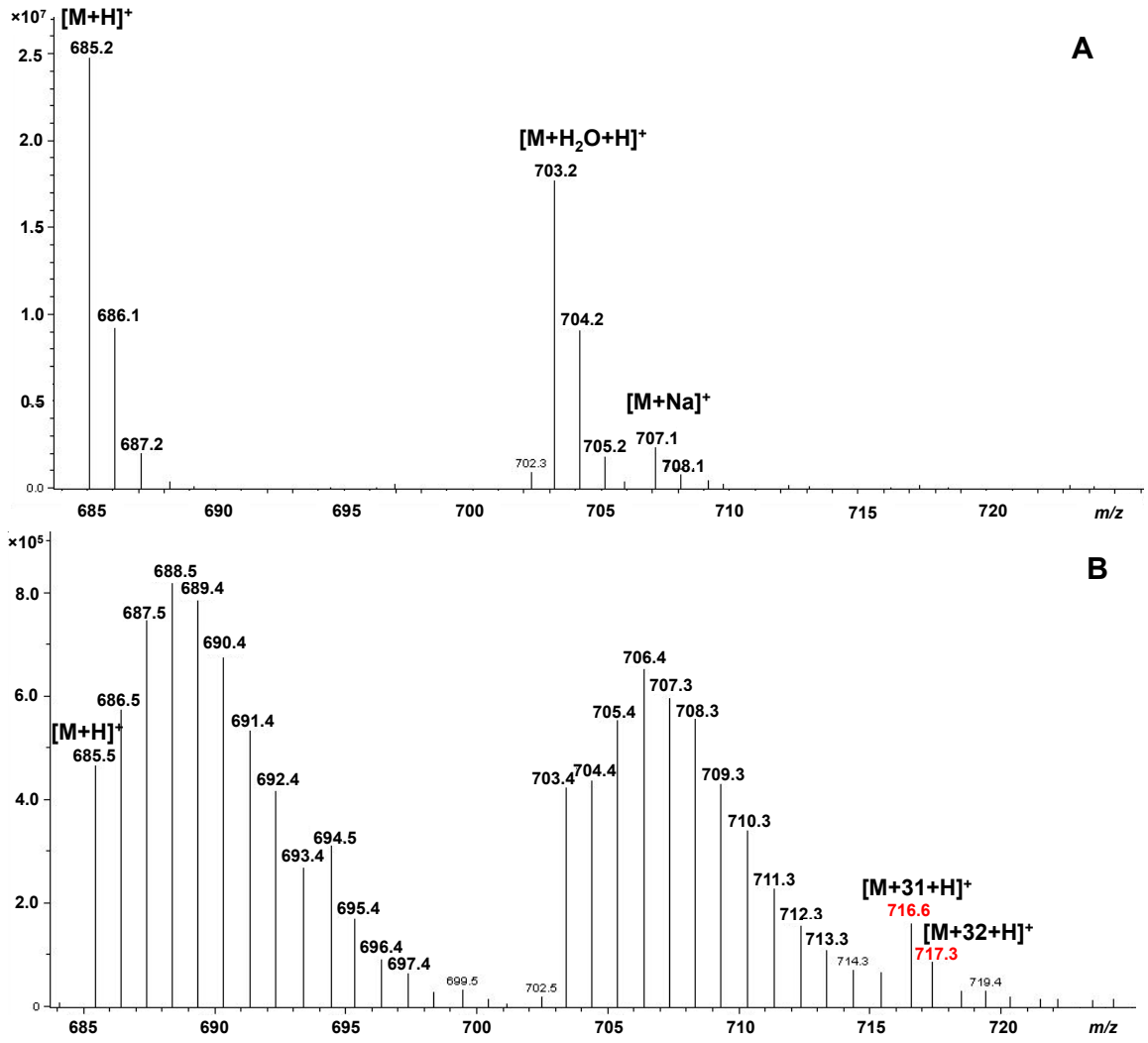

Figure 2.41 HPLC-ESI-MS spectra of natural abundance (A) and ^{13}C-enriched (B) brassicicolin A (**1e**) obtained from incubation of cultures with D-[U-$^{13}C_6$]glucose (**229a**)

2.3.2 Incorporation of L-[$^{2}H_{8}$]valine and L-[^{15}N]valine into brassicicolin A

Brassicicolin A (**1**) has isocyanoisovaleryl (C-9/9'–C-14/14') and 2-hydroxy-3-methylbutanoate (C-4/4'–C-8/8') groups connected to mannitol (**233**) through ester linkages. Since valine is likely a precursor of brassicicolin A (**1**), preliminary experiments using unlabeled valine were carried out to examine whether addition of valine to MM affects production of brassicicolin A (**1**). As a preliminary experiment, unlabeled valine was added to 48-h-old cultures (50 mg) and 96-h-old cultures (50 mg). After eight days, culture filtrates were extracted and brassicicolin A (**1**) was quantified. The amount of brassicicolin A (**1**) in standard MM at 30 °C increased by ca. 150 % in standard MM amended with valine at 30 °C.

A. brassicicola cultures were grown in standard MM at 30 °C. L-[$^{2}H_{8}$]Valine was administered to 48-h-old culture (50 mg in 100 mL MM) and 96-h-old culture (50 mg in 100 mL MM), where total amount of L-[$^{2}H_{8}$]valine was 100 mg in a 100 mL of standard MM. After 8 days, culture filtrates were extracted and the crude extracts were subjected to FCC. Purified brassicicolin A (**1**) (19.5 mg, see **Scheme 4.7**) obtained from incubation of cultures with L-[$^{2}H_{8}$]valine was analyzed by ^{1}H NMR and HRESI-MS.

The ^{1}H NMR of brassicicolin A (**1**) obtained from incubation of cultures with L-[$^{2}H_{8}$]valine was compared to that of natural abundance brassicicolin A (**1**) (**Figure 2.42**). Integration of the ^{1}H NMR spectrum revealed that the protons in isocyanoisovaleryl and 2-hydroxy-3-methylbutanoyl groups were replaced by deuteria. The reduced integration of ^{1}H NMR signals (H-6/6'–8/8' and H-12/12'–14/14') of ^{2}H-enriched brassicicolin A (**1**) suggest that L-[$^{2}H_{8}$]valine is incorporated into brassicicolin A (**1**) at H-6/6'–H-8/8' and H-12/12'–H-14/14'.

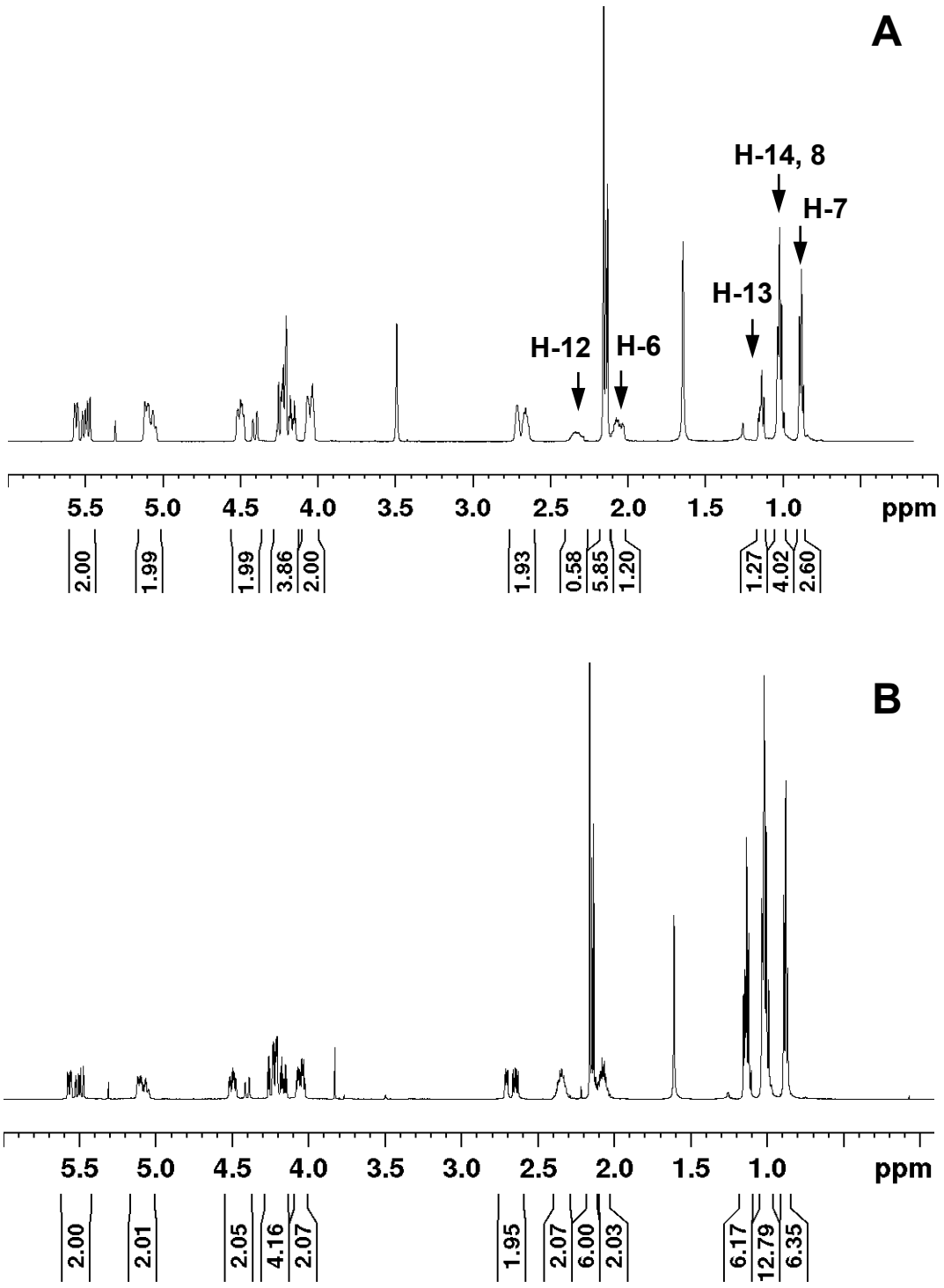

Figure 2.42 ^{1}H NMR spectra of ^{2}H-enriched brassicicolin A (**1j**) resulting from incubation of cultures with L-[$^{2}H_8$]valine and natural abundance brassicicolin A (**1**) (B). Arrows indicate the partial replacement of protons by deuteria.

The HRESI-MS spectrum confirmed incorporation of L-[$^2H_8$]valine into brassicicolin A (**1**) (**Figure 2.43**). Four quasimolecular ion peaks were detected in ^{2}H-enriched brassicicolin A (**1**) resulting from incubation of cultures with L-[$^2H_8$]valine. For example, a quasimolecular ion $[M+H]^+$ at *m/z* 692.3633 showed 7 mass units higher than natural abundance brassicicolin A (**1**) $[M+H]^+$ at 685.3224, suggesting the protons in either isocyanoisovaleryl or 2-hydroxy-3-methylbutanoate groups are replaced by deuteria (**Figure 2.44**). Similarly, a quasimolecular ion $[M+H]^+$ at *m/z* 713.4941 showed 28 mass units higher than natural abundance brassicicolin A (**1**), suggesting that the protons of two isocyanoisovaleryl and two 2-hydroxy-3-methylbutanoate moieties are replaced by deuteria. HRESI-MS suggests that the ^{2}H-enriched brassicicolin A (**1**) is present as a mixture of isotopologues (e.g., **1f** and **1j** are isotopologues) and isotopomers (e.g., **1f** and **1g** are isotopomers). Each quasi-molecular ion peak and the corresponding molecular formula are shown in **Table 14**.

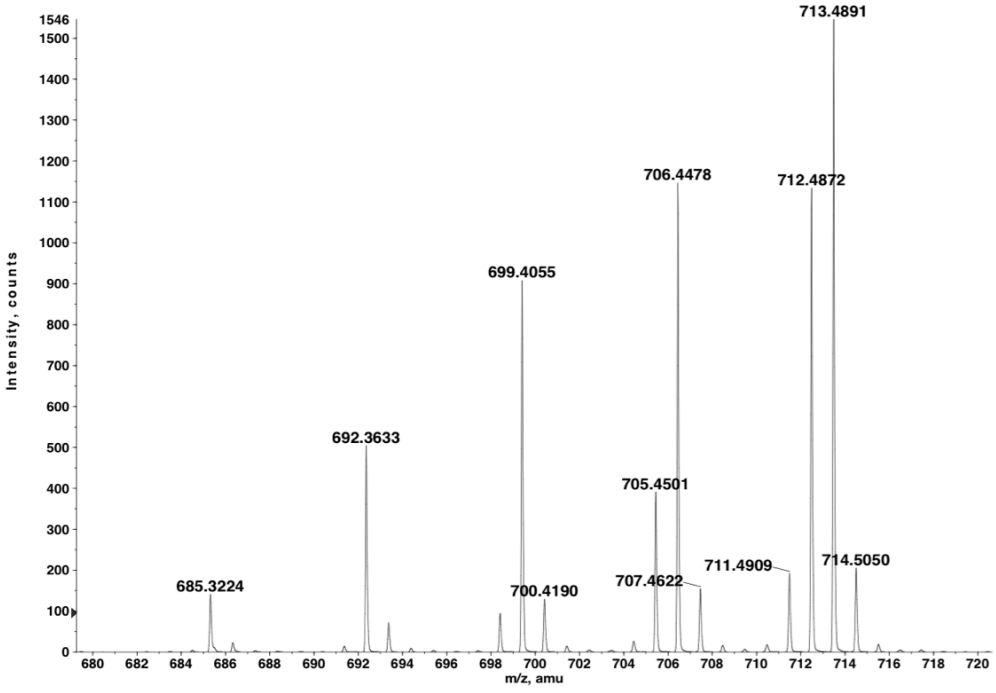

Figure 2.43 HR-MS spectrum of ^{2}H-enriched brassicicolin A (**1j**) obtained from administration of L-[$^2H_8$]valine.

Table 14 Quasi-molecular ions of ^{2}H-enriched brassicicolin A.

m/z	Molecular formula
685.3224	$[M+H]^+$, $C_{32}H_{49}N_2O_{14}$
692.3633	$[M+H+7]^+$, $C_{32}H_{42}{}^{2}H_7N_2O_{14}$
699.4055	$[M+H+14]^+$, $C_{32}H_{35}{}^{2}H_{14}N_2O_{14}$
706.4478	$[M+H+21]^+$, $C_{32}H_{28}{}^{2}H_{21}N_2O_{14}$
713.4941	$[M+H+28]^+$, $C_{32}H_{21}{}^{2}H_{28}N_2O_{14}$

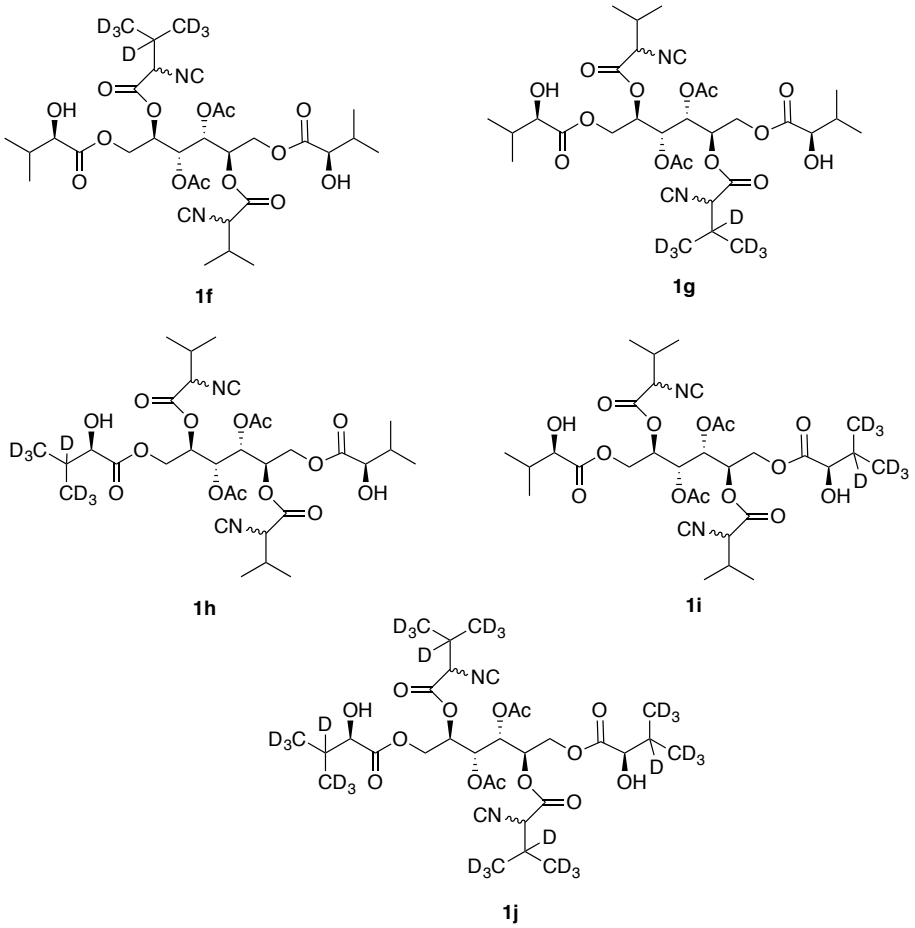

Figure 2.44 Examples of isotopologues and isotopomers of ^{2}H-enriched brassicicolin A.

To identify the biosynthetic origin of nitrogens in brassicicolin A (**1**), L-[^{15}N]Valine was administered twice to 48-h-old culture (50 mg) and 96-h-old culture (50 mg), where the total amount of L-[^{15}N]valine was 100 mg in a 100 mL of culture. After 8 days, culture filtrates

incubated with L-[^{15}N]valine were extracted and the crude extracts were subjected to FCC to isolate brassicicolin A. Brassicicolin A (13.3 mg **Scheme 4.7**) was obtained and the^{15}N-enriched brassicicolin A (**1m**) was analyzed by ^{1}H, ^{13}C, ^{15}N NMR and HRESI-MS.

The spin systems and chemicals shifts in the ^{1}H NMR spectrum of the ^{15}N-enriched brassicicolin A (**1**) were identical with those of natural abundance brassicicolin A (**1**) (**Figure 2.45**). The ^{13}C NMR spectrum of the ^{15}N-enriched brassicicolin A (**1**) was also identical with that of natural abundance of brassicicolin A (**1**) except for isocyanide carbon (C-11). More complex couplings at C-11 were detected in ^{15}N-enriched brassicicolin A (**1**) compared to the natural abundance molecules (**Figure 2.46**).

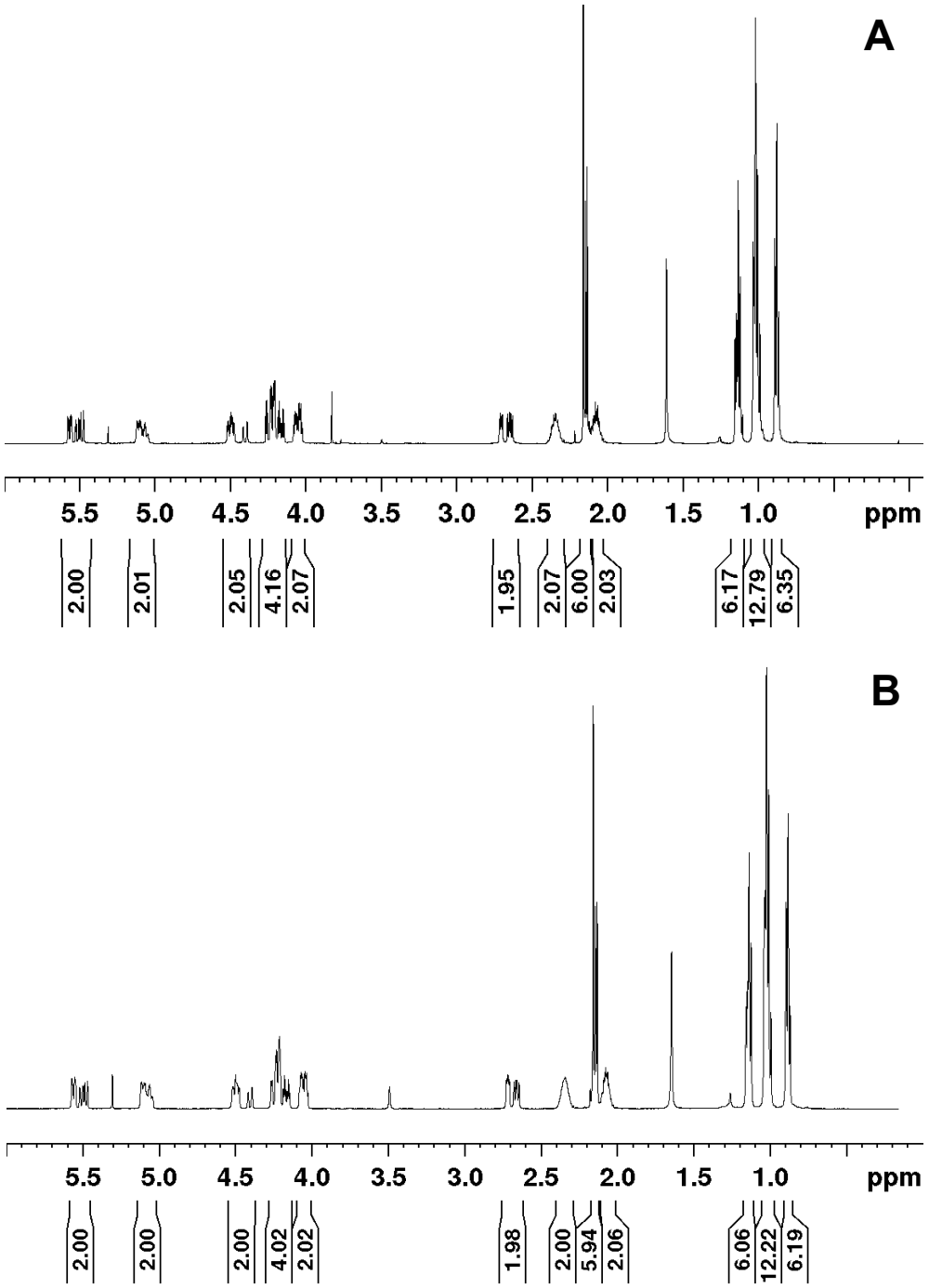

Figure 2.45 ^{1}H NMR spectra of ^{15}N-enriched brassicicolin A (**1m**) (upper) obtained from incubation of cultures with L-[^{15}N]valine and natural abundance brassicicolin A (**1**) (lower).

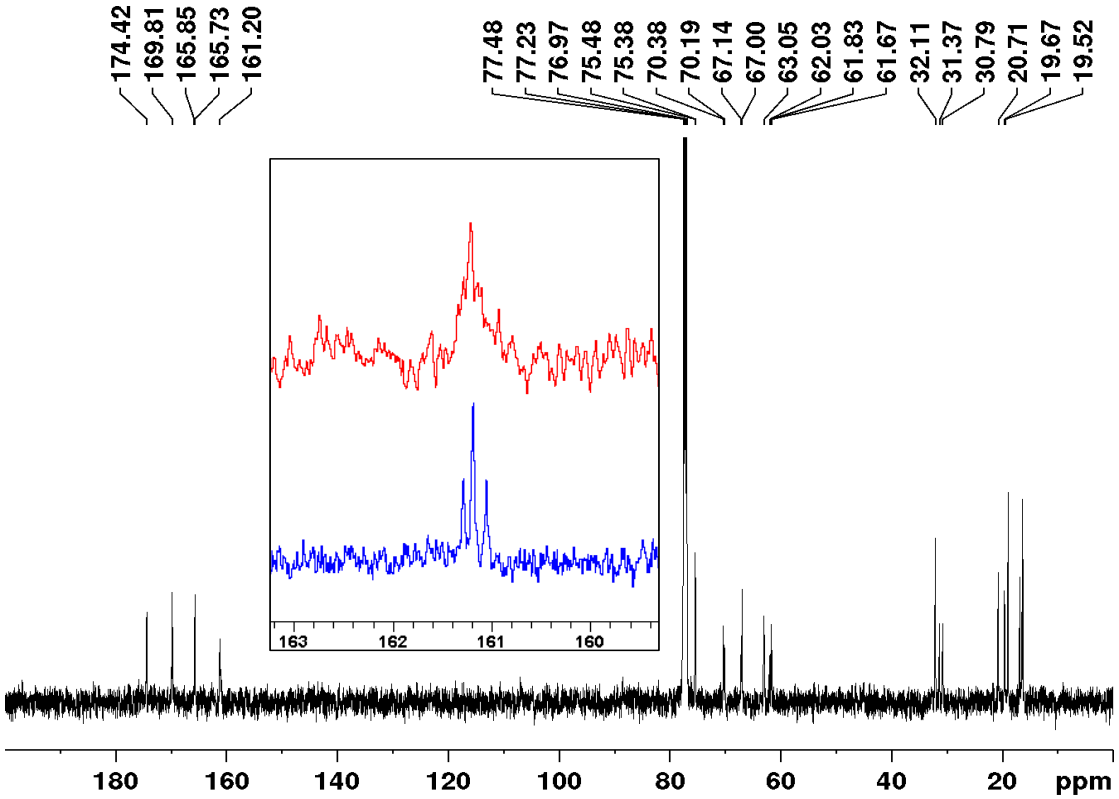

Figure 2.46 ^{13}C NMR spectrum of ^{15}N-enriched brassicicolin A (**1**) obtained from incubation of cultures with L-[^{15}N]valine. The insert shows C-11/C-11' resonance of ^{15}N-enriched brassicicolin A (red) and natural abundance brassicicolin A (**1**) (blue).

For ^{15}N NMR analysis, the ^{15}N resonances were externally referenced to the signal of liquid CH_3NO_2 (379.6 ppm relative to external liquid NH_3 as a zero-point standard) containing $CDCl_3$ (Wishart, Bigam *et al.*, 1995). The ^{15}N NMR of the ^{15}N-enriched brassicicolin A (**1m**) resulting from incubation of cultures with L-[^{15}N]valine showed three resonances (**Figure 2.47**). Brassicicolin A (**1**) is an equilibrium mixture of diastereomers; thus, three resonances in the ^{15}N NMR are indicative of three different diastereomers. The HRESI-MS spectrum of ^{15}N-enriched brassicicolin A (**1m**) revealed molecular ions $[M+H+1]^+$ at *m/z* 686.3174 and $[M+H+2]^+$ at *m/z* 687.3165, besides the natural abundance at *m/z* 685.3211 (**Figure 2.48**). Considering that brassicicolin A (**1**) has two nitrogens (next to C-11, and C-11'), detection of a peak at *m/z* 686.3174 indicates one nitrogen in two isocyanide groups is replaced with ^{15}N. That is, a mixture of two isotopomers (**1k** and **1l**) yielded detection of a peak at *m/z* 686.3174. In addition, detection of two peaks at *m/z* 686.3174 and 687.3165 in ^{15}N-enriched brassicicolin A indicates

the^{15}N-enriched brassicicolin A (**1m**) is a mixture of isotopologues of nitrogen (e.g., **1k** and **1m**) (**Figure 2.49**). Each quasi-molecular ion of ^{15}N-enriched brassicicolin A and the corresponding molecular formula are shown in **Table 15**.

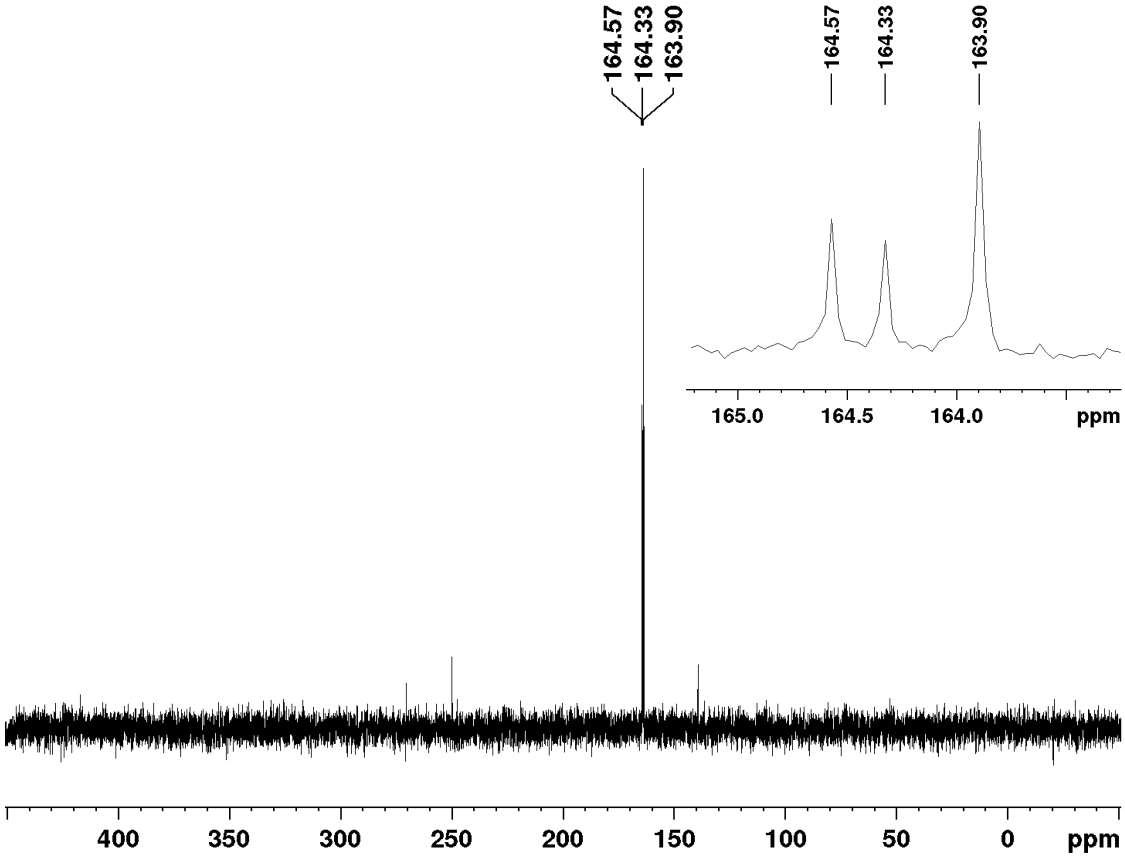

Figure 2.47 ^{15}N NMR (50.7 MHz, $CDCl_3$) of brassicicolin A (**1**) obtained from incubation of cultures with L-[^{15}N]valine.

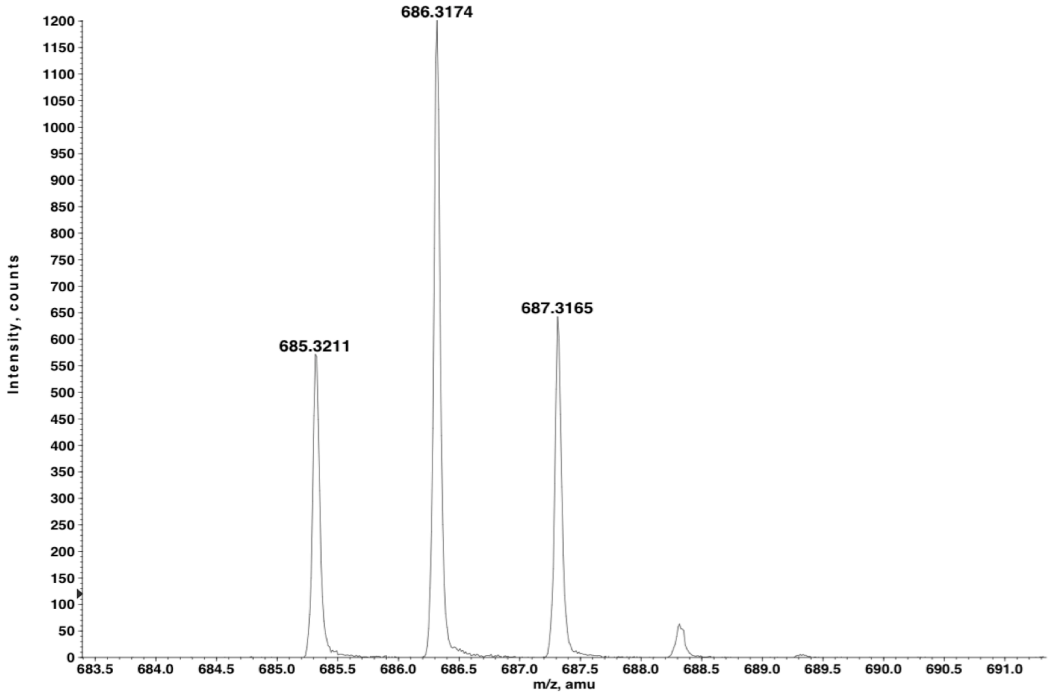

Figure 2.48 HRESI-MS spectrum of ^{15}N-enriched brassicicolin A (**1**) obtained from incubation of cultures with L-[^{15}N]valine.

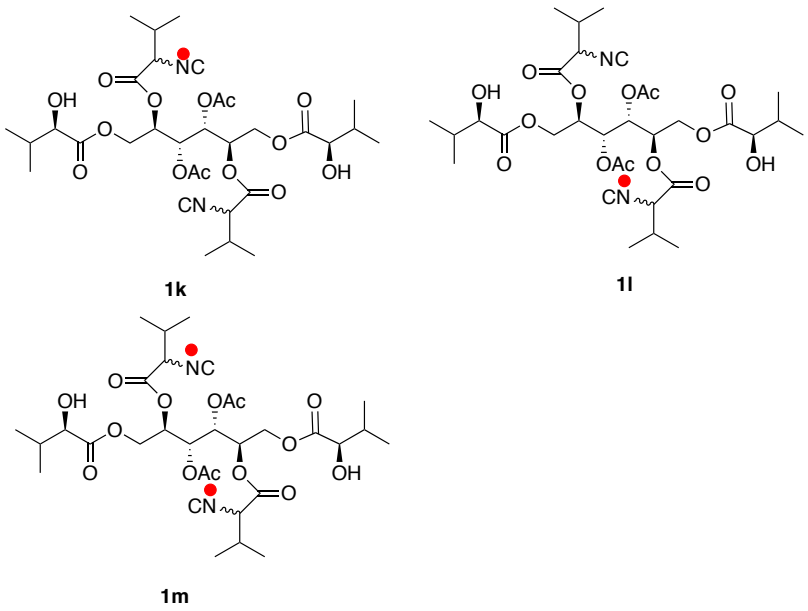

Figure 2.49 Isotopologues and isotopomers of ^{15}N-enriched brassicicolin A. Red circles refer to ^{15}N atoms.

Table 15 Quasi-molecular ions of ^{15}N-enriched brassicicolin A.

m/z	Molecular formula
685.3211	$[M+H]^+$, $C_{32}H_{49}NO_{14}$
686.3174	$[M+H+1]^+$, $C_{32}H_{49}{}^{15}NNO_{14}$
687.3165	$[M+H+2]^+$, $C_{32}H_{49}{}^{15}N_2O_{14}$

2.3.3 Discussion

Alternaria brassicicola produces various secondary metabolites. Ciegler and Lindenfelser (1969) first reported that the extracts of *Alternaria brassicicola* exhibited antibiotic activities (Ciegler and Lindenfelser, 1969). Gloer *et al*. elucidated the structure of the main component of antibiotic complex (named brassicicolin A) using NMR and MS spectrometry (Gloer, Poch *et al.*, 1988). More recently, Pedras *et al.* established that brassicicolin A (**1**) is a host-selective phytotoxin in *Brassica juncea* cv. Cutlass using a whole plant assay (Pedras, Chumala *et al.*, 2009). There are no reports regarding the biosynthetic studies on brassicicolin A (**1**).

All spectroscopic data of ^{13}C, ^{2}H, or ^{15}N-enriched brassicicolin A showed successful incorporation of labeled precursors into brassicicolin A (**1**), suggesting that brassicicolin A (**1**) is originated from those biosynthetic precursors (i.e., valine and glucose). To determine whether isocyanide carbons (C-11/C-11') in brassicicolin A (**1**) are labeled, natural abundance brassicicolin A (**1**) was analyzed by ^{13}C NMR using the identical parameters as those used for ^{13}C-enriched brassicicolin A (**1e**). A significant enhancement of C-11/C-11' carbon signals in ^{13}C-enriched brassicicolin A (**1e**) indicates the isocyanide carbons are labeled (**Figure 2.37**). A biosynthetic precursor of marine isocyanide compounds is most likely inorganic cyanide (Garson and Simpson, 2004), while the origin of the carbon in isocyalexin (**166**), a unique plant-derived isocyanide, is (*S*)-tryptophan (**155**) (Pedras and Yaya, 2013). In addition, it was reported that the isocyanide carbon of indole vinylisocyanide (**158**) was derived from ribulose-5-phosphate in the recombinant *E. coli* (Brady and Clardy, 2005b). Considering that brassicicolin A (**1**) is a terrestrial microbe-derived isocyanide, it is likely that the isocyanide carbon of brassicicolin A (**1**) is derived from glucose via ribulose-5-phophate (**156a**). Further experiments are needed to further establish the biosynthetic origin of the isocyanide carbons of brassicicolin A (**1**) using more advanced precursors (e.g., [2-^{13}C]ribose) than [U-$^{13}C_6$]glucose.

3 Conclusions and future work

A comprehensive investigation of secondary metabolites produced by *A. brassicicola* was carried out for a better understanding of the chemical interactions between *A. brassicicola* and its host plants. Previously, as described in the introduction, several metabolites including brassicicolin A (**1**), diterpenoides (**Figure 1.18**), polyketides (**Figure 1.19**) and siderophores (**176**, **179**, **184**) were reported. In this work, four metabolites—α-acetylorcinol (**210**), tyrosol (**219**), depudecin (**151**), and dihydrobrassicicolin A (**220**)—were isolated from the extracts of culture filtrates of *A. brassicicola* grown in MM or PDB under standard conditions. The chemical synthesis of α-acetylorcinol (**210**) was accomplished for the first time with an overall yield of 36% (Pedras and Park, 2015).

Secondary metabolic pathways of *A. brassicicola* are strongly dependent on culture conditions, specifically nitrogen sources, ferric ion and temperature. An increase in the incubation temperature (from 23 °C to 30 °C) of cultures increased the production of brassicicolin A (**1**), whereas the production of depudecin (**151**) was decreased at the higher temperature (30 °C). Nitrates appeared to down-regulate biosynthetic pathways of brassicicolin A (**1**), depudecin (**151**) and α-acetylorcinol (**210**). In the Fe^{3+}-deficient condition, *A. brassicicola* produced larger amounts of siderophores than in control cultures (ferric citrate 2 μM) or in high concentration of ferric citrate (200 μM). *A. brassicicola* hydrolyzed SAHA (**32**) to *N*-phenylacetamide (**227**) via hydrolysis of SAHA (**32**) followed by acetylation. Neither SBHA (**33**) nor 5-Aza (**35**) affected metabolite profiles of *A. brassicicola* in MM. These results suggest that *A. brassicicola* might be resistant to exogenous epigenetic modifiers (Pedras and Park, 2015).

Detached leaf assays were employed to determine the phytotoxicity of secondary metabolites of *A. brassicicola*. Neither α-acetylorcinol (**210**), tyrosol (**219**) nor phomapyrone A (**25**) showed necrosis on detached leaves of *B. juncea*, *B. napus*, and *S. alba* (Pedras and Park, 2015). However, a significant difference was observed between leaves of whole plants (no necrosis) and detached leaves (necrosis) of *S. alba* responding to brassicicolin A (**1**). Furthermore, detached leaves of *S. alba* infected with *A. brassicicola* exhibited disease symptoms, suggesting physical stresses (e.g. excision of leaves) might affect plant resistance. On the other hand, lower severity of disease symptoms in detached leaves of *S. alba* infected with *A.*

brassicicola suggested that other resistance mechanisms might be present in detached leaves of *S. alba*.

HPLC-ESI-MS analyses of SGFs collected from detached leaves of *B. juncea*, *B. napus*, or *S. alba* showed that all SGFs contained siderophores and phomapyrone A (**25**). It suggests that *A. brassicicola* might produce siderophores to obtain iron from host plants. However, further experiments are necessary to establish roles of phomapyrone A (**25**) in the chemical interactions of *A. brassicicola* and its host plants.

Incorporation of D-[U-$^{13}C_6$]glucose, L-[^{15}N]valine, or L-[$^{2}H_8$]valine into brassicicolin A was determined using ^{1}H , ^{13}C NMR, ^{15}N NMR spectroscopy, HRMS-ESI and HPLC-ESI-MS spectrometry. The ^{13}C NMR and INADEQUATE spectra of ^{13}C-enriched brassicicolin A (**1e**) showed ^{13}C-^{13}C coupling attributed to adjacent ^{13}C carbons. In addition, enhancement of the carbon resonances of isocyanide carbon of brassicicolin A (**1**) suggested that isocyanide carbons of brassicicolin A are labeled. Spectroscopic data including ^{1}H NMR, ^{15}N NMR, HRMS-ESI and HPLC-ESI-MS of brassicicolin A (**1**) indicated that both 2-hydroxyisopentanoyl and 2-isocyanoisopentanoyl residues are derived from valine.

Currently, it is unclear whether brassicicolin A (**1**) is a virulence factor or pathogenicity factor of *Alternaria* black spot disease in crucifers. One of the ways to prove the involvement of brassicicolin A (**1**) in disease is to establish pathogenicity or virulence using mutants that would not produce brassicicolin A (**1**). If the mutant deficient in brassicicolin A are less virulent to host plants than the wild type, brassicicolin A might be considered a key determinant of the disease. On this basis, the biosynthetic pathway of brassicicolin A could be a plausible target to control *A. brassicicola*. Design of selective inhibitors of enzymes involved in biosynthesis of brassicicolin A (**1**) would contribute to development of eco-friendly biocontrol agents (Cools and Hammond-Kosack, 2013; Pedras and Park, 2015).

4 Experimental

4.1 General

Chemicals were purchased from Alfa-Aesar (Ward Hill, MA, USA), Fisher Scientific Canada (Ottawa, ON), Sigma-Aldrich Canada (Oakville, ON) and TCI America (Portland, OR, USA). D-[U-$^{13}C_6$]Glucose (99%), L-[$^{2}H_8$]valine (98%), and L-[^{15}N]valine (98%) were purchased from Cambridge Isotope Laboratories (Tewksbury, MA, USA). All solvents were HPLC grade. Organic extracts were dried over Na_2SO_4 and solvents were evaporated under reduced pressure in a rotary evaporator.

Flash column chromatography (FCC) was carried out using silica gel grade 60 (mesh size 230–400 Å).

Analytical thin layer chromatography (TLC) was carried out on alumina sheets pre-coated with TLC silica gel 60 F_{254} (Merck, Germany). Bands on TLC plates were visualized under UV light and by dipping in a solution of 5% aqueous (w/v) phosphomolybdic acid containing 1% (w/v) ceric sulfate and 4% (v/v) H_2SO_4 followed by heating.

HPLC analyses were carried out with Agilent high performance liquid chromatographs equipped with quaternary pumps, automatic injector, and diode array detector (DAD, wavelength range 190–600 nm), and degasser. The HPLC methods (A, B, and C) are summarized in **Table 16**.

HPLC-ESI-MS analysis was carried out with an Agilent 1100 series HPLC system equipped with an autosampler, binary pump, degasser and diode array detector connected directly to a mass detector (Agilent G2440A MSD-Trap-XCT ion trap mass spectrometer) with an ESI source. Chromatographic separation was carried out at room temperature. The interface and mass parameters were as follows: nebulizer pressure, 70.0 psi (N_2); dry gas, N_2 (12.0 L/min); dry gas temperature, 350 °C; spray capillary voltage 3500 V; skimmer voltage, 40.0 V; ion transfer capillary exit, 100 V; scan range, *m/z* 100–2000. Ultrahigh purity He was used as the collision gas. The HPLC-ESI-MS method (method D) is summarized in **Table 16**.

Nuclear magnetic resonance (NMR) spectra (^{1}H, 500 MHz; ^{13}C, 125.8 MHz; ^{15}N, 50.7 MHz; COSY-correlation spectroscopy; HSQC-Heteronuclear Single Quantum Coherence;

HMBC-Heteronuclear Multiple Bond Coherence; INADEQUATE-Incredible Natural Abundance DoublE QUAntum Transfer) were recorded on Bruker Avance 500 spectrometers at room temperature, unless otherwise stated. The ^{15}N resonances were externally referenced to the signal of liquid CH_3NO_2 containing $CDCl_3$ (379.6 ppm relative to external liquid NH_3 as a zero-point standard) (Wishart, Bigam *et al.*, 1995). Data processing was carried out using TopSpin™ 3.2 software.

High resolution electron impact mass (HREI-MS) spectra were obtained from a VG70 SE mass spectrometer employing a solid probe. High resolution field desorption mass (HRFD-MS) spectra were obtained from JEOL AccuTOF GCv 4G by direct insertion. High resolution electrospray ionization mass (HRESI-MS) spectra were obtained from a QSTAR XL Mass Spectrometer (Hybrid Quadrupole-TOF LC/MS/MS) with turbo spray ESI source.

Specific rotations ($[\alpha]_D$) were determined at room temperature on a polarimeter using a 1 mL, 10 cm length cell; the units are 10^{-1} deg cm^2 g^{-1} and the concentration was g/100 mL.

Fourier transform infrared (FT-IR) spectral data were obtained from a Bio-Rad FTS-40 spectrometer and spectra were measured by the diffuse reflectance method on samples dispersed in KBr.

Statistical analysis was conducted by one-way ANOVA with Tukey's test at significance level $P < 0.05$ using SPSS version 22.0 (SPSS, Inc. Chicago, IL, USA).

Table 16 HPLC methods used for analysis of metabolites of *Alternaria brassicicola* and *Brassica* species[§].

	Time	**MeOH**	**H_2O**	**Flow rate**
Method A[a]	0	10	90	0.4 mL/min
	10	30	70	
	35	100	0	
Method B[a]	0	30	70	0.4 mL/min
	35	100	0	
	Time	**MeCN**	**H_2O**	
Method C[b]	0	0	100	1.0 mL/min
	25	50	50	
	35	75	25	
	40	100	0	
	Time	**MeCN (0.2% HCOOH)**	**H_2O (0.2 % HCOOH)**	
Method D[b]	0	25	75	1.0 mL/min
	35	75	25	
	40	100	0	

[§] All signals in HPLC analyses were detected at 210, 220, and 254 nm.
[a] Eclipse XDB C-18 column (3.5 μm particle size silica, 3.0 i.d. × 100 mm)
[b] Eclipse XDB C-18 column (5.0 μm particle size silica, 4.6 i.d. × 150 mm)

Cultures of A. brassicicola

Alternaria brassicicola isolate UAMH 7474 was obtained from the University of Alberta Microfungus Collection and Herbarium (UAMH). *A. brassicicola* isolate UAMH7474 was subcultured in potato dextrose agar (PDA) plates under constant light at 23 ± 1 °C for 14 days. The spores were collected by adding sterilized H_2O (10 mL) to each agar plate and by scraping off the agar surface followed by filtration and centrifugation (3,000 rpm for 30 min) of the spore suspension. The resulting pellets were suspended with sterile H_2O. The spores were counted under a microscope using a hemocytometer and stored at −20 °C**.**

Alternaria brassicicola UAMH 7474 was grown in a Erlenmeyer flask (250 mL) containing minimal medium (MM, 100 mL) inoculated with fungal spores (2×10^6 spores / 100 mL) and incubated on a shaker at 110 rpm, at 23 ± 1 °C and 30 ± 1 °C for 7 days, unless otherwise stated.

Composition of standard MM:

Solution 1: KNO_3 (3.1 g/L, 31 mM), K_2HPO_4 (0.75 g/L, 4.3 mM), KH_2PO_4 (0.75 g/L, 5.5 mM), NaCl (0.10 g/L, 1.7 mM), asparagine (0.28 g/L, 2.1 mM);

Solution 2: $CaCl_2 \cdot 2H_2O$ (0.10 g/L, 0.68 mM), $MgSO_4 \cdot 7H_2O$ (0.50 g/L, 2.0 mM);

Solution 3: $ZnSO_4 \cdot 7H_2O$ (0.40 mg/L, 1.4 μM), $CuSO_4 \cdot 5H_2O$ (0.079 mg/L, 0.32 μM), $MnSO_4 \cdot 4H_2O$ (0.041 mg/L, 0.18 μM), MoO_3 (85%, 0.018 mg/L, 0.12 μM), ferric citrate (0.54 mg/L, 2.0 μM), $Na_2B_4O_7 \cdot 10H_2O$ (0.038 mg/L, 0.10 μM);

Solution 4: thiamine (0.10 mg/L, 0.38 μM);

Glucose: (15 g/L, 83 mM).

Solutions 1, 3 and glucose were combined and the pH of the mixed solution was adjusted to 6.5, autoclaved, allowed to cool and combined with solutions 2 and 4, which were previously sterilized by autoclaving and filtering using a 0.2 μm membrane filter, respectively.

Potato dextrose broth (PDB) was prepared by suspending PDB powder (VWR, Canada) in distilled water (24 g/L) followed by sterilization. *A. brassicicola* UAMH 7474 (2×10^6 spores/100 mL) was incubated in a Erlenmeyer flask (250 mL) containing PDB (100 mL) on a shaker at 110 rpm, at 23 ± 1 °C and 30 ± 1 °C for 7 days, unless otherwise stated**.**

4.2 Isolation and structure elucidation of fungal metabolites

4.2.1 Metabolites produced in MM

A. brassicicola cultures (12 L at 23 °C and 10.6 L at 30 °C) grown in standard MM (7-day-old) were filtered followed by lyophilization (**Scheme 4.1**). Lyophilized culture filtrates were diluted with distilled water and extracted with EtOAc.

The extracts (1.1 g, 30°C) of culture filtrates were fractionated by flash column chromatography (FCC) using silica gel. The crude extracts of fungal culture filtrates were eluted with CH_2Cl_2:MeOH (100:0 to 80:20 (v/v), gradient) followed by CH_2Cl_2:MeOH (99:1 (v/v), isocratic) to obtain α-acetylorcinol (**210**, 2.5 mg) and tyrosol (**219**, 2.5 mg). Fractions 2–3 (93 mg) were combined and further purified by hexane:Et_2O (40:60 to 0:100, gradient) to obtain brassicicolin A (**1**, 77.3 mg) and phomapyrone A (**25**, 1.3 mg) (**Scheme 4.1**).

The crude extracts (1.1 g) of culture filtrates of *A. brassicicola* grown at 23°C were eluted with CH_2Cl_2:MeOH (100:0 to 80:20, gradient) followed by hexane:EtOAc (15:85 to 5:95 (v/v), isocratic) to obtain depudecin (**151** 57 mg) and hexane:EtOAc (95:5, isocratic) to yield phomapyrone A (**25**, 2.1 mg) (**Scheme 4.2**).

Phomapyrones E (**146**) and G (**148**) were isolated from *combined* crude extracts (1.3 g) of *A. brassicicola* culture filtrates. The combined crude extracts (1.3 g) were eluted with CH_2Cl_2:MeOH (99:1 to 80:20, gradient) followed by Et_2O:CH_2Cl_2 (50:50, isocratic) and Hexane:EtOAc (95:5, isocratic) to obtain phomapyrone G (**148**, 1.5 mg). Fraction 9 obtained from the first purification step was eluted with CH_2Cl_2:MeOH (97:3, isocratic) followed by Et_2O:CMeOH (97:3, isocratic) and Et_2O:Hx:MeOH (70:30:2, isocratic) to obtain phomapyrone E (**146**, 2.1 mg) (**Scheme 4.3**).

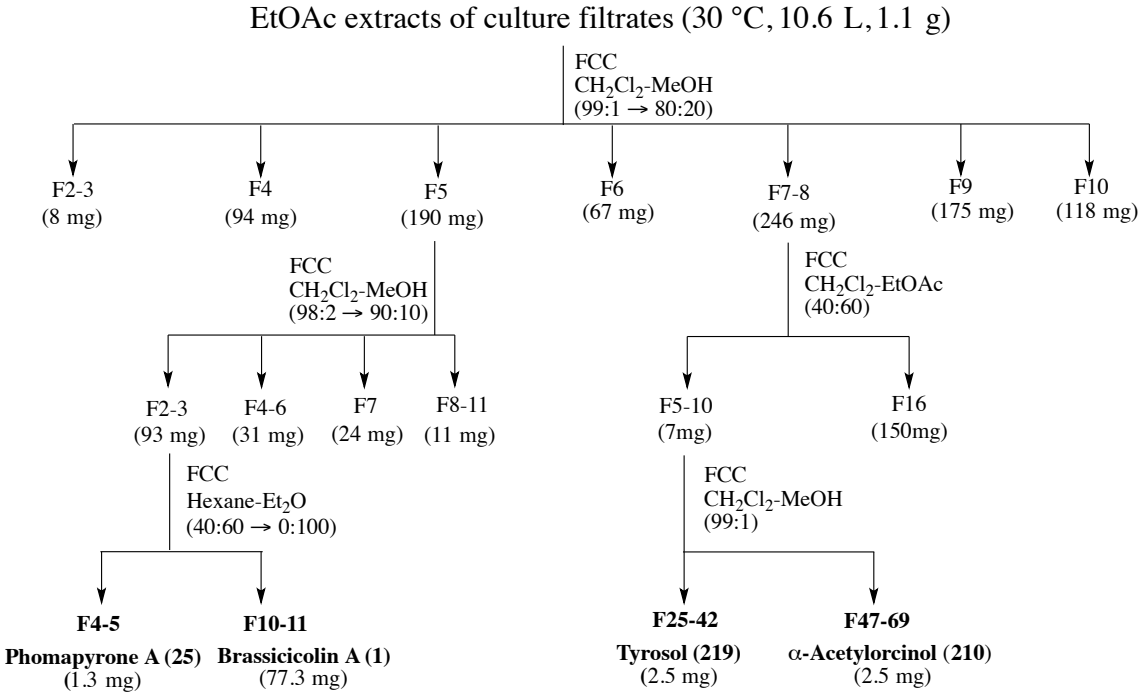

Scheme 4.1 Flow chart for isolation of metabolites of *Alternaria brassicicola* grown in standard MM at 30 °C.

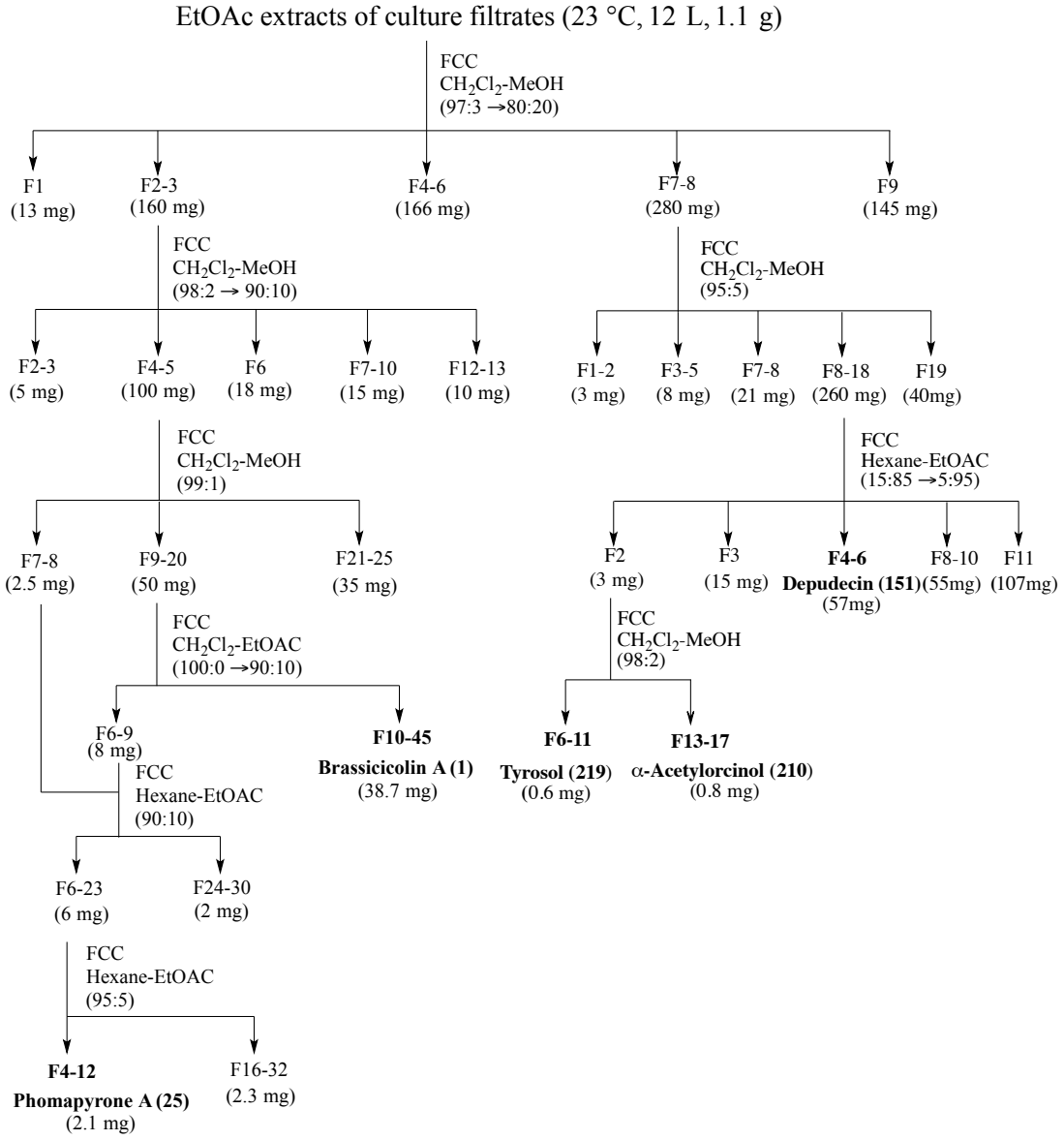

Scheme 4.2 Flow chart for isolation of metabolites of *Alternaria brassicicola* grown in standard MM at 23 °C.

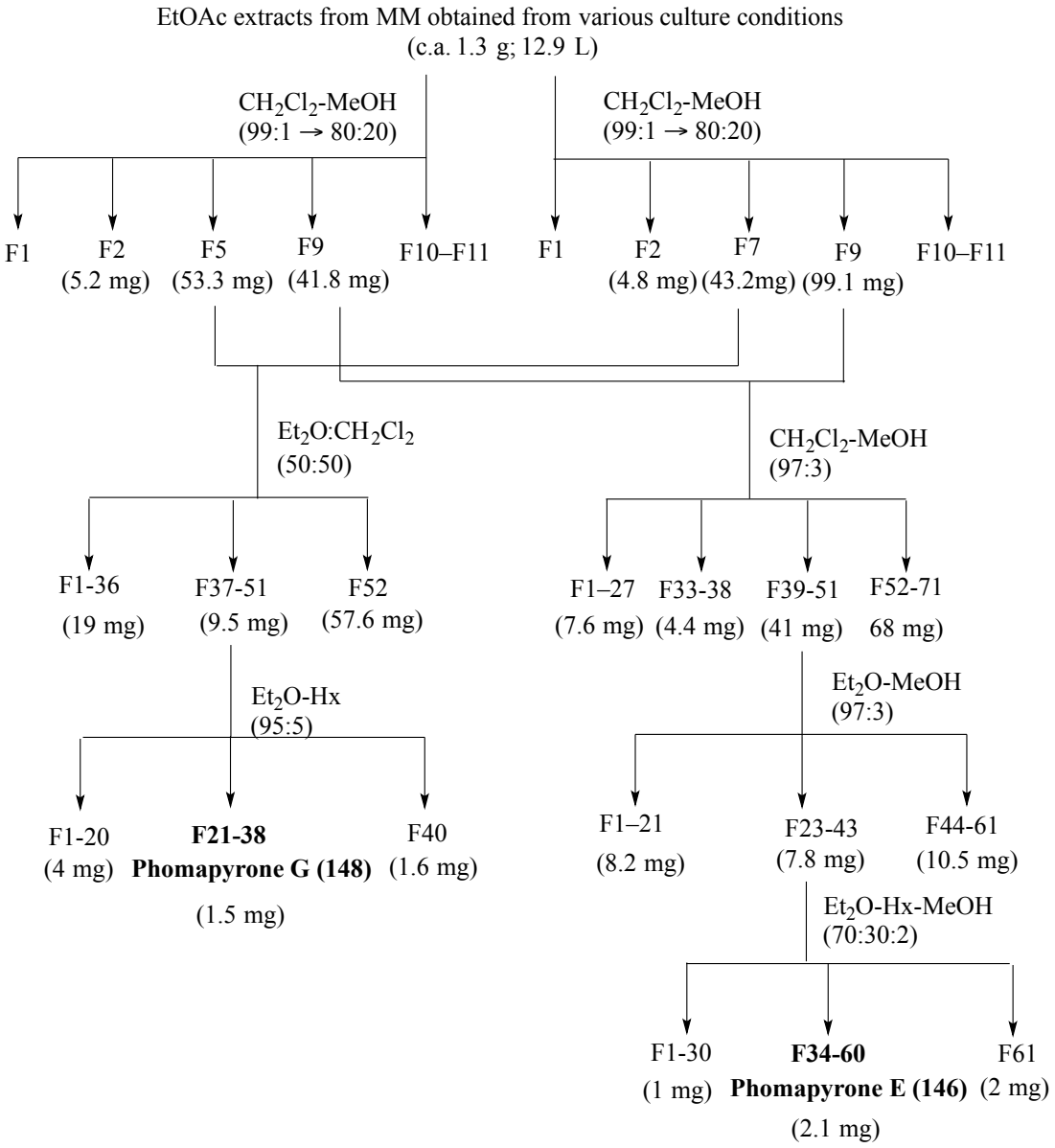

Scheme 4.3 Flow chart for isolation of metabolites of *Alternaria brassicicola* grown in standard MM at 23 °C and 30 °C.

4.2.1.1 α-Acetylorcinol (210)

HPLC t_R = 8.4 min, Method A.

^{1}H NMR (500 MHz, CD_3OD), ^{13}C NMR (125 MHz, CD_3OD) see **Table 5**.

HREI-MS: *m/z* 166.0626, $C_9H_{10}O_3$, calcd. 166.0629; *m/z* 166.0626 (100%), 123.0450 (65%).

FTIR (KBr): 3347, 1701, 1603, 1452, 1346, 1159, 1006, 842 cm^{-1}.

4.2.1.2 Tyrosol (219)

HPLC t_R = 9.2 min, Method A.

^{1}H NMR (500 MHz, CD_3CD), ^{13}C NMR (125 MHz, CD_3OD) see **Table 6**.

HREI-MS: *m/z* 138.0682, $C_8H_{10}O_2$, calcd. 138.0680; *m/z* 138.0682 (27%), 107.0497 (100%).

FTIR (KBr): 3392, 3170, 2953, 2958, 1514, 1360, 1345, 1238, 1051, 818cm^{-1}.

4.2.1.3 Depudecin (151)

HPLC t_R = 11.6 min, Method A.

^{1}H NMR (500 MHz, $CDCl_3$), ^{13}C NMR (125 MHz, $CDCl_3$) see **Table 7**.

FT-IR (KBr): 3388, 3083, 2976, 2144, 1743, 1666, 1379, 1223 cm^{-1}

$[\alpha]_D$ = -35 (*c* 0.50, MeOH).

Spectral data were consistent with those previously reported (Matsumoto, Matsutani *et al.*, 1992).

4.2.1.4 Phomapyrone A (25)

HPLC t_R = 24.7 min, Method B.

^{1}H NMR (500 MHz, $CDCl_3$): δ7.01(s, 1H), 6.16 (s, 1H), 5.66–5.62 (m, 1H), 3.92 (s, 3H), 2.04 (s, 3H), 1.95 (s, 3H), 1.83 (s, 3H), 1.76 (d, 3H, *J* = 7 Hz).

HRFD-MS: *m/z* 234.1264 calcd. $C_{14}H_{18}O_3$, 234.1256.

Spectral data were consistent with those previously reported (Pedras, Morales *et al.*, 1994).

4.2.1.5 Phomapyrone E (146)

HPLC t_R = 20.1 min, Method A.

^{1}H NMR (500 MHz, $CDCl_3$) diagnostic peaks of doublet at δ_H1.21 (3H, 6 Hz).

4.2.1.6 Phomapyrone G (148)

HPLC t_R = 24.1 min, Method A.

^{1}H NMR (500 MHz, $CDCl_3$) diagnostic peaks of quartet at δ_H3.47 (1H, 6 Hz).

HREI-MS: *m/z* 250.1207 calcd. $C_{14}H_{18}O_3$, 250.1205

4.2.2 Metabolites produced in PDB

The EtOAc extract (1.1g) of PDB culture filtrates was eluted with CH_2Cl_2:MeOH gradient to give 17 fractions. The resulting F7–10 (787 mg) was refractionated with hexane:EtOAc followed by CH_2Cl_2:MeOH to yield brassicicolin A (**1**, 208 mg) (**Scheme 4.4**). In addition, dihydrobrassicicolin A (**220**, 3.5 mg) was obtained from combined PDB extracts using reverse phase FCC (**Scheme 4.5**).

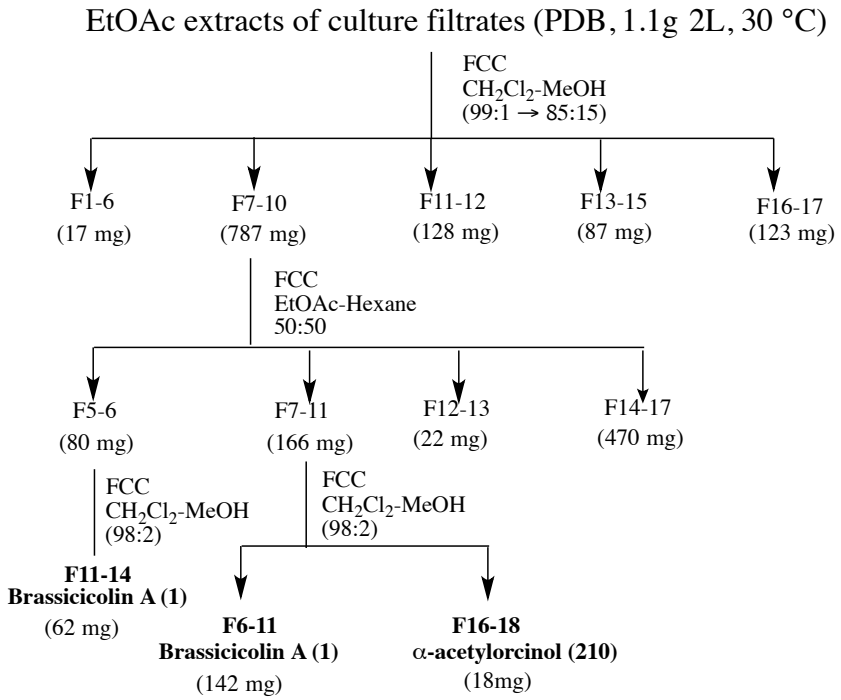

Scheme 4.4 Flow chart for isolation of metabolites of *Alternaria brassicicola* grown in PDB.

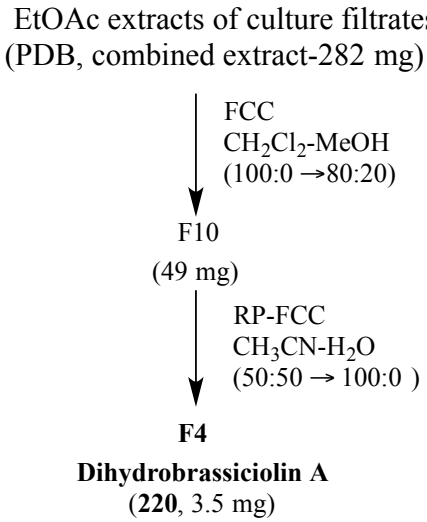

Scheme 4.5 Flow chart for isolation of dihydrobrassicicolin A (**220**) of *Alternaria brassicicola* grown in PDB.

4.2.2.1 Dihydrobrassicicolin A (220)

HPLC t_R = 23.3 min, Method B.

^{1}H NMR (500 MHz, $CDCl_3$) Doublets of the formamide group at δ 8.30 (d, J = 5 Hz) and 8.26 (d, J = 5 Hz).

HRESI-MS: *m/z* $[M\text{-}H_2O+Na]^+$ 725.3187, $C_{32}H_{50}N_2O_{15}Na$, calcd. 725.3103.

4.2.2.2 Brassicicolin A (1)

HPLC t_R = 25.5 min, Method B; t_R = 29.5 min, Method A

^{1}H NMR ^{13}C NMR (125 MHz, $CDCl_3$) see **Table 13**.

HRESI-MS: *m/z* $[M+H]^+$ 685.3190, $C_{32}H_{49}N_2O_{11}$, calcd. 685.3183.

Spectral data were consistent with those previously reported (Gloer, Poch *et al.*, 1988; Pedras, Chumala *et al.*, 2009)

Table 17 Production of fungal metabolites in standard MM and PDB.

Media	α-Acetylorcinol (**210**) (mg)	Tyrosol (**219**) (mg)	Depudecin (**151**) (mg)	Phomapyrone A (**25**) (mg)	Brassicicolin A (**1**) (mg)
MM-23 °C (12L, 1.1 g)	0.8	2.1	57	2.4	39
MM-30 °C (10.6L, 1.1 g)	2.5	2.5	-	1.3	77
PDB-30 °C (2L, 1.1 g)	18	-	-	-	204

4.2.3 Synthesis of α-acetylorcinol

4.2.3.1 Synthesis of 2-(3,5-dimethoxyphenyl)-*N*-methoxy-*N*-methylacetamide (218)

3,5-Dimethoxyphenylacetic acid (**211**, 50 mg, 0.26 mmol) in anhydrous CH_2Cl_2 (1 mL) was added to an oven-dried flask. *N,N*-dimethylformamide (DMF) (one drop) as a catalyst and oxalyl chloride (49 mg, 0.39 mmol) were added to the flask. The resulting mixture was stirred for 30 min at room temperature. The reaction mixture was concentrated to dryness *in vacuo* to remove excess of oxalyl chloride. *N,O*-dimethylhydroxylamine hydrochloride (38 mg, 0.39 mmol) in pyridine (100 μL) was added to the reaction mixture in anhydrous CH_2Cl_2 (1 mL). The resulting mixture was stirred for 30 min at room temperature. Diluted hydrochloric acid (2 M, 2 mL) solution was added to the reaction mixture. The reaction mixture was extracted with diethyl ether (4 mL × 3). The organic layer was dried over Na_2SO_4 and filtered using a cotton plug. Solvents in the filtrate were evaporated using a rotary evaporator. The crude residue gave 2-(3,5-dimethoxyphenyl)-*N*-methoxy-*N*-methylacetamide (**218**, 54 mg, 0.23 mmol, yield 92%) without purification**.**

*2-(3,5-Dimethoxyphenyl)-N-methoxy-N-methylacetamide (**218**)*

HPLC t_R = 21.6 min, Method A.

^{1}H NMR (500 MHz, $CDCl_3$): δ 6.47 (d, *J* = 2 Hz, 2H), 6.36 (t, *J* = 2 Hz, 1H), 3.78 (s, 6H), 3.71 (s, 2H), 3.62 (s, 3H), 3.20 (s, 3H).

^{13}C NMR (125 MHz, $CDCl_3$): δ 172.3, 161.0, 137.3, 107.5, 99.2, 61.5, 55.7, 39.8, 32.4.

HREI-MS: *m/z* 239.1166, $C_{12}H_{17}NO_4$, calcd. 239.1158; *m/z* 239.1166 (33%), 178.0623 (29%), 151.0756 (100%).

FTIR (KBr): 2937, 1661, 1594, 1460, 1380, 1205, 1151, 1064, 1007 cm^{-1}.

Spectral data were consistent with those previously reported (Wang, Denton *et al.*, 2011).

4.2.3.2 Synthesis of 1-(3,5-dimethoxyphenyl)propan-2-one (216)

A freshly prepared CH_3MgI in anhydrous Et_2O (1 mL) was added to 2-(3,5-dimethoxyphenyl)-*N*-methoxy-*N*-methylacetamide (**216**, 60 mg, 0.25 mmol) in anhydrous Et_2O (1 mL). The reaction mixture was stirred for 30 min at room temperature. Ammonium chloride (80 mg, 1.5 mmol) in water (2 mL) was poured into the reaction mixture. The reaction mixture was extracted with Et_2O (4 mL × 3) and the extract was dried over Na_2SO_4. The extract was concentrated to dryness *in vacuo*. The crude residue gave 1-(3,5-dimethoxyphenyl)propan-2-one (**2**, 37 mg, 0.19 mmol, yield 76%) after purification by FCC using silica gel (hexane:EtOAc = 60:40 (v/v)). Preparation of CH_3MgI: Mg (30mg, 1.25 mmol) and CH_3I (78 μL, 1.25 mmol) were stirred in anhydrous Et_2O (1mL) until Mg was completely consumed.

*1-(3,5-Dimethoxyphenyl)propan-2-one (**216**)*

HPLC t_R = 20.7 min, Method A.

^{1}H NMR (500 MHz, $CDCl_3$): δ 6.38 (t, *J* = 2 Hz, 1H), 6.36 (d, *J* = 2 Hz, 2H), 3.79 (s, 6H), 3.62 (s, 2H), 2.16 (s, 3H).

^{13}C NMR (125 MHz, $CDCl_3$): δ 206.5, 161.2, 136.6, 107.6, 99.2, 55.5, 51.5, 29.3.

HREI-MS: *m/z* 194.0944 $C_{11}H_{14}O_3$, calcd. 194.0943; *m/z* 194.0944 (95%), 151.0762 (100%), 69.0257 (30%).

FT-IR (KBr): 2941, 2839, 1710, 1595, 1462, 1431, 1349, 1205, 1155, 1066, 835 cm^{-1}.

4.2.3.3 Synthesis of α-acetylorcinol (210)

Iodocyclohexane (326 μL, 2.5 mmol) was added to 1-(3,5-dimethoxyphenyl)propan-2-one (**216**, 40 mg, 0.21 mmol) in dry DMF (1 mL). The resulting mixture was refluxed for 4 h, cooled, and poured into water (20 mL). The reaction mixture was extracted with EtOAc (20 mL × 3). The organic phase was washed with $NaHSO_3$ (5 mL) and brine, and dried over Na_2SO_4. Solvents in the organic layer were evaporated in a rotary evaporator. The crude residue was purified by FCC (Et_2O:hexane, 60:40 (v/v), isocratic) to afford α-acetylorcinol (**210**, 18mg, 0.11 mmol, 52% yield).

*α-Acetylorcinol (**210**)*

HPLC: t_R = 8.4 min, Method A.

^{1}HNMR (500 MHz, CD_3OD): δ 6.16–6.14 (m, 3H), 3.52 (s, 2H), 2.09 (s, 3H).

HREI-MS: *m/z* 166.0633, $C_9H_{10}O_3$, calcd. 166.0632; *m/z* 166.0633 (100%), 123.0445 (69%).

Spectral data were consistent with those of α-acetylorcinol (**210**) previously isolated from the extracts of fungal culture filtrates.

4.2.4 Hydrolysis of brassicicolin A

Brassicicolin A (**1**) (23 mg, 0.034 mmol) in MeOH (2 mL) was dissolved in HCl (0.10 mM, 2 mL) and kept at 4 °C for 2 h. The reaction was quenched with Na_2CO_3 (1 M, 4 mL), and extracted with EtOAc to yield dihydrobrassicicolin A (**220**). The extract was concentrated and the residue was analyzed by ^{1}H NMR, HPLC-ESI-MS, and HRESI-MS.

To examine hydrolysis of brassicicolin A (**1**) to dihydrobrassicicolin A (**220**) in media in the absence of *A. brassicicola* spores, brassicicolin A (**1**) (0.3 mM) in PDB was incubated at 30 °C. Seven days later, PDB media (20 mL) was withdrawn and extracted with EtOAc (20 mL × 2). After evaporation of solvents, the residue was dissolved in MeOH (1mL). Brassicicolin A (**1**) and dihydrobrassicicolin A (**220**) were quantified using calibration curves (**Table 18**).

Dihydrobrassicicolin A (**220**)

HPLC t_R = 28.5, Method A; t_R = 23.3 min, Method B.

HRESI-MS: *m/z* $[M\text{-}H_2O+Na]^+$, 725.3187, $C_{32}H_{50}N_2O_{15}Na$, calcd., 725.3103.

^1H NMR (500 MHz, $CDCl_3$): δ 8.30 (d, J = 5 Hz), 8.26 (d, J = 5 Hz) at formamide group. Spectral data were consistent with those of the metabolite previously isolated from the fungal culture extracts.

Table 18 Parameters used in HPLC-DAD quantification of fungal metabolites and synthetic compounds.

Metabolite or compound	**Method (detection at 220 nm) - t_R (min)**	**R^2 (calibration curve equation)**
α-Acetylorcinol (**210**)	A - 8.4	0.9995 (y = 8704x)
Tyrosol (**219**)	A - 9.2	0.9999 (y = 5010x)
Depudecin (**151**)	A - 11.6	0.9924 (y = 3680x)
Dihydrobrassicicolin (**220**)	B - 23.3	0.9995 (y = 196x)
Phomapyrone A (**25**)	B - 24.7	0.9997 (y = 2571x)
	C - 31.2	0.9993 (y = 2382x)
Brassicicolin A (**1**)	B - 25.5	0.9977 (y = 251x)
SAHA (**32**)	C - 16.3	0.9992 (y = 2023x)
N-Phenylacetamide (**227**)	A - 12.9	—
	C - 13.5	0.9981 (y = 1896x)

4.3 Modification of minimal media

Various culture conditions are summarized in **Table 8**. *A. brassicicola* spores (2×10^6 spores/100 mL) were incubated in modified MM or standard MM on a shaker at 110 rpm at 23 °C ± 1 and 30 °C ± 1 for 7 days. Cultures grown under various conditions (**Table 8**) were filtered to remove mycelia from culture broths, mycelia were weighted and the culture filtrates were extracted with EtOAc (150 mL × 1). After evaporation of solvents using a rotary evaporator, residues were dissolved in MeOH (500 μL) and analyzed by HPLC-DAD and HPLC-ESI-MS.

4.3.1 Carbon sources and other components

MM containing high glucose (entry 2, 45 g/L, 250 mM) or low glucose (entry 3, 5 g/L, 17 mM) was prepared. Sucrose (entry 4, 15 g/L, 44 mM), fructose (entry 5, 15 g/L, 83 mM); mannitol (entry 6, 15 g/L, 82 mM), or sorbitol (entry 6, 15 g/L, 82 mM) was substituted for glucose in standard MM.

Asparagine (entry 7) or thiamine (entry 8) was excluded from standard MM. For NaCl (entry 16), cultures were grown under standard MM, and then NaCl (10 g/100 mL) was added to 60-h-old cultures of *A. brassicicola*.

4.3.2 Nitrogen sources

MM containing low KNO_3 (entry 9, 0.31g /L, 3.1 mM), $NaNO_3$ (entry 10, 2.5 g/L, 29 mM), low $NaNO_3$ (entry 11, 0.25 g/L, 2.9 mM), no nitrate (entry 12, complete removal of KNO_3) or NH_4Cl (entry 13, 0.16 g/L, 3.1 mM) was prepared.

4.3.3 Iron source and siderophores

Ferric citrate (0.54 mg/L, 2 μM) was used as a sole iron source in standard MM. *A. brassicicola* was incubated in MM containing high ferric citrate (entry 14, 54 mg/L, 200 μM) or no ferric citrate (entry 15).

4.3.3.1 Purification of siderophores

MM was prepared with three different concentrations of ferric citrate (0, 2, and 200 μM). *A. brassicicola* spores (2 × 10^6 spore/100mL) were inoculated to MM. All cultures were incubated on a shaker at 110 rpm at 23 °C ± 1. The experiment was carried out in five replicates. After five days, cultures were filtered to separate fungal mycelia from culture broths. Each culture filtrate (100 mL) was divided into two 50 mL-portions.

One portion (50 mL) of culture filtrates was used to fractionate iron-binding compounds (reddish fractions) with the revised method based upon Oide et al (2006). Ferric chloride hexahydrate ($FeCl_3 \cdot 6H_2O$, 33 mg, 2.4 mM in 50 mL culture) was added to the culture filtrates. To fractionate siderophores, amberlite XAD-4 (5 g per 50 mL of culture-$FeCl_3$) preequlibrated with 50 mM KPO_4 buffer (pH = 7.5) was used. Culture filtrates containing $FeCl_3$ were loaded onto preequlibrated XAD-4 and then washed out with four column volumes of 50 mM KPO_4. Four column volumes of MeOH were used to elute iron-binding compounds (reddish fractions) from the XAD-4. Freshly prepared XAD-4 column was used for each separation. After evaporation of MeOH in a rotary evaporator, the residue was dissolved with a mixture of solvents (H_2O:MeOH, 90:10 (v/v), 500 μL) and analyzed by HPLC-ESI-MS and HRESI-MS.

The other portion (50 mL) of culture filtrates was used for extraction with EtOAc (50 mL × 2). After evaporation of solvents using a rotary evaporator, each extract was dissolved in MeOH (500 μL) and analyzed by HPLC-DAD.

4.3.4 Epigenetic modifiers

SAHA (**32**) and SBHA (**33**) were synthesized as described below and 5-Aza (**35**) was purchased from Alfa Aesar (Ward Hill, MA, USA). *A. brassicicola* was grown in standard MM containing suberoylanilide hydroxamic acid (SAHA, **32**), suberoyl *bis*-hydroxamic acid (SBHA, **33**), or 5-azacytidine (5-Aza, **35**). The experimental details were described below.

4.3.4.1 Synthesis of suberoylanilide hydroxamic acid (SAHA, 32)

A solution of suberic acid (**224**, 1.25 g, 7.2 mmol) in acetic anhydride (5 mL) was refluxed for 1 h. After cooling down, the reaction mixture was concentrated to dryness *in vacuo*. Aniline (**228**, 830 μL, 8.9 mmol) was added to the resulting mixture in THF. The mixture was

stirred for 1 h at room temperature. The mixture was poured into 1 M $NaHCO_3$ (100 mL) and extracted with EtOAc (100 mL × 2). The aqueous layer was acidified by adding concentrated HCl, and extracted with EtOAc (100 mL × 2). The extract was concentrated to dryness *in vacuo* to yield 7-(phenylcarbamoyl)heptanoic acid (738 mg, 2.9 mmol) (**226**) as white solid in 40% yield.

Methyl chloroformate (70 μL, 0.9 mmol) and Et_3N (167 μL, 1.2 mmol) were added to a solution of suberanilic acid (**224**, 150 mg, 0.6 mmol) in anhydrous THF (5 mL) in an ice-water bath and the reaction mixture was stirred for 20 min. The solid was filtered using a cotton plug and the filtrate was added to a freshly prepared hydroxylamine solution—hydroxylamine hydrochloride (168 mg, 2.4 mmol) in MeOH (3 mL) was added to a solution of KOH (138 mg, 2.4 mmol) in MeOH (3 mL)— and the mixture was stirred for 15 min in an ice-water bath. The mixture was filtered using a cotton plug and the filtrate was stirred for 15 min at room temperature. After evaporation of the solvents, the residue was recrystallized from MeCN to yield *N*-hydroxy-*N'*-phenyloctanediamide (**32**, suberoylanilide hydroxamic acid, SAHA) (88 mg, 0.33 mmol, yield 55%).

*SAHA (suberoylanilide hydroxamic acid, **32**)*

HPLC t_R = 16.3 min, Method C.

^{1}H NMR (500 MHz, CD_3OD): δ 7.53 (d, *J* = 7.0 Hz, 2H), 7.29 (t, *J* = 7.5 Hz, 2H), 7.08 (t, *J* = 7.5 Hz, 2H), 2.36 (t, *J* = 7.5 Hz, 2H), 2.09 (t, *J* = 7.0 Hz, 2H), 1.70 (t, *J* = 7.0 Hz, 2H), 1.63 (t, *J* = 7.0 Hz, 2H), 1.45–1.35 (m, 4H).

^{13}C NMR (125 MHz, CD_3OD): δ 174.8, 173.1, 140.0, 129.9, 125.3, 121.4, 38.0, 33.8, 30.1, 30.0, 29.7, 26.9, 26,7.

HRESI-MS: *m/z* $[M+H]^+$ 265.1550, $C_{14}H_{21}N_2O_3$, calcd. 265.1546.

FTIR (KBr): 3284, 2936, 2845, 1661, 1602, 1544, 1444, 1317, 975, 755, 691 cm^{-1}.

m.p.: 153–155 °C.

Spectral data were consistent with those previously reported (Mai, Esposito *et al.*, 2001).

4.3.4.2 Synthesis of suberoyl *bis*-hydroxamic acid (SBHA, 33)

Et_3N (197 μL, 1.4 mmol) and methyl chloroformate (291 μL, 3.7 mmol) were successively added to a solution of suberic acid (**224**, 81 mg, 0.47 mmol) in anhydrous THF (4mL). The reaction mixture was stirred for 1.5 h in an ice-water bath. The reaction mixture was filtered and the solvent in the filtrate was evaporated *in vacuo*. Freshly prepared hydroxylamine—hydroxylamine hydrochloride (82 mg, 1.2 mmol) in MeOH (3 mL) was added to a solution of Na_2CO_3 (62 mg, 0.6 mmol) in water (0.3 mL)—was added to a solution of the reaction mixture in anhydrous THF (0.5 mL). The resulting mixture was stirred for 1 h at room temperature. The reaction mixture was filtered, and the filtrate was dried over Na_2SO_4, and concentrated to dryness *in vacuo* to yield suberoyl bis-hydroxamic acid (**33**) (98 mg, 0.47 mmol) as a white powder quantitatively.

*SBHA (suberoyl bis-hydroxamic acid, **33**)*

^{1}H NMR (500 MHz, CD_3OD): δ 2.09 (t, J = 7.5 Hz, 4H), 1.65–1.56 (m, 4H), 1.39–1.31 (m, 4H).

^{13}C NMR (125 MHz, CD_3OD): δ 173.2, 33.8, 29.8, 26.7

HRESI-MS: *m/z* $[M-H]^-$ 203.1038, $C_8H_{15}N_2O_4$, calcd. 203.1037,

FTIR (KBr): 3257, 3059, 2943, 2845, 1781, 1665, 1465, 1426, 1075, 978 cm^{-1}

m.p.: 149–151 °C.

4.3.4.3 Preparation of fungal cultures with epigenetic modifiers

*SAHA (**32**)*

SAHA (**32**, 93 mg) was dissolved in MeOH (3.5 mL) and then added to standard MM to a final concentration of 0.50 mM. As control, MeOH (500 μL) was added to standard MM (100 mL).

*SBHA (**33**)*

SBHA (**33**, 61 mg) was dissolved in DMSO (3 mL) and then added to standard MM to a final concentration of 0.50 mM. As control, DMSO (500 μL) was added to standard MM (100 mL).

*5-Aza (**35**)*

5-Aza (**35**, 73mg) was dissolved in standard MM (50 mL) and sterilized using a 0.2 μm membrane filter. The resulting 5-Aza (**35**, 50 mL) was combined with standard MM (950 mL) to a final concentration of 0.30 mM.

A. brassicicola was grown in standard MM containing each epigenetic modifier on a shaker at 110 rpm at 23°C ± 1 or 30 °C ± 1 for 7 days. Cultures were filtered, mycelia were weighted and the culture filtrates were extracted with EtOAc. The residues were dissolved in MeOH (500 μL) and analyzed by HPLC-DAD. All experiments were carried out in triplicate.

4.3.4.4 Isolation of *N*-phenylacetamide (227)

To purify the peak at t_R = 12.9 min (Method A), a major metabolite of *A. brassicicola* grown in standard MM containing SAHA (**32**), the extracts of the culture filtrates were fractionated by silica gel flash column chromatography (Et_2O:hexane, 60:40 to 100:0 (v/v), gradient).

N-*phenylacetamide (**227**)*

HPLC t_R = 12.9 min, method A; t_R = 13.2 min, method C.

^{1}H NMR (500 MHz, $CDCl_3$): δ 7.50 (d, *J* = 8, 2H), 7.33 (t, *J* = 8, 2H), 7.11 (t, *J* = 8, 1H), 2.19 (s, *3*H).

^{13}C NMR (125 MHz, $CDCl_3$): δ 168.5, 138.1, 129.2, 124.5, 120.1, 24.8.

HREI-MS: *m/z* 135.0688, C_8H_9NO, calcd. 135.0684; *m/z* 135.0688 (45%), 93.0577 (100%)

Spectral data were consistent with those of the authentic compound.

4.3.4.5 Biotransformation of SAHA (32)

A. brassicicola (2×10^6 spores/100 mL) was grown in MM containing SAHA (**32**, 0.40 mM) at 23 °C and 30 °C. A 10 mL of cultures was withdrawn and extracted with EtOAc (10 mL × 3) every 24 hours for 5 days. Culture extracts were dissolved with MeOH (500 µL) and were analyzed by HPLC-DAD. To examine stability of SAHA (**32**) in MM, MM containing SAHA (**32**) (0.40 mM) was incubated without the fungal spores and a 10 mL of MM was extracted with EtOAc (10 mL × 3). All experiments were carried out in triplicate.

4.3.4.6 Biotransformation of aniline (228) to *N*-β-D-glucopyranosyl amine(230)

A. brassicicola (2×10^6 spores/100 mL) was grown in standard MM. The cultures were shaken at 110 rpm at 23 °C ± 1. After 48 h, aniline (**228**) was added to *A. brassicicola* culture to a final concentration of 0.20 mM. Cultures (10 mL) at different time intervals (0h, 4h, 8h, 12h, 24h, 18h, 24h, 48h, and 72h) were collected and lyophilized. Lyophilized cultures were dissolved with distilled water for HPLC analysis. Due to low solubility with distilled water, 48-h-old-cultures and 72-h-old-cultures were extracted with EtOAc (10 mL × 3). The EtOAc extracts were concentrated to dryness using a rotary evaporator, and the residue was dissolved with MeOH for HPLC analysis. Control cultures were shaken in the presence of aniline (**228**) with no fungal spores. All experiments were carried out in triplicate.

To test stability of aniline (**228**) in standard MM, aniline (**228**, 13 mg, 0.14 mmol) was dissolved in MeOH (1.4 mL), and then a 40 µL of 100 mM aniline was added to following solutions to a final concentration of 0.02 mM: a) standard MM (20 mL) b) MM (20 mL) with no glucose or c) H_2O (20 mL). All solutions were incubated at room temperature for 3 days. The 48--h or 72-h-old solutions were analyzed by HPLC-DAD (method C). All experiments were carried out in triplicate.

To confirm formation of *N*-β-D-glucopyranosyl amine (**230**) (HPLC t_R = 8.7 min, Method C) in standard MM, two reaction mixtures were prepared: five (90 mg, 0.5 mmol) or ten (180 mg, 1.0 mmol) equivalents of glucose (**229**) were prepared in distilled water (1 mL) (pH = 6 adjusted by 1 M HCl). Aniline (**228**, 10 µL, 0.11 mmol) was added to each glucose solution. Each reaction mixture was stirred at room temperature for 3 days. After lyophilization, both residues were analyzed by ^1H and ^{13}C NMR.. The ^1H and ^{13}C NMR spectroscopic data of both residues indicated the presence of mixtures of α- and β-D-glucopyranose and *N*-β-D-

glucopyranosyl aniline (**230**), consistent with the previously reported data (Bridiau, Benmansour *et al.*, 2007; Roslund, Tähtinen *et al.*, 2008).

4.3.5 Co-cultivation of *A. brassicicola* with *A. brassicae*

4.3.5.1 Collection of *A. brassicae* spores

Alternaria brassicae UAMH4936 was obtained from the University of Alberta Microfungus Collection and Herbarium. *A. brassicae* UAMH4936 was subcultured in freshly prepared V8 agar in the dark at 23 ± 1 °C for 10 days. The spores were collected by adding sterilized H_2O (10 mL) to each agar plate and by scrapping off agar surface followed by filtration and centrifugation of suspension. The resulting pellets were rinsed with sterile H_2O. The spores were counted under a microscope using a hemocytometer and stored at −4 °C.

Preparation of V8 agar plate: V8 juice 100mL, $CaCO_3$ 0.37g, and agar 7.5g were added to H_2O 400 mL. A 500 μL of rose bengal (40 mg/mL) was added to the autoclaved V8 juice mixture (500 mL).

4.3.5.2 Co-cultivation of *A. brassicicola* with *A. brassicae*

A. brassicae (1×10^4 spores), *A. brassicicola* (1×10^4 spores) and co-culture were incubated in 6-well plates (in triplicate), where each well contains 6 mL of either PDB or MM. The plates were placed on a shelf at 23 °C under constant light for two weeks. The cultures were extracted with EtOAc (10 mL × 2). After evaporation of solvent, the residues were dissolved in MeOH (200 μL) and then analyzed by HPLC-DAD.

4.3.6 Evaluation of biological activity of metabolites: conidia germination inhibition

A microplate reader (xMark Microplate Spectrophotometer, Bio-Rad Laboratories, Inc.) was used to assess the conidia germination of *A. brassicicola* in standard MM containing the fungal metabolites brassicicolin A (**1**), depudecin (**151**), α-acetylorcinol (**210**), and tyrosol **(219**). The assay was carried out in sterile, Nunclon 48 well plates, each well containing standard MM (400 μL) (Pedras et al. 2014). Each fungal metabolite was dissolved in DMSO then added to wells containing 1×10^5 spores/mL in standard MM to give final concentrations of 0.50 mM. Eight replicate wells were set up per treatment per experiment. The plates were sealed and

incubated at 25 ± 0.5 °C, shaken at medium speed and were read in kinetic mode at 595 nm; absorbance readings were automatically recorded every hour over the course of 36 h. The absorbance was measured using the Microplate Manager 6 Software (Bio-Rad). After processing the raw data, the absorbance was plotted against time using the Microsoft Office Excel Software (Version 2003, USA).

4.4 Analyses of metabolites produced on infected leaves

4.4.1 Whole plant assay to determine phytotoxicity

Brassica juncea cv. Cutlass (brown mustard, susceptible) and *B. napus* cv. Westar (canola, susceptible) were grown in a growth chamber at 20 ± 2 °C with an 18-h photoperiod (fluorescent and incandescent 410–450 μmol $s^{-1}m^{-2}$) and ambient humidity (ca. 50%) for two weeks. Six leaves were employed, where each leaf was gently scratched with a needle at six spots. Various concentrations (0.25, 0.50, 1.0, 2.5 and 5.0 mM) of purified compounds were prepared in MeOH-H_2O (1:1, v/v). A 10 μL droplet of each concentration was placed on the six spots per leaf. In addition, various mixtures of two compounds were prepared as follows: brassicicolin A (**1**) 1.0 mM + depudecin (**151**) 10 mM, 5.0 mM, 2.0 mM, 1.0 mM or 0.50 mM; brassicicolin A (**1**) 0.50 mM + depudecin (**151**) 10 mM, 5.0 mM, 2.0 mM, 1.0 mM or 0.50 mM; depudecin (**151**) 2.0 mM + brassicicolin A (**1**) 10 mM, 5.0 mM, 2.0 mM, 1.0 mM or 0.50 mM; depudecin (**151**) 1.0 mM + brassicicolin A (**1**) 10 mM, 5.0 mM, 2.0 mM, 1.0 mM or 0.50 mM. A 10 μL droplet of the mixtures was placed on the six spots per leaf. Control leaves were treated similarly with MeOH-H_2O (10 μL, 1:1, v/v). Whole plants were incubated in the growth chamber for one week. The visible necrotic areas were measured using a stencil having circles with different diameters and damage index was recorded by converting diameters to damage index scale. Lesion size scale is as follows: 0 = 0.0–1.9 mm; 1 = 2.0–2.9 mm; 2 = 3.0–3.9 mm; 3 = 4.0–4.5 mm; 4 = 4.6–5.5 mm; 5 = 5.6–6.5 mm; 6 = 6.5–7.5 mm (Pedras, Chumala *et al.*, 2009).

Sinapis alba cv. Westar (white mustard, resistant) was grown under the same conditions described above. Six leaves were employed, where each leaf was gently scratched with a needle

at six spots. A 10 µL droplet of brassicicolin A (**1**) (1.0, 0.50, and 1.0 mM) in MeOH-H_2O (1:1, v/v) was placed on the six spots. Control leaves were treated similarly with MeOH-H_2O (10 µL, 1:1, v/v). Whole plants of S. *alba* were incubated in the growth chamber for one week under the same conditions as described above.

4.4.2 Detached leaf assay to determine phytotoxicity

Brassica juncea cv. Cutlass, *B. napus* cv. Westar and *Sinapis alba* cv. Ochre were grown as described above. The six second or third leaves were excised at the base of the petiole, where each leaf was gently scratched with a needle at six spots. Three concentrations (0.1, 0.5 and 1.0 mM) of purified metabolites (α-acetylorcinol (**210)**, tyrosol (**219)**, depudecin (**151**), phomapyrone A (**25**), and brassicicolin A (**1**)) were prepared in MeOH-H_2O (1:1, v/v). A 10 µL droplet of each concentration was placed on the six spots. Control leaves were treated similarly with MeOH-H_2O (10 µL, 1:1, v/v). Each detached leaf was placed in a Falcon tube containing water for one week in an incubator at 23 ± 2 °C with an 18-h photoperiod. Visible necrotic areas were measured using a stencil having circles with different diameters and damage index was recorded by converting diameters to damage index scale, as described above (Pedras, Chumala *et al.*, 2009).

4.4.3 Analysis of spore germination fluids

Brassica juncea, B. napus, *and* Sinapis alba

Brassica juncea cv. Cutlass, *B. napus* cv. Westar, and *Sinapis alba* cv. Ochre were grown as described above. To prepare spore germination fluids (SGFs), *A. brassicicola* spores in water (1×10^5 spores/mL, 20 µL) were placed at 40 spots in each leaf of three species. Leaves (6 leaves per species) were prepared as follows: A leaf was excised at the base of petiole from *B. juncea*, *B. napus* and *S. alba*. The lower (or back) side of the excised leaf was gently scratched using a pipet tip. After inoculation of spores, each leaf was placed on a filter paper in a petri dish. Petiole of each leaf was covered with a moistened cotton plug. Petri dishes were covered with lids and then sealed with parafilm. Leaves in petri dishes were incubated for 72 hours in an

incubator under dark conditions at 23 ± 2 °C. The control leaves were treated similarly using distilled water. The germinated spore suspension droplets at inoculated sites were collected and filtered using a 0.2 μm-membrane filter to remove remaining spores and mycelia in SGFs. The filtrates of control and SGFs were lyophilized, dissolved with H_2O (500 μL), and analyzed by HPLC-DAD and HPLC-ESI-MS.

Arabidopsis thaliana *and its mutants*

Seeds of *Arabidopsis thaliana* Columbia ecotypes (Col-0), and two mutants (*pad3-1* and *pen2-1*) were purchased from The Arabidopsis Information Resource (TAIR). Additional seeds of mutants (*pad3-1* and *pen2-1*) were provided by Dr. Wei in Department of Biology, University of Saskatchewan, SK, Canada. Seeds of Col-0, *pen2-1* and *pad3-1* were grown according to the modified method using hydroponic kits (Tocquin, Corbesier *et al.*, 2003). Briefly, seeds were grown on the surface of seed-holders containing solidified 0.70% agar. Those seeds holders were placed onto hydroponic kits containing 2000-times diluted nutrient solutions (Tocquin, Corbesier *et al.*, 2003). To keep moisture of agar in each seed holder, a hydroponic kit was covered with a plastic bag. The resulting hydroponic kits were placed into an incubator at 23 ± 2 °C under a period of 18-h-light for 4–5 weeks.

The fungal spore suspension (1×10^6 spores/mL, 20 μL) was placed on to leaves of *A. thaliana* (4–5 spots per a seedling). Hydroponic kits were covered with plastic bags to keep moisture. All infected plants were incubated in an incubator at 23 ± 2 °C under a period of 18-h-light for 48 h. After collection of SGF, infected leaves of Col-0, *pen2-1* and *pad3-1* were extracted with MeOH. Each extract was dissolved in MeCN-MeOH (300 μL, 1:1, v/v) and analyzed by HPLC-DAD.

4.4.4 Time course analysis of metabolites in infected leaves

Brassica juncea cv. Cutlass, *B. napus* cv. Westar, and *Sinapis alba* cv. Ochre were grown as described above. Each detached leaf was placed in a falcon tube containing a mixture of diluted nutrient solutions (see above). Each detached leaf was gently scratched using a needle at 20 spots. The *A. brassicicola* spore suspension (1×10^6 spores/mL, 20 μL) was placed onto each spot. The falcon tubes were placed in a tray covered with a plastic bag to keep moisture. Distilled water (20 μL), or autoclaved spores (1×10^6 spores/mL, 20 μL) were placed onto spots and considered control treatments. Infected and control leaves were weighted every 24 h for five days. The leaves were frozen with liquid N_2, and extracted with MeOH (10 mL) for 1 h. After concentration, each residue was dissolved with MeCN-MeOH (300 μL, 1:1, v/v) and analyzed by HPLC-DAD and HPLC-ESI-MS. Plant and fungal metabolites were quantified using calibration curves built with authentic compounds (**Table 19**).

Table 19 Parameters used in HPLC-DAD quantification of plant metabolites.

Metabolite or compound	**Method (detection at 220 nm) - t_R (min)**	**R^2 (calibration curve equation)**
Glucobrassicin (**196**)[a]	C - 4.6 min	0.9999 (y = 26649x)
4-MeO-glucobrassicin (**161**)[a]	C - 6.1 min	0.9982 (y = 24293x)
Tryptophan (**155**)[b]	C - 9.4 min	0.9978 (y = 52535x)
Indole-3-acetonitrile (**188**)[b]	C - 22.4 min	0.9970 (y = 41528x)
Brassilexin (**185**)[a]	C - 22.7 min	0.9995 (y = 64611x)
Camalexin (**209**)[a]	C - 24.7 min	0.9992 (y = 16000x)
Rutalexin (**231**)[a]	C - 25.0 min	0.9969 (y = 21924x)
Sinalexin (**195**)[a]	C - 29.6 min	0.9979 (y = 29112x)
Cyclobrassinin (**186**)[a]	C - 32.8 min	0.9996 (y = 44889x)

[a] Compounds were provided by EE, VK, and AA

[b] Compounds are commercially available.

4.5 Biosynthesis of brassicicolin A

4.5.1 Administration of D-[U-$^{13}C_6$]glucose

Alternaria brassicicola (5×10^6 spores/100 mL) was incubated in MM (3 × 100 mL MM in a 250 mL Erlenmeyer flask) on a shaker at 110 rpm at 30 °C for 8 days. D-[U-$^{13}C_6$]glucose was administered to 72-h-old cultures (100 mg in 100 mL MM), and 120-h-old-cultures (100 mg in 100 mL). The cultures were combined, and filtered to remove mycelial debris. The culture filtrate was extracted with EtOAc, and the solvent was evaporated in a rotary evaporator. The residue was loaded onto silica gel FCC to isolate brassicicolin A (**1e**) (2.7 mg) (**Scheme 4.6**).

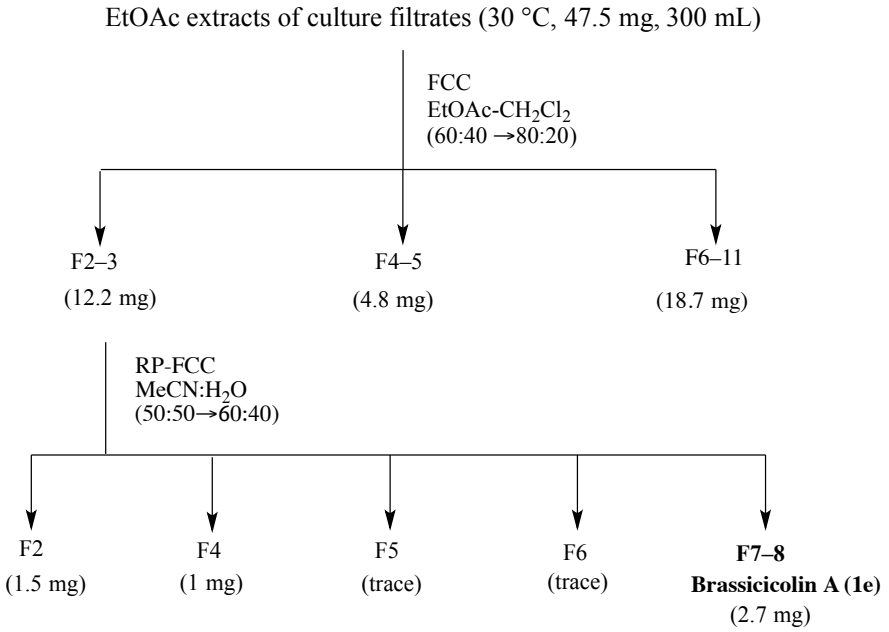

Scheme 4.6 Flow chart for isolation of ^{13}C-enriched brassicicolin A (**1e**) after incubation of cultures with D-[U-$^{13}C_6$]glucose.

Additionally, ^{13}C-enriched (2.7 mg) and natural abundance (2.7 mg) brassicicolin A (**1**) were analyzed by ^{13}C NMR (125.8 MHz, $CDCl_3$) under conditions as follows: Pulse sequence, the power-gated decoupling sequence (zgpg30, Bruker library); ^{13}C excitation pulse, 7.0 μs; dead time 6.0 μs; acquisition time, 1.1 s; relaxation delay, 2.0 s; number of scan, 17500, room temperature.

4.5.2 Administration of L-[$^{2}H_{8}$]valine and L-[^{15}N]valine

Alternaria brassicicola (2×10^{6} spores/100 mL) was incubated in MM (3 × 100 mL MM in a 250 mL Erlenmeyer flask) on a shaker at 110 rpm at 30 °C for 8 days. L-[$^{2}H_{8}$]valine was added to the cultures at 48-h (50 mg in 100 mL MM), and 96-h (50 mg in 100 mL MM). Similarly, L-[^{15}N]valine was administered twice to 48-h-old culture (50 mg in 100 mL MM) and 96-h-old culture (50 mg in 100 mL MM). After 8 days, cultures were filtered and the resultant culture filtrates were extracted with EtOAc. The crude extracts were fractionated using silica gel FCC to purify brassicicolin A (**1**). Purified brassicicolin A obtained from L-[$^{2}H_{8}$]valine or L-[^{15}N]valine was 19.5 mg or 13.3 mg, respectively (**Scheme 4.7**).

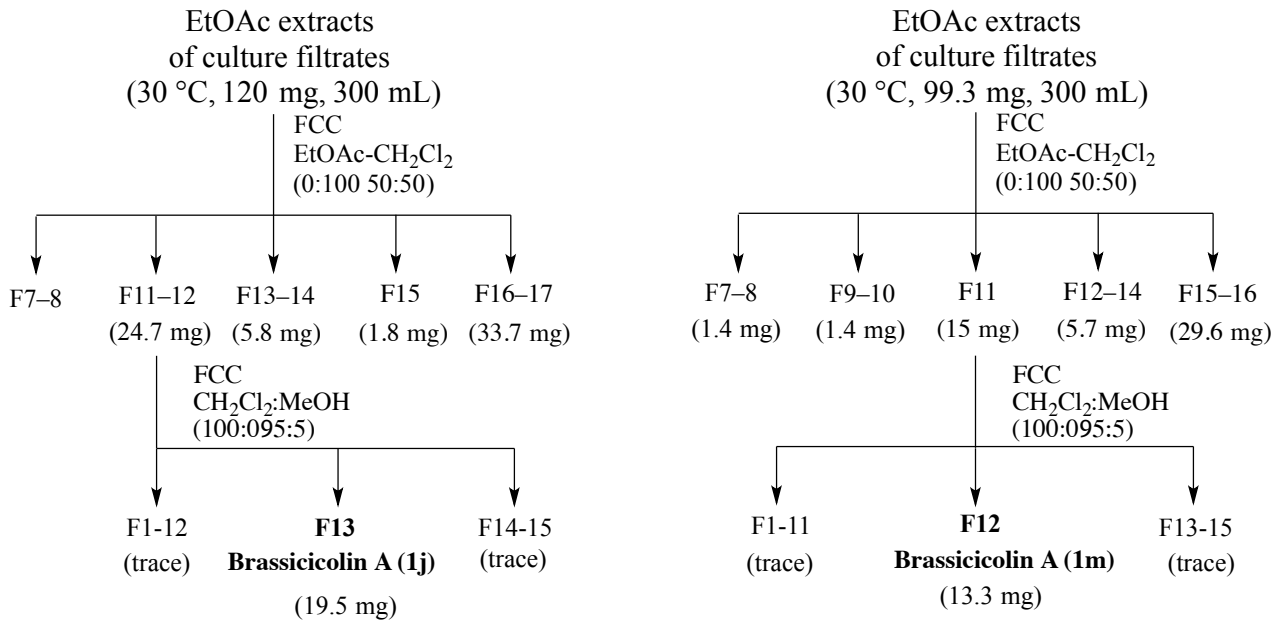

Scheme 4.7 Flow charts for isolation of ^{2}H-enriched brassicicolin A (**1j**) and ^{15}N-enriched brassicicolin A (**1m**) obtained from incubation of cultures with L-[$^{2}H_{8}$]valine and L-[^{15}N]valine, respectively.

5 References

Agerbirk, N., Olsen, C.E., 2012. Glucosinolate structures in evolution. Phytochemistry 77, 16–45.

Akimitsu, K., Tsuge, T., Kodama, M., Yamamoto, M., Otani, H., 2014. *Alternaria* host-selective toxins: determinant factors of plant disease. J. Gen. Plant Pathol. 80, 109–122.

Anyanwu, C.S., Sorensen, J.L., 2015. Secondary metabolites from a strain of *Alternaria tenuissima* isolated from northern Manitoba soil. Nat. Prod. Commun. 10, 39–42.

Asai, T., Chung, Y.M., Sakurai, H., Ozeki, T., Chang, F.R., Wu, Y.C., Yamashita, K., Oshima, Y., 2012a. Highly oxidized ergosterols and isariotin analogs from an entomopathogenic fungus, *Gibellula formosana*, cultivated in the presence of epigenetic modifying agents. Tetrahedron 68, 5817–5823.

Asai, T., Chung, Y.M., Sakurai, H., Ozeki, T., Chang, F.R., Yamashita, K., Oshima, Y., 2012b. Tenuipyrone, a novel skeletal polyketide from the entomopathogenic fungus, *Isaria tenuipes*, cultivated in the presence of epigenetic modifiers. Org. Lett. 14, 513–515.

Asai, T., Luo, D., Obara, Y., Taniguchi, T., Monde, K., Yamashita, K., Oshima, Y., 2012. Dihydrobenzofurans as cannabinoid receptor ligands from *Cordyceps annullata*, an entomopathogenic fungus cultivated in the presence of an HDAC inhibitor. Tetrahedron Lett. 53, 2239–2243.

Asai, T., Yamamoto, T., Chung, Y.M., Chang, F.R., Wu, Y.C., Yamashita, K., Oshima, Y., 2012a. Aromatic polyketide glycosides from an entomopathogenic fungus, *Cordyceps indigotica*. Tetrahedron Lett. 53, 277–280.

Asai, T., Yamamoto, T., Oshima, Y., 2011. Histone deacetylase inhibitor induced the production of three novel prenylated tryptophan analogs in the entomopathogenic fungus, *Torrubiella luteorostrata*. Tetrahedron Lett. 52, 7042–7045.

Asai, T., Yamamoto, T., Oshima, Y., 2012b. Aromatic polyketide production in *Cordyceps indigotica*, an entomopathogenic fungus, induced by exposure to a histone deacetylase inhibitor. Org. Lett. 14, 2006–2009.

Asai, T., Yamamoto, T., Shirata, N., Taniguchi, T., Monde, K., Fujii, I., Gomi, K., Oshima, Y., 2013. Structurally diverse chaetophenol productions Induced by chemically mediated epigenetic manipulation of fungal gene expression. Org. Lett. 15, 3346–3349.

Ayer, W.A., Browne, L.M., Feng, M.-C., Orszanska, H., Saeedi-Ghomi, H., 1986. The chemistry of the blue stain fungi. Part 1. Some metabolites of *Ceratocystis* species associated with mountain pine beetle infected lodgepole pine. Can. J. Chem. 64, 904–909.

Ayer, W.A., Peña-Rodriguez, L.M., 1987. Metabolites produced by *Alternaria brassicae*, the black spot pathogen of canola. Part 1, the phytotoxic components. J. Nat. Prod. 50, 400–407.

Baidyaroy, D., Brosch, G., Graessle, S., Trojer, P., Walton, J.D., 2002. Characterization of inhibitor-resistant histone deacetylase activity in plant-pathogenic fungi. Eukaryot. Cell 1, 538–547.

Bains, P.S., Tewari, J.P., 1987. Purification, chemical characterization and host-specificity of the toxin produced by *Alternaria brassicae*. Physiol. Mol. Plant Pathol. 30, 259–271.

Ballio, A., 1991. Non-host-selective fungal phytotoxins: Biochemical aspects of their mode of action. Experientia 47, 783–790.

Ballio, A., Brufani, M., Casinovi, C.G., Cerrini, S., Fedeli, W., Pellicciari, R., Santurbano, B., Vaciago, A., 1968. The structure of fusicoccin A. Experientia 24, 631–635.

Ballio, A., Chain, E.B., De Leo, P., Erlanger, B.F., Mauri, M., Tonolo, A., 1964. Fusicoccin: a new wilting toxin produced by *Fusicoccum amygdali* Del. Nature 203, 297–297.

Ballio, A., D'Alessio, V., Randazzo, G., Bottalico, A., Graniti, A., Sparapano, L., Bosnar, B., Casinovi, C.G., Gribanovski-Sassu, O., 1976. Occurrence of fusicoccin in plant tissues infected by *Fusicoccum amygdali* Del. Physiol. Plant Pathol. 8, 163–169.

Bashyal, B.P., Wellensiek, B.P., Ramakrishnan, R., Faeth, S.H., Ahmad, N., Gunatilaka, A.A.L., 2014. Altertoxins with potent anti-HIV activity from *Alternaria tenuissima* QUE1Se, a fungal endophyte of *Quercus emoryi*. Bioorg. Med. Chem. 22, 6112–6116.

Bednarek, P., Pislewska-Bednarek, M., Svatos, A., Schneider, B., Doubsky, J., Mansurova, M., Humphry, M., Consonni, C., Panstruga, R., Sanchez-Vallet, A., Molina, A., Schulze-Lefert, P., 2009. A glucosinolate metabolism pathway in living plant cells mediates broad-spectrum antifungal defense. Science 323, 101–106.

Beisler, J.A., 1978. Isolation, characterization, and properties of a labile hydrolysis product of the antitumor nucleoside, 5-azacytidine. J. Med. Chem. 21, 204–208.

Bertrand, S., Bohni, N., Schnee, S., Schumpp, O., Gindro, K., Wolfender, J.-L., 2014. Metabolite induction via microorganism co-culture: A potential way to enhance chemical diversity for drug discovery. Biotechnol. Adv. 32, 1180–1204.

Birch, R.G., Patil, S.S., 1985. Preliminary characterization of an antibiotic produced by *Xanthomonas albilineans* which inhibits DNA-synthesis in *Escherichia coli*. J. Gen. Microbiol. 131, 1069–1075.

Bode, H.B., Bethe, B., Höfs, R., Zeeck, A., 2002. Big effects from small changes: possible ways to explore nature's chemical diversity. ChemBioChem 3, 619–627.

Bornemann, V., Patterson, G.M.L., Moore, R.E., 1988. Isonitrile biosynthesis in the cyanophyte *Hapalosiphon fontinalis*. J. Am. Chem. Soc. 110, 2339–2340.

Brady, S.F., Clardy, J., 2005a. Cloning and heterologous expression of isocyanide biosynthetic genes from environmental DNA. Angew. Chem. Int. Ed. 44, 7063–7065.

Brady, S.F., Clardy, J., 2005b. Systematic investigation of the *Escherichia coli* metabolome for the biosynthetic origin of an isocyanide carbon atom. Angew. Chem. Int. Ed. 44, 7045–7048.

Brakhage, A.A., 2013. Regulation of fungal secondary metabolism. Nat. Rev. Microbiol. 11, 21–32.

Brakhage, A.A., Schroeckh, V., 2011. Fungal secondary metabolites - Strategies to activate silent gene clusters. Fungal Genet. Biol. 48, 15–22.

Bridiau, N., Benmansour, M., Legoy, M.D., Maugard, T., 2007. One-pot stereoselective synthesis of β-N-aryl-glycosides by N-glycosylation of aromatic amines: application to the synthesis of tumor-associated carbohydrate antigen building blocks. Tetrahedron 63, 4178–4183.

Brosch, G., Dangl, M., Graessle, S., Loidl, A., Trojer, P., Brandtner, E.M., Mair, K., Walton, J.D., Baidyaroy, D., Loidl, P., 2001. An inhibitor-resistant histone deacetylase in the plant pathogenic fungus *Cochliobolus carbonum*. Biochemistry 40, 12855–12863.

Browne, L.M., Conn, K.L., Ayert, W.A., Tewari, J.P., 1991. The camalexins: New phytoalexins produced in the leaves of *Camelina sativa* (Cuciferae). Tetrahedron 47, 3909–3914.

Brzonkalik, K., Herrling, T., Syldatk, C., Neumann, A., 2011. The influence of different nitrogen and carbon sources on mycotoxin production in *Alternaria alternata*. Int. J. Food Microbiol. 147, 120–126.

Buchwaldt, L., Green, H., 1992. Phytotoxicity of destruxin B and its possible role in the pathogenesis of *Alternaria brassicae*. Plant Pathol. 41, 55–63.

Cai, S., King, J.B., Du, L., Powell, D.R., Cichewicz, R.H., 2014. Bioactive sulfur-containing sulochrin dimers and other metabolites from an *Alternaria* sp. isolate from a Hawaiian soil sample. J. Nat. Prod. 77, 2280–2287.

Chagas, F.O., Dias, L.G., Pupo, M.T., 2013. A mixed culture of endophytic fungi increases production of antifungal polyketides. J. Chem. Ecol. 39, 1335–1342.

Chen, B., Shen, Q., Zhu, X., Lin, Y., 2014. The Anthraquinone derivatives from the fungus *Alternaria* sp XZSBG-1 from the saline lake in Bange, Tibet, China. Molecules 19, 16529–16542.

Chen, H., Fujita, M., Feng, Q., Clardy, J., Fink, G.R., 2004. Tyrosol is a quorum-sensing molecule in *Candida albicans*. Proc Natl Acad Sci U S A 101, 5048-5052.

Chen, L.-H., Yang, S.L., Chung, K.-R., 2014. Resistance to oxidative stress via regulating siderophore-mediated iron acquisition by the citrus fungal pathogen *Alternaria alternata*. Microbiology 160, 970–979.

Chung, Y.-M., El-Shazly, M., Chuang, D.-W., Hwang, T.-L., Asai, T., Oshima, Y., Ashour, M.L., Wu, Y.-C., Chang, F.-R., 2013. Suberoylanilide hydroxamic Acid, a histone deacetylase inhibitor, induces the production of anti-inflammatory cyclodepsipeptides from *Beauveria felina*. J. Nat. Prod. 76, 1260–1266.

Chung, Y.-M., Wei, C.-K., Chuang, D.-W., El-Shazly, M., Hsieh, C.-T., Asai, T., Oshima, Y., Hsieh, T.-J., Hwang, T.-L., Wu, Y.-C., Chang, F.-R., 2013. An epigenetic modifier enhances the production of anti-diabetic and anti-inflammatory sesquiterpenoids from *Aspergillus sydowii*. Bioorg. Med. Chem. 21, 3866–3872.

Cichewicz, R.H., 2010. Epigenome manipulation as a pathway to new natural product scaffolds and their congeners. Nat. Prod. Rep. 27, 11–22.

Ciegler, A., Lindenfelser, L.A., 1969. An antibiotic complex from *Alternaria brassicicola*. Experientia 25, 719–720.

Cociancich, S., Pesic, A., Petras, D., Uhlmann, S., Kretz, J., Schubert, V., Vieweg, L., Duplan, S., Marguerettaz, M., Noëll, J., Pieretti, I., Hügelland, M., Kemper, S., Mainz, A., Rott, P., Royer, M., Süssmuth, R.D., 2015. The gyrase inhibitor albicidin consists of *p*-aminobenzoic acids and cyanoalanine. Nat. Chem. Biol. 11, 195–197.

Cools, H.J., Hammond-Kosack, K.E., 2013. Exploitation of genomics in fungicide research: Current status and future perspectives. Mol. Plant Pathol. 14, 197–210.

Cotty, P.J., 1983. Production of zinniol by *Alternaria tagetica* and its phytotoxic effect on *Tagetes erecta*. Phytopathology 73, 1326–1326.

Cramer, R.a., La Rota, C.M., Cho, Y., Thon, M., Craven, K.D., Knudson, D.L., Mitchell, T.K., Lawrence, C.B., 2006. Bioinformatic analysis of expressed sequence tags derived from a compatible *Alternaria brassicicola-Brassica oleracea* interaction. Mol. Plant Pathol. 7, 113–124.

De Luca, L., Giacomelli, G., Taddei, M., 2001. An easy and convenient synthesis of Weinreb amides and hydroxamates. J. Org. Chem. 66, 2534-2537.

Dewick, P.M., 2002. Secondary metabolism: The building blocks and construction mechanisms. Medicinal natural products: A biosynthetic approach. John Wiley & Sons, pp. 7–38.

Dixon, R.A., 2001. Natural products and plant disease resistance. Nature 411, 843–847.

Dixon, S.J., Stockwell, B.R., 2014. The role of iron and reactive oxygen species in cell death. Nat. Chem. Biol. 10, 9–17.

Du, L., King, J.B., Cichewicz, R.H., 2014. Chlorinated polyketide obtained from a *Daldinia* sp. treated with the epigenetic modifier suberoylanilide hydroxamic acid. J. Nat. Prod. 77, 2454–2458.

Du, Z.-Y., Liu, R.-R., Shao, W.-Y., Mao, X.-P., Ma, L., Gu, L.-Q., Huang, Z.-S., Chan, A.S.C., 2006. α-Glucosidase inhibition of natural curcuminoids and curcumin analogs. Eur. J. Med. Chem. 41, 213–218.

Edenborough, M.S., Herbert, R.B., 1988. Naturally occurring isocyanides. Nat. Prod. Rep. 5, 229–245.

Elliott, C.E., Gardiner, D.M., Thomas, G., Cozijnsen, A., Van De Wouw, A., Howlett, B.J., 2007. Production of the toxin sirodesmin PL by *Leptosphaeria maculans* during infection of *Brassica napus*. Mol. Plant Pathol. 8, 791–802.

Expert, D., Enard, C., Masclaux, C., 1996. The role of iron in plant host-pathogen interactions. Trends Microbiol. 4, 232–237.

Expert, D., Franza, T., Dellagi, A., 2012. Iron in plant-pathogen interactions. In: Expert, D., O'Brian, M. R. (Eds.), Molecular Aspects of Iron Metabolism in Pathogenic and Symbiotic Plant-Microbe Associations. Springer Netherlands, pp. 7–39.

Faulkner, D.J., 1984. Marine natural products: metabolites of marine invertebrates. Nat. Prod. Rep. 1, 551–598.

Fisch, K.M., Gillaspy, A.F., Gipson, M., Henrikson, J.C., Hoover, A.R., Jackson, L., Najar, F.Z., Waegele, H., Cichewicz, R.H., 2009. Chemical induction of silent biosynthetic pathway transcription in *Aspergillus niger*. J. Ind. Microbiol. Biotechnol. 36, 1199–1213.

Fraenkel, D.G., Banerjee, S., 1972. Deletion mapping of *zwf*, the gene for a constitutive enzyme, glucose 6-phosphate dehydrogenase in *Escherichia coli.* Genetics 71, 481–489.

Fulton, N.D., Bollenbacher, K., Templeton, G.E., 1965. A metabolite from *Alternaria tenuis* that inhibits chlorophyll production. Phytopathology 55, 49–51.

Gamboa-Angulo, M.M., Escalante-Erosa, F., Garcia-Sosa, K., Alejos-Gonzalez, F., Delgado-Lamas, G., Peña-Rodriguez, L.M., 2002. Natural zinniol derivatives from *Alternaria tagetica*. Isolation, synthesis, and structure-activity correlation. J. Agric. Food Chem. 50, 1053–1058.

Gamboa-Angulo, M.M., García-Sosa, K., Alejos-González, F., Escalante-Erosa, F., Delgado-Lamas, G., Peña-Rodríguez, L.M., 2001. Tagetolone and tagetenolone: Two phytotoxic polyketides from *Alternaria tagetica*. J. Agric. Food Chem. 49, 1228–1232.

Garson, M.J., 1986. Biosynthesis of the novel diterpene isonitrile diisocyanoadociane by a marine sponge of the *Amphimedon* genus: incorporation studies with sodium [^{14}C]cyanide and sodium [2-^{14}C]acetate. J. Chem. Soc. Chem. Commun., 35–36.

Garson, M.J., Simpson, J.S., 2004. Marine isocyanides and related natural products-structure, biosynthesis and ecology. Nat. Prod. Rep. 21, 164–179.

Giese, H., Sondergaard, T.E., Sørensen, J.L., 2013. The AreA transcription factor in *Fusarium graminearum* regulates the use of some nonpreferred nitrogen sources and secondary metabolite production. Fungal Biol. 117, 814–821.

Gloer, J.B., Poch, G.K., Short, D.M., McCloskey, D.V., 1988. Structure of brassicicolin A: a novel isocyanide antibiotic from the phylloplane fungus *Alternaria brassicicola*. J. Org. Chem. 53, 3758–3761.

Graniti, A., 1991. Phytotoxins and their involvement in plant diseases. Experientia 47, 751–755.

Gross, H., 2007. Strategies to unravel the function of orphan biosynthesis pathways: Recent examples and future prospects. Appl. Microbiol. Biotechnol. 75, 267–277.

Haas, H., Eisendle, M., Turgeon, B.G., 2008. Siderophores in fungal physiology and virulence. Annu. Rev. Phytopathol. 46, 149–187.

Hanson, J.R., 2003. The classes of natural product and their isolation. In: Hanson, J. R. (Ed.), Natural Products: The Secondary Metabolites, vol. 17. The Royal Society of Chemistry, pp. 1–34.

Hayashi, N., 1990. Determination of host-selective toxin production during spore germination of *Alternaria alternata* by high-performance liquid chromatography. Phytopathology 80, 1088–1089.

Henrikson, J.C., Hoover, A.R., Joyner, P.M., Cichewicz, R.H., 2009. A chemical epigenetics approach for engineering the *in situ* biosynthesis of a cryptic natural product from *Aspergillus niger*. Org. Biomol. Chem. 7, 435–438.

Herbert, R.B., Mann, J., 1984. The incorporation of C1 units in the biosynthesis of tuberin and xanthocillin. J. Chem. Soc. Chem. Commun., 1474–1475.

Hider, R.C., Kong, X., 2010. Chemistry and biology of siderophores. Nat. Prod. Rep. 27, 637–657.

Höfs, R., Walker, M., Zeeck, A., 2000. Hexacyclinic acid, a polyketide from *Streptomyces* with a novel carbon skeleton. Angew. Chem. Int. Ed. 39, 3258–3261.

Hohn, T.H., 1997. Fungal phytotoxins: biosynthesis and activity. In: Carroll, G. C., Tudzynski, P. (Eds.), The Mycota: Plant relationships (Part A, Vol. VI). Springer Verlag, pp. 129–144.

Idris, A., Tantry, M.A., Ganai, B.A., Kamili, A.N., Williamson, J.S., 2015. Reduced perylenequinone derivatives from an endophytic *Alternaria* sp. isolated from *Pinus ponderosa*. Phytochemistry Lett. 11, 264–269.

IUPAC, 1997. IUPAC. Compendium of Chemical Terminology, 2nd ed. (the "Gold Book"). WileyBlackwell; 2nd Revised edition edition.

Jalal, M.a.F., van der Helm, D., 1989. Siderophores of highly phytopathogenic *Alternaria longipes* - structures of hydroxycoprogens. Biol. Met. 2, 11–17.

Jalal, M.F., Love, S., van der Helm, D., 1988. N^a -Dimethylcoprogens three novel trihydroxamate siderophores from pathogenic fungi. Biol. Met. 1, 4–8.

Johal, G.S., Briggs, S.P., 1992. Reductase activity encoded by the HM1 disease resistance gene in maize. Science 258, 985–987.

Karuso, P., Scheuer, P.J., 1989. Biosynthesis of isocyanoterpenes in sponges. J. Org. Chem. 54, 2092–2095.

Kawai, M., Rich, D.H., 1983. Total synthesis of the cyclic tetrapeptide, HC-toxin. Tetrahedron Lett. 24, 5309–5312.

Kawai, M., Rich, D.H., Walton, J.D., 1983. The structure and conformation of HC-toxin. Biochem. Biophys. Res. Commun. 111, 398–403.

Keller, N.P., Turner, G., Bennett, J.W., 2005. Fungal secondary metabolism - from biochemistry to genomics. Nat. Rev. Microbiol. 3, 937–947.

Kenmoku, H., Takeue, S., Oogushi, M., Yagi, Y., Sassa, T., Toyota, M., Asakawa, Y., 2014. Seed dormancy breaking diterpenoids, including novel brassicicenes J and K, from fungus *Alternaria brassicicola*, and their necrotic/apoptotic activities in HL-60 cells. Nat. Prod. Commun. 9, 351–354.

Kihara, J., Moriwaki, A., Ito, M., Arase, S., Honda, Y., 2004. Expression of THR1, a 1,3,8-trihydroxynaphthalene reductase gene Involved in melanin biosynthesis in the phytopathogenic fungus *Bipolaris oryzae*, is enhanced by near-ultraviolet radiation. Pigm. Cell Res. 17, 15–23.

Kim, H., Woloshuk, C.P., 2008. Role of AreA, a regulator of nitrogen metabolism, during colonization of maize kernels and fumonisin biosynthesis in Fusarium verticillioides. Fungal Genet. Biol. 45, 947–953.

Kimura, N., Tsuge, T., 1993. Gene cluster involved in melanin biosynthesis of the filamentous fungus *Alternaria alternata*. J. Bacteriol. 175, 4427–4435.

Kimura, Y., Tamura, S., 1973. Isolation of L-β-phenyllactic acid and tyrosol as plant growth regulators from *Gloeosporium laeticolor*. Agric. Biol. Chem. 37, 2925–2925.

Kitahara, N., Endo, A., 1981. Xanthocillin X monomethyl ether, a potent inhibitor of prostaglandin biosynthesis. J. Antibiot. (Tokyo) 34, 1556–1561.

Kodaira, Y., 1962. Studies on the new toxic substances to Insects, destruxin A and B, produced by *Oospora destructor*. Agric. Biol. Chem. 26, 36–42.

Kohmoto, K., Itoh, Y., Shimomura, N., Kondoh, Y., Otani, H., Kodama, M., Nishimura, S., Nakatsuka, S., 1993. Isolation and biological-activities of 2 host-specific toxins from the tangerine pathotype of *Alternaria alternata*. Phytopathology 83, 495–502.

Konetschny-Rapp, S., Huschka, H.-G., Winkelmanne, G., Jung, G., 1988. High-performance liquid chromatography of siderophores from fungi. Biol. Met. 1, 9–17.

König, C.C., Scherlach, K., Schroeckh, V., Horn, F., Nietzsche, S., Brakhage, A.A., Hertweck, C., 2013. Bacterium induces cryptic meroterpenoid pathway in the pathogenic fungus *Aspergillus fumigatus*. ChemBioChem 14, 938–942.

Kretz, J., Kerwat, D., Schubert, V., Grätz, S., Pesic, A., Semsary, S., Cociancich, S., Royer, M., Süssmuth, R.D., 2015. Total synthesis of albicidin: A Lead structure from *Xanthomonas albilineans* for potent antibacterial gyrase inhibitors. Angew. Chem. Int. Ed. 54, 1969–1973.

Kwon, H.J., Owa, T., Hassig, C.a., Shimada, J., Schreiber, S.L., 1998. Depudecin induces morphological reversion of transformed fibroblasts via the inhibition of histone deacetylase. Proc. Natl. Acad. Sci. U. S. A. 95, 3356–3361.

Lou, J., Fu, L., Peng, Y., Zhou, L., 2013. Metabolites from *Alternaria* fungi and their bioactivities. Molecules 18, 5891–5935.

MacKinnon, S.L., Keifer, P., Ayer, W.A., 1999. Components from the phytotoxic extract of *Alternaria brassicicola*, a black spot pathogen of canola. Phytochemistry 51, 215–221.

Maekawa, N., Yamamoto, M., Nishimura, S., Kohmoto, K., Kuwada, M., Watanabe, Y., 1984. Studies on host-specific AF-toxins produced by *Alternaria-alternata* strawberry pathotype causing Alternaria black spot of strawberry. 1. Production of host-specific toxins and their biological activities. Ann. Phytopathol. Soc. Jpn 50, 600–609.

Mai, A., Esposito, M., Sbardella, G., Massa, S., 2001. A new facile and expetedious synthesis of *N*-hydroxy-*N*′-phenyloctanediamide, a potent incuder of terminal cytodifferenciation Org. Prep. Proc. Int. 33, 391–394.

Mann, J., 1987. Introduction. In: Atkinson, P. W., Holker, J. S. E., Hoolliday, A. K. (Eds.), Secondary metabolism. Clarendon press Oxford, pp. 1–24.

Marre, E., 1979. Fusicoccin: A tool in plant physiology. Annu. Rev. Plant Physiol. 30, 273–288.

Matsumoto, M., Matsutani, S., Sugita, K., Yoshida, H., Hayashi, F., Terui, Y., Nakai, H., Uotani, N., Kawamura, Y., Matsumoto, K., 1992. Depudecin: a novel compound inducing the flat phenotype of NIH3T3 cells doubly transformed by *ras*- and *src*-oncogene, produced by *Alternaria brassicicola*. J. Antibiot. (Tokyo) 45, 879–885.

Meeley, R.B., Johal, G.S., Briggs, S.P., Walton, J.D., 1992. A biochemical phenotype for a disease resistance gene of maize. Plant Cell 4, 71–77.

Meeley, R.B., Walton, J.D., 1991. Enzymatic detoxification of HC-toxin, the host-selective cyclic peptide from *Cochliobolus carbonum*. Plant Physiol. 97, 1080–1086.

Metwaly, A.M., Fronczek, F.R., Ma, G., Kadry, H.A., El-Hela, A.A., Mohammad, A.-E.I., Cutler, S.J., Ross, S.A., 2014. Anti leukemic alpha-pyrone derivatives from the endophytic fungus *Alternaria phragmospora*. Tetrahedron Lett. 55, 3478–3481.

Mitchell, R.E., 1984. The relevance of non-host-specific toxins in the expression of virulence by pathogens. Annu. Rev. Phytopathol. 22, 215–245.

Morant, A.V., Jørgensen, K., Jørgensen, C., Paquette, S.M., Sánchez-Pérez, R., Møller, B.L., Bak, S., 2008. β-Glucosidases as detonators of plant chemical defense. Phytochemistry 69, 1795–1813.

Muria-Gonzalez, M.J., Chooi, Y.-H., Breen, S., Solomon, P.S., 2015. The past, present and future of secondary metabolite research in the Dothideomycetes. Mol. Plant Pathol. 16, 92–107.

Muromtsev, G.S., Voblikova, V.D., Kobrina, N.S., Koreneva, V.M., Krasnopolskaya, L.M., Sadovskaya, V.L., 1994. Occurrence of fusicoccanes in plants and fungi. J. Plant Growth Regul. 13, 39–49.

Nakatsuka, S., Ueda, K., Goto, T., Yamamoto, M., Nishimura, S., Kohmoto, K., 1986. Structure of AF-toxin II, one of the host-specific toxins produced by *Alternaria alternata* strawberry pathotype. Tetrahedron Lett. 27, 2753–2756.

Nishimura, S., Kohmoto, K., 1983a. Host-specific toxins and chemical structures from *Alternaria* species. Annu. Rev. Phytopathol. 21, 87–116.

Nishimura, S., Kohmoto, K., 1983b. Roles of toxins in pathogenesis. In: Daly, J. M., Deverall, B. J. (Eds.), Toxins and Plant Pathogenesis Academic Press, Sydney, pp. 137–157.

O'Brien, J., Wright, G.D., 2011. An ecological perspective of microbial secondary metabolism. Curr. Opin. Biotechnol. 22, 552–558.

Ohra, J., Morita, K., Tsujino, Y., Fujimori, T., Goering, M., Evans, S., Zorner, P., 1995. Production of two phytotoxic metabolites by the fungus *Alternaria cassiae*. Biosci. Biotechnol. Biochem. 59, 1782–1783.

Oide, S., Moeder, W., Krasnoff, S., Gibson, D., Haas, H., Yoshioka, K., Turgeon, B.G., 2006. *NPS6*, encoding a nonribosomal peptide synthetase involved in siderophore-mediated iron

metabolism, is a conserved virulence determinant of plant pathogenic ascomycetes. Plant Cell 18, 2836–2853.

Oka, K., Akamatsu, H., Kodama, M., Nakajima, H., Kawada, T., Otani, H., 2005. Host-specific AB-toxin production by germinating spores of *Alternaria brassicicola* is induced by a host-derived oligosaccharide. Physiol. Mol. Plant Pathol. 66, 12–19.

Orvehed, M., Haggblom, P., Soderhall, K., 1988. Nitrogen inhibition of mycotoxin production by *Alternaria alternata*. Appl. Environ. Microbiol. 54, 2361–2364.

Otani, H., Kohnobe, A., Kodama, M., Kohmoto, K., 1998. Production of a host-specific toxin by germinating spores of *Alternaria brassicicola*. Physiol. Mol. Plant Pathol., 285–295.

Païs, M., Das, B.C., Ferron, P., 1981. Depsipeptides from *Metarhizium anisopliae*. Phytochemistry 20, 715–723.

Parada, R.Y., Sakuno, E., Mori, N., Oka, K., Egusa, M., Kodama, M., Otani, H., 2008. *Alternaria brassicae* produces a host-specific protein toxin from germinating spores on host leaves. Phytopathology 98, 458–463.

Pedras, M.S.C., Abdoli, A., 2013. Metabolism of the phytoalexins camalexins, their bioisosteres and analogues in the plant pathogenic fungus *Alternaria brassicicola*. Bioorg. Med. Chem. 21, 4541–4549.

Pedras, M.S.C., Biesenthal, C.J., 1998. Production of the host-selective phytotoxin phomalide by isolates of *Leptosphaeria maculans* and its correlation with sirodesmin PL production. Can. J. Microbiol. 44, 547–553.

Pedras, M.S.C., Biesenthal, C.J., Zaharia, I.L., 2000. Comparison of the phytotoxic activity of the phytotoxin destruxin B and four natural analogs. Plant Sci. 156, 185–192.

Pedras, M.S.C., Chumala, P.B., 2005. Phomapyrones from blackleg causing phytopathogenic fungi: isolation, structure determination, biosyntheses and biological activity. Phytochemistry 66, 81–87.

Pedras, M.S.C., Chumala, P.B., 2011. Maculansins, cryptic phytotoxins from blackleg fungi. Nat. Prod. Commun. 6, 617–620.

Pedras, M.S.C., Chumala, P.B., Jin, W., Islam, M.S., Hauck, D.W., 2009. The phytopathogenic fungus *Alternaria brassicicola*: phytotoxin production and phytoalexin elicitation. Phytochemistry 70, 394–402.

Pedras, M.S.C., Irina Zaharia, L., Ward, D.E., 2002. The destruxins: synthesis, biosynthesis, biotransformation, and biological activity. Phytochemistry 59, 579–596.

Pedras, M.S.C., Khallaf, I., 2012. Molecular interactions of the phytotoxins destruxin B and sirodesmin PL with crucifers and cereals: metabolism and elicitation of plant defenses. Phytochemistry 77, 129–139.

Pedras, M.S.C., Minic, Z., Hossain, S., 2012. Discovery of inhibitors and substrates of brassinin hydrolase: Probing selectivity with dithiocarbamate bioisosteres. Bioorg. Med. Chem. 20, 225–233.

Pedras, M.S.C., Minic, Z., Sarma-Mamillapalle, V.K., 2009. Substrate specificity and inhibition of brassinin hydrolases, detoxifying enzymes from the plant pathogens *Leptosphaeria maculans* and *Alternaria brassicicola*. FEBS J. 276, 7412–7428.

Pedras, M.S.C., Montaut, S., Suchy, M., 2004. Phytoalexins from the crucifer rutabaga: structures, syntheses, biosyntheses, and antifungal activity. J. Org. Chem. 69, 4471–4476.

Pedras, M.S.C., Montaut, S., Zaharia, I.L., Gai, Y., Ward, D.E., 2003. Transformation of the host-selective toxin destruxin B by wild crucifers: probing a detoxification pathway. Phytochemistry 64, 957–963.

Pedras, M.S.C., Morales, V.M., Taylor, J.L., 1994. Phomapyrones: Three metabolites from the blackleg fungus. Phytochemistry 36, 1315–1318.

Pedras, M.S.C., Nycholat, C.M., Montaut, S., Xu, Y., Khan, A.Q., 2002. Chemical defenses of crucifers: elicitation and metabolism of phytoalexins and indole-3-acetonitrile in brown mustard and turnip. Phytochemistry 59, 611–625.

Pedras, M.S.C., Park, M.R., 2015. Metabolite diversity in the plant pathogen *Alternaria brassicicola*: factors affecting production of brassicicolin A, depudecin, phomapyrone A and other metabolites. Mycologia 107, 1138–1150.

Pedras, M.S.C., Taylor, J.L., Nakashima, T.T., 1993. A novel chemical signal from the blackleg fungus - beyond phytotoxins and phytoalexins. J. Org. Chem. 58, 4778–4780.

Pedras, M.S.C., Yaya, E.E., 2010. Phytoalexins from Brassicaceae: News from the front. Phytochemistry 71, 1191–1197.

Pedras, M.S.C., Yaya, E.E., 2012. The first isocyanide of plant origin expands functional group diversity in cruciferous phytoalexins: synthesis, structure and bioactivity of isocyalexin A. Org. Biomol. Chem. 10, 3613–3616.

Pedras, M.S.C., Yaya, E.E., 2013. Dissecting metabolic puzzles through isotope feeding: a novel amino acid in the biosynthetic pathway of the cruciferous phytoalexins rapalexin A and isocyalexin A. Org. Biomol. Chem. 11, 1149–1166.

Pedras, M.S.C., Yaya, E.E., 2015. Plant chemical defenses: are all constitutive antimicrobial metabolites phytoanticipins? Nat. Prod. Commun. 10, 209–218.

Pedras, M.S.C., Yaya, E.E., Glawischnig, E., 2011. The phytoalexins from cultivated and wild crucifers: chemistry and biology. Nat. Prod. Rep. 28, 1381–1405.

Pedras, M.S.C., Yu, Y., 2008a. Stress-driven discovery of metabolites from the phytopathogenic fungus *Leptosphaeria maculans*: structure and activity of leptomaculins A-E. Bioorg. Med. Chem. 16, 8063–8071.

Pedras, M.S.C., Yu, Y., 2008b. Structure and biological activity of maculansin A, a phytotoxin from the phytopathogenic fungus *Leptosphaeria maculans*. Phytochemistry 69, 2966–2971.

Pedras, M.S.C., Yu, Y., 2009a. Phytotoxins, elicitors and other secondary metabolites from phytopathogenic "blackleg" fungi: structure, phytotoxicity and biosynthesis. Nat. Prod. Commun. 4, 1291–1304.

Pedras, M.S.C., Yu, Y., 2009b. Salt stress induces production of melanin related metabolites in the phytopathogenic fungus *Leptosphaeria maculans*. Nat. Prod. Commun. 4, 53–58.

Pedras, M.S.C., Zaharia, I.L., Gai, Y., Smith, K.C., Ward, D.E., 1999. Metabolism of the host-Selective toxins destruxin B and homodestruxin B : probing a plant disease resistance trait. Org. Lett. 1, 1655–1658.

Pedras, M.S.C., Zaharia, I.L., Gai, Y., Zhou, Y., Ward, D.E., 2001. *In planta* sequential hydroxylation and glycosylation of a fungal phytotoxin: Avoiding cell death and overcoming the fungal invader. Proc. Natl. Acad. Sci. U. S. A. 98, 747–752.

Pedras, M.S.C., Zheng, Q.-A., Schatte, G., Adio, A.M., 2009. Photochemical dimerization of wasalexins in UV-irradiated *Thellungiella halophila* and in vitro generates unique cruciferous phytoalexins. Phytochemistry 70, 2010–2016.

Pedras, M.S.C., Zheng, Q.A., 2010. Metabolic responses of *Thellungiella halophila*/*salsuginea* to biotic and abiotic stresses: metabolite profiles and quantitative analyses. Phytochemistry 71, 581–589.

Pusztahelyi, T., Holb, I.J., Pócsi, I., 2015. Secondary metabolites in fungus-plant interactions. Front. Plant Sci. 6, 1–23.

Quayyum, H.a., Gijzen, M., Traquair, J.a., 2003. Purification of a necrosis-inducing, host-specific protein toxin from spore germination fluid of *Alternaria panax*. Phytopathology 93, 323–328.

Renshaw, J.C., Robson, G.D., Trinci, A.P.J., Wiebe, M.G., Livens, F.R., Collison, D., Taylor, R.J., 2002. Fungal siderophores: structures, functions and applications. Mycol. Res. 106, 1123–1142.

Rich, D.H., Mathiaparanam, P., 1974. Synthesis of the cyclic tetrapeptide tentoxin. effect of an *N*-methyldehydrophenylalanyl residue on conformation of linear tetrapeptides. Tetrahedron Lett. 15, 4037–4040.

Robeson, D.J., Strobel, G.A., 1984. Zinniol induces chlorophyll retention in barley leaves: the selective action of a non host-specific phytotoxin. Phytochemistry 23, 1597–1599.

Roslund, M.U., Tähtinen, P., Niemitz, M., Sjöholm, R., 2008. Complete assignments of the ^{1}H and ^{13}C chemical shifts and $J_{H,H}$ coupling constants in NMR spectra of D-glucopyranose and all D-glucopyranosyl-D-glucopyranosides. Carbohydr. Res. 343, 101–112.

Rothe, W., 1950. Vorläufige Mitteilung über eine neues Antibiotikum. Pharmazie, 190.

Ryan, G.F., Greenblatt, G., Al-Delaimy, K.A., 1961. Seedling albinism induced by an extract of *Alternaria tenuis*. Science 134, 833–834.

Scheffer, R.P., Livingston, R.S., 1984. Host-selective toxins and their role in plant diseases. Science 223, 17–21.

Scherlach, K., Hertweck, C., 2009. Triggering cryptic natural product biosynthesis in microorganisms. Org. Biomol. Chem. 7, 1753–1760.

Scherlach, K., Sarkar, A., Schroeckh, V., Dahse, H.-M., Roth, M., Brakhage, A.A., Horn, U., Hertweck, C., 2011. Two induced fungal polyketide pathways converge into antiproliferative spiroanthrones. ChemBiochem 12, 1836–1839.

Schneider, B., 2007. Nuclear magnetic resonance spectroscopy in biosynthetic studies. Prog. Nucl. Magn. Reson. Spectrosc. 51, 155–198.

Schroeckh, V., Scherlach, K., Nützmann, H.-W., Shelest, E., Schmidt-Heck, W., Schuemann, J., Martin, K., Hertweck, C., Brakhage, A.A., 2009. Intimate bacterial–fungal interaction triggers biosynthesis of archetypal polyketides in *Aspergillus nidulans*. Proc. Natl. Acad. Sci. U. S. A. 106, 14558–14563.

Schuhegger, R., Nafisi, M., Mansourova, M., Petersen, B.L., Olsen, C.E., Svatos, A., Halkier, B.A., Glawischnig, E., 2006. CYP71B15 (PAD3) catalyzes the final step in camalexin biosynthesis. Plant Physiol. 141, 1248–1254.

Shi, X., Wei, W., Zhang, W.-J., Hua, C.-P., Chen, C.-J., Ge, H.-M., Tan, R.-X., Jiao, R.-H., 2015. New tricycloalternarenes from fungus *Alternaria* sp. J. Asian Nat. Prod. Res. 17, 143–148.

Simpson, J.S., Garson, M.J., 2004. Biosynthetic pathways to isocyanides and isothiocyanates; precursor incorporation studies on terpene metabolites in the tropical marine sponges *Amphimedon terpenensis* and *Axinyssa* n.sp. Org. Biomol. Chem. 2, 939–948.

Strange, R.N., 2007. Phytotoxins produced by microbial plant pathogens. Nat. Prod. Rep. 24, 127–144.

Strauss, J., Reyes-Dominguez, Y., 2011. Regulation of secondary metabolism by chromatin structure and epigenetic codes. Fungal Genet. Biol. 48, 62–69.

Takasugi, M., Katsui, N., Shirata, A., 1986. Isolation of three novel sulphur-containing phytoalexins from the chinese cabbage *Brassica campestris* L. ssp. pekinensis (Cruciferae). J. Chem. Soc. Chem. Commun., 1077–1078.

Tanaka, M., Fujimori, T., Nabeta, K., 2000. Biosynthesis of depudecin, a metabolite of *Nimbya scirpicola*. Biosci. Biotechnol. Biochem. 64, 244-–247.

TheArabidopsisInitiative, 2000. Analysis of the genome sequence of the flowering plant *Arabidopsis thaliana*. Nature 408, 796–815.

Thomma, B., Nelissen, I., Eggermont, K., Broekaert, W., 1999. Deficiency in phytoalexin production causes enhanced susceptibility of *Arabidopsis thaliana* to the fungus *Alternaria brassicicola*. The Plant Journal 19, 163 - 171.

Thomma, B.P., 2003. *Alternaria* spp.: from general saprophyte to specific parasite. Mol. Plant Pathol. 4, 225–236.

Tocquin, P., Corbesier, L., Havelange, A., Pieltain, A., Kurtem, E., Bernier, G., Périlleux, C., 2003. A novel high efficiency, low maintenance, hydroponic system for synchronous growth and flowering of *Arabidopsis thaliana*. BMC Plant Biol. 3, 1–10.

Tsuge, T., Harimoto, Y., Akimitsu, K., Ohtani, K., Kodama, M., Akagi, Y., Egusa, M., Yamamoto, M., Otani, H., 2013. Host-selective toxins produced by the plant pathogenic fungus Alternaria alternata. FEMS Microbiol. Rev. 37, 44–66.

Tsuji, J., Jackson, E.P., Gage, D.A., Hammerschmidt, R., Somerville, S.C., 1992. Phytoalexin accumulation in *Arabidopsis thaliana* during the hypersensitive reaction to *Pseudomonas syringae* pv. *syringae*. Plant Physiol. 98, 1304–1309.

Tudzynski, B., 2014. Nitrogen regulation of fungal secondary metabolism in fungi. Front. Microbiol. 5, 1–15.

Ueno, T., Hayashi, Y., Nakashima, T., Fukami, H., Nishimura, S., Kohmoto, K., Sekiguchi, A., 1975. Isolation of AM-Toxin I, a new phytotoxic metabolite from *Alternaria mali*. Phytopathology 65, 82–83.

Ueno, T., Nakashima, T., Hayashi, Y., Fukami, H., 1975a. Isolation and structure of AM-Toxin III, a host specific phytotoxic metabolite produced by *Alternaria mali*. Agric. Biol. Chem. 39, 2081–2082.

Ueno, T., Nakashima, T., Hayashi, Y., Fukami, H., 1975b. Structures of AM-toxin I and II, host specific phytotoxic metabolites produced by *Alternaria mali*. Agric. Biol. Chem. 39, 1115–1122.

VanderMolen, K.M., Darveaux, B.A., Chen, W.-L., Swanson, S.M., Pearce, C.J., Oberlies, N.H., 2014. Epigenetic manipulation of a filamentous fungus by the proteasome-inhibitor bortezomib induces the production of an additional secondary metabolite. RSC Adv. 4, 18329–18335.

VanEtten, H.D., Mansfield, J.W., Bailey, J.A., Farmer, E.E., 1994. Two classes of plant antibiotics: Phytoalexins versus "Phytoanticipins". Plant Cell 6, 1191–1192.

Venkatasubbaiah, P., Baudoin, A.B.A.M., Chilton, W.S., 1992. Leaf spot of hemp dogbane caused by *Stagonospora apocyni*, and its phytotoxins. J. Phytopathol. 135, 309–316.

Vervoort, H.C., Drašković, M., Crews, P., 2011. Histone deacetylase inhibitors as a tool to up-regulate new fungal biosynthetic products: Isolation of EGM-556, a cyclodepsipeptide, from *Microascus* sp. Org. Lett. 13, 410–413.

Walton, J.D., 2006. HC-toxin. Phytochemistry 67, 1406–1413.

Wang, H., Denton, J.R., Davies, H.M., 2011. Sequential rhodium-, silver-, and gold-catalyzed synthesis of fused dihydrofurans. Org. Lett. 13, 4316–4319.

Wang, X., Sena Filho, J.G., Hoover, A.R., King, J.B., Ellis, T.K., Powell, D.R., Cichewicz, R.H., 2010. Chemical epigenetics alters the secondary metabolite composition of guttate excreted by an Atlantic-forest-soil-derived *Penicillium citreonigrum*. J. Nat. Prod. 73, 942–948.

Wang, X.-Z., Luo, X.-H., Xiao, J., Zhai, M.-M., Yuan, Y., Zhu, Y., Crews, P., Yuan, C.-S., Wu, Q.-X., 2014. Pyrone derivatives from the endophytic fungus *Alternaria tenuissima* SP-07 of Chinese herbal medicine *Salvia przewalskii*. Fitoterapia 99, 184–190.

Wang, Y., Yang, M.-H., Wang, X.-B., Li, T.-X., Kong, L.-Y., 2014. Bioactive metabolites from the endophytic fungus *Alternaria alternata*. Fitoterapia 99, 153–158.

Wheeler, H., Luke, H.H., 1963. Microbial toxins in plant disease. Annu. Rev. Microbiol. 17, 223–242.

White, G.A., Starratt, A.N., 1967. The production of a phytotoxic substance by *Alternaria zinniae*. Can. J. Bot. 45, 2087–2090.

Wiemann, P., Keller, N.P., 2014. Strategies for mining fungal natural products. J. Ind. Microbiol. Biotechnol. 41, 301–313.

Wight, W.D., Kim, K.-H., Lawrence, C.B., Walton, J.D., 2009. Biosynthesis and role in virulence of the histone deacetylase inhibitor depudecin from *Alternaria brassicicola*. Mol. Plant Microbe. Interact. 22, 1258–1267.

Williams, R.B., Henrikson, J.C., Hoover, A.R., Lee, A.E., Cichewicz, R.H., 2008. Epigenetic remodeling of the fungal secondary metabolome. Org. Biomol. Chem. 6, 1895–1897.

Wishart, D., Bigam, C., Yao, J., Abildgaard, F., Dyson, H.J., Oldfield, E., Markley, J., Sykes, B., 1995. ^{1}H, ^{13}C and ^{15}N chemical shift referencing in biomolecular NMR. J Biomol. NMR 6, 135–140.

Wu, C.T., Morris, J.R., 2001. Genes, Genetics, and Epigenetics: A Correspondence. Science 293, 1103–1105.

Xu, G.-B., Pu, X., Bai, H.-H., Chen, X.-Z., Li, G.-Y., 2015. A new alternariol glucoside from fungus *Alternaria alternate* cib-137. Nat. Prod. Res. 29, 848–852.

Zhang, L., Birch, R.G., 1997a. Mechanisms of biocontrol by *Pantoea dispersa* of sugar cane leaf scald disease caused by *Xanthomonas albilineans*. J. Appl. Microbiol. 82, 448–454.

Zhang, L., Xu, J., Birch, R.G., 1999. Engineered detoxification confers resistance against a pathogenic bacterium. Nat. Biotech. 17, 1021–1024.

Zhang, L.H., Birch, R.G., 1997b. The gene for albicidin detoxification from *Pantoea dispersa* encodes an esterase and attenuates pathogenicity of *Xanthomonas albilineans* to sugarcane. Proc. Natl. Acad. Sci. U. S. A. 94, 9984–9989.

Zuo, L., Yao, S.Y., Wang, W., Duan, W.H., 2008. An efficient method for demethylation of aryl methyl ethers. Tetrahedron Lett. 49, 4054–4056.